Biofilm Impacts on Water Quality in Drinking Water Distribution Systems

Yi Shi

School of Engineering

Cardiff University

This thesis is submitted in fulfilment of the requirement of the degree of

Doctor of Philosophy

2018

Declaration and Statements

DECLARATION

This work has not been submitted in substance for any degree or award at this or any other university or place of learning, nor is being submitted concurrently in candidature for any degree or other award.

Signed..... (Yi Shi) Date .....

STATEMENT 1

This thesis is being submitted in partial fulfilment of the requirements for the degree of Doctor of Philosophy (PhD).

Signed ..... (Yi Shi) Date .....

STATEMENT 2

This thesis is the result of my own investigation, except where otherwise stated. Other sources are acknowledged by giving explicit reference. The views expressed are my own.

Signed ..... (Yi Shi) Date .....

STATEMENT 3

I hereby give consent for my thesis, if accepted, to be available for photocopying and for inter-library loan, and for the title and summary to be made available to outside organizations.

Signed ..... (Yi Shi) Date .....

Acknowledgements

I would like to thank all the people who helped and supported me to complete this thesis during the four years. Firstly, I would like to sincerely appreciate my academic supervisors, Dr Akintunde Babatunde and Dr Bettina Bockelmann-Evans for their continued support and encouragement. I would also like to thank my colleagues, Dr Alya Mohammed, Dr Talib Zbala, Dr Mishari Khajah and Dr Abdullah Almatouq for their kind support, comments and feedback.

In addition, I am greatly appreciative for the assistance from Dr Angela Marchbank and Dr Gordon Webster (Cardiff University, Wales), especially for their contribution of both time and knowledge to the microbiological aspects of this study. I would also thank the School of Engineering technical staff, and in particular, Mr Harry lane, Mr Steffen Jones and Mr Marco Santonastaso for their practical knowledge to the build-up of the experimental facility.

I would like to reserve my greatest thanks to my parents, without their unconditional supports and encouragement I would never have completed my thesis.

Abstract

Drinking water distribution systems (DWDSs) account for the majority of the infrastructure for transporting water from treatment plants to customers' tap. During the transportation, water quality deteriorates due to the unavoidable accumulation of biofilm within the pipelines. The microbial activity and ecology within the biofilm have great impact on the water quality degradation process. Within DWDSs using chloramine as disinfectant, nitrification caused by nitrifying bacteria is increasingly becoming a concern as it poses a great challenge for maintaining water quality. In order to control nitrification in DWDSs, it is essential to consider both the nitrifying bacteria and their shelter. Hence, the overall aim of this study is to investigate nitrification properties under different operational conditions, in addition to biofilm characteristics in chloraminated water distribution systems.

To achieve the aim, nitrifying biofilm was firstly incubated within a flow cell experimental facility. A total of four test phases were conducted to investigate the effects on the extent of nitrification of five flow rates (2, 4, 6, 8 and10 L/min) and four disinfection strategies (total chlorine=1mg/L, Cl_2/NH_3=3:1; total chlorine=1mg/L, Cl_2/NH_3=5:1; total chlorine=5mg/L, Cl_2/NH_3=3:1; and total chlorine=5mg/L, Cl_2/NH_3=5:1). Physico-chemical parameters and nitrification indicators were monitored during the tests. The main results from the study indicate that nitrification is affected by hydraulic conditions and the process tends to be severe when the fluid flow transforms from laminar to turbulent (2300<Reynold number<4000). Increasing disinfectant concentration and optimizing Cl_2/NH_3 mass ratio were found to have limited efficacy for controlling nitrification. Furthermore, several nitrification indicators were evaluated for their prediction efficiency and the results suggest that the change of nitrite, together with total organic carbon (TOC) and turbidity can indicate nitrification potential more efficiently. At the end of the tests, genomic DNA from biofilm and bulk water from each flow cell unit running at different operational conditions were subjected to a next generation sequencing (NGS) analysis by Illumina MiSeq. The results obtained showed that the microbial community and structure was different between biofilm and water samples. There was no statistical difference in microbial community in biofilm identified between different hydraulic regimes, suggesting that biofilm is a stable matrix to environment. Results further showed that Cl_2/NH_3 mass ratio had obvious effect on microbial structure in biofilm. This suggests that excessive ammonia is an influencing factor for microbial activity within biofilm. Within bulk water, species richness and diversity tended to be higher at lower hydraulic regimes. This confirms the influence of hydraulic condition on biofilm mechanical structure and further material mobilization to water. Opportunic pathogens such as *Legionella* and *Mycobacterium* were detected in abundance in the experimental system. This confirms that nitrification can lead to a decrease of water quality and microbial outbreaks. The characteristics of extracellular polymeric substance (EPS) from biofilm conditioned under different operational conditions were also analysed. Carbohydrate was found to be the main components within biofilm's EPS. EPS composition and structure were found to be governed by operational conditions, but no simple linear relationship was found. This suggests the interactive effects of EPS properties, hydraulics and disinfectant strategies. EPS effects on disinfection were evaluated via disinfectant decay tests. EPS was confirmed to have an influencing in biofilm overcoming disinfection.

Table of Contents

List of Figures

List of Tables

List of Abbreviations

AOB	Ammonia oxidizing bacteria
BSA	Bovine serum albumin
C	Carbon
CDF	Chlorine demand free
CLSM	Confocal Laser Scanning Microscopy
Cl_2	Chlorine
C/P	Carbohydrate/protein
DO	Dissolve oxygen
DWDS	Drinking water distribution system
EDTA	Ethylenediaminetetraaccetic acid
EPS	Extracellular polymeric substance
Fm	Microbial decay factor
HDPE	High-Density Polyethylene
HPC	Heterotrophic plate count
IC	Inorganic carbon
LB	Luria-Bertani
MDS	Multi-Dimensional Scaling analysis
N	Nitrogen
NGS	Next generation sequencing
NH_4^+	Ammonium
NH_3	Ammonia
NOB	Nitrite oxidizing bacteria
NO_3^-	Nitrate
NO_2^-	Nitrite
NOM	Nature organic matter

RSA	Relative sequence abundance
SMP	Soluble microbial products
TC	Total carbon
TOC	Total organic carbon

Nomenclature

C	Concentration of reactant after decay
D_h	Hydraulic diameter
f	Fanning friction factor
k_1	Fast decay coefficient
k_2	Slow decay coefficient
k_c	Chemical decay rate coefficient
k_m	Microbial decay rate coefficient
K_s	Half saturation constant for ammonia oxidizing bacteria, mg/L-N
k_s	First-order decay coefficient of sample
k_t	Decay coefficients for unprocessed
Q	Average flow rate
Re	Reynold number
R_{gi}	The minimum total chlorine concentrations needed to prevent nitrification for any free ammonia concentration, mg/L-Cl_2
t	Time
U	Average flow velocity
U_{ave}	Average flow velocity
u_{max}	Maximum velocity
ρ	Water density
τ_w	Shear stress

Chapter 1 Introduction

1.1 Research Motivation

Water safety is one of the most important issues related to human health due to the fact that unsafe water may bring high risk of diseases (WHO, 2009). According to data provided by the WHO (2009), unsafe water is the leading cause of morbidity when compared with other environmental problems, such as air pollution and global warming. The situation has been amplified due to the increasing rate of urbanization and the resultant increase in demand for safe water (Karanja et al. 2011). In order to secure water quality, advanced water treatment techniques have been applied both in water treatment facilities and water distribution systems. Before water reaches the customer's tap, strategies for minimizing pathogens and chemicals entering into the distribution system have been widely introduced. However, studies have indicated that water quality is still being adversely impacted by physical, chemical, biological and operational conditions in both the treatment and distribution facilities, especially in ageing systems (UKWIR 2003). In addition, an increasing trend of waterborne illnesses and outbreaks have been identified (Liang et al. 2006), and this is possibly attributed to pathogens re-growth or chemicals re-introduce between the point of entry (after water treatment plants) and the point of use, i.e. taps, bottled water (Jørgensen et al. 2008). This situation leads to a significant concern about water quality in drinking water distribution systems (DWDS).

DWDS is the pipe system that transports finished water from treatment plant to the point of use. Before the water reaches customer taps, water quality deterioration can occur due to the influence of environmental conditions in the DWDS, and this is partly influenced by the system management (i.e. hydraulic and disinfection) and water composition (i.e. microorganisms and phisco-chemical parameters). Of particular concern is the biofilm formation. Biofilm refers to a complex microbiological slime layer, composed of aggregated microbial cells and embedded within a self-produced

matrix of extracellular polymeric substances (EPS) upon the pipe surface (for example, see Fig.1.1). This matrix has stable structure and high resistance to external disturbance (i.e. detachment shear force and disinfection) (LeChevallier et al. 1988; Douterelo et al. 2013). Its characteristics, which includes density, structure and community, are affected by various abiotic and biotic properties, and subsequently impact on features of DWDS. Furthermore, there is an impact from interaction between the pipe properties (surface roughness, resistance to corrosion and chemical composition of pipe materials) and microbial attachment/development (Niquette et al. 2000; Tsvetanova 2006; Nielsen et al. 2008). This relationship also indicates that the involvement of microorganisms in DWDS is a contributory factor in impairing water quality.

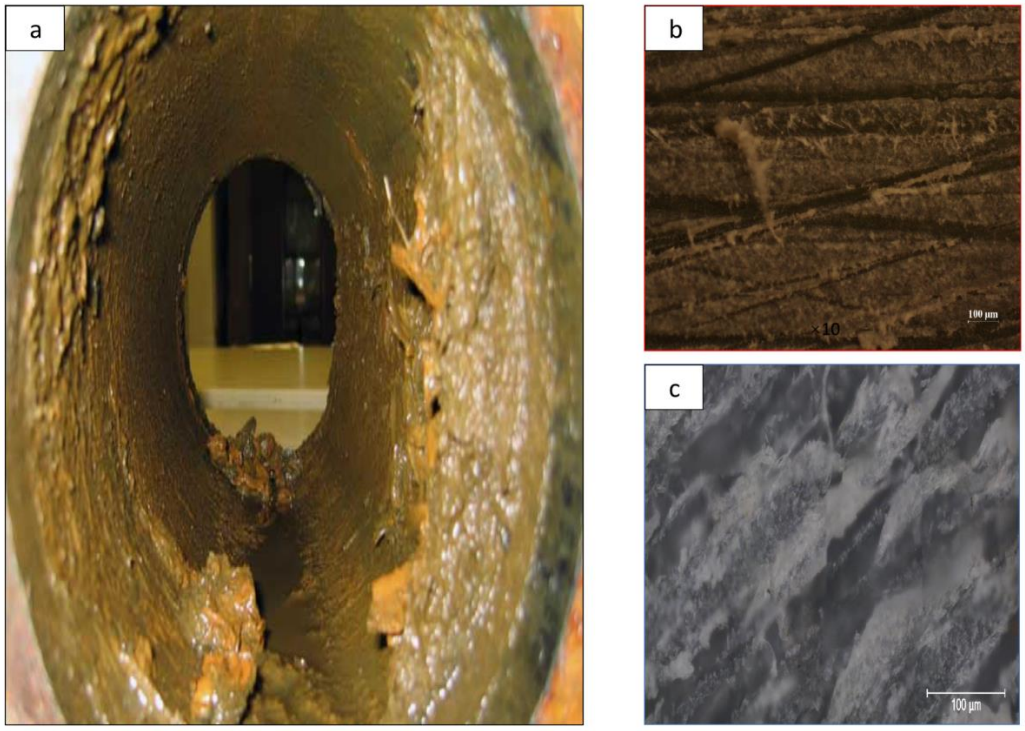

Figure 1.1 Biofilm within drinking water distribution systems: a. a cast pipe removed from service (Water quality Investigation, 2014); b and c: biofilm formatted upon coupons from current study, captured by a polarizing microscopy (Nikon ECLIPSE LV100) at × 10 and × 100 magnifications.

The presence of biofilm can lead to undesirable physical (pH, taste and odour and turbidity) and chemical (excessive ions, unexpected substance) changes in distribution system. Moreover, since biofilm itself is a great shelter for potential pathogens, and coupled with the property to sorb water chemicals, growth of pipe scales and biofilm conglomerates is recognized as an underestimated source of contamination in DWDS (Lytle et al. 2004). In order to control and remove biofilm in DWDS, actions like

flushing and disinfectant treatment are utilized to inhibit biofilm development according to their potential to remove and/or counteract the growth of biofilm (Hallam et al. 2001; Tsvetanova 2006; Zhou et al. 2009). Flushing is proved to be a valid method for removing biofilm when flow velocities are at a relatively high level (Percival et al. 1999; Douterelo et al. 2013). However, biofilm detachment and mobilization could in turn affect water quality (i.e. discoloration event). Theoretically, after disinfection treatment, the disinfectant residuals in DWDS can keep biomass growth in the system at safe level. Instead of expectation, disinfectant efficacy has been shown to be affected by the microbial community within DWDS, and the formation of disinfectant by-products is becoming another contaminant source.

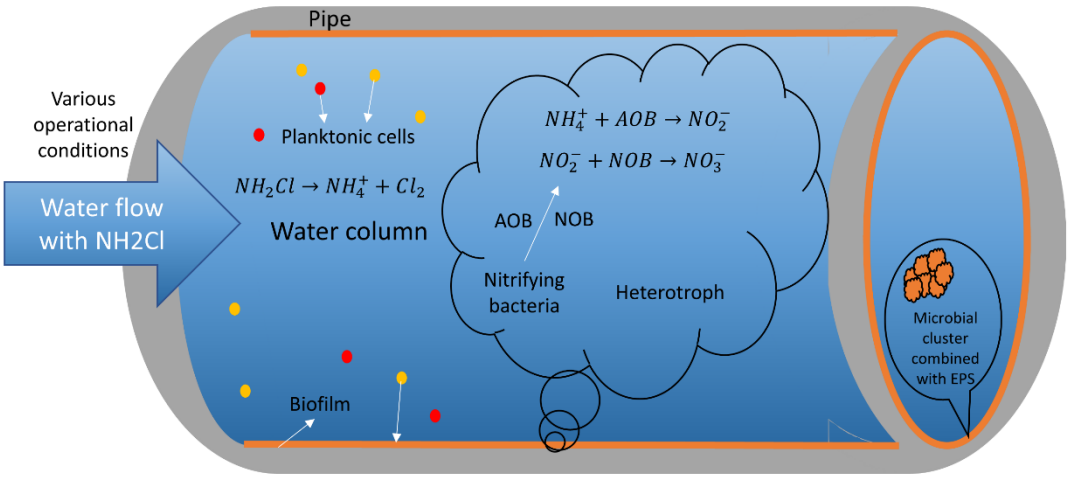

Figure 1.2 Effects of biofilm developed within drinking water distribution system using chloramine as disinfectant

In modem water treatment plants, chlorine and chloramine are the two main disinfectants applied due to their low cost and low risk for human health. Compared with chlorine, chloramine has relatively low activity and produces less disinfectant by products (DBPs). However, biofilm shows a resistance ability with chloramine and the concentration of disinfectant residual potentially decreased by nitrifiers (LeChevallier et al. 1990; Zhang and Edwards 2009a). As shown in Fig.1.2, in chloraminated DWDS, the free ammonia can provide nutrient substance for autotrophic ammonia oxidizing bacteria (AOB) and nitrite oxidizing bacteria (NOB). Through biological oxidation process, ammonia can be converted to nitrite and then nitrate by these two kinds of nitrifiers respectively, referred to nitrification. This reaction will not only reduce disinfectant efficacy but also bring about unintended impacts on pipe corrosion through

inducing pH drop, and thereby increasing metal ion leaching (Zhang et al. 2009b). Other impacts brought by nitrification can include increasing biofilm accumulation and escalating the possibility of regrowth events in distribution.

Nitrification is the unexpected bio-chemical process in DWDS utilizing chloramine as disinfectants. In order to provide advice about making efficient disinfectant procedure, previous studies have focused on nitrifying bacteria properties and relevant influencing factors on nitrification (Wolfe et al. 1990; Kirmeyer et al. 1995; Odell et al. 1996; Zhang et al. 2008; Zhang et al. 2009c). Nitrifiers have low activity compared with heterotrophic bacteria and their growth relay on the availably of inorganic substances (i.e. ammonia and nitrite) (Pintar and Slawson 2003). However, once this process is underway and become severe, it is difficult to control or inhibit (Cunliffe 1991; Odell et al. 1996; Seidel et al. 2005; Sathasivan et al. 2008). Traditional nitrification controlling strategies are aimed at inhibiting the activity of nitrifying bacteria by optimizing disinfectant schedules (Skadsen and Cohen 2006). Though nitrification could be controlled for a period within DWDS, the event is always recurring. The persistence of nitrification might be attributed to the support from biofilm, which enhances the stability and disinfection resistance of nitrifiers (Furumai and Rittmann 1994; Volk and LeChevallier 1999). In addition, due to the difficulty of acquiring biofilm samples from real DWDS, most of the previous researches only investigated nitrification process based on the change of water composition (Odell et al. 1996; Fleming et al. 2005, 2008; Zhang et al. 2009a) or observed nitrifying bacteria from water samples (Regan et al. 2002; Regan et al. 2003). However, it is suggested that nitrifiers have preference to aggregate within biofilm (Wilczak et al. 1996; Tarre and Green 2004) rather than live as free cells and hence their behaviour is not independent from the biofilm matrix. The increasing emphasis on water safety within drinking water systems with respect to disinfection efficiency of networks implies that it is important to control nitrification as well as biofilm via long-term effective approaches.

1.2 Research Aim and Objectives

The overall aim of this study is to investigate nitrification properties under different operational conditions, together with biofilm characteristics in chloraminated water distribution systems. The specific objectives are:

I. To investigate nitrification response to different operational conditions by measuring the change of water quality in a controlled laboratory flow cell facility.
II. To determine the impacts of operational conditions on microbial community within both water and biofilm via DNA sequencing analysis.
III. To understand the effect of operational conditions on biofilm EPS composition and to investigate EPS impacts on disinfectant decay.

1.3 Organization of the thesis

The thesis is organized into 7 chapters as briefly described below:

Chapter 1 gives an introduction to the current study, emphasizing the motivation for the research, the aim and the objectives.

Chapter 2 reviews relevant literature particularly with respect to current concerns about microbial water quality and typical biofilm formation process within DWDS. The interactive effects between biofilm and operational conditions are highlighted. Nitrification process, including its mechanism, effects, predictors and controlling strategies are also reviewed. A summary of the identified knowledge gaps is presented at the end of this chapter.

Chapter 3 presents the methodology and experimental design used in this study. Details including the setup and operations of the experimental facility, and approaches for sampling and measurements are described.

Chapter 4 addresses the first objective, which observes the change of water quality within flow cell units operated under different conditions and evaluates the prediction efficiency of major nitrification indicators. A possible direction for nitrification control is presented.

Chapter 5 addresses the second objective; it investigates the impact of operational conditions on microbial community within biofilm and bulk water.

Chapter 6 addresses the third objective; it characterizes the biofilm EPS composition and observes how disinfectant decay would be affected by EPS.

Chapter 7 highlights the contribution from this study and the conclusion. It also gives suggestion for further work.

Chapter 2 Literature Review

2.1 Introduction

A review of current literature on biofilm and nitrification within DWDS is presented in this Chapter. The overall aim is to critically review the impact of biofilms and EPS in DWDS, and the understanding on the nitrification process, effects on water quality and controlling methods. From the review, it is expected to identify the current knowledge gaps which will provide direction for the current study. The chapter begins by analysing the impact of biofilm on microbial water quality within DWDS. The key processes involved within biofilm formation and biofilm EPS matrix are then reviewed. The influence of environmental parameters, including hydraulics and disinfection on biofilm are highlighted and discussed. An overview of nitrification process in DWDS using chloramine as disinfectant is then presented. The chapter ends by summarising current review and suggesting new ideas for nitrification research.

2.2 Water quality in DWDS

Water quality deterioration during distribution brings various concerns for suppliers and customers. Within DWDS, challenges for maintaining water quality are increasing due to the fact that most of the DWDS are composed of diverse, ageing and deteriorating infrastructures (UKWIR 2003). In these less optimistic environments, water quality will be affected by several interacting chemical, physical and microbiological factors. Although the regulatory requirements always focus on the planktonic cells within water columns, the microorganisms are more commonly found in DWDS biofilm - defined as a matrix combination of microorganism that adhere to each other and/or to surfaces (Costerton et al. 1995). Compared to planktonic cells, biofilm is a relatively more concentrated carrier of cells: 10^3 to 10^5 cells ml^{-1} have been reported in water columns (Hammes et al. 2008; Vital et al. 2012), compared to 10^6 to 10^{11} cells cm^{-1} at the pipe walls (Zacheus et al. 2001). Although the units used to compare cell counts between planktonic and biofilm are different, it has been accepted

that most of the microorganisms are attached to the pipe surfaces and assembled to form biofilm. As water quality could be immediately affected by biofilm and other interactions (i.e. hydraulic condition and disinfectant), the interface between pipe wall and water is considered as the place where the occurrences of water quality problems are influenced (i.e. discoloration and corrosion).

2.2.1 Microbial drinking water quality

The primary concern about microbial drinking water quality is the possible outbreak of pathogens, and the resulting risks for human health. Although water treatment plants apply various disinfection strategies, occasional microbial water quality failure still happens even in developed countries, where water quality is commonly high. For instance, a population of around 57500 people were affected during an outbreak of *Cryptosporidium* in Yorkshire, UK in 2014 (Drinking water inspectorate, 2014). A total of 42 water-associated outbreaks were reported in USA from 2013 to 2014 and *Legionella* accounted for 57% of the events (Katharine et al. 2017). Water treatment failure is commonly attributed to large scale outbreaks, such as inadequate or interrupted treatment of water (Craun et al. 2010). However, as biofilm is a good shelter for microorganisms (Costerton et al. 1995), its existence increases the survival and growth opportunity of pathogens with low-level concentrations.

Regarding the non-pathogenic microorganisms either within or released from biofilms, water quality and DWDS operation might be affected by degrading aesthetics and reducing disinfection efficiency. According to industry reports (Customer Council for Water, 2014), the leading water quality problem related to aesthetics as given by customers is discoloration. Discoloration is associated with the mobilisation of accumulated materials from DWDS as reflected by the increasing turbidity (Vreeburg and Boxall 2007). This event often occurs with the change of hydraulic regimes (Husband et al. 2008) and the particulate accumulations within discoloured water is found to have a relationship with biomass (Gauthier et al. 1999), thereby making discoloration as a possible water safety issues. In addition, though the mechanisms of accumulations of discoloration materials have not been fully investigated, biological interactions were thought to be one of the material sources (Kirmeyer 2000).

Except influencing water quality as an entire structure, some specific microbial groups

within biofilm (i.e. nitrifying bacteria) could affect water quality through bio-chemical reactions. Nitrification is a process often observed within DWDS using chloramine as disinfectant, where nitrifying bacteria including ammonia oxidizing bacteria (AOB) and nitrite oxidizing bacteria (NOB) could utilize free ammonia as nutrient and produce nitrite/nitrate (Grady et al. 2011). This process will bring series of water quality problems and a fast decay of disinfectant residual is one of the major consequences (Cunliffe 1991; Odell et al. 1996; Sathasivan et al. 2008). A low-level disinfectant residual will result in an increased chance of pathogen outbreak, and simultaneously promote the development of biofilm which could make DWDS management to be difficult. To address this phenomenon, studies have focused on investigating the nitrifying community (Regan et al. 2002; Regan et al. 2003) and the physico-chemical factors relating to the process (Cunliffe 1991; Fleming et al. 2005, 2008). On the other hand, water utilities usually respond by increasing disinfectant residual, combined with system flushing (Seidel et al. 2005). However, the efficiency of such strategies remains limited. Details of this process are presented in Section 2.6.

Ultimately, reducing microbial water quality failures and increasing DWDS operation efficiency are of significant importance; and to do so requires further understanding of the processes and interactions involving biofilm characteristics and microorganisms within it. Consequently, research evaluating both operational effects on biofilm and microbial community at a molecular level is needed. This, could give insight into biofilm characteristics, and thereby provide feasible management suggestions for water utilities.

2.3 Biofilms within DWDS

2.3.1 The process of biofilm formation

Generally, biofilm formation process within DWDS pipeline is divided into four stages: first attachment, expansion, maturation and resistance. All the stages of biofilm development are governed and controlled by the environmental and operational conditions of the pipeline (see Fig.2.1). These stages are outlined below:

- *First attachment* -- this stage usually starts from when biological matter enters the pipeline, and the pipe surface functions as a water-solid interface for the

spontaneous adsorption and formation of a conditioning layer or film. The initial microbiological adhesion will then occur and will be encouraged predominantly by the conditioning film. This is due to its neutralisation of the surface charge, provision of increased source of nutrients and the polarisation of the forces that exist between the film and the microorganisms. Initially, the surface will consist of only a few randomly distributed cells, adhered to the surface via weak, reversible forces/bonds known as Van-der-Waals forces (Vigeant et al. 2002).

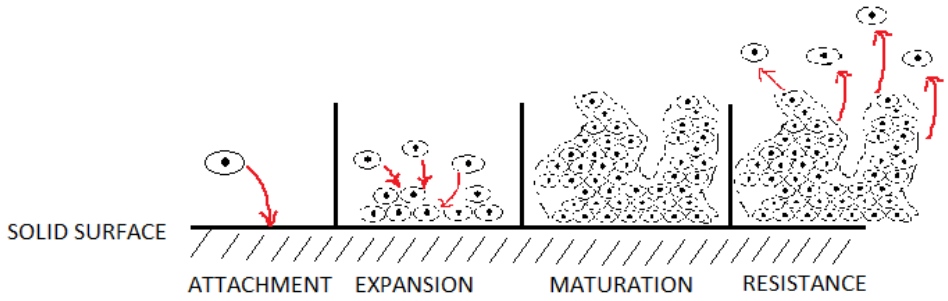

Figure 2.1 Biofilm development within DWDS

- *Expansion* -- during this stage, cell division and EPS secretion will follow first attachment, along with the formation of substantially stronger bonds, which anchor the now densely packed cells to the pipe surface (Melo and Bott 1997). Over time, further colonisation and growth can take place, resulting in an increasingly thicker and denser structure, which protrude further into the flow. This stage of development continues until a point of equilibrium is reached between the favourable and adverse growth conditions (i.e. nutrient availability, temperature, flow shear and disinfectants).
- *Maturation* -- in this stage, the biofilm structure becomes stable under an idealised condition (i.e. sufficient nutrient availability etc.) and operational conditions, and thus the flow velocity remain reasonably constant. The biofilm formed tends to reach a pseudo-steady state. Depending on the prevailing conditions this can take anywhere from 14 to 385 days (Hallam et al. 2001; Boe-Hansen et al. 2002), with the latter typically associated with low nutrient and DWDS conditions.
- *Resistance* -- this stage occurs when the circumstances become unfavourable

for biofilm growth (i.e. nutrient limited, flow velocity varies). Cells and/or cell clusters are sloughed off the surface and carried by the flow as floating biofilms, which then settle downstream when condition becomes suitable (Kjelleberg and Givskov 2007; Stewart 2012).

2.3.2 Extracellular polymeric substance (EPS) within biofilm

EPS is defined as an organic polymer which is of microbial origin in the biofilm (Characklis and KC 1990). It is responsible for binding cells and other particulate materials together, and to the surface (Flemming 2002; Flemming et al. 2007). This structure is essential to the biofilm, as it is not simply the 'glue' for biofilm, rather it endows the biofilm with particular features through its complex composition and structure (Flemming et al. 2007). Within DWDS, where flow shear and disinfectant are negative factors, EPS not only protects the component of biofilm from the surrounding environment, it also traps organic (i.e. carbon, phosphate and nitrogen) or inorganic substance (i.e. iron and manganese) for biofilm development under these oligotrophic conditions (LeChevallier et al. 1988; Srinivasan et al. 1995; Flemming et al. 2007; Bridier et al. 2011). For instance, Fish et al. (2017) compared biofilm structure and EPS composition before and after a flushing event within a drinking water pilot-scale experimental facility. It was found that although a reduction of biomass and a change of EPS composition were observed within biofilm, the biofilm could not be removed entirely (Fish et al. 2017).

In biofilm, the EPS matrix can account for 90% of the dry biomass (Flemming and Wingender 2010). Though it is still a challenge to purify EPS from other materials within biofilm matrix (i.e. cells) and to have comprehensive analysis of EPS composition (Nielsen and Jahn 1999), EPS is normally comprised of a wide variety of proteins, carbohydrates, nucleic acids, lipids and even deoxyribonucleic acid (DNA) (Goodwin and Forster 1985; Flemming et al. 2007; Flemming et al. 2010). However, the exact proportions of each component highly vary with time and space. This is because environmental conditions and the microbial community type have great effects on EPS structure and composition (Ahimou et al. 2007; Simões et al. 2007). Carbohydrate was observed to be the dominant component at higher shear stress (Ahimou et al. 2007; Fish et al. 2017) and its filamentous nature and ability to form

and fill cells supported the phenomenon (Ohashi and Harada 1994; Wloka et al. 2004a; Flemming et al. 2010). Contrary opinions were given by Houghton and Quarmby (1999), who suggested high proportion of protein would increase biofilm reliability and hence the ability to resist effects from high shear stress. This divergence might be attributed to the difference in microbial community and nutrient conditions between the studies. For example, *P. aeruginosa* and *P. putida* are microorganisms identified in water distribution systems and the EPS they produce are known as carbohydrate-based and protein-based, respectively (Hardalo and Edberg 1997; Jahn et al. 1999). It has also been documented that an increase of carbohydrate in EPS was associated with the reduced phosphate level (Hoa et al. 2003). In biofilms formed by heterogeneous microbial cultures, EPS production would be influenced by environmental factors, directly or indirectly through the change of microbial community structure (Kreft and Wimpenny 2001; Flemming et al. 2010; Fish et al. 2017). Kreft et al. (2001) found a decrease of biofilm growth with EPS production and suggested that more energy was available for EPS production when biofilm growth rate was slow.

The environmental impacts on EPS structure and composition will further affect the biofilm. Thicker and more diverse biofilm are likely to form under lower flow rates or shear stress (Rickard et al. 2004b; Wagner et al. 2009). This is because such conditions have less disturbances on biofilm growth and consequently less EPS is produced. Abe et al. (2012) found biofilms have stronger mechanical strength and resistant ability to detachment forces when they were developed under lower shear stress, potentially due to the reason that different EPS features were governed by hydraulics during development. By contrast, biofilm developed under highly varied flow condition was found to have greater detachment potential (Fish et al. 2017). This was similar to the findings from a two-dimensional model study (Picioreanu et al. 2001) which reported biofilm adhere weakly during detachment events because more energy was available for cell reproduction rather than EPS production.

In addition to the structural role on biofilm, EPS could protect the microorganisms within biofilm from disinfection and its components determine the protective mechanisms. Xue et al. (2013a) investigated the role of both carbohydrate-based and protein-based EPS on disinfection efficiency and the results show that EPS could provide protection for biofilm from different disinfectants (chlorine/monochloramine)

with different mechanisms. The EPS could either consume chlorine or limit monochlormine access to cell membrane, and thereby consequently prevent biofilm from inactivation (Xue et al. 2013a). Xue et al. (2014) did further research about the selective reactivity of monochloramine with EPS components. The polysaccharide EPS could obstruct monochloramine reactive sites on bacterial cells, while protein EPS would react with monochloramine and hence reduce the concentration of disinfectant (Xue et al. 2014). However, the EPS within these studies were extracted from biofilm developed by single bacteria strains under laboratory conditions. Therefore, it is unclear whether their components and structure can reveal the real situation, especially considering the effects of various environmental conditions on EPS features in DWDS.

2.4 Microbial community within DWDS

With the development of molecular techniques, insight into microbial community composition and diversity can be achieved. The microorganisms within DWDS are taxonomically diverse but bacteria are the one mostly studied and identified. In terms of phylum, members of *Proteobacteria* are dominant in both bulk water (Manz et al. 1993; Douterelo et al. 2013) and biofilm (Schmeisser et al. 2003; Emtiazi et al. 2004; Douterelo et al. 2013), regardless of hydraulic regimes (Douterelo et al. 2013), disinfections (Eichler et al. 2006) and pipe materials (Yu et al. 2010). However, environmental and engineering factors also do have influence on the microbial community; and its composition and structures vary within and between different networks (Revetta et al. 2010; Sun et al. 2014; Wu et al. 2015).

Difference in microbial community between biofilm and bulk water sample have been identified within systems (Martiny et al. 2005a; Douterelo et al. 2013). Due to the difficulty of obtaining in-situ biofilm samples from DWDS, a pilot-scale drinking water distribution facility was developed at The University of Sheffield, UK. From the facility, both biofilm and water samples were collected after a 28-day period and their microbial components and diversity were observed differently at both class and genus level though 454 pyrosequencing, a next generation sequencing technique (Douterelo et al. 2013). This difference was potentially due to different adherent capacity of bacteria to attach to surface and to form biofilm (Rickard et al. 2003; Rickard et al. 2004a). In freshwater ecosystems, the attachment ability of *Bate-Proteobacteria* to

surfaces was potentially stronger and they were found to be dominant within the biofilm (Manz et al. 1999; Araya et al. 2003). In addition, when considering the effects of hydraulic regimes, microbial community within biofilm developed under different hydraulic conditions potentially had different response to flushing event (Douterelo et al. 2013). For example, the abundance of *Grammaproterobacteria* formed at low varied flow condition tended to decrease after flushing, while *Pseudomnas* from biofilm incubated under steady state increased (Douterelo et al. 2013). Though no clear trend of this microbial community shifts was observed, such results emphasize the complexity and uncertainty of microbial community within DWDS.

As the surface for attaching during biofilm development, pipe materials were considered as a significant factor for determining microbial composition (Niquette et al. 2000; Waines et al. 2011). Liu et al. (2014) investigated the microbial community within biofilm formed on the surface made by PVC and cast iron respectively and identified significant difference between the biofilms. The corrosion-associated bacteria (i.e. *Acidithiobacillus* spp.) was only observed in cast iron biofilm (Liu et al. 2014), and this indicates that bacteria have different selectivity to the material they attach to. Similar conclusion was reached by Yu et al. (2010) who found that pipe materials have effects on both biofilm formation potential and microbial communities. Although the potential bacterial in biofilm differed between the pipe materials, the growth of biofilm on various materials increases the challenge of maintaining microbial water quality within DWDS.

To ensure water safety, disinfectant such as chlorine and chloramine are introduced before water enters the DWDS. However, bacteria were still identified and the microbial community showed different sensitivity to different disinfectant (Hwang et al. 2012; Mi et al. 2015). Through Illumina MiSeq sequencing, *Proteobacteria* was found to be dominant in chloraminated drinking water biofilm, while *Firmicutes* was found to be abundant in chlorinated water biofilm (Mi et al. 2015). The shifts of microbial community in drinking water were also observed to correlate with disinfectant types (Hwang et al. 2012). In chlorinated water, *Cyamobacteria, Methylobacteriaceae* and *Sphingngmonadaceae* were predominant, and *Methylophilaceae, Methylococcaceae* and *Pseudomonadaceae* were more abundant within chloraminated water (Hwang et al. 2012). In addition, *Gammaproteobacteria*,

which is a bacterial group that includes most of the opportunic pathogens (Mathieu et al. 2009), was observed to be dominant within biofilm developed in chlorinated water (Douterelo et al. 2013). The various groups of bacteria and potential pathogenic bacterial groups identified within disinfected DWDS increase the concern about drinking water safety.

Despite operational factors, microbial community within large distribution system are associated with location and season. Potgieter et al. (2018) investigated the spatial and temporal microbial community dynamics by collecting samples from drinking water distribution system that applies successive disinfection strategy. The results suggested a difference between samples collected from different location and time, also the disinfection strategy showed an effect on microbial community structure (Potgieter et al. 2018). Together with the influence identified from operational factors on microbial community in DWDSs, a comprehensive understanding of the microbial community influencing factors under various conditions (i.e. different water quality, location of systems) is important. This information could assist the operator to develop effective biofilm control strategies and hence to maintain higher water quality.

2.5 Operational effects and biofilm response

The features of DWDS vary greatly with respect to infrastructures (i.e. system materials and design), operational conditions (i.e. hydraulic conditions and disinfection) and water composition (i.e. physico-chemical and microbial components). Among these factors, only the operational conditions could be managed conveniently for controlling biofilm. In essence, biofilm development and structural characteristics (composition and physical sharp) are determined by many influences, from both external and internal. DWDS environmental factors would have complex interactive effects on biofilm, and the microorganisms within it would modify surrounding environment through the metabolic activity. As biofilms are ubiquitous and their thorough elimination is impossible, a better understanding of the interactions between biofilm and surrounding environment, in particular the operational conditions is necessary to ensure high water quality.

2.5.1 Hydraulic conditions

There is a relation between hydraulic condition and biofilm development and this is attributed to its influence on mass transfer (Beer et al. 1996; Beyenal and Lewandowski 2002; Wäsche et al. 2002) and surface accumulated material mobilization (Husband et al. 2008; Sekar et al. 2012). The hydraulic features (flow rate, turbulence and shear stress) within DWDS varied with water demand and network locations. The flow within DWDS is typically turbulent, but laminar condition or lower flow velocity is observed, especially at the dead end or areas with low water consumption. The flow turbulence influences the structure of boundary layer which is the region where biofilms are exposed to water. In laminar flow conditions, normally associated with low flow velocity, the boundary layer is relatively thicker, and theoretically the development of biofilm is easier due to the limited near wall shear forces (Stoodley et al. 1998). However, the mass transfer rate to the surface tends to be slow herein as such condition lacks sufficient mixing of materials, including microorganisms, dissolved oxygen and nutrients; thus potentially inhibiting biofilm growth. In contrast, when the flow condition is turbulent (or high flow velocity), the influx and diffusion of materials to surfaces will increase greatly with the increasing turbulent mixing. The resultant biofilm tends to be denser and more compact compared with that developed in laminar condition. However, different observations in respect of biofilm formation and mass transfer under various hydraulic conditions have raised doubts on whether material diffusion was crucial to biofilm development. For example, although biofilm density was observed to be promoted under high flow velocity, the nutrient diffusion was simultaneously inhibited (Beyenal et al. 2002). Converse result was found in an alternative experiment, in which both the penetration of nutrients and biofilm density increased with increasing flow velocity (Vieira and Melo 1999). Nonetheless, such studies still highlight the importance of taking into account the interactions between hydraulic and mass diffusion in biofilm development.

In addition to affecting mass transfer, hydraulic govern water retention time within DWDS. When the flow velocity is slow, long hydraulic retention time or water age would likely benefit biofilm growth (Eisnor and Gagnon 2003). Within older water, the concentration of disinfectant residual tends to be extremely low due to substances auto-decay and reactions with network materials (Rossman et al. 1994; Wu et al. 2005)

which results in a decrease of biocide efficiency. This then, increase the potential bacterial activity and facilitating the growth of microorganisms within biofilm. In addition, the extended resistance time increases the contact time between cells and materials, and hence other biofilm related water quality problems, such as discoloration, nitrification, corrosion and disinfectant by products formation, would become severe (AWWA 2002).

In addition to the effects on biofilm composition, structure and density, hydraulic was suggested to impact the mechanical properties of biofilm, especially the cohesive strength, which is related to biofilm detachment (Beyenal et al. 2002; Purevdorj et al. 2002; Ochoa et al. 2007; Böl et al. 2009; Paul et al. 2012). Biofilm thickness and biomass have been observed to decrease with increasing turbulent flows (high shear stress and up to 13 Pa), while a reverse trend was found for biofilm density (Paul et al. 2012). When biofilm is exposed to various shear stresses, Paul et al. (2012) found that the cohesive strength was stronger within biofilm developed under turbulent flow but the strength was not consistent. This was attributed to both detachment and compression force from the increasing shear stress. By contrast, Abe et al. (2012) found that more force was required to remove biofilm formed under lower shear stress (0.12 Pa) than higher shear stress (0.23 Pa) conditioned biofilm. It should be noted that, compared with the average shear stress in real DWDS (i.e. ~0.3 Pa), the conditioning shear force in this study was relative low. Moreover, the force reported to detach the biofilm was extremely higher than typical flows (~ 10 Pa). In addition, both Abe et al. (2012) and Lehtola et al. (2006) reported a relationship between the force required to remove biofilm with biomass, but converse trends were suggested. The contrasting observations were potentially due to the use of different reactors and operational conditions. Furthermore, the uncertainty of biofilm behaviour under experimental condition makes it more difficult to evaluate how they will be affected by hydraulics within real DWDS.

Biofilm will detach from the surface when the shear stress increases and overcome the biofilm internal cohesive strength (Paul et al. 2012). Simultaneously, the concentration of planktonic cells, turbidity and materials related to discoloration (i.e. iron and magnesium) will increase in water columns (Lehtola et al. 2006; Sekar et al. 2012). The positive correlation between planktonic cells and flow rates (Sekar et al. 2012)

supports the occurrence of biofilm mobilization by external forces which could result in a decrease of water quality. However, the typical shear force within DWDS could not remove all biofilm materials. Moreover, biofilm cohesive strength seemed to increase after exposure to detaching shear force (Paul et al. 2012), possibly due to the hypothesis that the biofilm layer remaining after detachment would be further compressed by external shear stress and consequently their resistance to high external forces increased (Paul et al. 2012). In addition to explaining the persistent physical structure of biofilm during detachment events, Liu and Tay (2001) provided an insight into biofilm metabolic response to changing shear stress. Biofilm was hypothesised to regulate their metabolic pathway by utilizing more energy for anabolism than for catabolism when shear stress increased, and this in turn resulted in a denser biofilm (Liu et al. 2001). In addition, considering the adhesive property of biofilm EPS, this matrix might provide mechanical support for biofilm to overcome the detachment forces (Neu and Lawrence 2009). Although the theory has yet to be fully understood, previous studies observed that EPS components (polysaccharide and protein) had different responses to hydraulic conditions (Simoes et al. 2003; Simões et al. 2007). Simoes et al. (2003) investigated the stability of *Pseudomonas fluorescens* biofilm in low and turbulent flow, and observed a positive correlation between protein and shear stress while polysaccharide was negatively correlated. Another study demonstrated that *B. cereus* biofilm produced less EPS, but more resistance to shear stress than *P. fluorescens* biofilm (Simões et al. 2007). However, these studies used a single bacterial strain, which cannot reveal the complex composition within biofilm developed within operational DWDS, and hence no clear conclusion could be made regarding the relationship between EPS and biofilm stability. Nonetheless, the EPS and/or cells within biofilm were possibly conditioned by shear stress and show different resistance ability to further detachment forces. Further research is required to explore mixed culture biofilms and their EPS response to various hydraulic conditions.

2.5.2 Disinfection

To meet growing water demands and maintain biological stability in water distribution systems, disinfection is an important procedure which is applied in water treatment plants. Chlorination and chloramination are two kinds of primary methods used to disinfect water and are largely justified by their effectiveness in inactivating pathogens,

ease of use and reasonable cost. Commonly, disinfectants, such as chlorine or chloramine are applied to inactivate microorganisms at treatment works and to inhibit microbial growth during distribution by relying on the disinfectant residuals. The hydrodynamics, microbial concentration and water chemistry will determine disinfection efficiency (Beyenal et al. 2002). After exposure to disinfectant residuals, biofilm activity was supposed to decrease (Hallam et al. 2001). Hallam et al. (2001) observed two orders of magnitude reduction in biofilm activity (measured as pg adenosine triphosphate (ATP) per cm^2) after chlorination. However, chemical disinfectants can injure or damage microbial cells to some degree, but cannot prevent the formation of biofilm (Chandy and Angles 2001; Williams and Braun-Howland 2003). The penetration of chlorine into biofilm was suggested to be difficult (LeChevallier et al. 1988; Beer et al. 1994) and biofilms rich in EPS would increase chlorine demand (Power and Nagy 1989). The increasing chlorine demand results in an increase in application of chlorine and subsequently, the risks of DBPs formation increases.

As an unintentional consequence of chemical disinfection, DBPs are formed by the reaction between organic/inorganic matter and disinfectants (Doederer et al. 2014). DBPs in drinking water have been associated with possible public health risks (Richardson et al. 2007; Sedlak and von Gunten 2011) through routes of ingestion, inhalation and dermal adsorption. Several epidemiological studies have found association between consumption of chlorinated drinking water and increased risk of certain health outcomes, particularly bladder cancer (Nieuwenhuijsen et al. 2009). Compared with chlorine, chloramine was suggested to be more effective and safer as it is less reactive and produces less DBPs (Neden et al. 1992; Norton and LeChevallier 1997). However, other non-regulated DBPs have been detected after chloraminaton, especially nitrogenous DBPs (N-DBPs) which are very toxic and present great risk to public health. Previous DBP research has focused on the study of how water physico-chemical parameters and compositions affect their formation during the production of drinking water (Hua et al. 2006; Lyon et al. 2012). It has been noted that biofilm EPS is expected to pose a greater risk to DBP formation than natural organic matters (NOM) in water, due to their higher contribution to toxic N-DBP formation (Lee et al. 2007; Richardson et al. 2007; Plewa et al. 2008). Moreover, studies suggested a relationship

between EPS components and the type of DBPs (Wang et al. 2012a; Wang et al. 2013). Wang et al. (2012a) observed a greater amount of N-DBP yield from the reaction between chlorine and *P. putida* EPS, which is protein based, than polysaccharide based EPS extracted from *P. aeruginosa* biofilm. Considering that single strain biofilm was investigated in these studies rather than mixed culture biofilm, further research is required to investigate the disinfection and EPS interactions within DWDS.

Regardless of working as biocide agents, chloramine may serve as a nutrient supplier for some autotrophs within DWDS biofilms. Within chloraminated DWDS, nitrifiers were detected within biofilm and water samples (Regan et al. 2002; Regan et al. 2003). This bacterial groups could utilize the free ammonia introduced from the decay of chloramine and produce nitrite/nitrate (Grady et al. 2011). This phenomenon can further reduce water quality by accelerating chloramine decay and consequently promote the growth of heterotrophs. In addition, although chloramine was suggested to be more efficient due to its greater penetration ability into biofilm than chlorine (LeChevallier et al. 1988), Gagnon et al. (2004) found that chloramine was the least efficient disinfectant in a bacterial inactivation experiment. As previously discussed in Section 2.4, disinfectant types have been observed to affect microbial community, and hence the difference in biofilm structure between studies might potentially contribute to the uncertainty of disinfectant efficiency. Therefore, further disinfectant research needs to consider the microbial diversity and community which are interacting with the disinfectants.

It was suggested that biofilms, including the planktonic cells in water columns have different metabolic responses to the presence of disinfectant (Gagnon et al. 2004). For instance, biofilm has been observed to have higher growth rate, but to be less dense after exposure to chlorine, indicating that there might be a protective mechanism for bacteria in the presence of disinfectant (Butterfield et al. 2002). Furthermore, compared with planktonic cells, the resistance ability of biofilm to disinfection tends to be stronger (Bridier et al. 2011; Hageskal et al. 2012) and hence leading to greater threats to water quality. Several possible mechanisms of biofilm resistance to biocides have been proposed in previous studies (Tuomanen et al. 1986; Bridier et al. 2011). Except the possible protection contributed from biofilm EPS (Xue et al. 2013a), bacterial cultures within biofilm tend to reduce their growth rate to withstand antimicrobial

agents (Mah and O'Toole 2001). In addition, bacteria might reduce the permeability of their cell membrane by altering the membrane-protein compositions, thereby protecting cells from disinfectants (Mah et al. 2001). Currently, no mechanism has been proved to be the main cause for the high resistance ability of biofilm to biocide agents. These mechanisms might work together or be induced based on the type of disinfectants and biofilm community. An overall consideration of interactions involving biofilm, biofilm EPS and disinfection in further research might provide insight into biofilm resistance behaviour over antimicrobial agents.

2.6 Nitrification process

As has been described above, chloramine is more persistent in water than chlorine and it is widely used as chemical disinfectant within DWDS (Norton et al. 1997). However, its disinfection efficiency has been observed to be highly affected by microbial composition in both biofilm and bulk water. Nitrification process, which is a bio-chemical process induced by the occurrence of nitrifiers and free ammonia, has considerable influence on the inactivation efficiency of chloramine and subsequently affects drinking water quality.

The implementation of chloramination as a disinfection strategy has resulted in increased levels of free ammonia within the distribution system, which serves as an energy source for indigenous autotrophic ammonia oxidizing bacteria (AOB) (Pintar et al. 2003). Growth of these microorganisms mediates the process of nitrification, resulting in production of nitrite, episodic loss of disinfectant residual and increased biofilm accumulation, thus escalating the possibility of regrowth events in the distribution system (Kirmeyer et al. 1995). The following two equations described the two-step microbiological process referring to nitrification in DWDS (Grady et al. 2011):

$$NH_4^+ + 1.38O_2 + 0.172HCO_3^- + 0.069CO_2 \rightarrow 0.0172C_5H_7O_2N + 0.983NO_2^- + 0.966H_2O + 1.97H^+ \quad \text{Equation 2.1}$$

$$NO_2^- + 0.00875NH_4^+ + 0.035H_2CO_3 + 0.00875HCO_3^- + 0.456O_2 + 0.00875H_2O \rightarrow 0.00875C_5H_7O_2N + 1.0NO_3^- \quad \text{Equation 2.2}$$

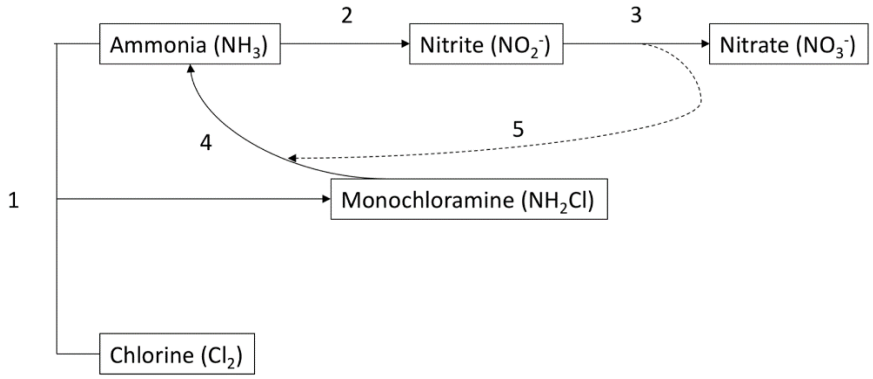

Figure 2.2 Key bio-chemical processes related to nitrification within chloraminated DWDS; 1. Formation of monochloramine; 2. Ammonia oxidation by AOB/AOA; 3. Nitrite oxidation by NOB; 4. Monochloramine decomposition; 5. Nitrite oxidation reaction with monochloramine. (Vikesland et al. 2001; Yang et al. 2008)

As shown in Eq.2.1, ammonia is oxidized to nitrite and the overall acid producing reaction yields 2 molecules of H^+ for every mole of ammonia-N conversion. This is the first step of nitrification, which is mediated by nitrifying bacteria, including the *Bacteria* (ammonic-oxidizing bacteria, AOB) and *Archaea* (ammonia-oxidizing archaea, AOA) groups. Subsequently, nitrite produced at this step can be further utilized by nitrite-oxidizing bacteria (NOB) and converted to nitrate (Eq.2.2). Moreover, within chloraminated DWDS, nitrite can be chemically oxidized by chloramine and hence to introduce more free ammonia to water (Yang et al. 2008). This reaction, together with the products of nitrification, will promote ammonia oxidation and accelerate chloramine decay through a self-reinforcing feedback loop. Fig.2.2 illustrates the key processes of this loop. In such conditions, some free ammonia is in the water after leaving the treatment plants and its concentration will increase via monochloramine auto decomposition (step 4) and oxidative reaction involving NH_2Cl, nitrite and other organic matters (step 5). Simultaneously, AOB/AOA converts free ammonia to nitrite (step 2), which is further oxidized to nitrate by NOB (step 3). In addition to these processes, Zhang et al. (2008) suggested that nitrate can be recycled to ammonia through reactions with corrosion products.

Owing to the development of molecular analytical techniques, nitrifying bacteria have been identified and classified. Most AOB relevant to fresh water have been suggested to be members of the *Nitrosospira* and *Nitrosomonas* groups (Moel et al. 2007). Via culture independent technique, Regan et al. (2003) detected both of these two AOB

types within a chloraminated drinking water system, with *Nitrosomonas* observed to be predominant and *Nitrosospira* found with small proportion. Within the same study, *Nitrosomonas oligotropha* was observed to be the most abundant AOB cluster (Regan et al. 2002; Regan et al. 2003). This is, potentially attributed to their high affinity with ammonia and hence to outcompete other clusters in such an oligotrophic environment (Stehr et al. 1995). NOB are mostly represented by members of *Nitrobacter* and *Nitrospira* (Moel et al. 2007). However, some studies only detected *Nitrospira* NOB in drinking water related systems (Regan et al. 2003; De Vet et al. 2009). Previous studies have suggested that the abundance of nitrifying bacteria groups relates with their substrate-utilizing ability (Blackburne et al. 2007). Considering the low availability of ammonia in DWDS, AOB/NOB presented are characterized with high affinity for substrates (ammonia and nitrite), thereby increasing their survival opportunity (Bollmann et al. 2002a; Bollmann and Laanbroek 2002b).

2.6.1 Factors affecting nitrification within DWDS

Researches have indicated that the occurrence of nitrification in drinking water systems is influenced by many factors relevant to the growth of nitrifying bacteria, such as free ammonia concentration, dissolved oxygen, temperature, light, pH and alkalinity (Wolfe and Lieu 2001; Zhang et al. 2009c). Several other factors relating to nitrification were identified, which include nutrients, pipe materials and house hold treatment methods (Fleming et al. 2005, 2008; Zhang et al. 2009b). Herein, several key factors affecting the occurrence and kinetics of nitrification within chloraminated DWDS are reviewed.

2.6.1.1 Presence of ammonia

Rather than utilizing organic compounds, the growth of autotrophic bacteria relies on converting inorganic substances to organic nourishments. In the case of nitrifying bacteria, ammonia and nitrite are the only external energy source. From Eqs.2.1 and 2.2, the first step of nitrification is induced by the presence of ammonia. Within DWDS, free ammonia could be released from the decomposition of monochloramine and their level has been suggested to have relationship with the initial dosing ratio of chlorine to ammonia used to form chloramine (Fleming et al. 2005, 2008). Traditionally, utilities use 3:1 chlorine to ammonia dosing ratio, to optimize monochloramine formation, unpleasant tastes and odours, and dichloramines (Letterman and AWWA 1999).

However, nitrification tends to be encouraged at this relative low ratio (<4:1) since excess ammonia was introduced (Skadsen 1993).

Although there is no doubt on the importance of ammonia on nitrification, whether the tendency of occurrence of nitrification is correlated with ammonia concentration remains uncertain. In a full-scale chloraminated system, the overdose of ammonia was potentially linked with the increase of nitrification episodes (Skadsen 1993). Lipponen et al. (2002) reported a high correlation (Spearman correlation coefficient = 0.74) between ammonia concentration and AOB abundance through analysing water samples from a finished DWDS. By contrast, Odell et al. (1996) and Zhang et al. (2010) suggested that the ammonia concentration had no significant influence on nitrification and the initial availability of ammonia (determined by chlorine to ammonia ratio) did not affect nitrification.

2.6.1.2 pH

Studies have observed the occurrence of nitrification over a wide range of pH, from 4.6 (Wolfe et al. 2001) to 11.2 (Prakasam and Loehr 1972). The optimal pH for nitrification is between 7 and 8 (Odell et al. 1996; Villaverde et al. 1997; Wolfe et al. 2001). Considering the typical pH value (weakly alkaline or neutral) within DWDS, the growth of nitrifying bacteria could be favoured within such environment.

pH is an essential factor for both chemical and biological reactions and its effects seem to be complex. Commonly, pH affects nitrification in DWDS by influencing the decay of chloramine and the level of free ammonia concentration (Zhang et al. 2009c). Lower pH tended to promote auto-decomposition of monochloramine (Vikesland et al. 2001), while the occurrence of free ammonia is inhibited when pH is less than 6 (Stein and Arp 1998). In addition, pH has effects on the growth of nitrifying bacteria by impacting the inactivation rate of monochloramine. With the increase of pH from 7 to 9, the Chick-Watson disinfection rate for a specie of AOB decreased (Oldenburg et al. 2002). In terms of controlling nitrification, these mechanisms may act in opposition to each other. Studies have investigated whether nitrification could be inhibited by altering aqueous pH (Skadsen 2002; Fleming et al. 2008). Skadsen (2002) observed that there was lower tendency for nitrification by setting pH above 9.3. Based on the nitrification potential curve model, Fleming et al. (2008) proposed that raising the pH in DWDS

may be feasible to reduce the risks of nitrification. This potential control strategy was argued by Oldenburg et al. (2002), who suggested that although chloramine auto-decomposition and nitrifying bacteria grow rate could be less under a pH of 8.5, the inactivation rate of chloramine decreased as well. Considering the differences in operational conditions and experimental infrastructures between the studies, no clear conclusion can be made and further research is required.

2.6.1.3 Temperature

As a microbial process, temperature could affect nitrification by influencing nitrifying bacteria activities. Bio-reactions involving enzyme and substance diffusion rates to cell will be impacted by the change of temperature (Grady et al. 2011). Although nitrifiers are observed under a wide range of temperature (i.e. 4~45°C) (Zhang et al. 2009c), the optimal temperature for nitrifiers in drinking water systems is narrow and reported to be 25~30°C (Odell et al. 1996; Wolfe et al. 2001). Compared with lower temperature, higher temperature could increase both the substance consumption and microbial growth rates (Groeneweg et al. 1994). Wilczak et al. (1996) reported a higher extent of nitrification during summer based on surveys undertaken in DWDSs. Wolfe et al. (1990) found no nitrifiers when the temperature was less than 18°C. However, in a bench-scale experiment conducted by Pintar et al. (2003), AOB was observed under both 22°C and less optimal temperature (12°C). Furthermore, when the temperature decreased to 6°C, the activity of the established nitrifying biofilm was not affected (Pintar et al. 2003). This observation is of importance to water utilities and it indicates that in addition to challenging the water quality during warmer seasons, nitrification is an issue that should be focused on all the time.

2.6.1.4 Disinfectant residual

To limit microbial growth, the disinfectant residual is required to be maintained at a reasonable level, normally no less than 1 mg/L at the end of the distribution system (Wilczak et al. 1996). In terms of controlling nitrification, Odell et al. (1996) found that AOB regrowth potential was much less at higher chloramine dose: AOB was observed to regrow within 26% and 77% of total samples when the residual was respectively 2.5 mg/L and 1.7 mg/L. However, since monochloramine is formed via the combination of chlorine (biocide for nitrifiers) and ammonia (energy source for nitrifiers), the

inactivation rate on nitrifying bacteria of chloramine could be affected by these two adverse effects (Edwards et al. 2005; Fleming et al. 2008).

Fleming et al. (2005) and Fleming et al. (2008) have explicitly addressed the dependency of chlorine disinfectants and free ammonia substrates in their work. A nitrification potential curve is proposed based on Eq. 2.3 (Fleming et al. 2005, 2008):

$$[\text{Total chlorine}] = \frac{R_{gi}[\text{free ammonia}]}{K_s + [\text{free ammonia}]} \qquad \text{Equation 2.3}$$

Where [Total chlorine] = the sum of free chlorine, monochloramine and dichloramine concentration, mg/L-Cl_2

R_{gi}: the minimum total chlorine concentrations needed to prevent nitrification for any free ammonia concentration, mg/L-Cl_2

K_s: half saturation constant for ammonia oxidizing bacteria, mg/L-N

[Free ammonia]: the sum of ammonia (NH_3) and ammonium (NH_4^+) concentrations, mg/L-N

In essence, this equation illustrates that if the death rate of nitrifying bacteria via disinfection exceeds the growth rate from ammonia consumption, then nitrification becomes difficult to be established. Conversely, if the nitrifier growth rate exceeds the death rate, then serious nitrification problems can occur even under continuous flow conditions present in water distribution systems (Fleming et al. 2005, 2008). Fig.2.3 shows the outputs from the simulation of above model using data from a Bango (Marine) water district distribution system (Fleming 2008). Based on the curve, the authors suggested that chlorine concentration of 1.6 mg/L was a threshold value to control nitrification (Fleming et al. 2005, 2008), which meant that nitrification would be prevented when the chloramine concentration in the system was above the value without considering the concentration of ammonia, whilst below the value the chlorine to ammonia dose ratio would affect the occurrence of nitrification (Fleming et al. 2005, 2008).

In general, nitrification can be prevented by a relatively high chloramine dose and most of the nitrification events were relevant to low chloraminated treatment (Skadsen 1993; Odell et al. 1996; Wilczak et al. 1996). Nevertheless, nitrification has been observed in systems with high chloramine concentration. For instance, Cunliffe (1991) observed nitrifying bacteria within a quarter of the total water samples with chloramine dose greater than 5 mg/L. This phenomenon might be attributed to the fact that nitrification has occurred before applying high chloramine dose to the water reservoir that was

studied. The decay of monochloramine would be accelerated by the produced nitrite and hence the disinfection residual would not be sufficient enough to limit the growth of nitrifying bacteria. On the other hand, nitrifiers within DWDS could be protected by biofilm structure and heterotrophic bacteria. To better understand disinfectant effects on nitrification, research about the interactions between nitrifiers and other heterotrophic bacterial groups is required.

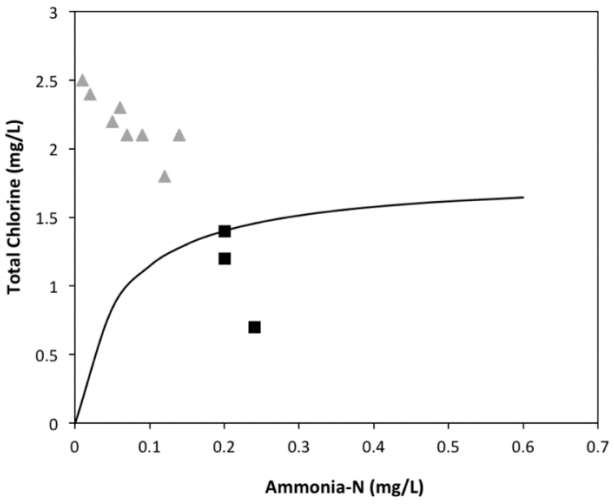

Figure 2.3 Constructed nitrification potential curve from the model of Fleming et al. (2005) by using data from a Bango (Marine) water district distribution system (Fleming et al. 2008). Curve coefficients are R_{gi}=1.8 and K_s=0.057; The triangle represents distribution system observed with no nitrification while the square is for sites undergoing nitrification.

2.6.1.5 Organic carbon and HPC

Although nitrifiers are autotrophic bacteria, the availability of organic carbon can promote their growth to some extent. With the presence of pyruvate, yeast extract and peptone, Watson et al. (1989) observed the growth rate of *Nitrospira marina* was faster than that in condition with only inorganic source. Within DWDS, where the concentration of organic carbon is limited and natural organic matters (NOM) dominates the total organic carbon (TOC), NOM was expected to impact on nitrification by increasing chloramine demand and hence accelerating the decay of chloramine (Zhang et al. 2010). Consequently, the growth of nitrifying bacteria could be stimulated indirectly.

Rather than having a positive effect on nitrification, some studies suggested that increasing TOC level resulted in competition between heterotrophic bacteria and nitrifiers (Verhagen and Laanbroek 1991). Since nitrifiers have to transfer inorganic

carbon to organics via energy-cost reactions, when sufficient organic carbon is available, their competitiveness is weaker than heterotrophs, which can immediately take advantage of exoteric organic substances (Rittmann and Manem 1992). In addition, heterotrophs seem to have better affinity with nutrients than nitrifiers (Rosswall 1982; Grady et al. 2011). Based on this theory, Verhagen et al. (1991) illustrated that there was a critical carbon to nitrogen (C/N) ratio to determine the growth of nitrifiers. Above this ratio, heterotrophs would outcompete nitrifiers for ammonia, while heterotrophs become carbon-limited and nitrifiers could utilize excess ammonia when C/N falls below the ratio (Verhagen et al. 1991).

In addition to the competition for nutrients, nitrifiers and heterotrophs in water distribution system can benefit from each under some conditions. These synergistic effects between the two bacterial groups are magnified within biofilm from DWDS experiencing nitrification. Due to low growth rate, nitrifiers have weak resistance to shear force. By benefiting from the EPS produced by heterotrophs, nitrifiers can aggregate into biofilm and further be protected by outer heterotrophic bacteria from detachment (Verhagen et al. 1991). Moreover, organics that are toxic to nitrifiers can be degraded by some heterotrophic bacteria (Pan and Umbreit 1972), while nitrifies can be stimulated by the metabolic products excreted from heterotrophs (Hockenbury et al. 1977). Meanwhile, heterotrophic bacteria can use the soluble microbial products (SMP) produced by nitrifiers for growth and enhance their stability within oligotrophic environment (Rittmann et al. 1994). In conditions with low C/N ratio (~1), studies have found that nitrifiers fixed the inorganic carbon to SMP, which accounted for 40% of the organic carbon that the heterotrophs utilized (Furumai and Rittmann 1992; Rittmann et al. 1994).

2.6.1.6 Cell attachments

Within DWDS, nitrifiers can survive as free living cells or aggregate to the surface to form biofilm. Compared with free cells, nitrifier within biofilm tends to have better stability and disinfection resistance ability (Furumai et al. 1994). The nature of biofilm makes it to be a good material reservoir (Volk et al. 1999) and hence nitrifiers accumulated within biofilm seem to be more resistant to nutrient-limited environment. In addition, Tarre et al. (2004) observed nitrification under less optimal pH ranges,

which was potentially due to the support from biofilm and its aggregates. The evidence of detecting nitrifiers within DWDS biofilm (Wilczak et al. 1996) supported the idea that biofilm can provide growth advantage for nitrifying bacteria, and help them to be persistent in such a turbulent and oligotrophic environment.

The preference of nitrifiers to attach to solid surface increases the difficulty of controlling nitrification within DWDS, since these systems are always have stagnant water or excessive water age which favour biofilm formation (Cunliffe 1991; Skadsen 1993). Consequently, to limit the growth of nitrifiers and to suggest effective nitrification control strategies to utilities, research about nitrification needs to take into consideration the effects from biofilm and its characteristics (structure, diversity and composition).

2.6.2 Nitrification monitoring and impacts within DWDS

Based on the features of nitrification, utilities normally monitor nitrification via the detection of relevant microorganisms or measurements of the change of nitrification indicator. Most probable number (MPN) is an approach that can enumerate nitrifiers by culturing AOB/NOB with selective media and it is widely used for nitrification quantification (Zhang et al. 2008; Zhang et al. 2009b). However, it will take at least three weeks for incubation and hence the data provided cannot reveal the current water quality. Compared with molecular techniques, this method is time consuming and less efficient. In the past few years, culture independent techniques have been developed, which can use nucleic acids to acquire genetic information from various kind of samples. (Regan et al. 2002; Regan et al. 2003) used terminal restriction fragment length polymorphism (T-RFLP) analysis and 16S rRNA cloning and sequencing to characterize the community of nitrifying bacteria within a pilot-scale chloraminated distribution system. By targeting gene that are specific for AOB/NOB (i.e. *amoA* for AOB/AOA), nitrifiers can be identified and quantified. Limpiyakorn et al. (2011) observed a relationship between ammonium concentration and the abundance of AOA *amoA* genes via quantitative real-time PCR (q-PCR) technique. Such approaches have been widely applied in researches and information they provide can help to gain insight into the interactions of environmental factors, heterotrophs and nitrifiers. Combined with analysing and quantifying other microbial communities by q-PCR, Krishna et al.

(2013) investigated how nitrifying bacterial community changed with chloramine residual and nitrification metabolites (nitrite concentration). However, for drinking water utilities which require timely detection of water quality risks, molecular techniques are still less convenient and slower than directly monitoring nitrification indictors.

From Eqs.2.1 and 2.2, nitrification process brings an increase of nitrite/nitrate concentration and a decrease of ammonia-nitrogen. Since the nitrite is usually below detection levels within DWDS, its increase is considered as a good indicator of nitrification. Kirmeyer et al. (2004) proposed a critical threshold for nitrification, with a concentration of 0.05 nitrite-N mg/L. However, Sathasivan et al. (2008) suggested that this value was too high to predict severe nitrification. Ongoing growth of microorganisms, including nitrifiers occurred in mildly nitrifying system (nitrite-N <0.001 mg/L) and severe nitrification was then observed associated with a drop of chloramine residual (below 0.4mg/L) (Sathasivan et al. 2008). This was supported by Cunliffe (1991) who proposed to predict nitrification by considering the change of both disinfectant residual and nitrite. Within microbial stable and well-operated DWDS, the variability of disinfectant residual is relatively limited. Once nitrification occurs, the decay of monochloramine is accelerated by the consumption of ammonia, oxidizing reactions with produced nitrite and increased chloramine demand caused by increasing microorganisms and organic matters (Vikesland et al. 2001; Yang et al. 2008). Therefore, an unusual decline of disinfectant residual could be an early warning sign for nitrification.

Although nitrification can contribute to a change of free ammonia concentration, this parameter is not sensitive to predicting nitrification. In pilot-scale experiments, Liu et al. (2005) observed ammonia increased firstly, then decreased in correspondence to severe nitrification. Similar observation was found from the simulation results of nitrification model developed by Yang et al. (2007) and Yang et al. (2008). This model is based on the mass balance of both chemicals and microorganisms related to nitrification (Yang et al. 2007). Fig.2.4 shows an example of the outputs from this model (Yang et al. 2008). From this figure, it could be noticed that during a nitrification event, a quick decline of chloramine was observed before the increase of nitrite, while ammonia increased and remained stable before any visible rise of nitrite (Yang et al.

2008). According to these references, it is difficult to evaluate whether nitrification is ongoing by monitoring ammonia due to its concentration either increasing or decreasing during a nitrification event. Nevertheless, it is still necessary to consider the change of ammonia since its obvious increase might suggest a fast decline of chloramine and nitrification can be induced by sufficient ammonia (Verhagen et al. 1991).

Another consequence on water quality brought by nitrification is the potential increase of heterotrophic plate counts (HPC). Associated with the decrease of chloramine residual caused by nitrification, the growth of heterotrophs is stimulated. Wilczak et al. (1996) and Skadsen (1993) reported high HPC accompanying nitrification in surveys of water utilities and a positive correlation between HPC and nitrite in DWDS. Conversely, Pintar et al. (2003) did not find any correlation between HPC and nitrification in a full-scale distribution system. Although HPC was suggested to be an indicator of nitrification (Odell et al. 1996), it is better to apply this in combination with other predictors (i.e. disinfectant residual and nitrite) since the level of HPC could be affected by other factors.

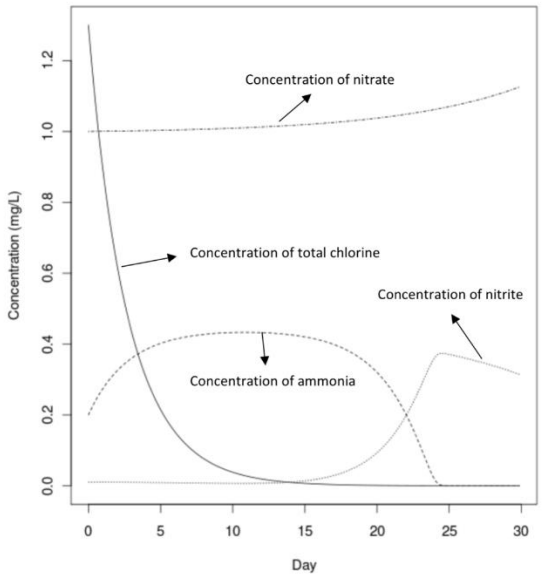

Figure 2.4 Outputs of nitrification risks model developed by Yang et al. (2008).

It has been noted that severe nitrification will result in low concentration of disinfectant residual (close to 0), and hence the risks of water quality increasing. Therefore, it is essential to provide early warning of nitrification for utilities. However, ongoing nitrification cannot be easily detected when it is not severe. Considering the

contribution of nitrification to increasing chloramine demand, Sathasivan et al. (2005) developed an approach to predict nitrification potential. This method hypothesised that chemical and microbial demands on chloramine determine the total chloramine decay rate (Sathasivan et al. 2005). The nitrification potential can then be predicted by calculating the ratio of microbial chloramine decay rate to total decay rate (defined as Fm ratio). The detailed process of this approach is presented in Section 3.6.2. Based on this method, a difference of 0.8 in Fm ratio was observed between water samples with nitrite concentration of 0.001 and 0.003 mg/L; this suggests that this method might be more sensitive to nitrification than traditional indicators (nitrite) (Sathasivan et al. 2005). This method was further proposed to work well in mildly nitrification systems (Sathasivan et al. 2008), wherein nitrifiers account for the main microbiologically associated disinfectant decay. The author thus suggested that with this approach, utilities can take actions before nitrification becomes severe.

As water quality would be difficult to maintain when nitrification is severe, a sensitive and quick nitrification detecting method is required urgently. Recently, a new chloramine decay index (C.D.I) was developed via using multiple wavelength Ultraviolet (UV) (Moradi et al. 2017). This index was defined as a beneath area that between two specific wavelength for detecting high performance size exclusion chromatography (HPSEC) (Moradi et al. 2017). Based on this index, nitrification was suggested when the index value was greater than that of water experiencing no nitrification.

2.6.3 Nitrification control methods within DWDS

To avoid or limit nitrification within DWDS, it is essential for utilities to keep sufficient monitor of nitrification related parameters and to initiate timely control methods before threats to water quality due to severe nitrification (Skadsen et al. 2006). Depending on the specific conditions within DWDS, different control methods can be applied and their effectiveness varies. The control strategies typically used are basically aimed at limiting the growth of microorganisms or damaging their shelter (biofilm) via either chemical (i.e. increasing chloramine dose and breakpoint chlornation) or physical (flushing) methods.

Increasing chloramine dose or optimizing chlorine to ammonia ratio are effective when

there is no severe nitrification (Lieu et al. 1993; Seidel et al. 2005). Harms and Owen (2004) suggested nitrification could be prevented by increasing chloramine concentration to a range between 2 and 4 mg/L. Once nitrification occurred, studies observed increasing chloramine failed to inhibit the process, even with concentration as high as 8 mg/L (Skadsen 1993). Moreover, high chloramine dose can bring more total ammonia to the system and the excess ammonia due to the decay of monochloramine might lead to increased risks of nitrification. Increasing chlorine to ammonia ratio can reduce the availability of free ammonia within water and hence limit the growth nutrients of nitrifiers. When setting the ratio as 5:1, no free ammonia exists (Kirmeyer et al. 1995). Wolfe et al. (1988) proposed that this method worked effectively to prevent nitrification in a water reservoir. By contrast, Wilczak et al. (1996) found no significant correlation between the ratio and nitrification events based on a survey of 438 utilities. The uncertainty of this method might be attributed to the difference in affinity to nutrients (i.e. ammonia) of nitrifying bacteria strains between different systems. Odell et al. (1996) reported observing nitrification in water systems with a very low level of ammonia, and this was suggested to be potentially due to the occurrence of nitrifying bacteria that have high affinity to ammonia.

As another chemical control strategy, breakpoint chlorination is adapted periodically by utilities (Seidel et al. 2005). Without bringing excess ammonia, chlorine can inactivate systems and inhibit the growth of nitrifiers once nitrification is underway (Odell et al. 1996). However, the increasing chlorine level may result in the formation of toxic DBPs (i.e. N-DBP - nitrogenous disinfectant by products) (Muellner et al. 2007). Schreiber and Mitch (2007) found a significant increase in formation of nitrosamine after chlorination.

Once nitrification is underway, efforts required to eliminate it tend to be more since nitrifiers potentially have great resistance ability to disinfectants. Combined with optimizing disinfection strategy, utilities flush the system to remove attached materials (biofilm and aggregates) to increase disinfection efficiency (Seidel et al. 2005; Skadsen et al. 2006). This joint method works temporarily and can only last for a short period with disinfectant residual back to a low level in two days (Skadsen 1993). In addition, material mobilized from surfaces and the increasing disinfectant dose will affect the colour, taste and odour of the water (Skadsen 1993; Husband et al. 2008). To optimize

the method, research is required to investigate the effective velocity/shear stress to remove biofilms containing nitrifiers.

2.7 Summary and Identification of Knowledge Gap

In this chapter, the current understanding of biofilms and nitrification within DWDS are reviewed. Several gaps in knowledge were identified based on current review and they are summarized below:

- According to previous studies, environmental parameters have interactive effects with biofilm, including its structure, composition and community. Although no clear conclusion or mechanism have been identified, it has been highlighted that hydraulic affect and govern biofilm characteristics via affecting material exchange and detachment forces. However, since previous studies were conducted within either real systems or laboratory facilities with different operational conditions, microbial community varied and potentially resulted in different conclusions between the studies. Further research is required to have a comprehensive investigation of biofilm responses to environmental factors, especially the relationship between microbial community and operational conditions. Such study is expected to provide effective biofilm management strategies, and this will help to sustain the water quality.
- To limit the development of biofilm, the properties of biofilm EPS matrix influencing biofilm stability and enhancing disinfection resistant ability have been studied. However, few of these studies investigated EPS responses to environmental parameters by using mixed culture biofilm and therefore, could not reveal the real condition in DWDS. Further research needs to consider the ecological complexity of biofilm and bridge the gap between laboratory and field.
- Nitrification, which is a microbial water quality issue was reviewed with respect to its mechanism, affecting factors, predictors and corresponding control strategies process within chloraminated DWDS. In addition, although the issue of nitrification was reasonably described 70 years ago (Hulbert 1933; Feben 1935; Larson 1939), studies have focused predominantly on limiting nitrification by inhibiting nitrifiers activity, while few studies related their

behaviour and response to operational parameters (hydraulics and disinfection) together with biofilm characteristics. Specifically, there have been no recent studies explicitly examining the inter-relationships between nitrification and hydraulic condition in drinking water distribution system. Furthermore, although previous studies share some opinions about nitrification properties, there is no consensus due to variation of microbiological features and, biofilm characteristics between studies.

Ultimately, to achieve better biofilm management and suggest effective nitrification control strategies, it is essential to have insight into the interactions of biofilm, operational factors and nitrification. Further research about nitrification needs to investigate whether nitrifiers activity is affected by the interactive effects between hydraulics and biofilm (community and EPS). This can be addressed by monitoring nitrification in systems operated with different hydraulic regimes, together with analysing microbial community and evaluating the corresponding EPS composition and structure. This will provide new insights into nitrification and suggest another idea for controlling within DWDS.

Chapter 3 Materials and Methods

3.1 Introduction

Based on the objectives of this study, a facility which could be operated under various hydraulic conditions and which will enable biofilm and water quality monitoring was required. The design and operation of such a flow cell arrangement is described comprehensively in this chapter. The experiments undertaken within the facility, including relevant sample analytical protocols and operating conditions are also presented in detailed.

3.2 Experimental facility

3.2.1 General description

There are several laboratory scale biofilm reactors capable of investigating biofilm properties and changes in water quality by simulating the environmental conditions within pipelines. These include annular reactors (Gjaltema et al. 1994; Lawrence et al. 2000; Altman et al. 2009; Zhou et al. 2009), simple batch reactors (Manuel et al. 2007) and flow cell systems (Hallam et al. 2001; Manuel et al. 2007; Teodosio et al. 2011). Among these reactors, the flow cell facilities have been applied wildly to study biofilm growth due to its flexible design which allows for an easier removal of inserts for scale and biofilm analysis (Eisnor et al. 2003). In addition, through numerical and physical investigation, a flow cell style reactor could simulate the hydraulic regimes accurately and hence provide reliable results that are associated with different operating conditions (Teodosio et al. 2011; Teodosio et al. 2013). Furthermore, compared with other reactors, the economic efficiency of flow cell was another advantage – cost under £200 for a unit.

In the current study, a flow cell arrangement was applied to simulate the conditions of a pipeline within drinking water distribution systems. Its specific hydrodynamic conditions have been simulated by numerical methods using computational fluid dynamics (CFD) by Cowles (2015) in previous study. The results proved that the flow

cells applied within the current study could accurately emulate pipe flow and represent known flow development criteria. In this study, six individual reactors were designed and procured. The flow cell system is shown in Fig.3.1 and it was located within the Characterisation Laboratories for Environmental Engineering Research (CLEER) laboratory at Cardiff University School of Engineering.

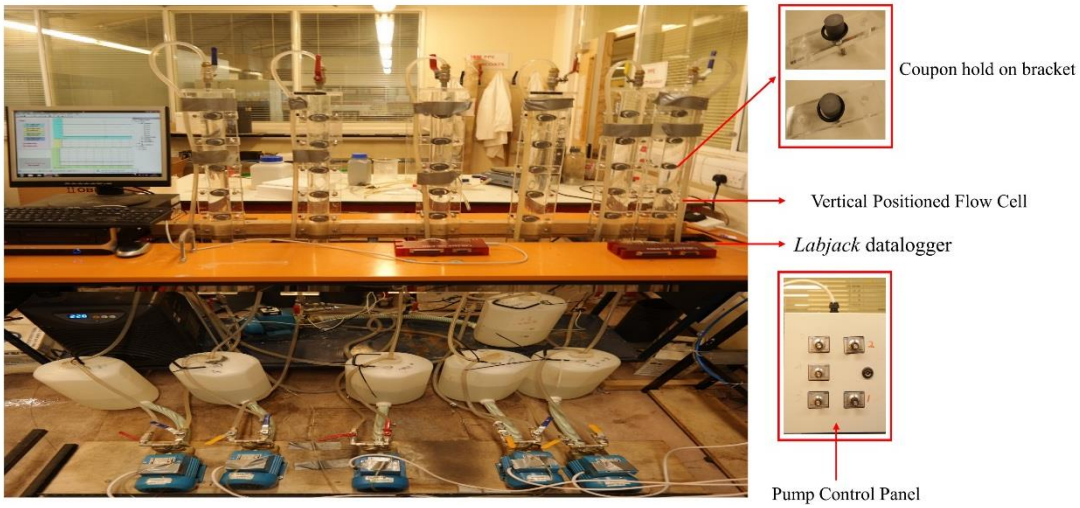

Figure 3.1 A series of flow cell systems in Characterisation Laboratories for Environmental Engineering Research laboratory at Cardiff University School of Engineering

3.2.2 Components

The flow cell unit utilized in this study was designed by Cowles (2015), who followed the design concepts outlined by (Teodosio et al. 2011; Teodosio et al. 2013) and (Pereira et al. 2000; Pereira et al. 2002). The detailed design diagram is shown in Fig.3.2. The flow cell units were made of acrylic and had a length of 100cm. The unit composed of a 4cm diameter semi-circular acrylic duct, and this was adhered on a planner and hence provided an equivalent hydraulic diameter and area of 2.44cm and 6.28 cm^2, as shown in Table 3.1. There are five equally spaced apertures along the planar surface of the flow cell, and these allow to fit 5 removable circular adhesion High-Density Polyethylene (HDPE) coupons, measuring 20mm in diameter. Given the circular nature of the apertures and coupons, the standard size 'O' ring-type seals were used to seal the systems. The first aperture is positioned 51.5 cm from the flow cells inlet. The four remaining apertures are positioned every 10 cm from the first. The purpose of this separation is to minimise potential disruptions in boundary shear caused by the respective downstream coupons. The last aperture is located 15 cm from the

flow cells outlet. During all experiment, the flow cells are positioned vertically to minimise trapped air within the system.

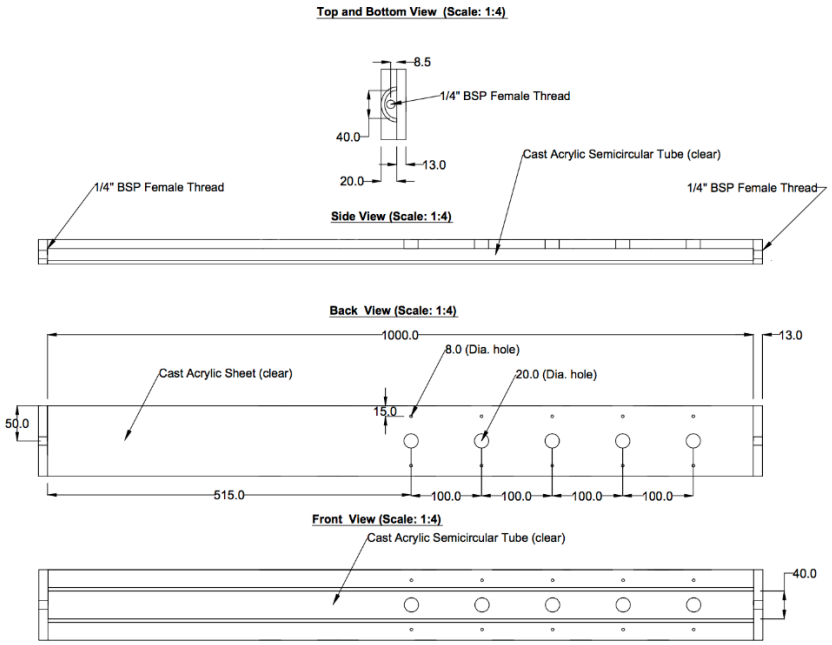

Figure 3.2 Design diagram of flow cell unit (Cowles 2015)

Table 3.1 Key characteristics of the flow cells used in the study (Cowles 2015)

Parameter	***Value***
Material	Acrylic
k_s	0.009 mm
Hydraulic diameter	2.44 cm
Flow area	6.28 cm^2
Wetted perimeter	10.28 cm
Hydraulic radius	0.61 cm
Length	100 cm
Internal volume	628.3 cm^3
Volume/Area	100 cm
Biofilm sampling points	5
Biofilm sampling area	3.14 cm^2

Polyethylene was selected to make the coupons as it is one of the most dominant and representative pipe material used in distribution system world-wide (Douterelo et al. 2013). In order to compare and evaluate the surface changes after experiment, images of each coupon surface were captured by a polarizing microscope (Nikon ECLIPSE LV100) before and after testing (Appendices Figs.A-4 to A-6). Due to the requirement for independent coupon position adjustment and convenient biofilm sampling, a separate holding bracket was used for holding the coupon (shown in Fig.3.1). The design allowed each coupon to be positioned perfectly with the internal surface of the flow cell, and the characterization of the composition of the in-situ biofilm assemblages quantitatively and qualitatively. However, it should be noted that any protrusions or depressions would disrupt the boundary layer flow conditions.

A 0.33 kW centrifugal water pump (*Clarke* CEB 102) was used for pumping water and the flow rate in each cell was controlled independently by two ¼'' ball valves. These were located at the inlet and outlet of the respective flow cells. The flow rate of each cell was monitored by an inline turbine flow meter (*RS* 511-4772). In order to avoid bias brought by temperature variation, the feed water was regulated by an external cooling unit (*D&D* DC-750) in order to maintain a constant temperature within system. The cooling unit is capable of cooling volumes between 200 and 600 liter to within ±1℃, over the temperature, T range of 4℃ < T < 28℃.

A *LabJack* multifunction 24-bit data logger (Model: U6-Pro) streamed all data recorded by a respective flowmeter to a desktop PC. DAQ factory (*AzeoTech*) data acquisition software was used to develop an interface to manage and export all measurement readings. The flow rate within each flow cell was monitored constantly and then maintained at a stable hydraulic condition.

3.3 Pre-testing Maintenance and sterilization

Before experiments commenced, the facility was disinfected with concentrated chlorine solution. The system was flushed for 48h at maximum flow rate (around 10L/min) and left to stand for another 24h after flushing. Fresh water was introduced to flush the system again at the maximum flow rate until the chlorine level became negligible. The insert coupons were sterilized with 80% ethanol solution for 24h and then left to dry in a clean fume cupboard for a further 24h. The above procedures were

repeated before each experimental regime. The maintenance regime outlined hereby was based on that described by Douterelo et al. (2013) for a pilot DWDSs.

3.4 Water physico-chemical properties

The feed water was collected from a tap located in the Characterisation Laboratories for Environmental Engineering Research (CLEER) lab in the Engineering School of Cardiff University (Room W0.24). It should be noted that the water was not immediately taken from the distribution system, a water tank was used for storage and hence there was extra disinfectant before the water reaching the tap.

Table 3.2 Physico-chemical properties of drinking water

Parameter	***Local drinking water***		***Reported Values***	***Reference***
	Measured in lab	***Measured by Welsh Water****		
T (℃)	23.00 ± 0.20	12.89-21.30	15.50-25.0	Sathasivan et al. (2005), Lehtola et al. (2006), Manuel et al. (2007), Douterelo et al. (2013)
pH	7.2 ± 0.25	-	6.90-8.96	LeChevallier et al. (1987), Lehtola et al. (2004), Momba and Makala (2004), Teng et al. (2008), Lipponen et al. (2002), Douterelo et al. (2013)
Turbidity (NTU)	0 ± 1	0.12 ± 0.12	0.06-1.2	Lipponen et al. (2002)
Conductivity (ms/cm)	0.300 ± 0.04	0.261 ± 0.04		
TOC (mg/L)	1.07 ± 0.35	1.21 ± 0.54	1.49-5.10	LeChevallier et al. (1987), Lehtola et al. (2004), Manuel et al. (2007), Wang et al. (2012)
TN (mg/L)	1.78 ± 0.14	-	0.50-2.10	Lipponen et al. (2002)
NH_3 (mg/L)	0.04	0.004 ± 0.002	0.20-1.66	Sathasivan et al. (2008)
NO_3^- (mg/L)	1.36 ± 0.02	1.18 ± 1.10	0.01-2.47	Manuel et al. (2007), Sathasivan et al. (2008), Lipponen et al. (2002)
NO_2^-(mg/L)	0.01	0.01	<0.01	Manuel et al. (2007)
Cl_2 (mg/L)	0.5 ± 0.02	0.5-0.9	0.05-3.00	Sathasivan et al. (2008), Lehtola et al. (2004), Manuel et al. (2007), Douterelo et al. (2013)

*Physico-chemical properties of local drinking water as measured by Welsh Water between 01/01/2016 to 31/12/2016

Table 3.2 gives the average of local physico-chemical parameters measured directly from the tap water collected from Cardiff University Engineering School, and the equivalent parameters measured by Welsh water, as outlined in their independent national database. The values of equivalent parameter from published literature were summarized in the table as well. Compared with the values from both Welsh Water and other studies, it can be seen that the measured parameters were within or close to the typical local values and hence the bias from the feed water could be neglected in further analysis.

As the current study was aimed at determining biofilm impacts on water quality within DWDSs utilizing chloramine as disinfectant, before preparing the feed water, all water collected from the tap had extra sodium thiosulfate added to remove free chlorine.

3.5 Facility set-up and operation

This section describes the facility set-up, and the operating condition undertaken within the current experiment. It comprises of four testing phases, with each phase consisting of two main stages, namely:

Stage 1. Inoculation and biofilm development – here nitrification process is established, and biofilm develop within the flow cell system before testing.

Stage 2. Testing phases – to assess water quality under different operational conditions, including hydraulic condition, disinfectant concentration and the mass ratio of chlorine and ammonia nitrogen. In total four test phases were undertaken and the details of the operating conditions are shown in Section 3.5.2.

3.5.1 Inoculation and biofilm development

In order to investigate how water quality changes under different operational conditions within chloramined DWDSs experiencing nitrification, nitrification process and biofilm were developed before applying different operating conditions within the flow cell systems. In addition, the distribution and growth of biofilm was expected to be as even as possible, so as to minimize bias from biofilm distribution in later discussion. For this purpose, every discrete flow cell unit was connected in series and fed with

water from the same water tank. Fig.3.3 showed the schematic of the set-up during this stage. A 0.33 kW centrifugal water pump (*Clarke* CEB102) was used to recirculate water through the system to a 10 L maximum capacity PE storage tank. The flow rate in each cell is controlled independently by two ¼'' ball valves which are located at the inlet and outlet sides of the respective flow cell. An inline turbine flow meter was used to monitor the flow rate within each cell.

3.5.1.1 Operating condition

Within the current study, the temperature was maintained by a cooling unit at 16℃±1℃ all the time. Based on previous report (Douterelo et al. 2013) 16℃ was representative of the typical temperature expected within DWDSs in the UK, and as a result, the flow cell system could be considered as reflecting of a real system with respect to temperature.

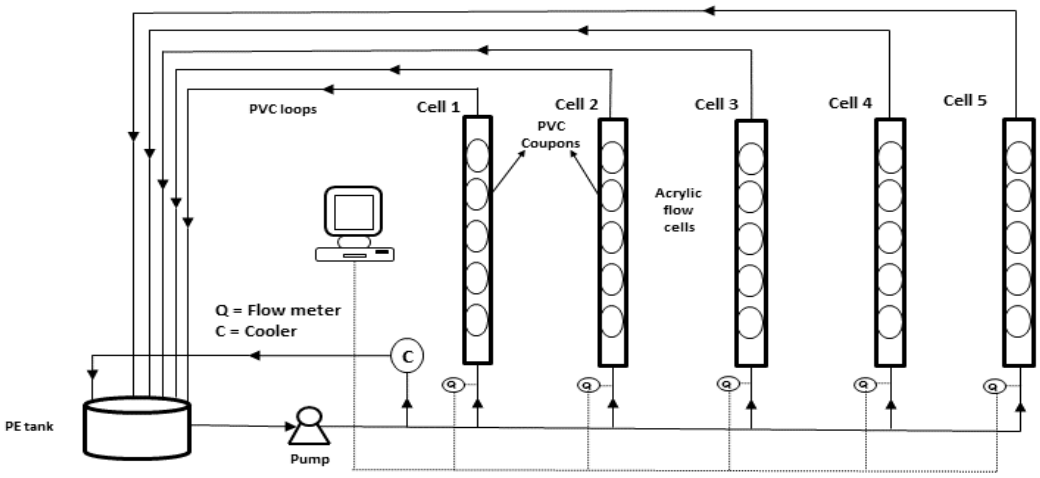

Figure 3.3 Schematic diagram of the flow cells during nitrification and biofilm development stage (five cells applied in first two testing phases and then change to six at next two phases)

To develop system with biofilm and establish nitrification process, the system was fed with dechlorinated tap water containing high concentration of ammonia (50 mg/L NH3-N) and adjusted to pH 8.0 with 5% (w/v) $NaHCO_3$. No other additions (i.e. carbon, tracers or metals) were added. 10 L of the feed water was fed with a flow rate of 2L/min. All cells were fully covered by shading material to protect nitrifiers from light. Water samples were collected regularly to monitor nitrogenous compounds, which include the concentration of nitrite nitrogen (NO_2^--N), nitrate nitrogen (NO_3^--N) and ammonia nitrogen (NH_3-N). Before every test phase, this process was repeated until a decrease

of 50% of ammonia nitrogen within the feed water.

3.5.2 Testing phases

After a stable nitrification process is established and an even and well distributed biofilm developed within all flow cells from the last stage, the facility was re-connected for the different experimental scenarios. Fig.3.4 shows the facility set-up during the test phases. In comparison to the last stage, flow in each flow cell was individually controlled to generate different hydraulic condition. Each flow cell was run in parallel and fed by an independent pump and return to the corresponding water tank.

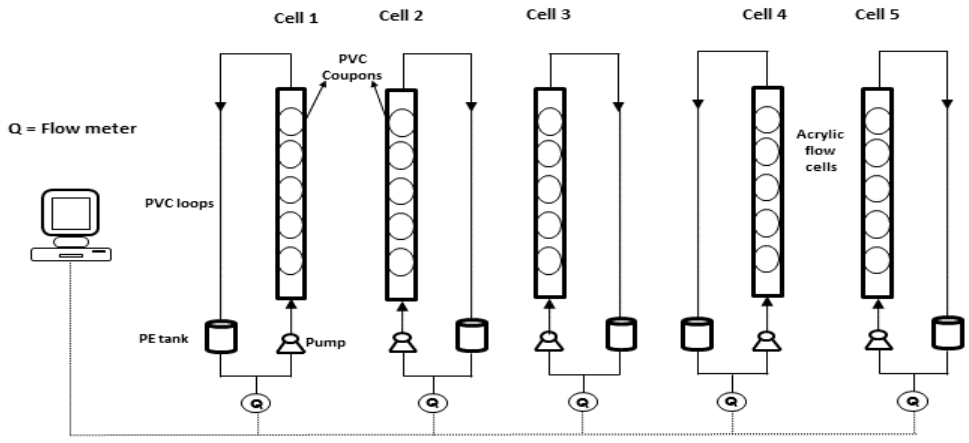

Figure 3.4 Schematic diagram of the flow cells during testing phases (five cells applied in first two testing phases and then change to six at next two phases)

3.5.2.1 Hydrodynamic characteristics

In the current study, a total of five flow regimes were evaluated, ranging from laminar to turbulent. The range of flow rates and water age that were used were chosen based on previous research and report (Manuel et al. 2007; Husband et al. 2008; Douterelo et al. 2013). Husband et al. (2008) documented that the average values of flow, Reynold number (Re) and shear stress (τ_w) were respectively about 0.06m/s, 4200 and 0.28 N/m^2. Manuel et al. (2007) incubated drinking water biofilm within a flow cell reactor at flow velocity of 0.21m/s and the corresponding Re was 5000. The flow rate used in the current study ranged from 2L/min to 10L/min. The corresponding Reynolds number and shear stress range were respectively 1107~5535 and 0.018~0.286. The hydraulic regimes included within the current study were therefore comparable to equivalent

studies and representative of actual systems. The average water age reported was around 1-3 days (AWWA 1992). To ensure enough reaction time for presenting representative water quality change, the water age within the current study was set as three days.

The hydrodynamic characteristics of the flow cells in this study were calculated based on the relationship between the Fanning friction factor (*f*) and Re (Stoodley et al. 2001). 2001). The *f* and Re are found from the average flow velocity (U_{ave}) and flow cell geometry. The Reynolds number is calculated from Eq.3.1:

$$\mathrm{Re} = \frac{\mathrm{U_{ave} * D_h}}{\mu} \qquad \text{Equation 3.1}$$

Where D_h is the hydraulic diameter and μ is the kinematic viscosity. The D_h in current study is 2.44 cm.

The friction factor (*f*) is predicted by the Hagen-Poiseuille equation (Characklis et al. 1990) in laminar region (Eq.3.2):

$$\mathrm{f} = \frac{16}{\mathrm{Re}} \qquad \text{Equation 3.2}$$

and the Blasius formula (Characklis et al. 1990) in the turbulent region:

$$\mathrm{f} = \frac{0.079}{\mathrm{Re}^{0.25}} \qquad \text{Equation 3.3}$$

The wall shear stress (τ_w) in laminar and turbulent region can be estimated from Eqs.3.4 and 3.5 respectively (Sommerfeld 1977; Characklis et al. 1990):

$$\tau_\mathrm{w} = \frac{4\mu \mathrm{u_{max}}}{\mathrm{D_h}} \qquad \text{Equation 3.4}$$

$$\tau_\mathrm{w} = \frac{\mathrm{f}\rho \mathrm{u_{ave}^2}}{2} \qquad \text{Equation 3.5}$$

where u_{max} is the maximum velocity. For a circular pipe $u_{max} = 2u_{ave}$. ρ is the water density.

Table 3.3 shows the summary of flow velocity/rate, equivalent boundary shear stress and Reynolds number for flow cells within current study.

Table 3.3 Experimental flow cell velocity, flow rate and determined boundary shear stresses

Average flow Rate Q (L/min)	***Average flow velocity U (m/s)***	***Reynolds number (Re)***	***Shear stress $(N/m)^2$***
2	0.05	1107	0.018
4	0.10	2214	0.036
6	0.15	3321	0.117
8	0.20	4428	0.194
10	0.25	5535	0.286

3.5.2.2 Experimental programme

Before the testing phases commenced, the facility was emptied and then refilled with fresh dechlorinated water to remove the remaining ammonia from the last stage. The system was emptied and filled three times and then left running for 24 h. In order to avoid damaging the attached biofilm, the flow rate was still maintained as 2L/min during this period. After the process, the level of free ammonia should be below detection.

The experimental programme comprised of four testing phases over a period of one year. Test coding for the corresponding phases and operational conditions are summarised in Tables 3.4 and 3.5. Test phases 1 and 2 comprised five steady state hydraulic regimes, each flow cell ran parallel at flow rate of 2L/min, 4L/min, 6L/min, 8L/min and 10L/min for 33 days, with three primary objectives:

- To investigate whether on-going nitrification in drinking water system is affected by hydraulic regimes.
- To determine the influence of mass ratio of chlorine and ammonia nitrogen on controlling nitrification.
- To assess microbial community within biofilm and bulk water collected from flow cell units operated under different operational conditions.

After these two experimental rounds, biofilm and bulk water sample were collected for DNA extraction and next generation sequencing (NGS). The details for sampling and molecular analysing are presented in Section 3.7.

Two other testing phases were conducted and the experiment scenarios are shown in

Table 3.5. Different from previous tests, only three hydraulic regimes were evaluated within these two rounds. The main objectives of these two rounds were:

- To verify the results from last two rounds that nitrification process would be severe when flow turbulence is between laminar and turbulent.
- To investigate the effect of different chloramine dose concentration on on-going nitrification, with different hydraulic regimes.
- To assess biofilm EPS composition from different operational conditions.

Table 3.4 Experiment scenarios (A)

Parameters controlled	Cell 1	Cell 2	Cell 3	Cell 4	Cell 5
	Round 1				
Water age (days)	3	3	3	3	3
Cl2 dose mg/L	1	1	1	1	1
Cl2:NH3-N mass ratio	3:1	3:1	3:1	3:1	3:1
Flow rate (L/min)	2	4	6	8	10
Test code	2A	4A	6A	8A	10A
	Round 2				
Water age (days)	3	3	3	3	3
Cl2 dose mg/L	1	1	1	1	1
Cl2:NH3-N mass ratio	5:1	5:1	5:1	5:1	5:1
Flow rate (L/min)	2	4	6	8	10
Test code	2B	4B	6B	8B	10B

Table 3.5 Experiment scenarios (B)

Parameters controlled	Cell 1	Cell 2	Cell 3	Cell 4	Cell 5	Cell 6
	Round 3					
Water age (days)	3	3	3	3	3	3
Cl2 dose mg/L	1	1	1	5	5	5
Cl2:NH3-N mass ratio	3:1	3:1	3:1	3:1	3:1	3:1
Flow rate (L/min)	2	6	10	2	6	10
Test code	2A_R3	6A_R3	10A_R3	2B_R3	6B_R3	10B_R3
	Round 4					
Water age (days)	3	3	3	3	3	3
Cl2 dose mg/L	1	1	1	5	5	5
Cl2:NH3-N mass ratio	5:1	5:1	5:1	5:1	5:1	5:1
Flow rate (L/min)	2	6	10	2	6	10
Test code	2A_R4	6A_R4	10A_R4	2B_R4	6B_R4	10B_R4

3.5.2.3 Water collection and preparation for feed

Water was collected from the tap located in CLEER lab (Cardiff University) and then stored in four 25 litre plastic water containers before been fed into the flow cell systems. Chlorine (from a stock solution of 500mg/L total chlorine) was then added into source water until a final concentration of approximately 1.0 mg Cl_2/L (or 5.0 mg Cl_2/L) was achieved in all containers. After 24h, the chlorine in the containers was re-adjusted and ammonia (from pure ammonium chloride solids) was added (maintaining a total chlorine to total ammonia nitrogen ratio of 3:1 or 5:1) into the container until a chloramine residual (measured as total chlorine) of 1.0/5.0 mg/L was achieved. Subsequently pH in the water was adjusted to 8.0 ± 0.1 after chloramination and from here on, this water will be referred to as the feed water.

The disinfectant concentration and the chlorine to ammonia mass ratio selected within the current study are based on the common operational conditions within real water infrastructures. Moradi et al. (2017) developed a chloramine decay model based on data collected from two sites in Australia, where the chloramine concentration measured in the inlet was ~4 mg/L with Cl_2:NH_3-N mass ratio of 4.5:1. Another research about microbial community distribution along distribution systems was conducted within various DWDSs with an average chloramine concentration of 1 mg/L (Potgieter et al. 2018). Therefore, the disinfection strategy operated within the current study can reveal the basic water chemistry in real systems.

Overall, via designing an experimental flow cell facility which can reveal the real hydraulic condition as much as possible and introducing water with representing physic-chemical characteristics within DWDSs, the tests conducted in the current study can provide meaningful referencing data for water utilities.

3.6 Analytical methods

Water samples were collected and analysed every three days. Frequent measurements (daily sampling) were undertaken from the 9th day of each experimental phase until the 16th day. Each sample was divided into three subsamples to perform repetitive analysis and the value reported is the average of the three replicates.

Within the current experiment, several water quality parameters were monitored

including pH, dissolved oxygen (DO), conductivity, turbidity, total and free chlorine, ammonia nitrogen (NH_3-N), nitrite and nitrate nitrogen (NO_2^- - N, NO_3^- - N), total organic carbon (TOC), dissolve organic carbon (DOC), total nitrogen (TN), heterotrophic plate count (HPC) and microbiological decay factor (F_m). The measurement details are described below.

3.6.1 Physico-chemical parameter measurement

The measurements of pH, DO and conductivity were made using a benchtop meter (SevenExcellence S600) and probes. A HACH portable machine is used for turbidity analysis in this test (HACH DR 900) based on standard method 2130 (APHA 1998). Total and free chlorine, nitrite nitrogen, nitrate nitrogen and free ammonia nitrogen were measured using a Benchtop Spectrophotometer (DR3900, *Hach*-Lange) and relevant standard reagent assays (produced by *Hach* Lange). In particular, total and free chlorine concentrations were determined by N,N-diethyl-p-phenylenediamine (DPD) method (Method 8167 and 8021, HACH). Whereas, diazotization and cadmium reduction method kit were used to measure NO_2^- - N and NO_3^- - N respectively (Method 8507 and Method 8171, HACH). Ammonia nitrogen (NH_3-N) concentrations (including all NH_4^+-N and free NH_3-N) were measured using a Nessler reagent kit (Method 8038, HACH).

TOC was measured by a TOC analyser (TOC-V_{CPH} *Shimadzu*). The TOC concentration was estimated by determining the concentrations of total carbon (TC) and inorganic carbon (IC) (TOC = TC –IC). The TN was analysed by using the TOC analyser's TNM-1 accompanying unit. Typical calibration curve for TC, IC and TN are presented in Appendices in Fig.A-1 and A-2.

To ensure the accuracy of the monitored parameters, total three subsamples for single sample point were taken and measured. The data used in the current study was the average value of these three samples.

3.6.2 Bio-parameters

HPC was determined by R2A agar plate following the standard method 9215 (APHA 1998). The microbiological decay factor (F_m) evaluates the contribution of microbiology to the overall monochloramine decay in the bulk water as described by Sathasivan et al. (2005). The method is outlined herein.

The water sample was divided into two subsamples. One of them was with no further process, while the other goes to 0.2μm filter for removing possible microbiological agents. After filtration, inhibitor ($AgNO_3$) was added to the second subsamples to make a total 100μg-Ag/L as well as to ensure monochloramine decay caused by chemical means only. The two subsamples were then incubated at a constant temperature of 20℃ without light. The monochloramine residual was measured regularly when the total chlorine residual in the unprocessed sample reached 0.5mg/L.

First-order reaction kinetics is used to describe all decay rate in this method. The integrated form is given by Eq.3.6:

$$C_{NH_2Cl} = C_{NH_2Cl,0}\exp(-k_s t) \qquad \text{Equation 3.6}$$

where $C_{NH2Cl,0}$ is the initial monochloramine concentration in mg/L (i.e., at t=0), C_{NH2Cl} is the monochloramine concentration in mg/L, k_s is the first-order decay coefficient of sample S at 20℃, and t is elapsed time in hours.

The decay coefficients for unprocessed and inhibited sub-sample are k_{total} and k_c respectively. The difference between chemical decay (k_c) and total decay (k_{total}) is attributable to microbiological agents including nitrifiers. The difference is defined as the microbial decay coefficient and is denoted as k_m (Eq.3.7).

$$K_m = k_t - k_c \qquad \text{Equation 3.7}$$

F_m is the ratio of the microbial decay rate coefficient (k_m) and the chemical decay rate coefficient (k_c) as shown in equation Eq.3.8.

$$F_m = \frac{k_m}{k_c} \qquad \text{Equation 3.8}$$

3.7 Molecular analysis

Herein the molecular analysis taken within current study is described in detail. All the following analysis were undertaken at the Cardiff School of Bioscience. The microbial community within biofilm and bulk water samples from the experimental phases 1 and 2 were evaluated by next generation DNA sequencing (Illumina MiSeq sequencer). The extracellular polymeric substance (EPS) was extracted and quantified from biofilm sample of all test phases.

3.7.1 Sampling of biofilm and bulk water

To study the microbial community within the biofilm, coupons installed in every

discrete flow cell (five for each) were collected after the experimental phases 1 and 2. In order to remove the attached biofilm thoroughly, the coupon was immersed into 10ml sterilized phosphate-buffered saline (PBS) and then sonicated in an ultrasonic water bath (Kerry 2593) for 10 mins at approximately 50Hz. After all the five coupons have been washed, the 10ml suspended culture was divided into three subsamples: 4.5ml suspension was centrifuged (*Eppendorf,* centrifuge 5424) at 14,000×g for 2 mins to pellet the cells for DNA extraction and microbial analysis; another 4.5ml culture was centrifuged to cell pellets for EPS extraction and quantification; the remaining 1ml solution was for HPC counting and storage (combined with 20% glycerine).

Biofilm sample was collected from experimental phases 3 and 4 as well for EPS extraction and evaluation only. Only two sub-samples were prepared from the 10ml suspension: 9ml solution was centrifuged to cell pellets for EPS analysis and the rest of 1ml suspension was used for HPC counting and storage.

The water sample was collected from every discrete water tank after experimental phases 1 and 2. For every single flow cell unit, 1 litre of bulk water was taken directly from the tank and filtered through 0.22 μm nitrocellulose membrane filters (Millipore, Corp). A total of 10 biofilm samples and 10 filters containing water samples were collected and stored at -80°C for subsequent DNA extraction and Miseq analysis.

3.7.2 EPS and DNA extraction protocol

The protocol used within the current study for EPS is as described by Brown and Lester (1980). The phenol: chloroform based method and chemical lysis approach (Zhou et al. 1996) was used for DNA extraction. The details of method are outlined herein.

3.7.2.1 EPS extraction protocol

From the sub-sample collected in the last step, the cell pellets were firstly washed with 0.25ml PBS and then re-suspended in 1.25ml PBS. Combined with the 0.25ml suspension from the washing step, the 1.5ml suspension was transferred to a clean centrifuge tube and then 1.5ml of 2% ethylenediaminetetraacetic acid (EDTA) in PBS was added. The solution was then sonicated for 30s (Kerry 2593) and incubated for 3h at 4°C. After the incubation period, the solution was centrifuged at 20000×g for 20mins to pellet the cells. The supernatant was then filtered through 0.2μm filters to remove

possible microorganisms before EPS evaluation.

3.7.2.2 DNA extraction and quantification

Based on the type of sample, the biofilm sample went through the extraction procedure immediately, whilst the filters with water sample required pre-treatment to remove the cells. In brief, the filter within 50ml centrifuge tube was washed by the filter wash buffer which was prepared by adding 6µl of Tween 20 to 3ml of PBS, and then mechanically shaken (*Lab Line*, Multi Wrist Shaker) for 10 mins. The cell suspension was transferred to a clean micro centrifuge tube and then the cells were pelleted by centrifuging the tube at 14,000×g for 2 mins. The suspension was discarded.

For DNA extraction, the Metagenomic DNA Isolation Kit for water was used within the current study. In brief, the cell pellet was firstly re-suspended in 300µl TE buffer (10 mM Tris-HCl [pH 7.5], 1mM EDTA) in a 1.5 ml centrifuge tube and then the cell suspension had 2µl of Ready-Lyse Lysozyme solution and 1µl of RNase A added. Vortexing (WhirliMixer) was required for fully mixture. After incubation at 37°C in water bath (*Julabo* TW12) for 30 mins, 300µl of Meta-Lysis Solution and 1µl of Proteinase K was added to the same tube and mixed by vortexing. The sample was then incubated at 65°C in a heating block (Eppendorf) for 15 mins. Subsequently, 350µl of MPC Protein Precipitation Reagent was added to the tube after cooling, then the debris were pelletised by centrifuging at 14,000×g for 10 mins in a micro centrifuge at 4°C (*Eppendorf*, Centrifuge 5417R). The supernatant was then transferred to a new 1.5ml tube and 570µl of isopropanol was added. The DNA was pelletised by centrifuging for 10 mins at 14,000×g and then washed by 500µl of 70% ethanol. Another centrifugation was followed by the washing step and the DNA pellet was dried and re-suspended in 50µl of TE buffer.

Qualification and quantification of extracted DNA were carried out, respectively on the TapeStation and Qubit respectively. Agilent genomic DNA protocol (Agilent Technologies, 2013) was used for the Tapestation analysis, while the quantification process followed the Qubit assay (Life Technologies, 2014) . Thereafter, DNA in all samples was normalized to a final concentration of 15ng/µl and its quality was ~4.7. The raw data of Qubit DNA concentration and DNA quality are presented in

Appendices in Table A-1.

3.7.3 16S rRNA sequencing with Illumina Miseq for characterising bacterial communities

A dual-index sequencing strategy was performed on the Miseq Illumina sequencing platform for characterizing bacterial communities, and examining their relative abundance and diversity in water and biofilm samples. Miseq Illumina is a next generation sequencer, which allows a clonal amplification, sequencing, cluster and data analysis in a single run. Within the current study, the extracted DNA was sent to the Heath Hospital, Cardiff University for bacterial 16S rRNA sequencing. One-step PCR amplification (30 cycles) was performed using the primers V4f and V4r (Kozich et al. 2013) to construct 16S rRNA gene libraries. The sequencing procedure was described in detail by Kozich et al. (2013).

3.7.4 Sequence analysis

Within this study, a total of 63129~136456 valid 16S rRNA gene sequence were recovered from each biofilm and water sample through Illumina MiSeq sequencing analysis. With the obtained sequences, two independent analyses were undertaken by the Bioscience Department, Cardiff University. One of the analyses was aimed at obtaining taxonomical assignments from sequences and the other one was carried out to estimate alpha- and beta- diversity, which are two different terms to measure diversity in an ecosystem Whittaker (1960, 1972). Alpha- diversity is about the diversity of a specific sample (i.e. how many different bacteria are in a sample), while beta- diversity refers to the difference between samples.

3.7.4.1 Mothur taxonomic analysis

Within the current study, Mothur (Version1.38.1) which is a custom Perl and C++ software, was used to take paired-end Illumina sequence reads, discover associated taxonomy and create a matrix of the count of each sequence in each sample. The pipeline required to implement the analysis are within the mother software package and specified on the mother website (http://www.mothur.org/wiki/Miseq_SOP) (Schloss et al. 2009). Following the method presented by Kozich et al. (2013), contigs that have any ambiguous bases (i.e., N), a homo-polymer run of more than 7 of the same base, or was shorter than 245 or longer than 275 bp were removed. Subsequently, the

sequence size was reduced to 2,334,474 by looking for contigs with identical sequence. The sequences were further aligned to reference alignment (Silva.Bacterial.fasta). Poorly aligned sequences were then removed and alignment was trimmed to remove positions that aren't informative (Schloss 2009, 2010, 2013). The sequences were trimmed to the ends to have them all start and end at the same alignment coordinates (Schloss 2013). In order to further remove duplicate sequences within each sample, a pre-clustering algorithm was applied after identifying the unique sequences and their frequency (Schloss et al. 2011). UCHIME (Edgar et al. 2011) was utilized for screening PCR chimeras within resulting sequences. The sequence was then classified by the Bayesian classifier against the Ribosomal Database Project (RDP) 16S rRNA gene training set (version 9). Sequences were removed if they did not classify to the level of kingdom or were classified as *Archaea, Eukaryota,* chloroplasts, or mitochondria. Finally, sequences were clustered into operational taxonomic units (OTU) at a 0.03 dissimilarity level and then a data matrix of each OTU in each sample as well as its abundance was made. The chimeras were identified based on mock community data and the sequencing error rates were calculated based on the method described by (Schloss et al. 2011).

3.7.4.2 Alpha- and beta- diversity analysis with R

Before the estimation of alpha- and beta diversity, each OTU was classified to get consensus taxonomy and the distance between sequences. A *biom* formatted file was then made for import into R software (Version 3.3.2). The sequences were representatives for each OTU subsequently. A phylogenetic tree was built using the FastTree algorithm (Price et al. 2009) for UniFrac distance matrix construction.

With the R software, a phyloseq package was introduced for diversity analysis within the current study. To study the alpha- diversity (diversity within samples), a rarefaction analysis was performed for each sample based on hydraulic regimes, habitat type and testing rounds. Two different alpha-diversity metrics were included, which are Chao1 richness estimator (Chao 1984) and Shannon diversity index (Shannon and Weave 1949). To compare bacterial diversity between samples (beta-diversity), Unifrac distance metric was applied (Lozupone et al., 2011) to calculate pairwise distance between communities in terms of their evolutionary history. Both un-weighted

(presence/absence information) and weighted (considering relative abundance of each OTU) UniFrac analysis were undertaken.

3.7.4.3 Statistical analyses

To assess the similarity of community within different samples, the Bray-Curtis similarity matrixes were introduced using the R software (Version 3.3.2). The multiple-dimensional scaling (MDS) diagrams was used to have the matrixes visualised. A DEseq2 package (Version 1.16.1) (Love et al. 2017), which used the negative binominal generalized linear model, was applied for determining the significant difference between biofilm and bulk water community.

3.7.5 EPS characterisation

EPS is a comprehensive term for organic macromolecules including polysaccharides (i.e. carbohydrates), proteins, nucleic acids and lipids (Staudt et al. 2004). EPS may vary in their physical and chemical properties, but they are primarily composed of protein and carbohydrate (representing over 50%) (Donlan and Costerton 2002; Donlan 2002; Flemming et al. 2017). In addition, the mechanical stability and cohesion properties of biofilm are found to be influenced by EPS (Wloka et al. 2004a; Flemming et al. 2010; Simoes et al. 2010). Consequently, protein and carbohydrate were the two components from extracted EPS quantified within the current study. The methods are detailed herein.

3.7.5.1 Total extracellular protein concentration

The total concentration of protein was determined using the standard Bradford assay (*Sigma* B6916) with bovine serum albumin (BSA) as standard. Following the procedure outlined by Bradford (1976), a protein standard curve ranging from 0 to 20μg/l was built. The absorbance was measured at 595nm using a Spectrophotometer (Model U-1900 by Hitachi High-Technologies).

3.7.5.2 Total extracellular carbohydrate concentration

The total carbohydrate concentration within extracted EPS was measured using a standard phenol-sulphuric acid based assay kit (*Sigma* MAK104) with glucose (2.0mg/l solution) as standard. A calibration standard in the range 0-20μg/50μl was built based on the procedure outlined by the manufacturer. The details are outlined herein.

The required glucose standard was firstly prepared by adding 0, 2, 4, 6, 8 and 10 μl of glucose concentrations (2mg/ml) to a 96 well plate. The total volume of each well was brought to 50μl to reach a final concentration of 0 (blank), 4, 8, 12, 16 and 20 μg/well. The EPS sample of volume of 50μl was added to the well as well. 150μl of concentrated sulfuric acid was added to each well. The solutions were then incubated for 15 mins at 90°C in a heating block (*Techne* Dri-Block-3). Light was avoided during incubation. Subsequently, 30μl of phenol-based developer was added to each well and then left for 5 mins at room temperature before measuring. A Spectrophotometric multiwall plate reader (*Tecan* infinite M200Pro) was used for measuring the absorbance with a wavelength setting at 490nm.

Typical standard curves for protein and carbohydrate are presented in Appendices in Fig.A-3. It should be noted that all standard curves used within current study had R^2 of at least 0.95.

3.8 Summary

This chapter presents details of the design and key components of the flow cell facility used in the current study. The maintenance of the facility and the physico-chemical characteristics of the water utilized were described, respectively in Sections 3.3. and 3.4.

A comprehensive description of the facility set-up for different experimental stage was outlined in Sections 3.5.1 and 3.5.2. The experimental programs undertaken within the flow cell system were presented in Section 3.5.2.2.

The analytical methods and instruments for both physico-chemical and bio parameters were described in Section 3.6. All sampling protocols and analytical techniques for molecular substance were outlined in detail in Section 3.7.

Chapter 4 Effect of hydraulic and disinfection strategies on nitrification in chloraminated flow cell facility

4.1 Introduction

This chapter presents the results of water quality parameters related to nitrification measured in the four test phases. The objective of this chapter is to investigate and determine the effect of hydraulic regimes and disinfectant strategies on on-going nitrification in chloramined DWDS. To achieve this, water quality parameters, nitrification episodes and microbial water quality indicators were compared separately between different operational conditions. The effects of hydraulic regimes and disinfection strategies on the nitrification process were also analysed in detail. The effect of hydraulic regimes on nitrification process was firstly suggested based on the statistical analysis. Combined with the results from the test phases 3 and 4 which used higher concentration of chloramine (5 mg/L), a joint action was suggested to control nitrification by increasing both flow turbulence and disinfectant concentration. In addition, water quality parameters were evaluated in terms of their efficiency to predict or indicate the extent of nitrification extent.

4.2 Results

Water quality parameters, which include pH, free chlorine, turbidity, total organic carbon (TOC), nitrite, nitrate, ammonia nitrogen, total nitrogen, HPC and microbial decay factor, were monitored within all flow cell units over the four testing phases.

Statistical analysis were performed using PASW Statistics 18.SPSS. As the water quality parameters were not normally distributed, the Kruskal-Wallis test (for comparison>2 datasets) or Mann-Whitney U test (for 2 datasets, $p<0.05$ two tailed) were used to identify whether there was difference in parameter concentrations between each operational condition. The correlation between each water quality

parameter and operational conditions was determined by calculating the non-parametric Spearman's rank correlation coefficients. Results of the Kruskal-Wallis test and Mann-Whitney U test are shown in Appendices (Sections B.2 and B.3).

4.2.1 Water quality parameters

Data for pH, free chlorine residual, turbidity and TOC are presented in boxplots in Figs.4.1 to 4.4. The boxplots shown in this chapter included the median and mean values of data within a box. From the top to bottom line of the box represented the third quartile and first quartile of all data respectively. Whiskers extended to cover the range of minimum and maximum of all the data; outliers of the data were plotted as individual circles.

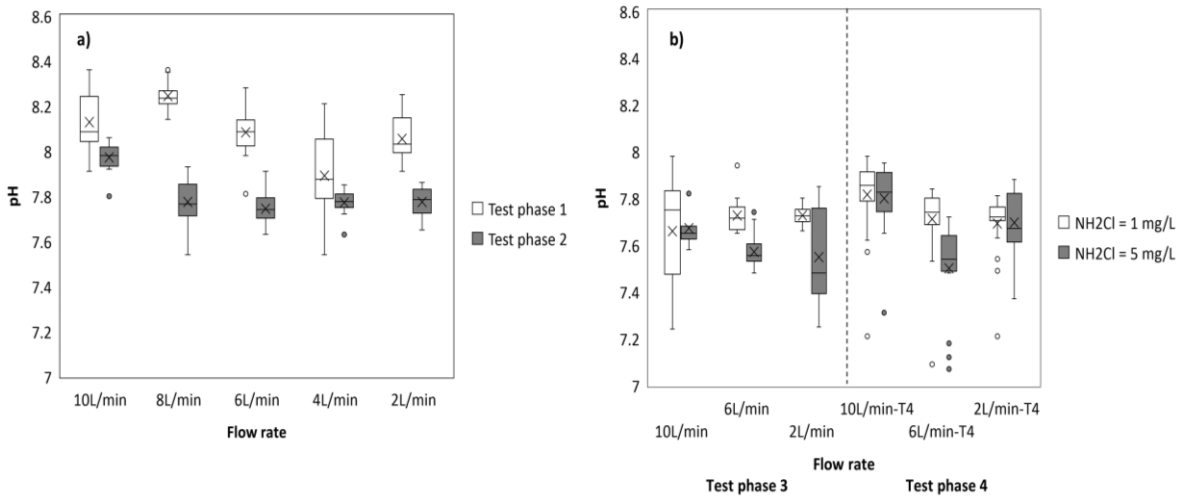

Figure 4.1 pH value in different operational conditions in four test phases. a) for test phase1 and 2; b) for test phase 3 and 4. The colour represents different monochloramine concentration.

In Fig.4.1, the variations of pH within each flow cell unit in all the four test phases were small, but the range differed among the different test phases. According to the results from Mann-Whitney U test (the data is shown in Appendices B, Table B-2), significant difference was observed between each operational condition in test phase 1 ($n=20$, $p<0.05$), except the flow cell running at 6 L/min between that running at 2 L/min and 10 L/min. The condition was not the same at different test phases. When the Cl_2/NH_3-N mass ratio was changed to 5:1 in test phase 2, only the difference in pH in the flow cell operated at 10 L/min was observed between other hydraulic regimes ($n=16$, $p<0.05$) (the data is shown in Appendices B, Table B-3). In test phase 3, the three flow cell units were used for repeating the operational conditions (2, 6, 10 L/min) conducted

in test phase 1. No statistical differences of pH were observed between these three hydraulic regimes (the data is shown in Appendices B, Table B-4). The result is similar to that in test phase 1, except for the cell running at 2 and 10 L/min ($n=17$, $p<0.05$) (the data is shown in Appendices B, Table B-4). Within the same test phase, another three units were fed with higher concentration of NH_2Cl (5 mg/l), but at the same three hydraulic conditions. Unlike those fed with lower concentration, there was difference in pH between each cell. When using the Mann-Whitney U test for identifying whether there was difference in pH between different NH_2Cl concentration at the same hydraulic condition, the results indicate significant difference in cells running at 2 and 6 L/min. Similar to the test phase 3, a repeat of the experiment for the three hydraulic regimes in test phase 2 was conducted in three of the flow cell units in test phase 4, and the Mann-Whitney U test confirmed the results in test phase 2 ($n=21$, $p<0.05$) (the data is shown in Appendices B, Table B-5). For the other three flow cells fed with 5 mg/L NH_2Cl, significant differences were found between the hydraulic regimes. However, the difference in pH between the different feed water was only observed in cells operated at flow rate of 6 L/min (the data is shown in Appendices B, Table B-5).

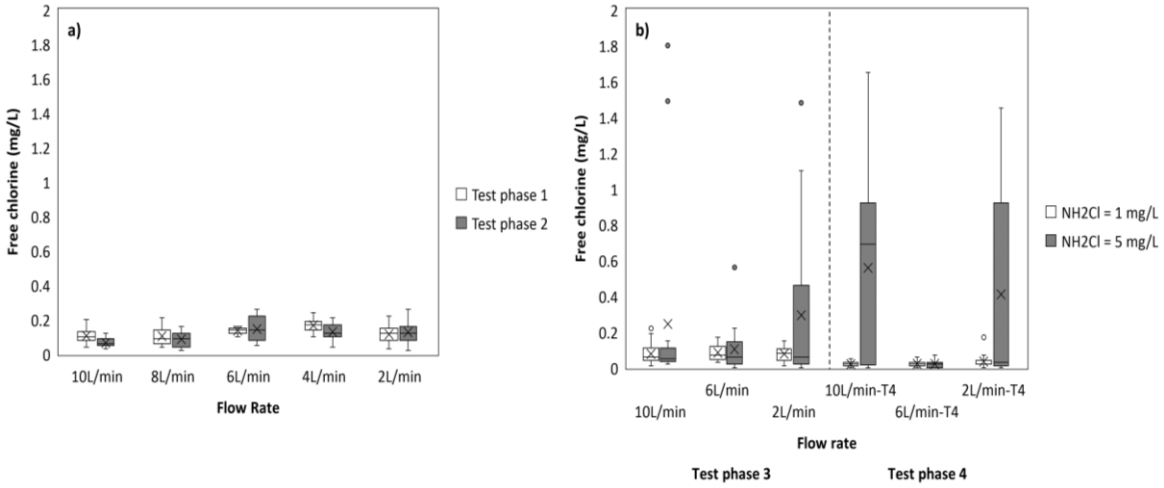

Figure 4.2 Concentration of free chlorine residual in different operational conditions in four test phases. a) for test phase1 and 2; b) for test phase 3 and 4. The colour represents different monochloramine concentration.

Fig.4.2 presents the free chlorine residual monitored along the four test phases. The disinfectant residual in all operational conditions was maintained at a low level. In test phases 1 and 2 and part of cell units in phases 3 and 4 where the total chlorine concentration was 1 mg/L in feed water, the residual could only reach an average of

0.05~0.2 mg/L in the experimental facility. Even though a higher concentration of total chlorine (5 mg/L) was also used in test phase 3 and 4, the average residual was below 0.5 mg/L (Fig.4.2b). From the Kruskal-Wallis test, significant difference in chlorine residual between different operational conditions was observed in test phases 1 and 2 (the data is shown in Appendices B, Tables B-6 and B-7). However, the difference was not found in all cases when comparing two separate operational conditions. This was further confirmed in the repeat experiment in test phases 3 and 4. When the chloramine concentration was changed to 5 mg/L, no significant difference was found in the test phase 3, while the concentration in the cell running at 10 and 2 L/min was significantly higher than that at 6 L/min in test phase 4 ($n=21$, $p<0.05$) (the data is shown in Appendices B, Tables B-4 and B-5). In addition, chloramine concentration did not affect the disinfectant residual when compared with that under the same hydraulic regimes ($p\geq0.269$) (the data is shown in Appendices B, Tables B-4 and B-5), except in cells running at flow rate of 10 L/min in test phase 4 ($n=21$, $p=0.003$) (the data is shown in Appendices B, Table B-5).

The turbidity in the water sample fluctuate and the range of values varied between the different operational conditions in the four test phases (Fig.4.3). Hydraulic regimes did not significantly affect the change of turbidity along the experiment in test phase 1 ($n=20$, $p=0.094$) (the data is shown in Appendices B, Table B-6). While in test phase 2, the water was more turbid in the cell running at lower flow rates ($\leq$ 6 L/min) when compared with that in the unit operated at flow rate of 8 and 10 L/min ($n=16$, $p<0.005$) (the data is shown in Appendices B, Table B-3). Similar with test phase 1, hydraulic regime was not a factor influencing the difference in turbidity of the water samples either in the repeat experiments or in cells fed with higher concentration of disinfectant in test phase 3 ($n=17$, $p\geq0.104$) (the data is shown in Appendices B, Table B-4). Conversely, when the Cl_2/NH_3-N mass ratio was 5:1 in test phase 4, the water was observed to be more turbid in the cell at flow rate of 6 L/min than that in the units at the other two hydraulic regimes under both disinfectant concentrations ($n=21$, $p<0.001$) (the data is shown in Appendices B, Table B-5). When compared with different disinfectant concentration at the same hydraulic regimes, no significant differences were observed in both test phases 3 and 4 ($p\geq0.360$) (the data is shown in Appendices B, Tables B-4 and B-5).

The concentration of TOC varied during the experiment in the four test phases and the range of values differed under different hydraulic regimes (Fig.4.4). Similar to the trend of turbidity, the concentration of TOC in both test phases 1 and 2 was higher in cells running at lower flow rate (≤ 6 L/min) (n=20, p≤0.023) (the data is shown in Appendices B, Tables B-2 and B-3), while no significant differences were found within these three lower flow rates (2, 4, 6 L/min) (n=20, p≥0.112) (the data is shown in Appendices B, Tables B-2 and B-3). The peak location of TOC was also observed in the cells at flow rate of 6 L/min in test phase 4 (n=21, p≤0.031) (the data is shown in Appendices B, Table B-5). However, no significant difference was found between hydraulic regimes in test phase 3 (n=17, p≥0.095) (the data is shown in Appendices B, Table B-4).

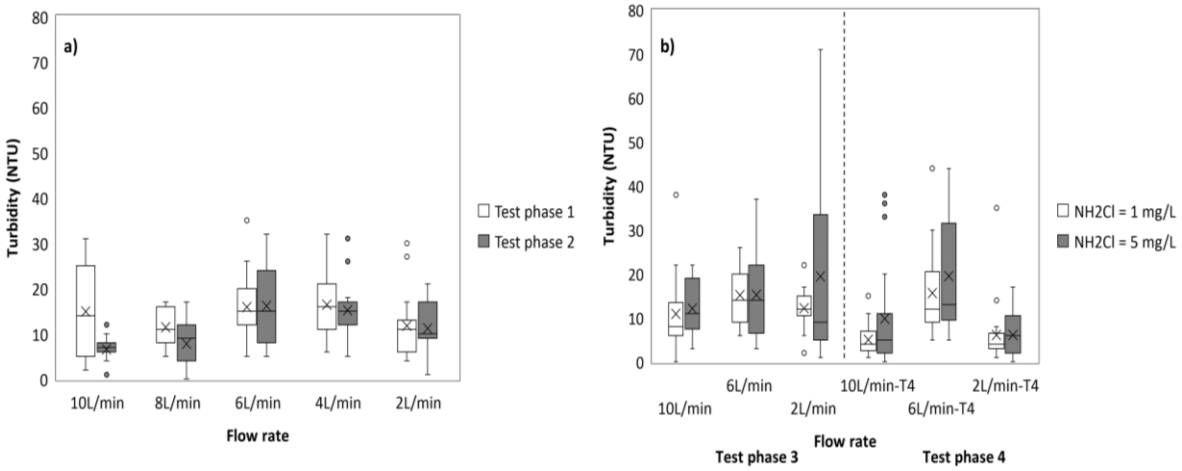

Figure 4.3 Turbidity value in different operational conditions in four test phases. a) for test phase1 and 2; b) for test phase 3 and 4. The colour represents different monochloramine concentration.

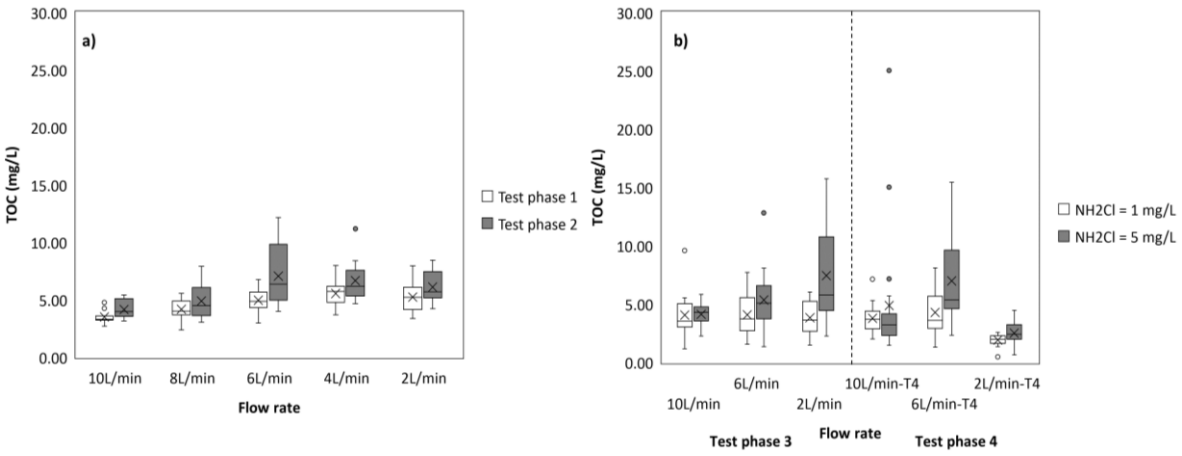

Figure 4.4 The concentration of TOC in different operational conditions in four test phases. a) for test phase1 and 2; b) for test phase 3 and 4. The colour represents different monochloramine concentration.

4.2.2 Physico-chemical indicators of nitrification

As the current study was conducted within the facility fed with chloraminated water and nitrification was established during the incubation stage (Section 3.5.1), nitrification related parameters were measured. The most common indicators used in water distribution system for monitoring nitrification are the change of nitrite, nitrate and ammonia concentrations. These measurements were aimed at investigating the effects of operational conditions on on-going nitrification within the experimental facility. In this section, time-series plots of nitrite (Figs.4.6, 4.8, 4.10, 4.12) and plots of all the three parameters (Figs.4.7, 4.9, 4.11, 4.13) were made for different hydraulic regimes for all the test phases. Boxplots (Fig.4.5) were made as well to compare nitrite production within different operational conditions.

In test phase 1, five hydraulic regimes were evaluated and according to the nitrite threshold (0.015 mg-N/L) given by AWWA (2006), the average production of nitrite during the test in all flow cell units exceeded the value, suggesting that nitrification was ongoing during the test (Fig.4.5a). However, unlike other hydraulic regimes which experienced nitrification along with the whole test, in the unit running at the flow rate of 10 L/min, no severe nitrification was observed during the first 15 days of the test (Fig.4.6). This might suggest that nitrification is inhibited to some extent in the early stage of the experiment when flow rate was 10L/min. During the test period, the nitrite concentration for all the hydraulic regimes fluctuated and NO_2^- - N in water from the cell running at flow rate of 6 L/min was found to be higher than that in the other operational conditions ($n=20$, $p \leq 0.001$) (the data is shown in Appendices B, Table B-2). The nitrate concentration in the five flow cells all indicated a declining trend along with the test (Fig.4.7). No significant differences in nitrate were observed between the different hydraulic regimes ($n=20$, $p \geq 0.130$) (the data is shown in Appendices B, Table B-2). The changing patterns between free ammonia and nitrite concentration was not consistent in all the hydraulic regimes (i.e. a decrease of NH_3-N with the rise of NO_2^- - N). An increase of ammonia (in day 13) was monitored before a quick rise of nitrite production (in day 15) in cell operated with flow rate of 10 L/min (Fig.4.7a). While in cell running at the flow rate of 4 L/min, the change of these two parameters had the same pattern (Fig.4.7d).

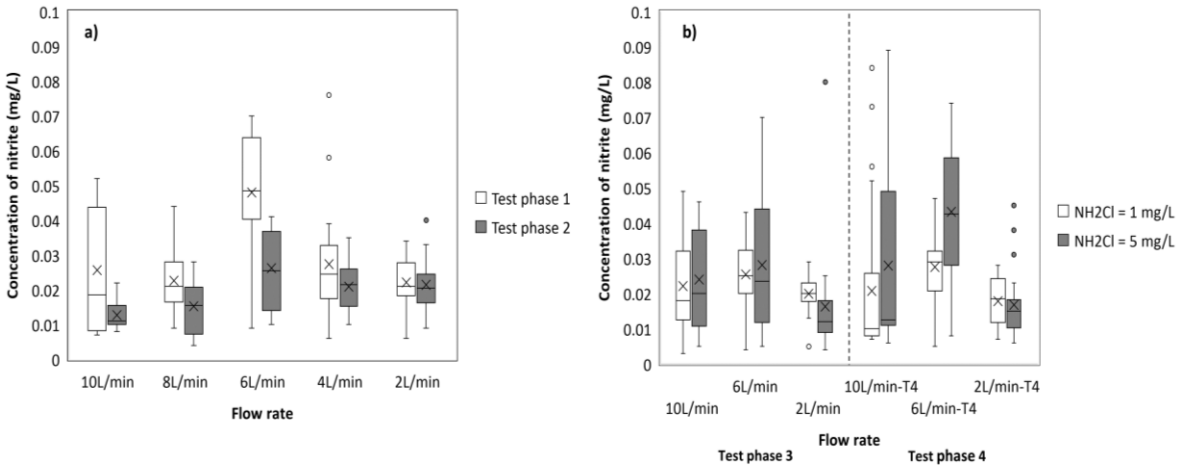

Figure 4.5 The concentration of nitrite in different operational conditions in four test phases. a) for test phase1 and 2; b) for test phase 3 and 4. The colour represents different monochloramine concentration.

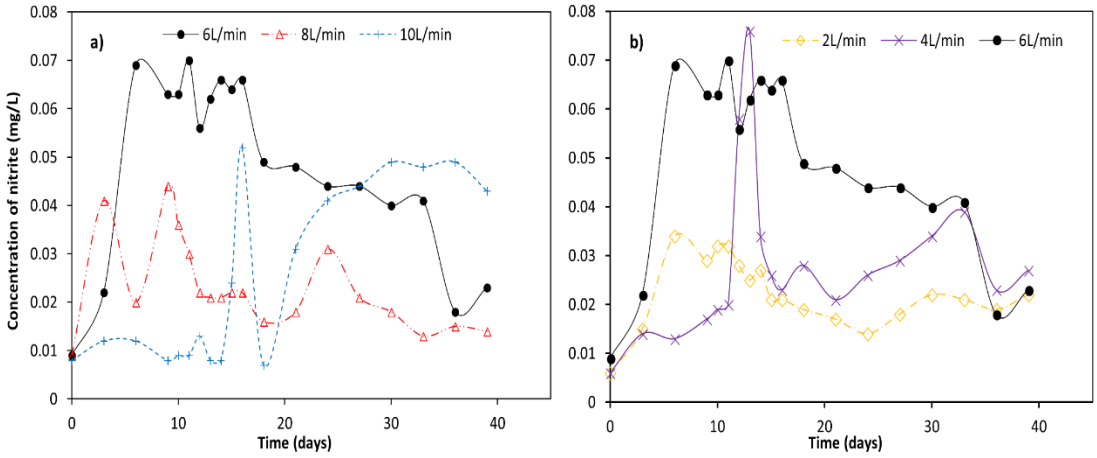

Figure 4.6 Time-series of nitrite measured as mg-N/L at each hydraulic regimes in test phase 1. a) for flow rates of 6, 8, 10 L/min; b) for flow rates of 2, 4, 6 L/min.

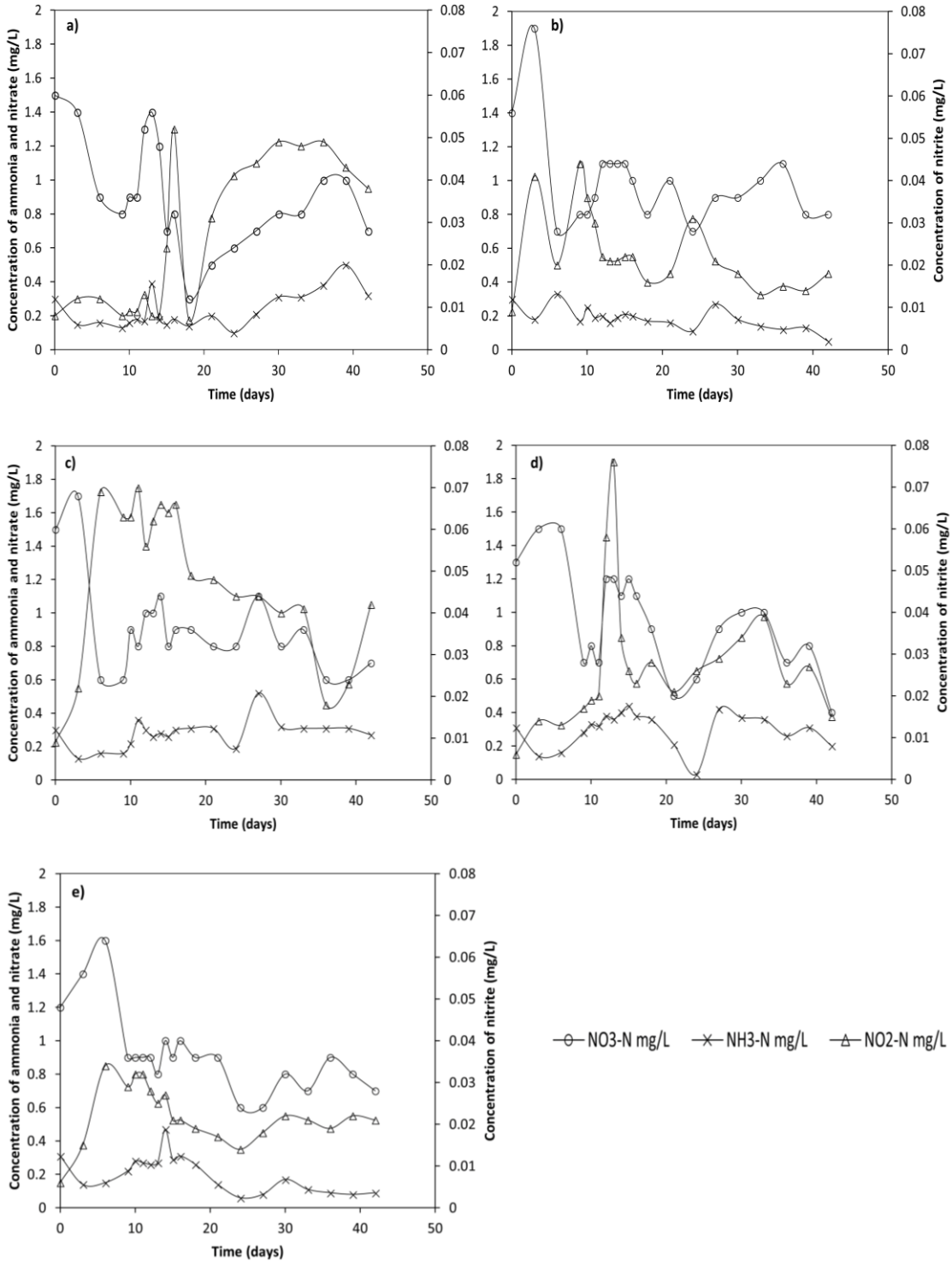

Figure 4.7 Time-series of nitrate, nitrite and ammonia measured as mg N/L at each hydraulic regime in test phase 1. a) for flow rate of 10 L/min; b) for flow rate of 8 L/min; c) for flow rate of 6 L/min; d) for flow rate of 4 L/min and e) for flow rate of 2 L/min.

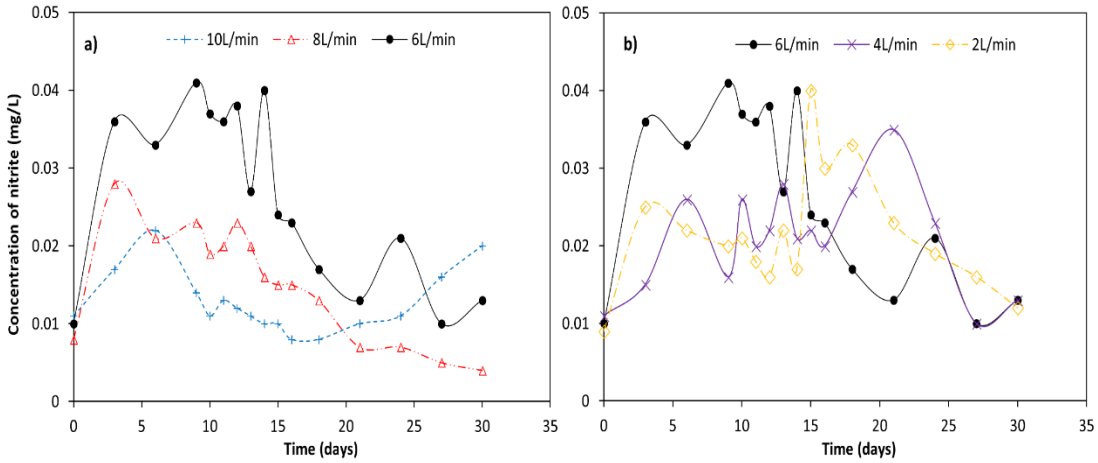

Figure 4.8 Time-series of nitrite measured as mg-N/L at each hydraulic regimes in test phase 2. a) for flow rates of 6, 8, 10 L/min; b) for flow rates of 2, 4, 6 L/min.

To assess whether optimizing the chlorine to ammonia mass ratio can control nitrification, a higher Cl_2/NH_3-N mass ratio (5:1) was applied in test phase 2 compared with that in test phase 1 (3:1). Similar to the observation in phase 1, the concentration of nitrite in all the hydraulic regimes varied with time and nitrification process was suggested to exist in all conditions (average nitrite above 0.015 mg/L) (Fig.4.5a). The production of nitrite was observed to decline with the increase of flow rate from 6 to 10 L/min ($n=16$, $p\leq0.006$) (the data is shown in Appendices B, Table B-3). However, hydraulic regimes below 6 L/min did not affect nitrite production during the test period ($n=16$, $p\geq0.119$) (the data is shown in Appendices B, Table B-3). In terms of ammonia and nitrite, a pattern of synchronous increase or decrease was observed under the five hydraulic regimes (Fig.4.9). In addition, unlike the corresponding decline of ammonia relative to the increase of nitrite in the first three days of experiment in test phase 1 (Fig.4.7), the concentration of ammonia remained stable or even increased when an increased production of nitrite was observed within all the flow cells in test phase 2 (Fig.4.9). The concentration of nitrate was not observed to be significantly impacted by the different hydraulic regimes ($n=16$, $p\geq0.204$) (the data is shown in Appendices B, Table B-3).

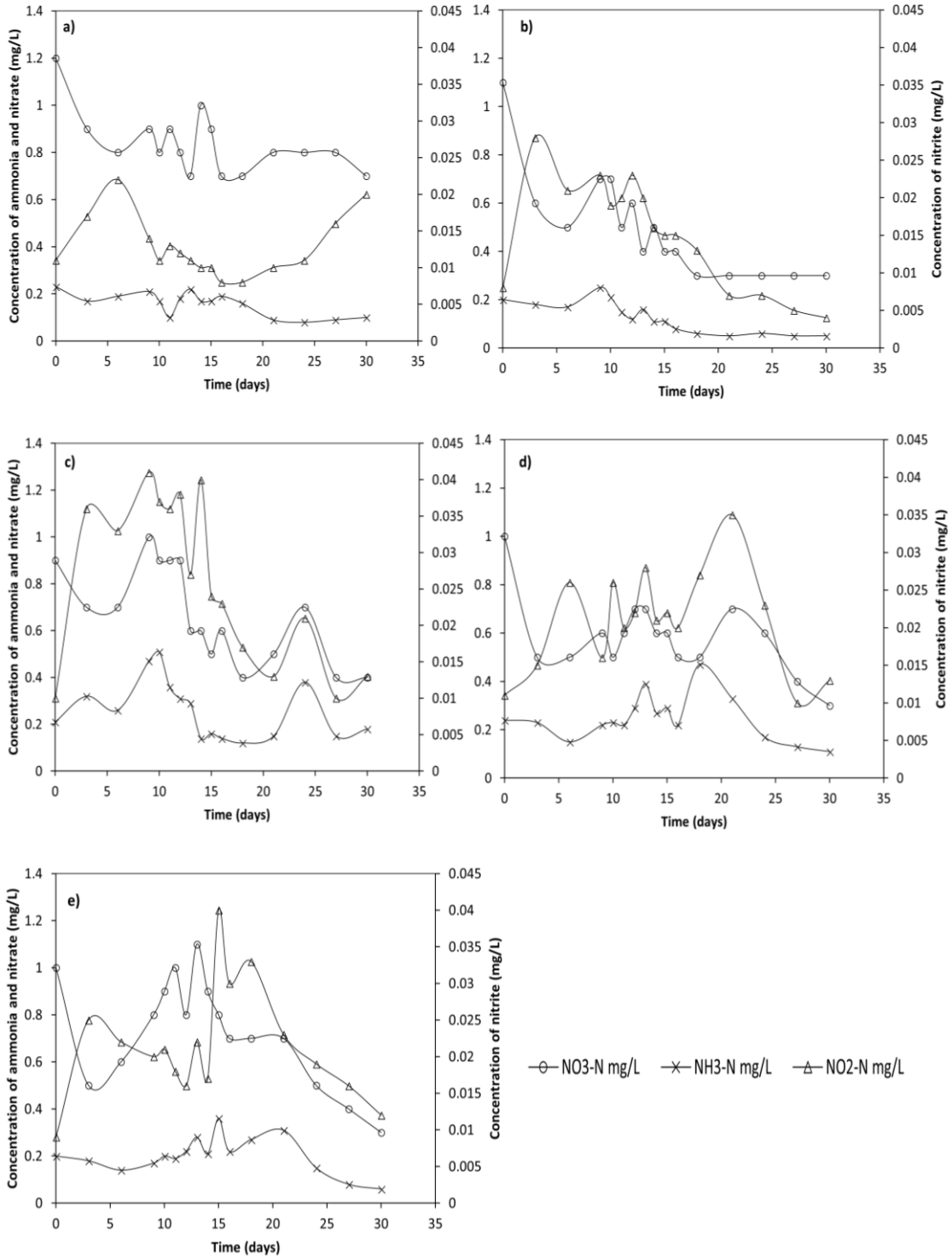

Figure 4.9 Time-series of nitrate, nitrite and ammonia measured as mg N/L at each hydraulic regime in test phase 2. a) for flow rate of 10 L/min; b) for flow rate of 8 L/min; c) for flow rate of 6 L/min; d) for flow rate of 4 L/min and e) for flow rate of 2 L/min.

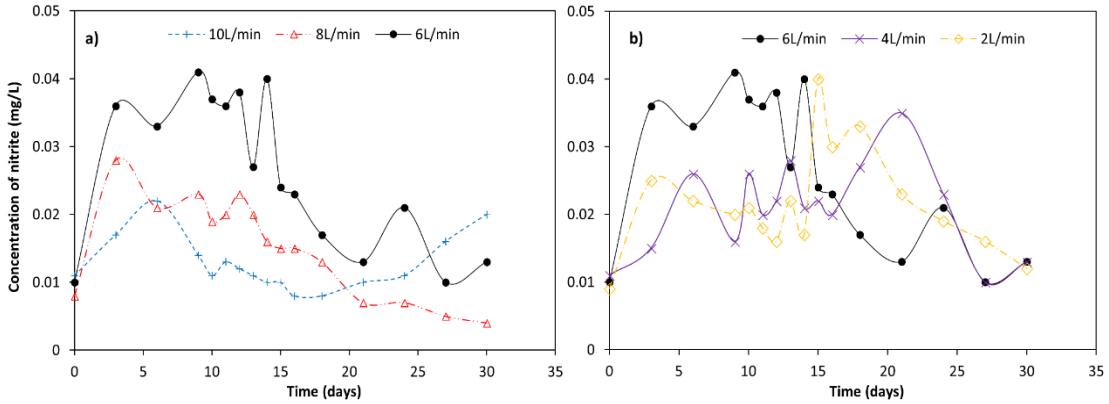

Figure 4.10 Time-series of nitrite measured as mg-N/L at each hydraulic regimes in test phase 3. a) for cells fed with 1 mg/L NH_2Cl (Cl_2/NH_3-N = 3:1) and run with flow rates of 6, 8, 10 L/min; b) for cells fed with 5 mg/L NH_2Cl (Cl_2/NH_3-N = 3:1) with flow rates of 2, 4, 6 L/min.

In test phase 3, three flow cell units were fed with the same water as in test phase 1 and operated at the flow rates of 10, 6 and 2 L/min. From Figs.4.10a and 4.11a, b, c, similar observations to that in phase 1 were found when the cells were running at 6 and 2 L/min. Under these two hydraulic regimes, nitrification was evidenced in the test period and nitrite production was higher in the cell at flow rate of 6 L/min than that in the cell at 2 L/min ($n=17$, $p\leq0.005$) (the data is shown in Appendices B, Table B-4). However, compared with the results from the cell at flow rate of 10 L/min in test phase 1, the increase of nitrite concentration was observed at the beginning of the experiment within this phase. Furthermore, no significant difference in nitrite was found at the flow rate of 10 and 6 L/min ($n=16$, $p\geq0.143$) (the data is shown in Appendices B, Table B-4). This inconsistent observation might be attributed to the difference in the incubated biofilm between these two test phases, although the incubating conditions remained the same with each test phase.

Fig.4.10b and Figs.4.11d, e, f presents the results for the other three flow cells which were fed with higher concentration (5 mg/L) of chloramine but operated at the same three hydraulic regimes. The results indicate that although a fast increase of nitrite concentration was observed later than that in the facility fed with less chloramine, nitrification could not be prevented even under conditions with high concentration of disinfectant. In addition, water from the cell operated at the flow rate of 6 L/min was found to have more nitrite than that in cells running under the other two hydraulic regimes ($n=16$, $p\leq0.049$) (the data is shown in Appendices B, Table B-4). The other two parameters (NO_3^- - N and NH_3-N) were not impacted by hydraulic regimes ($n=16$,

p≥0.134) (the data is shown in Appendices B, Table B-4).

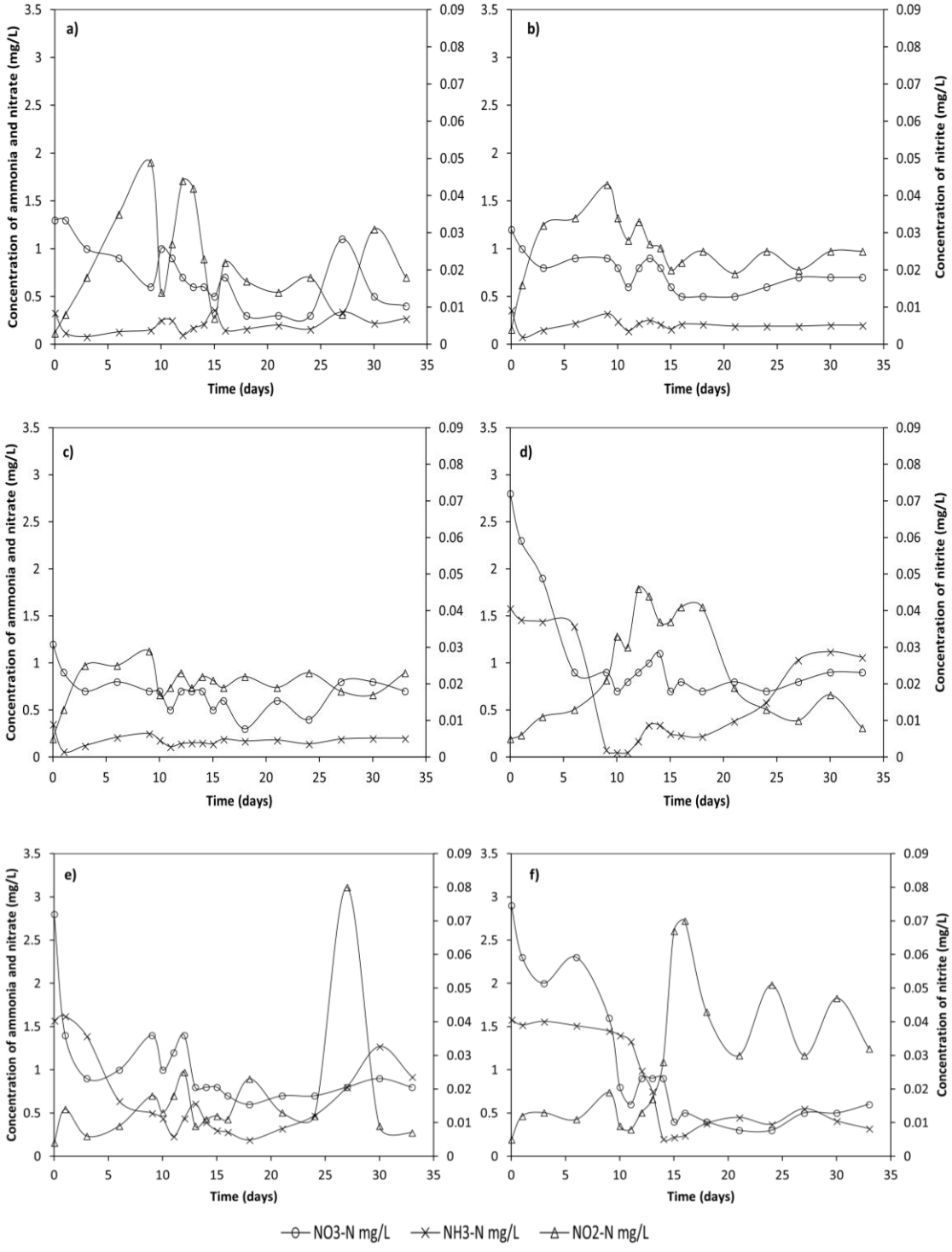

Figure 4.11 Time-series of nitrate, nitrite and ammonia measured as mg N/L at each hydraulic regime in test phase 3. a) for flow rate of 10 L/min (NH_2Cl = 1 mg/L, Cl_2/NH_3-N = 3:1); b) for flow rate of 6 L/min (NH_2Cl = 1 mg/L, Cl_2/NH_3-N = 3:1); c) for flow rate of 2 L/min (NH_2Cl = 1 mg/L, Cl_2/NH_3-N = 3:1); d) for flow rate of 10 L/min (NH_2Cl = 5 mg/L, Cl_2/NH_3-N = 3:1); e) for flow rate of 6 L/min (NH_2Cl = 5 mg/L, Cl_2/NH_3-N = 3:1); f) for flow rate of 2 L/min (NH_2Cl = 5 mg/L, Cl_2/NH_3-N = 3:1).

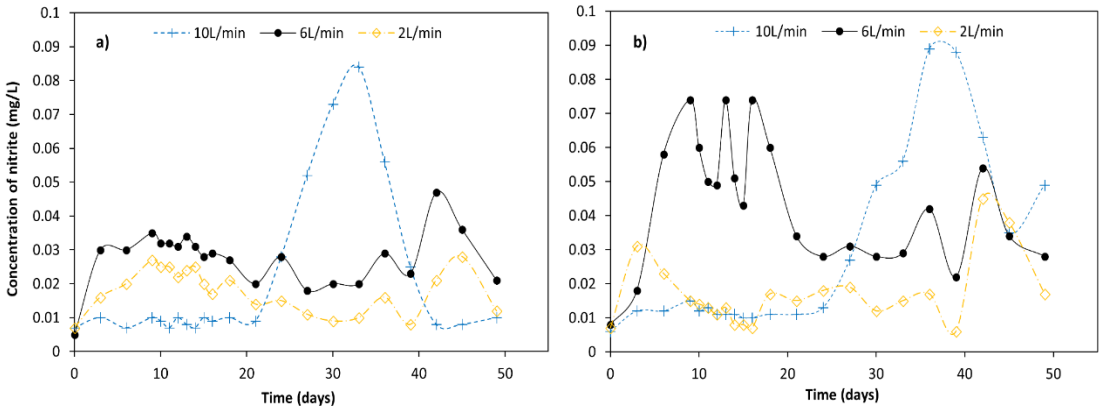

Figure 4.12 Time-series of nitrite measured as mg-N/L at each hydraulic regimes in test phase 4. a) for cells fed with 1 mg/L NH_2Cl (Cl_2/NH_3-N = 5:1) and run with flow rates of 6, 8, 10 L/min; b) for cells fed with 5 mg/L NH_2Cl (Cl_2/NH_3-N = 5:1) with flow rates of 2, 4, 6 L/min.

As a repeat experiment for test phase 2, the results from three flow cells in test phase 4 confirmed the impact of hydraulic regimes on nitrite production when the chloramine concentration is 1 mg/L and Cl_2/NH_3-N mass ratio is 5:1 (Fig.4.12a and Figs.4.13a, b, c). The results showed that the concentration of nitrite in water from the cell with flow rate of 6 L/min was the highest among the three hydraulic regimes ($n=21$, $p\leq0.05$) (the data is shown in Appendices B, Table B-5). However, unlike the consistent low level of nitrite production in cell running at the flow rate of 10 L/min in test phase 2, some outliers that were far above the average value were identified in this phase (Fig.4.5b and Fig.4.12a). This sudden increase of nitrite might be due to the regrowth of nitrifying bacteria within the facility when the disinfectant residual was kept at a low level (<0.1 mg/L), and a higher growth rate than the detachment rate caused by shear forces. The changing patterns of nitrate and ammonia were similar to that in test phase 2.

Flow rate of 6 L/min was suggested to be a condition that promote the production of nitrite when increasing the disinfectant concentration to 5 mg/L in test phase 4 as well ($n=21$, $p\leq0.005$) (the data is shown in Appendices B, Table B-5). However, the peak value of nitrite among the three hydraulic regimes was found in the cell running at the flow rate of 10 L/min (Fig.4.12b). In addition, a significant increase of nitrite concentration was observed earlier (from day 3) in the cell operated at flow rate of 6 L/min than in those running at the other two hydraulic regimes (Fig.4.12b). The concentration of ammonia in cell at flow rate of 6 L/min dropped quicker and then remained constant at a relatively low level along the test when compared with that in cells at the other two flow rates (Figs.4.13d, e, f).

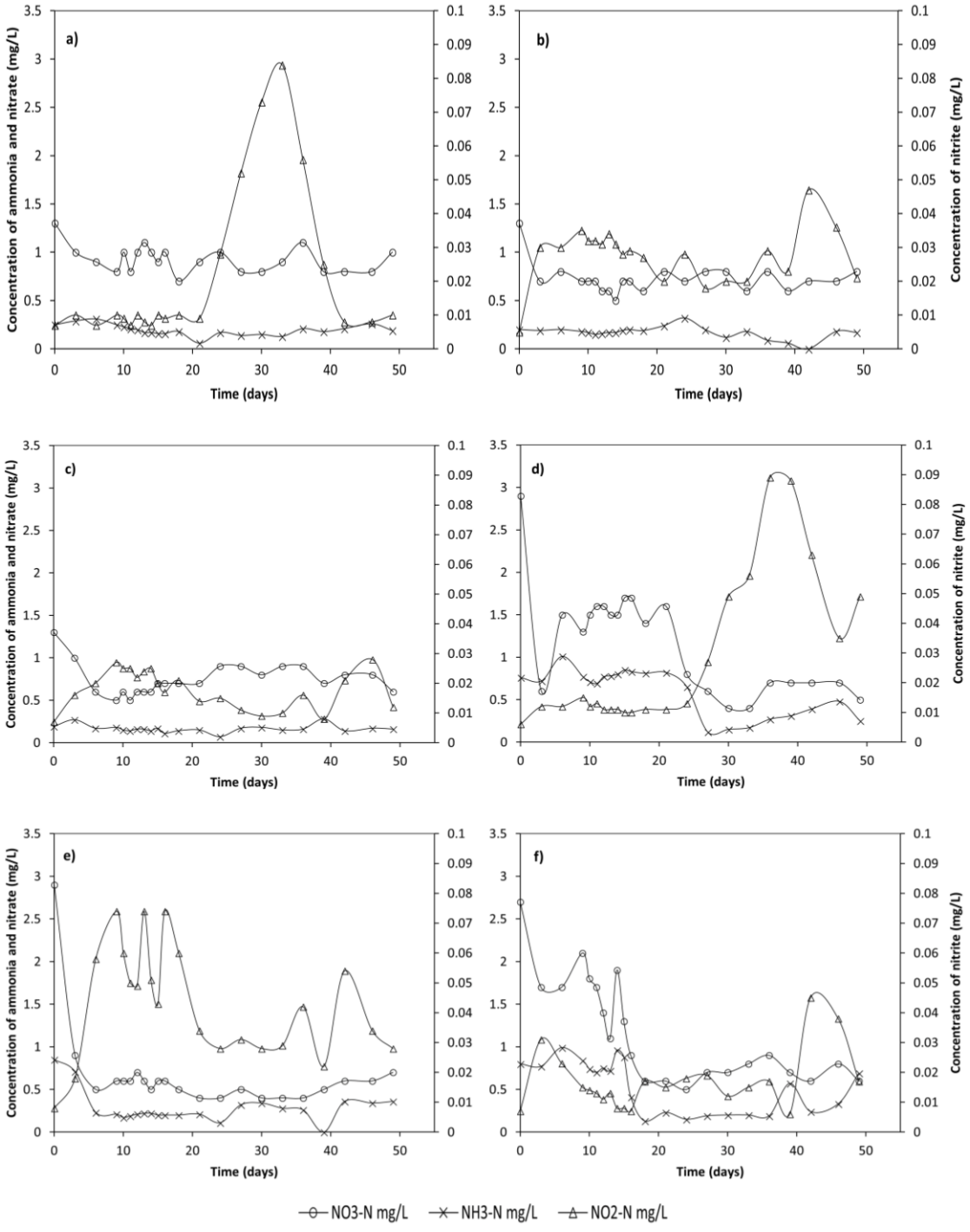

Figure 4.13 Time-series of nitrate, nitrite and ammonia measured as mg N/L at each hydraulic regime in test phase 4. a) for flow rate of 10 L/min (NH_2Cl = 1 mg/L, Cl_2/NH_3-N = 5:1); b) for flow rate of 6 L/min (NH_2Cl = 1 mg/L, Cl_2/NH_3-N = 5:1); c) for flow rate of 2 L/min (NH_2Cl = 1 mg/L, Cl_2/NH_3-N = 5:1); d) for flow rate of 10 L/min (NH_2Cl = 5 mg/L, Cl_2/NH_3-N = 5:1); e) for flow rate of 6 L/min (NH_2Cl = 5 mg/L, Cl_2/NH_3-N = 5:1); f) for flow rate of 2 L/min (NH_2Cl = 5 mg/L, Cl_2/NH_3-N = 5:1).

4.2.3 HPC and Microbial Decay Factor (Fm ratio)

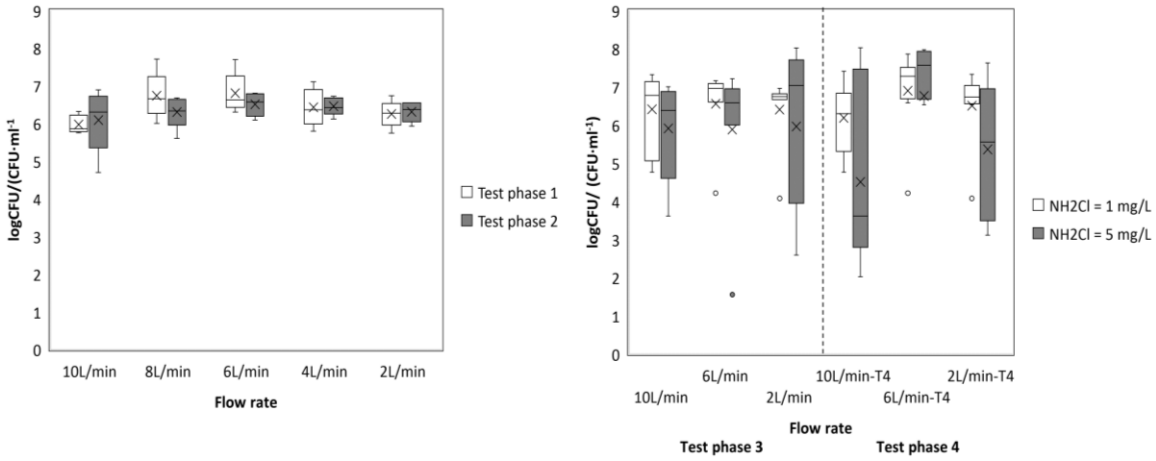

Figure 4.14 Heterotrophic bacteria (HPC) summarized for each operational condition in four test phases. a) for test phase 1 and 2; b) for test phase 3 and 4 and the colour represents different monochloramine concentration.

Heterotrophic plate counts (HPC) were measured at several time points along the four tests and presented as colony forming units (CFU) per ml. Fig.4.14 summarized the HPC results for each operational condition of every test phase as logarithm CFU/ml. For all the conditions, the number of HPC in the water was presented as logarithm growth during the experiment but with different increasing rates. These high values suggested a decrease of water quality. In test phase 1, no significant difference between the hydraulic regime were identified ($n=5$, $p\geq0.117$) (the data is shown in Appendices B, Table B-2), except for the HPC from cells running at the flow rate of 6 L/min and 8 L/min which were found to be more than that in the cell operated at 10 L/min (Fig.4.14a). For the other three test phases, hydraulic regimes did not significantly affect the value of HPC ($p\geq0.059$) (the data is shown in Appendices B, Tables B-2 to B-5). In terms of different disinfectant chloramine concentration (Fig.4.14b), no statically significant difference in HPC was observed in the flow cells that were operated under the same hydraulic regimes ($p\geq0.165$).

Microbial decay factor (expressed as Fm ratio) was used to evaluate the contribution of microorganisms to the total decay of chloramine. In this chapter, as with HPC measurements, the Fm ratio was measured at the same time points as in the test phases. In test phases 1 and 2 (Fig.4.15a), the largest value was observed in cell running at flow rate of 6 L/min ($p\leq0.047$) (the data is shown in Appendices B, Tables B-2 and B-3).

This was verified with the repeat experiments within the test phases 3 and 4 (Fig.4.15b). However, no significant difference in the ratio between different hydraulic regimes was found when changing the feed water with higher concentration of disinfectant ($p \geq 0.127$) (the data is shown in Appendices B, Tables B-4 and B-5). In addition, Figs.4.14 and 4.15 indicate that a greater value of Fm ratio did not always correspond to more heterotrophic bacteria.

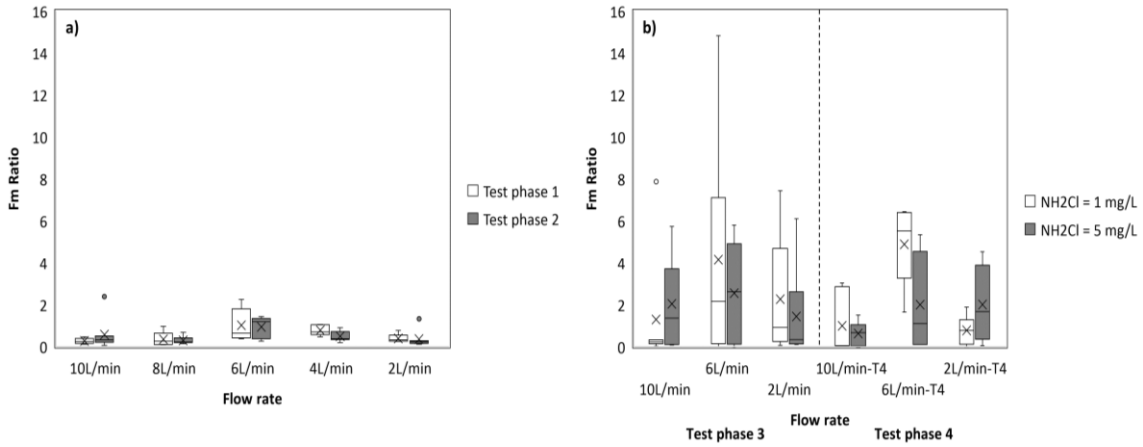

Figure 4.15 Microbial decay factor (Fm ratio) summarized for each operational condition in four test phases. a) for test phase 1 and 2; b) for test phase 3 and 4 and the colour represents different monochloramine concentration.

4.2.4 Correlation analysis

According to the results presented in Fig.4.5, nitrification was observed in the experimental facility used within the current study. In order to identify whether there are correlations between the water quality parameters, and therefore give possible suggestions for monitoring nitrification, the non-parametric correlation analysis was made. Tables 4.1 to 4.4 presents the detailed results of the analysis, which include the Spearman correlation coefficients and the statistical significance for each correlation for the four test phases.

Table 4.1 Non-parametric Spearman correlations between parameters from test phase 1

	Nitrite-N	pH	Turbidity	Chlorine	Nitrate-N	Ammonia-N	TN	TOC	HPC
pH	-0.260**								
Turbidity	0.540**	-0.263**							
Chlorine	0.302**	NS	0.363**						
Nitrate-N	NS	0.343**	NS	NS					
Ammonia-N	0.350**	-0.206*	0.526**	0.394**	0.207*				
TN	-0.353**	0.476**	NS	NS	0.611**	NS			
TOC	0.420**	-0.256*	0.410**	0.409**	NS	0.446**	NS		
HPC	NS	-0.582**	NS	NS	NS	NS	NS	NS	
Fm	0.485*	-0.539**	0.417*	NS	NS	NS	-0.615**	NS	NS

n=100 for nitrite-N, pH, turbidity, chlorine, nitrate-N, ammonia-N, TN and TOC; n=25 for HPC and Fm; **p<0.01, *p<0.05; NS = p>0.05; two-tailed test was used.

Table 4.2 Non-parametric Spearman correlations between parameters from test phase 2

	Nitrite-N	pH	Turbidity	Chlorine	Nitrate-N	Ammonia-N	TN	TOC	HPC
pH	-0.225*								
Turbidity	0.823**	NS							
Chlorine	0.506**	-0.446**	0.612**						
Nitrate-N	NS	NS	NS	0.543**					
Ammonia-N	0.569**	-0.247*	0.792**	0.814**	0.496**				
TN	0.259*	0.238*	0.403*	0.471**	0.763**	0.630**			
TOC	0.745**	NS	0.848**	0.495**	NS	0.661**	0.275*		
HPC	NS	NS	NS	NS	NS	NS	NS	NS	
Fm	NS	NS	NS	NS	NS	NS	NS	NS	NS

n=80 for nitrite-N, pH, turbidity, chlorine, nitrate-N, ammonia-N, TN and TOC; n=25 for HPC and Fm; **p<0.01, *p<0.05; NS = p>0.05; two-tailed test was used

Table 4.3 Non-parametric Spearman correlations between parameters from test phase 3

	Nitrite-N	pH	Turbidity	Chlorine	Nitrate-N	Ammonia-N	TN	TOC	HPC
pH	NS								
Turbidity	0.477**	-0.254**							
Chlorine	NS	0.286**	-0.286**						
Nitrate-N	-0.438**	NS	-0.507**	0.615**					
Ammonia-N	-0.474**	-0.229*	NS	0.207*	0.437**				
TN	-0.530**	NS	-0.269**	0.196*	0.638**	0.833**			
TOC	0.361**	NS	0.632**	NS	-0.189*	NS	NS		
HPC	NS	NS	NS	NS	NS	NS	NS	NS	
Fm	NS	NS	NS	NS	NS	NS	NS	NS	NS

n=108 for nitrite-N, pH, turbidity, chlorine, nitrate-N, ammonia-N, TN and TOC; n=42 for HPC and Fm; **p<0.01, *p<0.05; NS = p>0.05; two-tailed test was used

Table 4.4 Non-parametric Spearman correlations between parameters from test phase 4

	Nitrite-N	pH	Turbidity	Chlorine	Nitrate-N	Ammonia-N	TN	TOC	HPC
pH	-0.313**								
Turbidity	0.607**	-0.318**							
Chlorine	-0.313**	0.220*	-0.491**						
Nitrate-N	-0.616**	0.377**	-0.505**	0.499**					
Ammonia-N	-0.255**	NS	NS	0.412**	0.440**				
TN	-0.456**	0.270**	NS	0.411**	0.599**	0.805**			
TOC	0.572**	NS	0.606**	-0.417**	-0.425**	NS	NS		
HPC	NS	NS	NS	NS	NS	NS	NS	NS	
Fm	NS	NS	NS	NS	NS	NS	NS	NS	NS

n=132 for nitrite-N, pH, turbidity, chlorine, nitrate-N, ammonia-N, TN and TOC; n=47 for HPC and n=36 for Fm; **p<0.01, *p<0.05; NS = p>0.05; two-tailed test was used

Correlations were identified between most of the selected parameters in the four test phases, but the relationship and statistical significance were not consistent. As can be seen in Tables 4.1to 4.4, nitrite-N, turbidity and TOC were positively correlated with each other ($p<0.05$). There were correlations between nitrite-N and ammonia-N and TN as well. However, for nitrite-N and ammonia-N, positive correlations ($p<0.01$) were found in test phases 1 and 2 (Tables 4.1 and 4.2) while the correlation was negative in test phase 3 and 4 (Tables 4.3 and 4.4). For nitrite-N and TN, negative correlations ($p<0.01$) were observed, except in test phase 2, where it was positive ($p<0.05$). Although nitrite-N was not correlated with nitrate-N in the first two test phases, strong negative correlations ($p<0.01$) were found in the test phases 3 and 4. The correlations between nitrite-N and chlorine were not clear, as it was positive ($p<0.01$) in test phase 1 and 2, while no statistical correlation was identified in test phase 3 but turned out to be negative in test phase 4 ($p<0.01$). In addition, ammonia was strongly positively correlated with TN in the later three test phases (Tables 4.2 to 4.4), and there were positive correlations between nitrate and ammonia-N and TN within all the four test phases.

As microbial parameters, HPC or microbial decay factor (Fm) was not correlated with most of the water quality parameters, except few correlations that were observed in test phase 1 (Table 4.1).

4.3 Discussion

4.3.1 Hydraulic impacts on water quality

In the current study, five hydraulic regimes are investigated for their impacts on water quality within chloraminated flow cell facilities, which has been incubated with biofilm and had nitrification established before tests. Although the same incubation conditions were controlled in different flow cell units before testing, significant differences in water quality parameters were found between the cells running at different hydraulic regimes during the test phases. Since biofilm has been incubated before test and the flow rate was the only controlling factor within the single test phase, the difference in water quality might be explained by the impacts of the hydraulic condition on biofilm. In addition, since nitrification has been established before testing and significant difference in nitrite concentration was observed after changing the hydraulic conditions,

the difference in water quality could also be a result of the hydraulic impacts on the nitrification process.

Hydraulic condition is considered to be an influencing factor due to its impact on mass transfer to biofilm, including nutrients, disinfectants, oxygen and microorganisms (Vieira et al. 1993; Beer et al. 1996; Beyenal et al. 2002), and also on biofilm density, composition and structural characteristics (Beyenal et al. 2002; Purevdorj et al. 2002; Abe et al. 2012). However, although researches have investigated the interactions between hydraulics and biofilm under different conditions (LeChevallier et al. 1987; Beyenal et al. 2002; Lehtola et al. 2006), the conclusions varied. For instance, biofilm density was found to be promoted under higher velocity, while nutrient diffusion was inhibited under this condition (Beyenal et al. 2002). In contrast, both increased mass penetration and greater bacterial density were observed within *Pseudomoas fluorescens* culture when incubated with increasing velocity (Vieira et al. 1993). Lehtola et al. (2006) observed similar results within pilot distribution system, where biofilm formation was favoured by increased flow velocity and accompanied with increasing consumption of nutrients.

Within the current study, nitrification was observed and as nitrification is a microbial process, the density and activity of both the nitrifiers and heterotrophic bacteria within the biofilm was hypothesised to affect this process. If the previous theory was true, nitrification would be promoted under higher hydraulic regimes due to the potential increases in density of nitrifying bacteria in the biofilm. However, as the most common indicator of nitrification, the concentration of nitrite was observed to have an increasing trend at the flow rates between 2 and 6 L/min, while it tends to decrease between 6 L/min and 10 L/min (Fig.4.5). Nitrification was observed to be more severe when the flow rate was 6 L/min. In addition, nitrification was inhibited to some degree at the beginning of test in cell units running at the flow rate of 10 L/min (Fig.4.6, 4.8, 4.10, 4.12). This might be explained by the fact that the increasing test flow rate not only promote the nutrient diffusion (especially ammonia for nitrification) into the biofilm, but it also increases the detachment of biofilm to bulk water and hence reduces the available nitrifiers that participated in the nitrification process. The impact of increasing flow velocity on biofilm removal from surface has been observed by Lehtola et al. (2006) and Sekar et al. (2012), who both found a positive correlation between

flow velocity and planktonic cell counts in bulk water. To overcome the detachment force, biofilm tends to respond with an increasing cohesive strength (Paul et al. 2012) and higher microbial growth rates (Liu et al. 2001). In the current study, the flow turbulence was under the transition stage from laminar to turbulent when the flow rate was 6 L/min (Re=3321). Under this condition, biofilm/nitrifier growth could take full advantage of the increasing mass transfer by flow, while their detachment rate was lower than the growth rate. Hence, the most possible favourable hydraulic condition for nitrification was observed at the flow rate of 6 L/min within the current study.

Table 4.5 Measured TOC in feed water in test phase 2

Time (day)	TOC (mg/L)
1	1.64
2	0.96
3	2.28
4	1.88
5	1.91
6	1.56
7	1.49
8	1.5
9	1.35
10	1.61
11	1.87
12	1.56
13	1.79
14	2.29
15	1.57
16	1.54
17	1.83
18	1.74
19	1.72
20	1.51
21	1.62
22	1.58
23	1.46
24	1.69
25	1.88
26	2.83
27	2.91
28	2.67
29	1.66
30	2.17

To verify the hypothesis, other water quality parameters related to nitrification potential were evaluated. Though previous studies suggested parameters including pH, turbidity, chloramine residual, ammonia nitrogen, nitrate, TOC and HPC were related to

nitrification process (Odell et al. 1996; Wilczak et al. 1996; Wolfe et al. 2001; Liu et al. 2005; Yang et al. 2008), only TOC and turbidity were observed to have consistent positive correlation with nitrite in all the test phases (Tables 4.1 to 4.4). The organic carbon within drinking water system was suggested to be an indirect stimulating factor in terms of nitrifying bacteria growth, as it could react with chloramine and further reduce the inactivation of nitrifier and support the formation of biofilms (Kirmeyer et al. 1995; Zhang et al. 2010). Based on the water quality data from feed water (Appendices Table B-1) for the current experiment, the TOC within source water was around 1~2 mg/L. Table 4.5 also shows the measured TOC concentration in feeding water in test phase 2. During the tests, there was a great increase of organic carbon in bulk water under all operational conditions observed (Fig.4.4). The source of increasing organic carbon in drinking water system was thought to be the result of increasing HPC (Fig.4.14) in water, and also the release of microbial metabolism materials (Wolfe et al. 1990; Yang et al. 2008; Noguera et al. 2009). In addition, autotrophs, such as nitrifiers could also transfer inorganic carbon to organics and this could partly explain the positive correlation between TOC and nitrite concentration. Similar to the correlation analysis results within the current study, positive correlation between nitrifying bacteria and TOC level was observed as suggested by Zhang et al. (2010), who fed a simulated drinking water system with high/low TOC chloraminated water and the results indicated that nitrification was promoted under higher concentration of TOC. Therefore, the level of TOC in bulk water might be used as an indicator of nitrification potential. Within the current study, the level of TOC was observed to have similar pattern with nitrite between different hydraulic regimes (Fig.4.4). When the flow rate was between 2 and 6 L/min, the TOC concentration was higher than that in the flow cells operated at higher flow rates (8 and 10 L/min. This provides further support for the hypothesis raised above.

Turbidity was monitored as it can reflect water condition by detecting light scattering of fine particles in the flow (Twort et al. 2000). As a water quality indicator, turbidity in water is caused by the presence of suspended materials, such as clay, silt, organic or inorganic matter, plankton and other microscopic organisms (McCoy and Olson 1986; APHA 1998). This was verified from the observation that a significant positive correlation existed between TOC and turbidity in the current study (Tables 4.1 to 4.4).

In addition, similarly with the TOC, increased level of turbidity may be used as another parameter for evaluating water quality issues, such as bacterial or chemical contamination (LeChevallier et al. 1981; McCoy et al. 1986). Specifically, Lipponen et al. (2002) reported an increase of turbidity associated with increasing number of nitrifying bacteria in an investigation within 15 chloraminated DWDSs; it was suggested that turbidity could be an indicator of nitrification. Although the nitrifying bacteria was not measured within the current study, strong positive correlation between nitrite and turbidity was found (Tables 4.1 to 4.4). Together with the monitoring results of nitrite and turbidity, these two parameters followed similar trend between different hydraulic conditions (Fig.4.3 and 4.5). This was different from previous study, which observed increasing turbidity was associated with the detachment of materials from pipe surface caused by increased flow velocity (or shear stress) (Husband et al. 2008). This difference might provide further evidence that the water quality within the current study was mostly affected by hydraulic impacts on nitrification process, rather than directly by the hydraulics itself.

Combined with the discussion above, the hydraulics was supposed to have an impact on nitrification, but the influence could not be explained by simple linear relationship. Nitrification will be severer when potential for promoting it from hydraulic to nitrifying bacteria growth within biofilm was greater than the detachment force brought by increasing shear force. Within the current study, nitrification was suggested to be favoured when the flow rate is 6 L/min (Re=3321), which related to a transforming stage of flow from laminar to turbulent. Combined with the results from flow cell running at turbulent conditions (Q=8 and 10 L/min, Re=4428 and 5535), the potential of nitrification was observed to be inhibited when the flow is turbulent. In other words, without relating to a specific Re number, nitrification potential is suggested to be mainly correlated with the fluid conditions. To verify the results and to have better understand of the phenomenon, the abundance of nitrifying bacteria is suggested to be monitored along the test in further research.

4.3.2 Disinfectant schedule impacts on water quality

Monochloramine was applied as disinfectant within the current study and produced by the combination of free chlorine and ammonia at a mass ratio of 3:1 or 5:1. A 5 to 1

mass ratio would achieve the maximum formation of monochloramine without free ammonia left, while the 3 to 1 mass ratio would ensure monochloramine to be the dominant form, but will result in an excess of free ammonia in the feed water (Fleming et al. 2005, 2008). Due to the nitrifying biofilm been established during the incubation stage within the current study, the higher Cl_2/NH_3 mass ratio was supposed to control nitrification due to the limited amount of free ammonia available (Fleming et al. 2005, 2008). In test phases 1 and 2, the same concentration of total chlorine (1 mg/L) was used but the chlorine to ammonia nitrogen mass ratio was 3:1 and 5:1. In terms of inhibiting nitrification, neither of these two ratios could control the process effectively, and this is in agreement with an industry survey made by Wilczak et al. (1996). However, when considering nitrite data in conjunction with the free ammonia nitrogen data (Figs.4.7 and 4.9), it was noted that at the beginning of test phase 1 ammonia level dropped after a corresponding increase in nitrite concentration, but a converse observation was found in test phase 2. In the repeat experiment within test phases 3 and 4, this phenomenon was also confirmed. The difference was suggested to be caused by whether free ammonia is the major form of total ammonia within water. When the Cl_2/NH_3 mass ratio was 3:1, the extra free ammonia in bulk water would firstly be consumed if nitrification process was on-going, and hence a decrease of free ammonia concentration would be observed. By contrast, due to no free ammonia existing when the Cl_2/NH_3 mass ratio was 5:1, free ammonia would be released from monochloramine either by auto-decomposition or reactions between organic or inorganic species (Valentine 1998). Once nitrification occurred, the release of free ammonia would be promoted and its concentration would increase if the consumption rate was less than the production. Though the initial increase of ammonia before nitrification was reported in previous studies (Liu et al. 2005; Yang et al. 2008), no explicitly discussions about it have been done. From the results within the current study, Cl_2/NH_3 mass ratio was suggested to be a factor to be considered, especially for utilities using ammonia as nitrification indicator.

In test phase 1 and 2, the total chlorine maintained in the feed water was 1 mg/L. The chloramine residual dropped dramatically (close to 0.1 mg/L) at the beginning of tests and remained consistently low (<0.05 mg/L) in all conditions. Considering nitrifying biofilm has been established before the tests, the rapid loss of disinfectant was

considered to be the result of reactions involving nitrifiers and heterotrophic bacteria. In addition, the uninhibited nitrification would further increase the decay rate of chloramine (Cunliffe 1991) and hence result in a continuous low level of chloramine. In test phases 3 and 4, a concentration of 5 mg/L monochloramine (measured as total chlorine) was applied for investigating whether nitrification could be controlled by higher disinfectant. Liu et al. (2005) suggested that nitrification rarely occurred when disinfectant residual was above 1 mg/L and Cl_2/NH_3 mass ratio was greater than 5. However, in the current study though nitrification has been inhibited for a period within some instances, especially when the Cl_2/NH_3 mass ratio was 5 (Figs.4.10b and 4.12b), the increase of nitrite was monitored after the drop of chloramine residuals (Fig.4.16a). Once nitrification occurred, the produced nitrite further accelerated the decay of chloramine and the residual decreased to a low level. This could be explained by the high resistance ability of nitrifiers to disinfectant, which was observed to survive in the system with more than 5 mg/L monochloramine dose (Cunliffe 1991). Furthermore, in flow cells running at the flow rate 6 L/min, the chlorine residual declined extremely fast at the beginning of the test and the nitrification process could not be controlled at all (Fig.4.16b). This observation suggested that hydraulic regime could be another factor inhibiting the disinfection efficiency, as the nitrite production rate is high enough to consume chloramine and hence accelerate disinfectant decay under a specific range of hydraulic conditions. The results in the current study proved that increasing chloramine amount is an inefficient control method, and this has also been reported in full-scaled utilities experiencing nitrification (Odell et al. 1996), where disinfectant residuals could not be regained easily once lost and the activity of nitrifying bacteria was observed to increase simultaneously. The difficulty in controlling on-going nitrification was emphasized in the current study and a long-term efficient management method is urgently required.

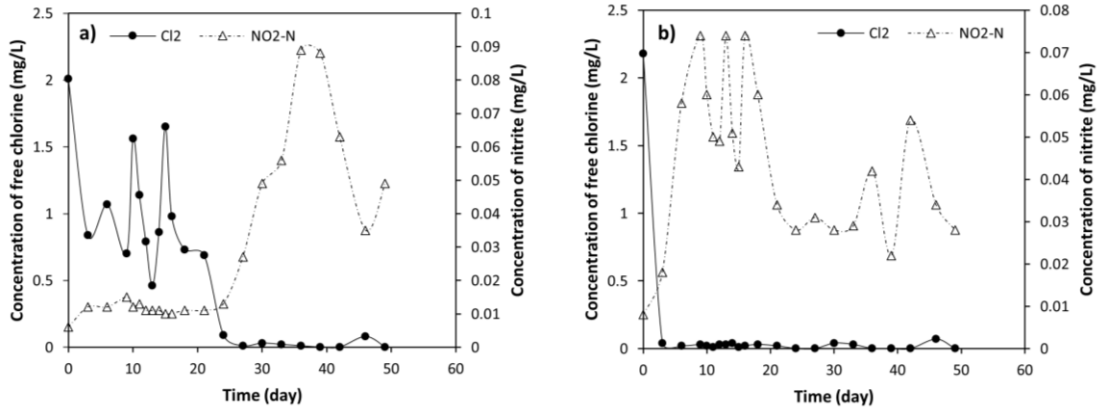

Figure 4.16 Free chlorine and nitrite concentration measured in flow cell operated with different flow rates in test phase 4. a) for flow cell running at 10 L/min and fed water with total chlorine concentration of 5 mg/L; b) for flow cell running at 6 L/min and fed water with total chlorine concentration of 5 mg/L

In addition to the previous discussion, although nitrification was observed under all operational conditions within the current study, increasing the flow rate to turbulent conditions and increasing the disinfectant residual simultaneously within DWDSs could still be considered as a joint method for controlling nitrification. Lower flow rate was not proposed (i.e. 2 L/min) for the reason that other water quality problems could be associated with increase of hydraulic retention time (Machell et al. 2009; Tinker et al. 2009), although the level of nitrite produced under the lower flow rate was relatively low based on the current results. The failure to inhibit nitrification for a long-term in flow cells operated with flow rate of 10 L/min and fed with 5 mg/L monochloramine within the current study was thought to be due to the long water age (3 days). This water age was thought to be the worst scenario in real systems, but it was chosen for the purpose of magnifying the physico-chemical changes of water quality under different operational conditions. To further verify the proposed management method, shorter water age is required to minimize the decline in disinfectant residual caused by the extended residence time (Machell et al. 2009). In addition, as turbulent flow (flow rate = 10 L/min, Re = 5535) was suggested to inhibit nitrification process to some degree within the current experimental facility, whether this fluid condition works in real systems requires further investigation.

4.3.3 Evaluate water quality indicators of nitrification

As mentioned in Section 4.3.2, several water quality parameters related to nitrification were monitored along the tests. pH was suggested to be a significant factor influencing

nitrification (Odell et al. 1996; Wilczak et al. 1996; Wolfe et al. 2001) and can work as a nitrification indicator since hydrogen ion would be produced during the oxidation reactions involving AOB and ammonia (Wilczak et al. 1996). A shift of pH toward lower value would be expected if this reaction takes the major place. Within the current study, a negative correlation was found between pH and nitrite concentration in three of the four test phases (Tables 4.1 to 4.4). Meanwhile, from Fig.4.1, although the difference in pH between the different operational conditions was found, no clear corresponding relationship to nitrification potential was observed. This result supports the possible function of pH in predicting nitrification. However, in terms of evaluating nitrification potential, pH value was not considered as a sensitive parameter due to the fact that it would be affected by various physico-chemical or microbial process, rather than nitrification on its own.

The accelerated loss of disinfectant residual is regarded as the major consequence of nitrification and suggested to be the early indication of nitrification (Burlingame and Brock 1985; Wolfe et al. 1988; Wilczak et al. 1996). However, from the correlation analysis, except the negative correlation between free chlorine and nitrite concentration found in test phase 4 (Table 4.4), it was surprising to observe that free chlorine was positively correlated with nitrite concentration in test phases 1 and 2 (Tables 4.1 and 4.2), while no significant correlations were found in phase 3 (Table 4.3). The positive correlations found within the current study might be due to the fact that nitrifying biofilm has been established before testing and then both the produced nitrite, microorganisms and organic matters would expedite the decay of chloramine. Since chloramine is decomposed to free chlorine and ammonia, more chlorine will be released when there is more nitrite. A positive correlation might occur when the production rate of nitrite was higher than the rate of loss of free chlorine. If this explanation was verified, the correlation analysis results found in test phase 3 could be expected as the result of the rapid loss of free chlorine and its later impact on nitrification was negligible. According to the inconsistent correlations observed within current study, the level of disinfectant residual might be taken as a predictor of nitrification or an indicator of water quality decline, but it was suggested not to be an effective parameter to evaluate nitrification potential within systems experiencing nitrification.

Nitrate was another reaction outcome from nitrification process and hence its increase is normally used as an indicator of nitrification within DWDSs. However, without indicating the correlation with nitrification potential, the concentration of nitrate was observed to decline under all operational conditions (Figs.4.7, 4.9, 4.11, 4.13). Although nitrate is suggested not to be as sensitive as nitrite to nitrification since it has more background variability from source water variations, the trend found in the current study was not expected. A probable explanation for this phenomenon is the possible existence of denitrifying bacteria in the system. Theoretically, the living of denitrifying bacteria always requires an anaerobic condition. Within the current study, the general environment during tests within the flow cell units was suggested to be aerobic through regular dissolve oxygen measurement (data shown in Appendices B, Table B-2). However, anaerobic environment might still occur at some potions within the systems, such as the attaching surface between coupon and the walls of flow cell units. Meanwhile, the abundance of NOB was limited and hence nitrate was continuously consumed. This hypothesis was partially supported by the positive correlation identified between nitrate and total nitrogen (Tables 4.1 to 4.4), as nitrate was supposed to transform to nitrogen by the denitrifying process, and hence a loss of total nitrogen was associated with the release of nitrogen gas. However, further microbial analysis regarding these specific bacterial groups is required for confirmation.

A decrease of total ammonia is suggested to be a consequence of nitrification and can work as the indicator associated with the change of nitrite/nitrate (Wilczak et al. 1996). However, together with the inconsistent correlation between nitrite and free ammonia (Tables 4.1 to 4.4), and the different responses of free ammonia to nitrification process observed within the current study, the concern about whether ammonia could be an effective nitrification indicator was raised again. This result was not a surprise as previous researches have reported the difficulties of using ammonia as nitrification indicator in practice (Wilczak et al. 1996). Based on a simulation model by Yang et al. (2008), the ammonia levels could either increase, decrease or not change during a nitrification event (Fig.2.4), and this was consistent with the observation in the current study (Figs.4.7, 4.9, 4.11, 4.13). This uncertainty trend of ammonia concentration could be attributed to the measurement taken at various stages of nitrification and hence the change of ammonia was not suggested to predict nitrification without considering other

main indicators.

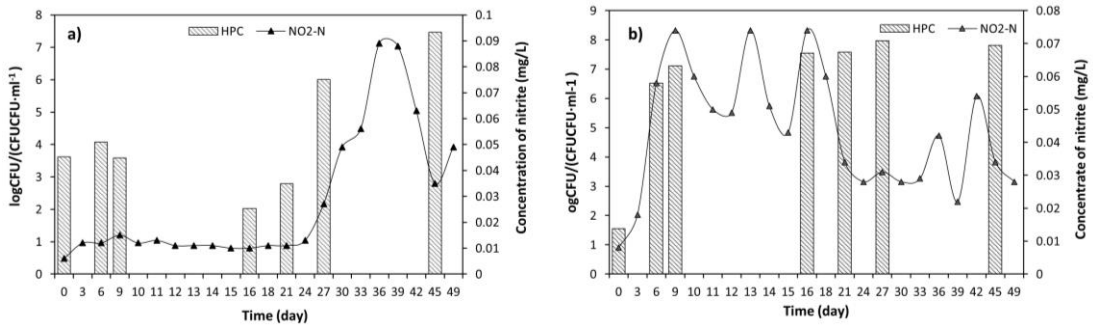

Figure 4.17 HPC and nitrite concentration measured in flow cell operated with different flow rates in test phase 4. a) for flow cell running at 10 L/min and fed water with total chlorine concentration of 5 mg/L; b) for flow cell running at 6 L/min and fed water with total chlorine concentration of 5 mg/L

The increase of HPC, which is suggested to be as a result of nitrification or a promoting factor to this process was considered as an important indicator in terms of predicting nitrification (Wolfe et al. 1990; Wilczak et al. 1996). Within the current study, logarithm increase of HPC was observed in all the operational conditions, and the rate of increase was extremely high when nitrite concentration began to increase (Fig.4.17). Once nitrification occurred, the growth rate became relatively stable and no significant change of HPC was observed. In addition, no correlation was found between HPC and nitrite concentration within the current study. These observations confirmed the role of HPC in predicting nitrification, but suggested a weaker function of evaluating nitrification potential within utilities experiencing nitrification. However, in terms of explaining the fluctuation of nitrite monitored within the experimental facilities, this stable high level of heterotrophic bacteria in water could be considered as a factor since heterotrophs could outcompete nitrifying bacteria, especially at the nutrient limited conditions of drinking water systems. This explanation was supported by previous studies, which reported a better capacity of heterotrophs to utilize dissolve oxygen (Grady et al. 2011) and ammonium (Rosswall 1982) than nitrifiers. Furthermore, the C/N ratio increased with increasing level of TOC in the current study (Fig.4.4). According to the theory raised by Verhagen (1991), the activity of nitrifying bacteria could be inhibited at higher C/N ratio due to the stronger affinity of heterotrophic bacteria with ammonia.

Microbial decay factor (Fm ratio) was firstly introduced by Sathasivan et al. (2005), who suggested this factor could indicate the presence of AOB activity by determining

microbial contribution to total chloramine decay (Sathasivan et al. 2008). If this works, an increase of Fm ratio would be observed to be associated with the occurrence of nitrification, and its value could reflect the nitrification potential to some extent. Within the current study, similar to the results from a batch test made by Sawade et al. (2016), the increases of Fm ratio was monitored in some cases where nitrite concentration increased (Fig.4.18), however, no significant correlation was found between its value and nitrite (Tables 4.1 to 4.4). In addition, low value of Fm (<0.1) was observed in cell units with severe nitrification (Fig.4.18), suggesting that this factor might not be an effective tool to predict nitrification. Considering the mechanism of this method, which assumed AOB activity was the main microbiological cause of chloramine decay, the results obtained in the current study do not seem to be in agreement. The low value of Fm ratio in conditions with severe nitrification (nitrite>0.05mg/L) might have resulted from high concentration of soluble microbial products remaining within the water sample (Krishna et al. 2012), and oxidation reactions between chloramine and nitrite (Krishna and Sathasivan 2010). Despite the inefficiency of Fm ratio in predicting nitrification, the high chloramine decay rate measured in the 0.2μm filtered water strongly emphasized the difficulty of maintaining chloramine residual in systems with nitrification, and the importance of finding solutions to isolate or stop the formation of materials accelerating chloramine decay in further study.

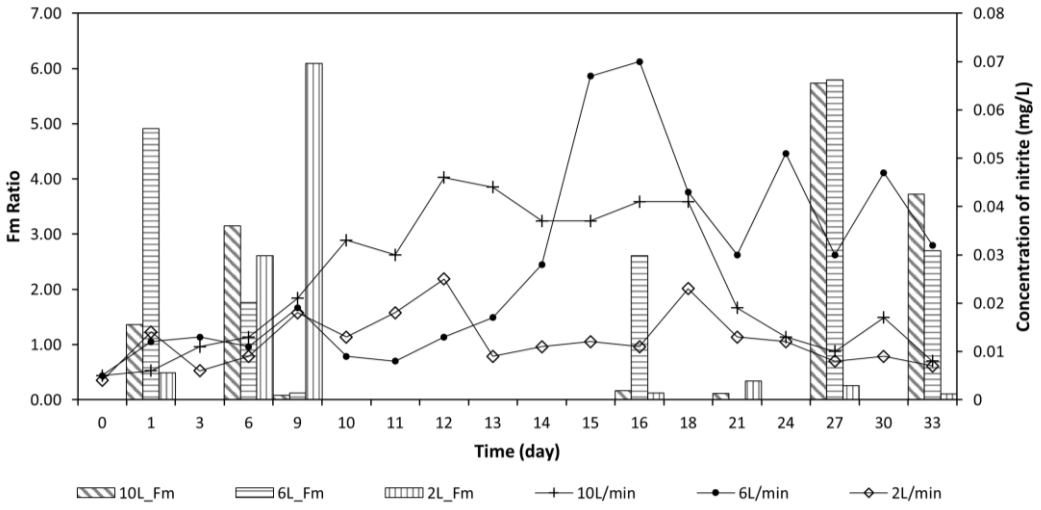

Figure 4.18 Fm ratio and nitrite concentration measured in flow cells operated at different flow rates and fed water with total chloramine concentration of 5 mg/L. The lines with different markers represent nitrite concentration measured at different flow rates; The column filled with different pattern represent the Fm ratio measured under different flow rates.

Based on the current analysis, nitrification could not be predicted based on any single water quality paratmeter, especially when nitrification has occurred within facilities, the difficulty of evaluating nitrification potential increased. Nevertheless, using nitrite concentration, together with turbidity and TOC, might be considered as a way to assess the extent of nitrification through the results from the current study. This suggestion was contrary to (Wilczak et al. 1996), who did not detect an obvious change of turbidity or TOC in nitrifying drinking water sites. Therefore, further research is required to investigate whether these suggested nitrification indicators can be universally applied within different utilities.

4.4 Summary

Maintaining water quality and sufficient disinfectant residual in chloraminated DWDSs was challenged by the nitrification process. To suggest efficient control strategies, operational conditions including hydraulic regimes and disinfectant schedules were controlled within the flow cell experimental facilities, and four test phases were conducted to investigate their impacts on nitrification process. Based on the results, the main outcomes are summarized below:

- Hydraulic regimes have effect on nitrification process and it was suggested to influence it via affecting the nutrient transfer rate to biofilm enriching with nitrifiers and biofilm adherence/detachment in facilities.
- Although no direct linear relationship was observed between nitrification extent and hydraulic conditions, nitrification potential was found to be most severe when the flow rate was 6 L/min, while it tended to be weaker under 10 L/min. Considering the effects of fluid condition on biofilm, the activity of nitrifying bacteria was hypothesised to be favoured when the fluid flow is transforming from the laminar stage to the turbulent stage ($2300<Re<4000$).
- Increasing total chlorine and ammonia nitrogen mass ratio from 3:1 to 5:1 was not suggested to be as an effective nitrification control strategy. On the other hand, the different response of ammonia to the change of nitrite observed between these two ratios might explain why the changing pattern ammonia varied in different utilities before nitrification.
- Increasing total chlorine concentration was found to inhibit nitrification for a

short period in some cases, while it was totally inefficient in the cell running at the flow rate of 6 L/min. Combined with the less severe nitrification that was observed in the flow cells operated at higher flow rate (10L/min), a joint action is suggested to control nitrification by increasing both flow turbulence to a proper range and chloramine concentration within DWDSs.

- To indicate nitrification, water parameters including pH, free chlorine residual, nitrite, turbidity, TOC and HPC were found to be efficient. In terms of evaluating nitrification extent in systems experiencing nitrification within the current study, it was feasible by taking into account nitrite, turbidity and TOC together.
- It was found that ammonia and nitrate were parameters that could neither predict nor indicate nitrification from the current results. Microbial decay factor (Fm ratio) was also suggested not to be an efficient tool to predict nitrification event, but its low value measured from severe nitrifying water indicated microbial community was not the only main cause of microbiological chloramine decay.

The results reveal the effect from hydraulic regimes on the nitrification process. The findings highlight the difficulty in controlling nitrification, but also provide information for water utilities to propose possible nitrification control method. Further research is required to verify the suggested strategy in various facilities.

Chapter 5 Influence of operational conditions on bacterial structure and composition in an experimental flow cell system

5.1 Introduction

Chloramine is the secondary disinfectant used within DWDSs for managing water quality. Due to its low contribution to the formation of disinfectant by products and also relatively stable chemical properties, chloramine is increasingly applied worldwide. However, maintaining the chloramine residual to secure water quality in the DWDSs is still a challenge due to its own decomposition process and more significantly, the chemical decay caused by microbial metabolites. As a result, it is urgently required to have a comprehensive understanding of the microbial community composition and structure in chloraminated systems. In the current study, biofilm and bulk water sample were collected from a flow cell experimental facility, which was fed with chloraminated water, and was run at different hydraulic regimes. Two test phases were undertaken in this system and five different hydraulic regimes and two Cl_2/NH_3-N mass ratios were applied. Genomic DNA from biofilm and bulk water from each flow cell unit running at different operational conditions was subjected to a next generation sequencing (NGS) analysis by Illumina MiSeq. The overall aim of this chapter was to investigate the impact of operational conditions, including hydraulic regimes and Cl_2/NH_3-N mass ratio on bacterial community composition and structure in biofilm and bulk water.

5.2 Results

Following the method for analysing sequences (Section 3.7.4), the results of both the alpha- and beta- diversity analysis are presented herein. In addition, in order to investigate the relationships between the water physico-chemical variables and relative sequence abundance at class level within the biofilm samples, non-parametric

Spearman's rank correlation coefficients were calculated using PASW Statistics 18.SPSS.

5.2.1 Water physico-chemical analysis

As shown in Table 5.1, pH value was maintained at weakly alkaline conditions (7.54~8.28) for all the flow cell units within the two test phases. Free chlorine level dropped significantly due to the disinfectant decay. The concentration of nitrite nitrogen, TOC and TN all increased after the tests and were different for each hydraulic regime. Due to on-going nitrification in the simulated experimental facility, the level of free ammonia nitrogen declined in most of the cases. Turbidity was found to be higher for flow cells running with higher flow rates.

It should be noted that Table 5.1 only lists the measured data before and after the test, although there was variation of the water physico-chemical parameters during the test process. These were previously discussed in Chapter 4.

Table 5.1 Physico-chemical properties of bulk water from the flow cell facility before and after test

	Test code	pH	Shear (N/m^2)	Turbidity (NTU)	Free Cl2 (mg/L)	NO_2^--N (mg/L)	NH3-N (mg/L)	NO_3^-N (mg/L)	TOC (mg/L)	TN (mg/L)
Test phases 1	2A	8.14	0.05	0	0.72	0.006	0.31	1.2	2.38	2.119
		8		4	0.08	0.021	0.09	0.7	2.98	1.208
	4A	8.16	0.1	0	0.81	0.006	0.31	1.3	2.18	2.119
		7.79		7	0.1	0.015	0.20	0.4	3.2	0.5447
	6A	8.23	0.15	0	0.9	0.009	0.30	1.5	2.85	2.214
		8.11		17	0.13	0.042	0.27	0.7	3.97	1.097
	8A	8.27	0.2	0	1.08	0.009	0.30	1.4	1.19	2.111
		8.22		6	0.05	0.018	0.05	0.8	2.45	1.636
	10A	8.28	0.25	0	0.98	0.008	0.30	1.5	2.72	2.164
		7.96		28	0.16	0.038	0.32	0.7	3.7	0.8738
Test phases 2	2B	7.65	0.05	0	0.49	0.005	0.2	1	2.22	1.638
		7.89		1	0.02	0.01	0.04	0.3	4.09	0.248
	4B	7.72	0.1	0	0.5	0.004	0.24	1	2.4	1.743
		7.83		4	0.03	0.012	0.05	0.4	3.9	0.2645
	6B	7.65	0.15	0	0.5	0.005	0.21	0.9	2.35	1.777
		7.88		19	0.11	0.013	0.32	0.5	6.93	0.9285
	8B	7.54	0.2	0	0.64	0.003	0.2	1.1	2.16	1.639
		7.77		5	0.03	0.004	0.06	0.3	3.9	0.2789
	10B	7.80	0.25	0	0.75	0.004	0.23	1.2	2.23	1.852
		7.93		11	0.09	0.021	0.11	0.8	6.11	0.8888

Corresponding to each test code, the above line was data collected before test and the below one was measured after test.

5.2.2 Correlation between physico-chemical data and relative sequence abundance

As shown in Table 5.1, there was no significant correlation between most of the bulk water quality parameters and the relative sequence abundance (RSA), and only a positive correlation identified with the concentration of ammonia nitrogen ($p < 0.05$).

However, significant correlations were observed between several water quality parameters. pH, nitrate-N and total nitrogen (TN) were strongly positively correlated with each other ($p < 0.01$). Ammonia-N was also significantly positively correlated with turbidity and total organic carbon (TOC) ($p < 0.01$).

Table 5.2 Spearman's correlation coefficients for water physico-chemical factors and the percentage of relative sequence abundance at class level within biofilms

	Biofilm							
	RSA	pH	Shear	Turbidity	Nitrite-N	Ammonia-N	Nitrate-N	TOC
pH	NS							
Shear	NS	NS						
Turbidity	NS	NS	NS					
Nitrite-N	NS	0.744*	NS	0.719*				
Ammonia-N	0.648*	NS	NS	0.804**	NS			
Nitrate-N	NS	0.793**	NS	NS	0.785**	NS		
TOC	NS	NS	NS	0.717*	NS	0.781**	NS	
TN	NS	0.842**	NS	NS	0.738*	NS	0.979**	NS

n=10; **p<0.01, *p<0.05, NS = p >0.05; a two-tailed test was used

RSA = Relative sequence abundance at class level.

5.2.3 Comparison of biofilm and bulk water bacterial diversity

As can be seen from Fig.5.1, the dominant bacterial phyla within the biofilms, was *Actinobacteria* followed by *Alphaproteobacteria, Betaproteobacteria*, *Planctomycetia*, *Gammaproteobacteria* and *Cytophagia*. The percentage of each of these bacterial groups varied depending on the particular hydraulic regime and disinfection strategies. These bacteria were also found in the bulk water samples, though with different abundance. Within bulk water, *Alphaproteobacteria* clearly dominated the bacterial community composition (average of total number of samples up to 46%) and to a lesser extent *Betaproteobacteria*, *Actinobacteria* and *Sphingobacteriia* were also abundant (Fig.5.1). At genus level (Fig.5.2), *Mycobacterium*, *Gemmata*, *Legionella* and *Azospira* were predominant within biofilms and *Mycobacterium, Sphingomonas, Sphingobium, Legionella, Flavisolibacter* and *Porphyrobacter* within bulk water samples (Fig.5.2). It should be noted that within the genus detected in the current study, *Mycobacterium, Legionella* and *Sphingomonas* were all considered as opportunic pathogens.

Based on the differential analysis, a total of 48 OTUs were identified as showing

significant difference of relative abundance ($p<0.01$) between biofilm and bulk water samples. Among them, 21 OTUs were clustered at the genus level (Table 5.1).

The alpha-diversity analysis presented both Chao 1 richness estimator and Shannon diversity index of biofilm and water samples. From Fig.5.3, it can be seen that the richness and diversity within biofilms were all higher than that in the bulk water samples.

Non-metric Multi-Dimensional Scaling analysis (MDS) indicates a clear difference between biofilm and bulk water samples (Fig.5.4). The results from UniFrac analysis (both Un-weighted and Weighted) also showed a separation based on sample types (Fig.5.5 and Fig.5.6).

Table 5.3 Differential analysis of relative OTU abundance in class level within biofilm and water samples

P-value	Genus
1.16E-04	*Mycobacterium*
1.16E-04	*Clostridium_sensu_stricto*
1.25E-04	*Dyadobacter*
1.80E-04	*Flavisolibacter*
2.93E-06	*Aquisphaera*
1.43E-04	*Prosthecobacter*
3.20E-05	*Thiobacillus*
1.19E-04	*Aquabacterium*
1.30E-08	*Azospira*
1.85E-11	*Cupriavidus*
3.01E-07	*Azoarcus*
4.74E-06	*Stenotrophomonas*
5.35E-06	*Pseudoxanthomonas*
5.89E-10	*Hyphomicrobium*
5.19E-07	*Phenylobacterium*
4.78E-07	*Hoeflea*
1.11E-10	*Altererythrobacter*
8.32E-07	*Novosphingobium*
3.55E-08	*Sphingobium*
7.87E-12	*Sphingomonas*
1.22E-03	*Peredibacter*

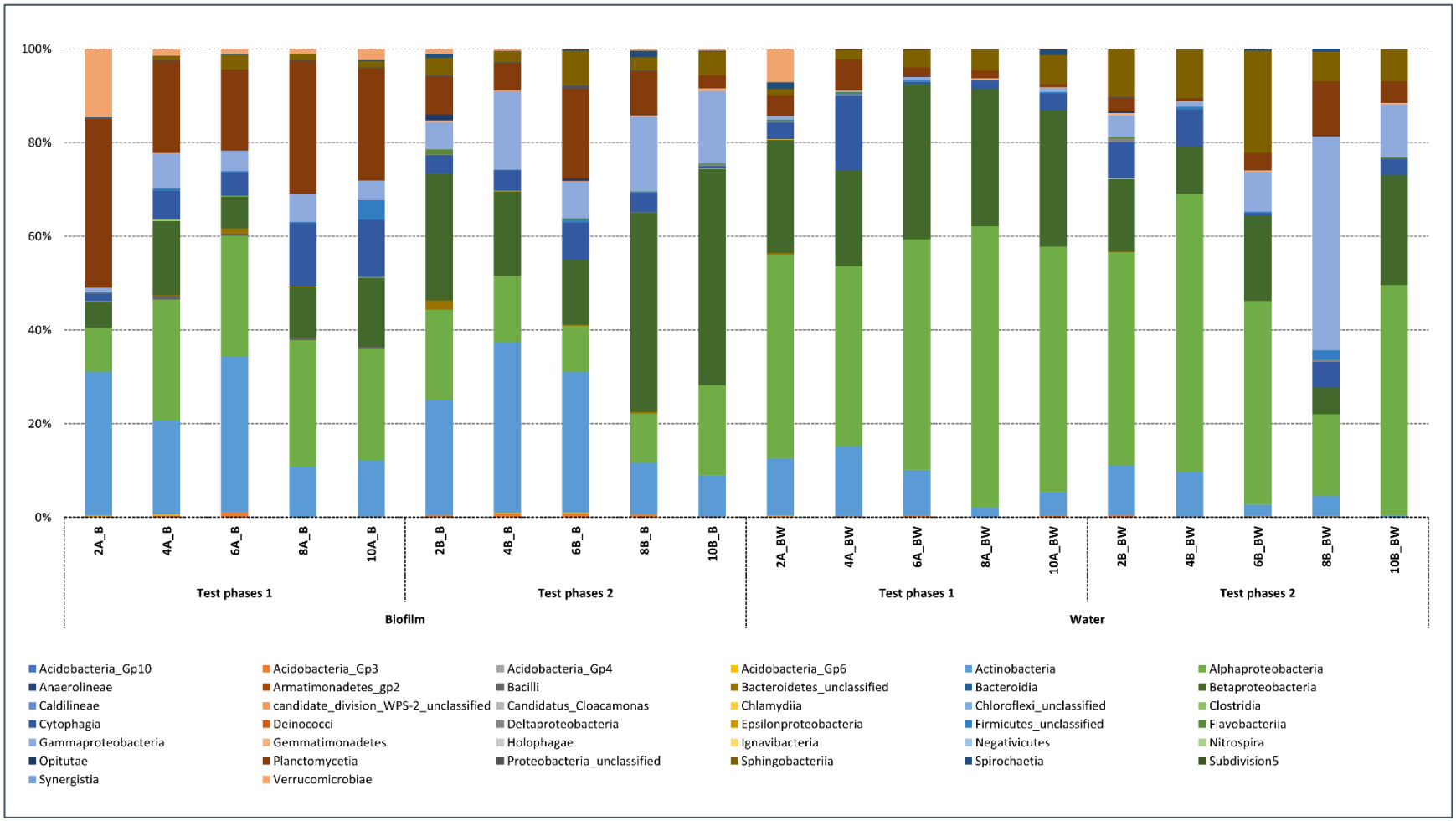

Figure 5.1 Comparison of the relative abundance of the major phylotypes (class level) found in biofilms and bulk water under the different operation conditions.

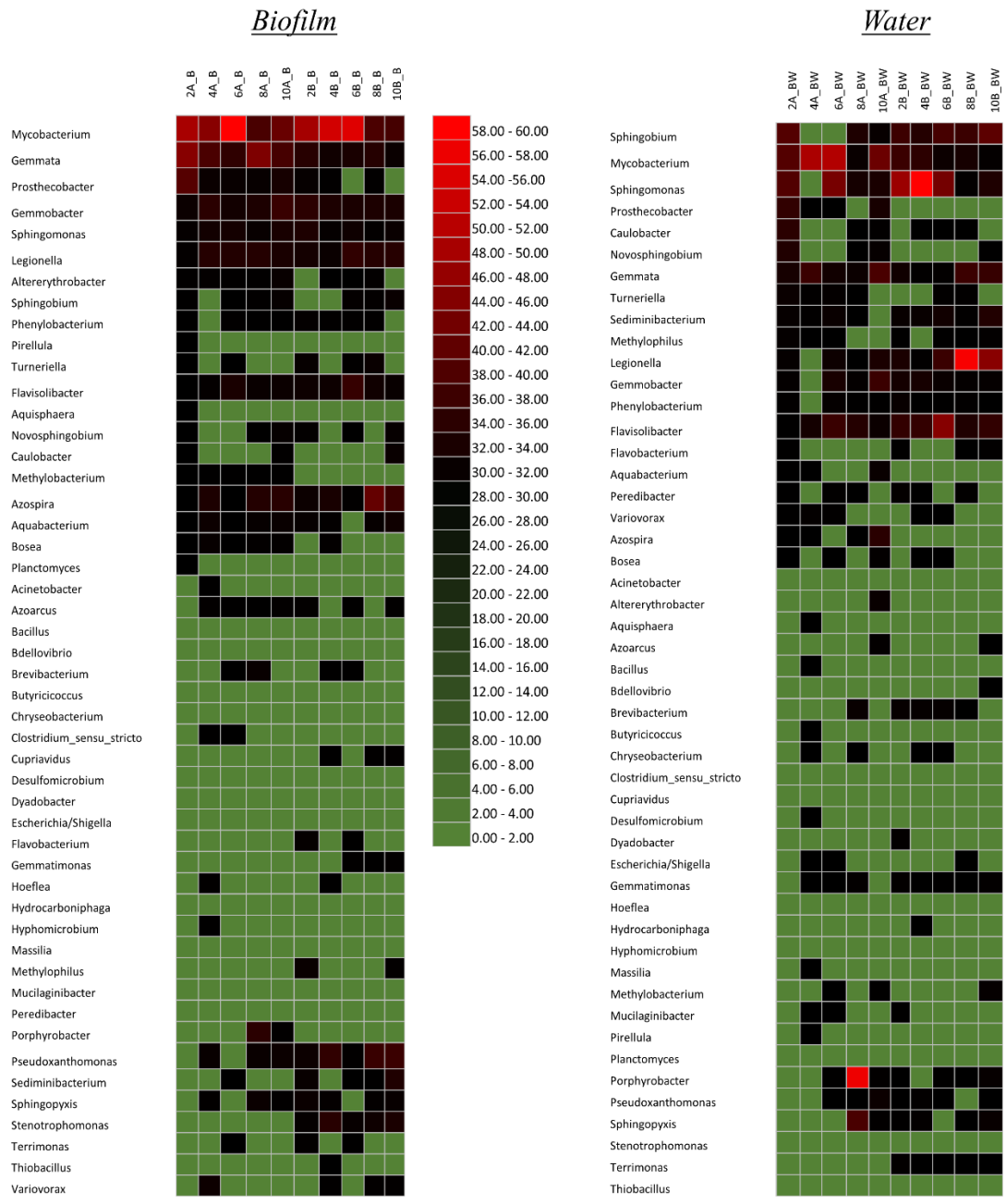

Figure 5.2 Heatmaps show the percentages of most abundant species at genus level within bulk water and bioiflms. A_B (biofilm sample from test phase 1); B_BW (bulk water sample from test phase 2).

5.2.4 Influence of hydraulic regimes on microbial community

In the current study, both biofilm and water samples from different hydraulic regimes shared most of the same components in class level, but the relative abundance differed in most cases. *Planctomycetia* was the predominant group within the biofilms formed under flow rates of 2L/min, 8L/min and 10L/min (36%, 28% and 24% respectively) in test phase 1 (Cl_2/ NH_3 mass ratio = 3:1) samples. While running at 4L/min and 6L/min,

Alphaproteobacteria and *Actinobacteria* were abundant (up to 26% and 33% respectively) (Fig.5.1). However, the structure of the bacterial community differed under most of the hydraulic conditions between test phase 1 and 2. Except in condition with flow rate at 6L/min where *Actinobacteria* remained dominant, the presence of this group increased in cells with flow rate at 4L/min when the chlorine and ammonia mass ratio changed to 5:1 in test phase 2 (from 20% to 36%). On the other hand, *Betaproteobacteria* was found to be more dominant in the rest three cells (from 6%, 11% and 15% to 27%, 43% and 46%) (Fig.5.1). *Gammaproteobacteria* and *Cytophagia* were the other main predominant phylogenetic groups within the biofilms from test phase 2.

In the bulk water, the different hydraulic regimes did not clearly influence the composition of the water samples at class level. *Alphaproteobacteria* was predominant in most of the samples (except the cells running at 8L/min in test phase 2), followed by *Betaproteobacteria, Sphingobacteriia* and *Actinobacteria* under these different operation conditions. Despite the high similarity found in the distribution of bacterial groups in water samples, *Gammaproteobacteria* was only abundant in the 8L/min in test phase 2 (up to 46%), where Cl_2/NH_3 mass ratio was 5:1 (Fig.5.1).

Mycobacterium was the genus predominant in the composition of most biofilm samples, especially in cells running at 6L/min (total up to 60%). The microbial composition differed in cells running with flow rate at 8L/min between the two test phases, where *Gemmata* and *Azospira*, were respectively most dominant (Fig.5.2). In the biofilms conditioned at 4L/min, 8L/min and 10L/min in test phase 2, *Pseudoxanthomonas* was more abundant when compared with those in biofilms incubated at the other two hydraulic regimes (2 and 6 L/min). The percentages of these bacterial genera were different between operational conditions but did not show a clear trend (Fig.5.2).

The hydraulic regimes significantly influenced the community composition of bulk water samples at genus level. In most of the conditions, the predominant group differed. In test phase 1, *Sphingobium, Porphyrobacter* and *Sphingomonas* were the most abundant in bulk water from the cells operated at 2L/min, 8L/min and 10L/min (total of these three were 19%, 54% and 40% respectively). *Mycobacterium* accounted for

the most predominant group in bulk water from cells at 4L/min and 6L/min (39% and 40%). In test phase 2, *Sphingomonas* was dominant in 2L/min and 4L/min condition (up to 35% and 58% respectively). *Flavisolibacter* accounted for 31% in 6L/min cell and *Legionella* was dominant in 8L/min and 10L/min (up to 56% and 31%) (Fig.5.2).

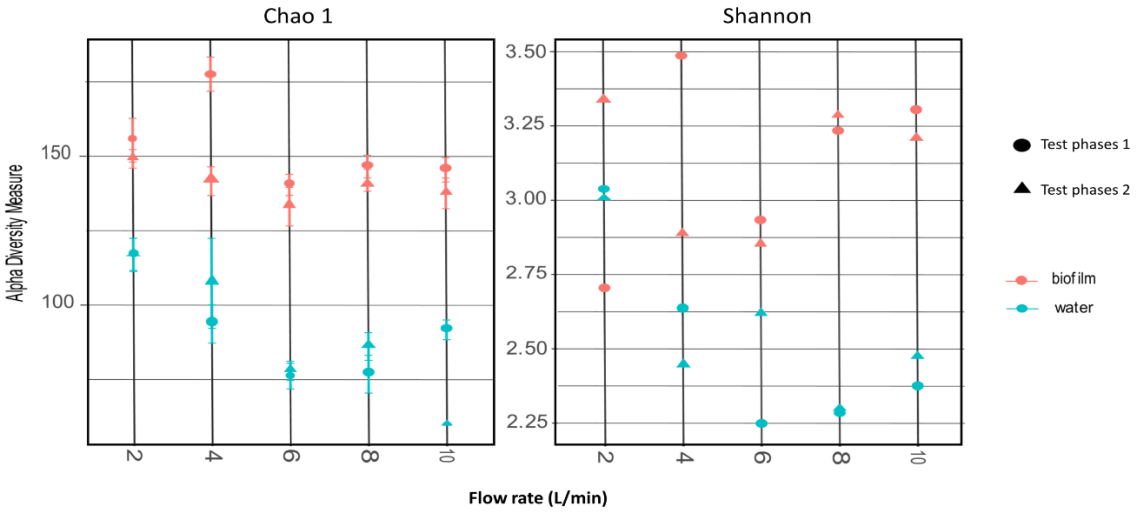

Figure 5.3 Alpha-diversity results for both biofilm and bulk water samples under different operation conditions

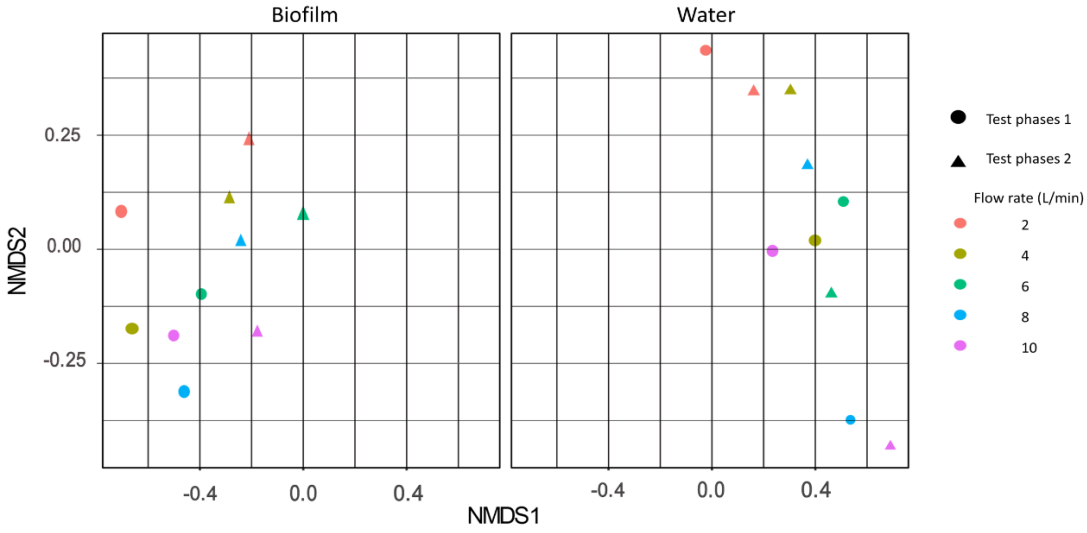

Figure 5.4 Two –dimensional plot of the Multi-Dimensional Scaling (MDS) analysis based on Bray-Curtis similarities of the percentage sequence abundance. Symbols and colour representing individual samples and sample type.

The species richness (Chao1 estimator) within the biofilm samples showed a declining trend with increasing flow rate in test phase 2; while flow cell running at 4L/min in test phase 1 showed the highest richness (Fig.5.3). The diversity (Shannon index) varied under different hydraulic regimes and test phases. In both test phases, the diversity was

relatively higher under lower flow rate (2L/min and 4L/min), and it showed an increasing trend with increasing flow rate ranging from 6~10 L/min.

Within bulk water samples, both richness and diversity indicated a higher potential under lower hydraulic regime (i.e. 2~4 L/min), compared with flow rate ranging from 6 to 10 L/min (Fig.5.3).

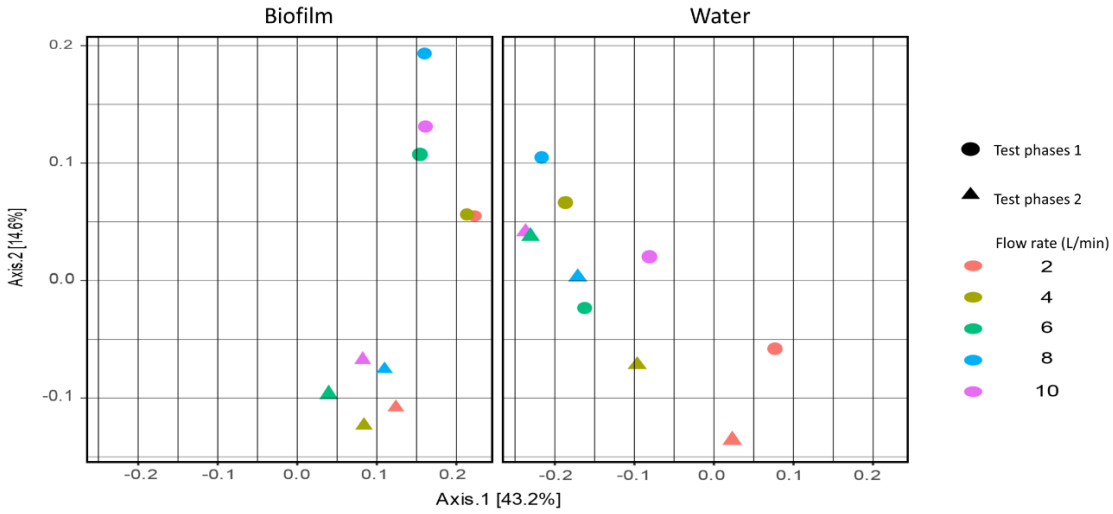

Figure 5.5 Two dimensional coordinates plots of Un-Weighted UniFrac analysis (n = 20) showing the phylogenetic clustering of bacterial communities within both biofilm and water samples at 97% similarity. The axes are scaled based on the percentage of variance that they are explaining.

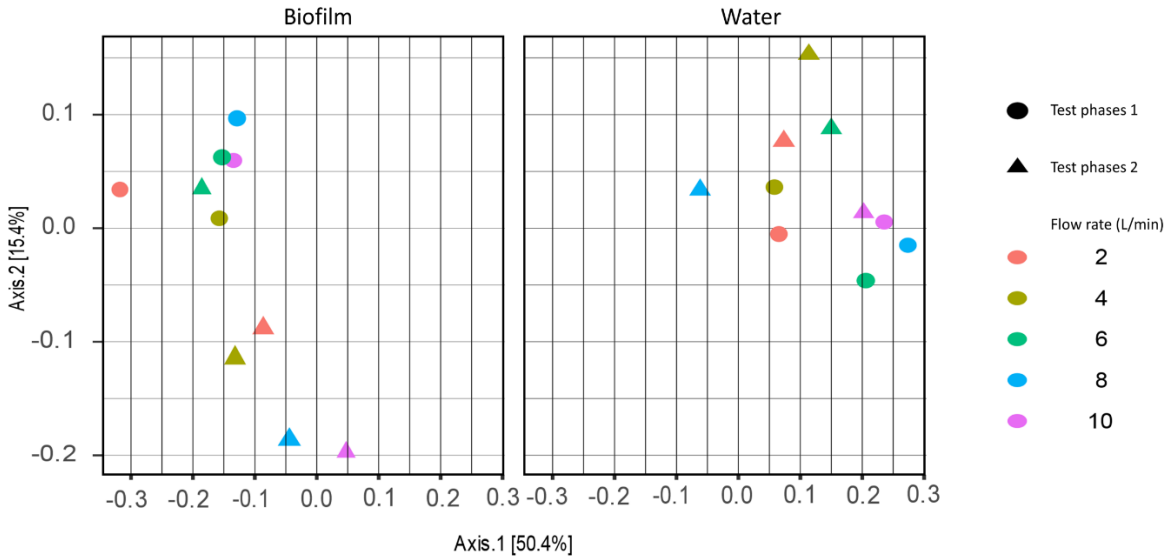

Figure 5.6 Two dimensional coordinates plots of weighted UniFrac analysis (n = 20) showing the phylogenetic clustering of bacterial communities within both biofilm and water samples at 97% similarity. The axes are scaled based on the percentage of variance that they are explaining.

The non-metric MDS based on relative abundance of sequence and the un-weighted UniFrac metrics, did not cluster in the distribution of biofilm samples from different

hydraulic regimes (Fig.5.4 and Fig.5.5). Results from the weighted UniFrac metrics did not show clear patterns in biofilm sample from test phase 1, while for test phase 2, there was a better cluster for biofilm sample based on hydraulic condition (Fig.5.6). Compared with biofilm samples, the MDS clearly separated the water samples between the different hydraulic regimes (Fig.5.4). Despite this, the un-weighted/weighted UniFrac metrics did not clearly cluster water samples based on the hydraulic regimes (Figs.5.5 and 5.6).

5.2.5 The effects of Cl_2/NH_3-N mass ratio on microbial community

There were differences in the bacterial community composition between both biofilm and bulk water sample from the different Cl_2/NH_3 mass ratio states (test phases 1 and 2). This is reflected in the different percentages of relative sequence abundance detected at different phylogenetic levels (Fig.5.1 and Fig.5.2). In the biofilm samples, *Planctomycetia* percentage tended to be smaller in the 5:1 state (test phase 2). The presence of *Betaproteobacteria* and *Gammaproteobacteria* was greater in the 5:1 state in all hydraulic conditions. The difference of *Betaproteobacteria* abundance was remarkable, and it was 6%, 16%, 7%, 11% and 15% at each flow condition (2L/min, 4L/min, 6L/min, 8L/min and 10L/min respectively) in the 3:1 state; and 17%, 18%, 14%, 43% and 47% in the 5:1 state (Fig.5.1). At the genus level, the abundance of certain bacterial within biofilm also differed (Fig.5.2). For example, the percentage of *Gemmata* that was accounted for was much greater in biofilm sample in the 3:1 condition than that in the 5:1 state (i.e. 31% at 2L/min in 3:1, while it was 9% in 5:1). At 4L/min, 8L/min and 10L/min condition, Pseudoxanthomonas was relatively higher in the 5:1 state (11%, 13% and 14% respectively), where there were all around 2% in the 3:1 state. The structures of microbial composition at 6L/min in each state were similar at genus level.

Within bulk water samples, different mass ratio did not significantly affect the community composition at class level (Fig.5.1). Only when the flow cell was run at 8L/min was *Gammaproteobacteria* the most dominant in the 5:1 state (up to 46%), which was only 0.07% in the 3:1 state. The relative abundance of *Alphaproteobacteria* and *Betaproteobacteria* was quite smaller in 5:1 (18% and 6% respectively) when compared with that in the 3:1 state (60% and 29% respectively) (Fig.5.1). At genus

level, the community composition at all hydraulic conditions in the two states were remarkably different (Fig.5.2). For instance, *Mycobacterium* was the most dominant at 4L/min in the 3:1 state (up to 39%), while it was only 10% in the 5:1 state. *Sphingomonas* was negligibly small in the 3:1 state (around 0) and was the predominant species in the 5:1 state (up to 58%). The difference in the bulk water samples in cells at 8L/min and 10L/min was also obvious. *Porphyrobacter* and *Mycobacterium* were predominant within samples in the 3:1 state (54% and 24% respectively), while their percentage were 0.1% and 1% in the 5:1 state. *Legionella* accounted for the largest percentage (56% and 31% respectively) in both flow conditions when the Cl_2/NH_3 mass ratio was 5:1, and this was quite small in 3:1 state (0.07% and 6%).

There was no significant difference in species richness between the two test phases under most of the hydraulic conditions (Fig.5.3). Only slight differences were identified in biofilm samples from flow cell running at 4L/min and also bulk water samples at 10L/min condition. For species diversity (Shannon index), only biofilm samples from cells with flow rate of 2 and 4 L/min presented differences according to the Cl_2/NH_3 mass dose ratios. Nether richness nor diversity variation followed a clear trend.

The MDS analysis clearly clustered the biofilm sample from the two test phases based on Cl_2/NH_3 mass ratio (Fig.5.4). There was a significant difference in the community composition within biofilm samples according to Cl_2/NH_3 mass ratio within un-weighted and weighted UniFrac metrics (Fig.5.5 and Fig.5.6). However, no clear separations in the distribution of water samples based on test phases were observed (Fig.5.4, 5.5 and 5.6).

5.3 Discussion

Difference in microbial community between biofilm and bulk water sample was identified according to dissimilarity analysis and UniFrac metrics (Fig.5.4 ~Fig.5.6). The alpha- diversity analysis also indicated higher species richness and diversity within biofilm when compared with that in bulk water samples (Fig.5.3), and this is in agreement with the results from a pilot-scale experimental DWDSs (Douterelo et al. 2013). Previous work has shown that some bacterial community presented better ability for attaching to material and forming biofilm (Rickard et al. 2003; Rickard et al. 2004a).

These bacteria could produce more high-quality polymers to form biofilm and hence increase the capacity to withstand the hydraulic attack. As a result, the biofilm which can work as a shelter for protecting bacteria from outer interference such as low nutrient, disinfectant and flushing; attract more bacteria to accumulate (LeChevallier et al. 1987). This might explain the difference in bacterial community and diversity between biofilm and bulk water.

In order to control water quality and to prevent possible microbial contamination through DWDS, water utilities are expected to apply disinfection to the water before it enters the system, and to also maintain the disinfectant residual at a reasonable level. Chlorine and chloramine are the two main disinfectants used worldwide. In particular, the application of chloramine has increased due to its low contribution to the formation of disinfectant by products (DBPs) (Neden et al. 1992). In the current study, chloramine was applied as the disinfectant. According to previous studies, bacterial groups showed different sensitivity to disinfectant (Williams et al. 2005; Gomez-Alvarez et al. 2012). The results from the current study are in agreement with researches on microbial structure detected in systems with chloraminated water (Williams et al. 2004; Yilmaz et al. 2008; Hwang et al. 2012; Mi et al. 2015), where *Alpha-* and *Betaproteobacteria* were dominant in biofilm and water samples (Fig.5.1). In addition, *Actinobacteria* and *Planctomycetia* were also the abundant bacterial groups identified in biofilm samples in the current study. Krishna et al. (2013) observed that the former group dominated in high chloramine containing water system, while Mi et al. (2015) found the latter group in annual reactor fed with low concentration of NH_2Cl (0.06mg/L).

At genus level, unlike chlorinated systems where *Pseudomonas* was always abundant (Martiny et al. 2005b; Douterelo et al. 2013), *Mycobacterium* was dominant (17%~60%) within biofilm samples in the current study (Fig.5.2). This is in agreement with the results in previous studies about bacterial community in monochloramine-treated drinking water biofilms (Williams et al. 2005; Revetta et al. 2013). In addition, high presence of species relative to *Mycobacterium* were also detected in biofilm from chloraminated DWDSs (Falkinham and LeChevallier 2001; Beumer et al. 2010). Other genera that dominated within the current study was *Sphingomonas*, which has been reported to be abundant in chloraminated environment (Regan et al. 2002; Williams et al. 2004; Krishna et al. 2013). Moreover, compared with chlorinated systems, this

group present the ubiquity in chloramine-treated systems (Yilmaz et al. 2008), and it was considered as an indicator of the onset of nitrification (Krishna et al. 2013). *Legionella* was also observed to be predominant within the current study. This group is always considered as the opportunic pathogens, and it is the most frequent causative agent of drinking water related disease outbreaks (Brunkard et al. 2011). Other abundant genera species in this study, such as *Gemmata* and *Porphyrobacter* have been observed in drinking water samples and suggested to be adapted to oligotrophic conditions in DWDSs (Revetta et al. 2010; Kwon et al. 2011; Liu et al. 2014).

The bacterial community composition and structure of biofilm and water samples differed between the different hydraulic regimes (Fig.5.1 and Fig.5.2). However, only statistical difference was observed within water samples (Fig.5.4). The consistency of the biofilm samples might be expected since the biofilm within each flow cell unit was firstly developed at the same condition before the test, and a common recirculation tank was used for all cells. The bacterial structure in biofilm was more stable and resistant to the change of outer environment than that in water, although distinctive microbial community within biofilm was observed under similar developing conditions (Henne et al. 2012). In addition, as the biofilm samples in current study were only collected at the end of the test, and the sequencing technology used only detected possible organisms without differentiating the live/dead status, further research in terms of monitoring microbial community over time is needed. In contrast with the results observed by Douterelo et al. (2013) who found similar community composition in water under different hydraulic regimes, the microbial community in water sample was clustered separately between different flow rate conditions in the current study (Fig.5.4). This phenomenon might be explained by the observation in previous studies that hydraulic condition showed effects on the material build up and subsequent mobilization within pipe-scale DWDSs (Boxall and Prince 2006; Husband et al. 2008; Husband and Boxall 2010). Sekar et al. (2012) also provided evidence by analysing bacterial abundance and structure from real WDS and suggested that the bacterial composition varied and was possibly associated with system hydraulics.

The alpha- diversity analysis provided comparison of species richness and diversity between different hydraulic regimes and the results reveal that both richness and diversity tended to be higher at lower flow rate conditions (Fig.5.3). In the test phase

1, both the highest species richness and diversity occurs in biofilms conditioned at 4 L/min. On the other hand, the species diversity within biofilm presented an increasing trend at flow rate ranging from 6 ~ 10 L/min. The high richness and diversity in biofilms from lower flow rate condition was potentially due to a less survival pressure from the damage caused by excessive shear stress. In addition, previous studies have suggested that higher flow might favour the development and growth of biofilm due to the promotion of transport and diffusion of nutrient within biofilms at high velocities (Beyenal et al. 2002). This may explain why there was an increasing trend in diversity associated with the increase of flow rates within current study. In contrast, both Rochex et al. (2008) and Rickard et al. (2004b) reported a decrease of biofilm diversity under higher shear stress, and this might slow down the process of biofilm maturation. The promotion and inhibiting effects from increasing shear stress on biofilm structure might work interactively, and hence result in the variation between studies. However, the cited research was undertaken in annual reactors in which nutrient and operational conditions varied with each other. Consequently, there was not enough evidence to support how the microbial community in the biofilm respond to different hydraulic conditions in real systems.

The species richness and diversity were observed to be higher within water samples at lower hydraulic regimes (Fig.5.3). This trend was expected to be a result of interaction between biofilm mechanical properties and hydraulics. Studies have suggested that a more dense and compact biofilm would develop under higher shear stress condition, and greater detachment force was then required to remove bacterial material (Manuel et al. 2007; Paul et al. 2012). Similar observation was noted by Vrouwenvelder et al. (2010) who found that biofilm formed under lower shear stress condition was easily removed. Sharpe et al. also reported less material mobilized to bulk water under higher conditioning shear stress and there were materials remaining on pipe coupons even after flushing events. Consequently, biofilm developed under higher flow rate condition in the current study resulted in less microbial material mobilized into the bulk water.

The current study uses chloramine as disinfectant and investigated two Cl_2/NH_3-N mass ratio (3:1 and 5:1) in two separate test phases. The results from similarity analysis and UniFrac matrix suggest a difference in composition and structure of biofilm

samples between the two ratios (Fig.5.4 ~ Fig.5.6). The difference between these two mass ratios was that there was excessive ammonia when monochloramine was prepared with smaller ratio (3:1). Lee et al. (2011) used microelectrodes to monitor the penetration of disinfectant and dissolved oxygen into nitrifying biofilm developed in an annual reactor. Lee et al. (2011) suggested that the excessive ammonia would further promote the chemical decay of chloramine and hence accumulate more free ammonia. This excessive ammonia would affect the penetration of chloramine and DO into the biofilm, where the disinfectant was impeded and the oxygen was consumed by free ammonia (Lee et al. 2011). Based on the information, the microbial activity and the level of inactivation by disinfectant within biofilm would be influenced when compared with the system using larger mass ratio (5:1). However, Lee et al. (2011) did not analyse the microbial composition after disinfection. In addition, even though the biofilm was developed under the same condition before the two test phases, the bacterial composition and structure might be different from each other. Furthermore, without working as a single influencing factor, interaction between hydraulic regimes and disinfection strategy might cause the difference in microbial community within biofilms from these two test phases. Further research into microbial succession in biofilms within the current experimental facility is required to verify the impact of Cl_2/NH_3-N mass ratio on microbial composition and structure.

Although the onset of nitrification was observed based on physico-chemical analysis within the current study (Table 5.1), few nitrifier (AOB/NOB) related sequences were detected (Fig.5.1 and Fig.5.2). Only small relative abundance of *Nitrospira* (< 0.01%) was classified in three biofilm samples in test phase 1. This low rate of detection might be due to the fact that the nucleus of this community available for sequencing was limited, and also the sequencing depth was not enough to acquire sufficient information. Sawade et al. (2016) used both MiSeq and qPCR to detect microbial community within onset of nitrification batch test, and the results suggested a very low fraction of nitrifier detected from MiSeq sequencing even in system with high production of nitrite. In comparison, the qPCR was relatively sensitive and the results indicated correlations between community abundance and nitrification (Sawade et al. 2016). In order to characterize the AOB and NOB within chloraminated DWDS, Regan et al. (2002) applied terminal restriction fragment length polymorphism (T-RFLP) analysis and this

technology indicated the occurrence of related sequence successfully. Therefore, in order to better understand the relationship between operational conditions and abundance of nitrification related microbial community, techniques targeting particular species such as qPCR and T-RFLP are needed in further research. On the other hand, the limited nitrifying community available for detecting might be result of the change of living environment, as a much higher concentration of NH_3-N (50mg/L) was used in the pre-incubation stage, while the available free ammonia dropped tremendously during test phases (only around 0.2 to 1 mg/L). Compared with the incubation period, the later limited nutrient experimental condition requires nitrifiers to have better affinity with substance. However, such kind of nitrifying community might not be fully enriched during incubation and hence lead to an increasing difficulty to identify nitrifiers within the after-test samples.

The bacterial composition results have confirmed that even under limited nutrient conditions, the drinking water system could still be a robust ecological niche for microbes. Moreover, opportunic pathogens including *Legionella* and *Mycobacterium* were observed to be abundant within the current study. From the physico-chemical parameter analysis, there was a dramatic decline of disinfectant in all the flow cell units (Table 5.1). On one hand, this low disinfectant residual was due to a three-day water age which would increase the level of disinfectant auto-decomposition and allow for a long reaction time between disinfectant and existing water chemicals (Krishna et al. 2010; Krishna et al. 2012). The onset of nitrification process was another key factor that accelerated the decay of chloramine. Both Krishna et al. (2013) and Sathasivan et al. (2008) monitored a high chloramine decay rate along with the nitrification process. The excessively high disinfectant decay rates would reduce the impact from outer environment on the growth of bacteria, and consequently increase the chance of appearance of opportunic pathogens.

Both the increase of nitrite concentration during the tests and the detection of *Sphingomonas* in the current study indicate the onset of nitrification within systems (Krishna et al. 2013). The pathogens observed in current study further confirmed the importance of maintaining disinfectant residual and controlling nitrification within DWDSs. Based on the results from this study, neither high shear stress nor large Cl_2/NH_3-N mass ratio was an effective approach to maintain water quality in system

with the onset of nitrification. However, it is still important to understand the microbial community and structure within systems under different operational conditions. Such information could assist in investigating the relationship between bacterial growth and environmental factors, and improve the effectiveness of management strategy by providing microbial indicator of water quality. Further research, using target sequencing technology and monitoring the community composition over time will help to better understand the occurrence of bacteria in different operating conditions, and to develop maintenance strategy for securing public health.

5.4 Summary

Nitrification in chloraminated DWDSs has received much consideration due to its impact on water quality and public health. However, there is less research conducted on microbial community under different hydraulic regimes and Cl_2/NH_3-N mass ratios in systems experiencing the onset of nitrification. The results of application of high throughout Illumina MiSeq analysis to chloraminated experimental flow cell systems, which yields new and unique data about the impact of operational conditions on bacterial community composition and structure in biofilms and bulk water. The outcomes of this study are summarized below:

- The bacterial community composition and structure were different between biofilm and bulk water. This difference suggests that microorganism within biofilm presented better capacity to produce high resistance polymers to form biofilm. On the other hand, the bacterial groups identified within the bulk water were different to those found in chlorine water DWDSs, and it was expected that these groups have better resistance to chloramine.
- Overall, species richness and diversity in biofilm tend to be higher at lower flow rates, while the diversity increases with the increase of shear stress when the flow rate is between 6 and 10 L/min. This suggests the uncertainty of hydraulic effects on biofilm development.
- There was no statistical difference in microbial structure identified in biofilm between different hydraulic regimes and this suggested the stability of biofilm to outer environment.
- Different hydraulic regimes affect the bacterial community composition and

structure within bulk water, with a tendency of higher richness and diversity detected at lower hydraulic regimes. This confirms the influence of hydraulic condition on biofilm mechanical structure and further material mobilization to water.

- Cl_2/NH_3-N mass ratio showed obvious effect on microbial structure in biofilm, suggesting excessive ammonia would be a factor affecting chloramine penetration to biofilm and the microbial activity within biofilm.
- Opportunic pathogens such as *Legionella* and *Mycobacterium* were detected in abundance in the experimental system. This confirms that biofilm could be a suitable reservoir for these microorganisms and further suggests that nitrification can lead to decrease of water quality and microbial outbreaks.

Chapter 6 Extracellular polymeric substance (EPS) characterization and its impact on disinfectant decay

6.1 Introduction

Extracellular polymeric substance (EPS) has been studied in terms of its composition and structure within biofilm (Flemming et al. 2007; Wagner et al. 2009). However, the interactions between operational conditions, especially hydrodynamics, and EPS, and also the role of EPS on disinfection process have not been sufficiently investigated. In this chapter, EPS was extracted from biofilm incubated in a series of flow cell facility running at different operational conditions. A total of three hydraulic regimes (Q = 2 L/min; 6L/min; 10L/min) and four different disinfection schedules (total Cl_2 = 1mg/L, Cl_2/NH_3 =3:1 or 5:1; total Cl_2 = 5mg/L, Cl_2/NH_3 =3:1 or 5:1) were investigated within the facility. The EPS composition structure of the incubated biofilm were analysed, and the EPS extracted from regrown biofilm were reacted with chlorine and chloramine to investigate their impacts on disinfectant decay. The overall aim of this chapter is to investigate whether the operational conditions affect the EPS characteristics and determine the possible role of EPS in disinfection process.

6.2 Material and Methods

6.2.1 Culture and Extracted EPS Preparation

Mixed species biofilm (total 10 samples) collected from test phases 3 and 4 were used to analyse the molecular composition of the EPS. Due to the limited amount of extracted EPS from the experimental facility, the mixed biofilm was regrown in 200ml $1/10^{th}$ strength Luria-Bertani (LB) broth at 30°C until the late exponential phase. The cells were harvested by centrifugation at 2,000 × g for 15 min (*Eppendorf,* centrifuge 5424), allowing for minimal removal of EPS. They were then washed with pH 7

chlorine demand free (CDF) phosphate buffer (0.54g Na_2HPO_4 and 0.88g KH_2PO_4 per litter) to remove growth media before EPS extraction. The disinfectant decay experiment described in this chapter used EPS extracted from regrown culture. Considering possible changes of EPS composition due to growth and nutrient condition (Wang et al. 2013), a comparison between the EPS extracted directly from biofilm and regrown culture was made.

EPS extraction from biofilm was performed using the procedure described in Section 3.7.2.1. In terms of the extracted volume, there is a difference when extracting EPS from regrown culture and the details are outlined herein. After the washing step described above, the centrifuged cell from regrown culture was re-suspended in 7.5 ml CDF buffer and thereafter 7.5 ml 2% EDTA was added in CDF solution. The incubation and centrifuge steps were the same as described previously. The details of EPS quantification were outlined in Section 3.7.5.

To verify and compare the EPS composition between different samples, both the cell numbers in biofilm and cultures, and total organic carbon within extracted EPS supernatant were evaluated by HPC counting and a TOC analyser (TOC-V_{CPH} *Shimadzu*) respectively. The measurement details are presented in Sections 3.6.1 and 3.6.2.

6.2.2 Preparation of Disinfectant Solution

In order to verify the water quality data acquired from the current experimental facility, the disinfectant concentration and Cl_2/NH_3 mass ratio at the disinfectant decay tests were selected as the same with that in test phases 3 and 4. In addition, to avoid interference on disinfectant decay from possible soluble material, all disinfectant experiment within the current study were conducted with CDF buffer. Chlorine solution was prepared by adding stock solution of 500 mg-Cl_2/L sodium hypochlorite to the buffer until a chlorine residual of 1.0 or 5.0 mg/L was achieved. Monochloramine solution (1mg/L or 5mg/L measured as total chlorine) was prepared by weighting corresponding ammonium chloride powder to the chlorine solution in a 3:1 (or 5:1) chlorine-to-ammonia-nitrogen mass ratio. The disinfectant solutions were prepared before the disinfectant decay experiments. Following the method described in Section 3.6.1, both the chlorine and monochloramine initial dose and residual were measured.

6.2.3 Disinfectant Decay by Extracted EPS

Based on the water quality results from the current experimental facility (Fig.4.4), the TOC within bulk water ranged from 2 to 20 mg/L. As the EPS belongs to the soluble organic matter, the extracted EPS was diluted to a series of concentration ranging from 2 to 20 mg/L based on the TOC concentration, and this was done to evaluate the effect of EPS on disinfectant decay. In addition, since 2% EDTA solution was used for EPS extraction and the EDTA is also organic, the same concentration range of EDTA was prepared as blank.

According to the growth condition of biofilm, the initial disinfectant concentration reacted with prepared EPS was identical to the test in the experiment facility (i.e. the initial monochloaramine or chlorine concentration would be 1mg/L and Cl_2/NH_3-N mass ratio is 3:1 if the EPS was extracted from biofilm grown in flow cell, with test code as 2A_R3, 6A_R3 and 10A_R3 in test phases 3). For control, the EDTA solution was reacted with monochloramine and chlorine with the concentration used in this test.

All the experiments were performed in 200ml amber glass bottles at room temperature (22°C ± 2). Parallel tests were undertaken and average values were calculated as results. During the decay test, disinfectant concentrations were measured at each sample point to determine the reaction kinetics. To evaluate the reactivity of EPS and tested disinfectant, a two-phase decay model adapted from EPA 1998 model (Eq.6.1) was used. In this model, k_1 and k_2 were the rate constants that represented the decay rate of the two phases during disinfectant decay, where k_1 dominates the fast decay phase while k_2 is the slow decay phase.

$$C = C_0 * [A * e^{-k_1 t} + (1 - A) * e^{-k_2 t}] \qquad \text{Equation 6.1}$$

6.3 Results

6.3.1 Isolated biofilm and regrown culture EPS Properties

Fig.6.1 presents the extracellular carbohydrate and protein concentration obtained from both isolated biofilm and regrown culture. To compare their properties and to verify the results of the disinfectant decay test, the concentration was expressed as μg per total organic carbon (mg) detected within the samples. Within isolated biofilm, carbohydrate was the dominant components and varied under different operational conditions

(Figs.6.1A and C). Between the different hydraulic regimes, the peak value of extracellular carbohydrate was obtained from biofilm isolated from flow cell running with flow rate at 6L/min when the total chlorine in feed water was 1 mg/L. However, when the concentration of monochloramine was 5mg/L in both test phases, carbohydrate concentration was found to decrease with increasing hydraulic regimes.

Unlike the EPS component fraction of isolated biofilm, protein was the major component in EPS from regrown culture, but it also varied with the original isolation conditions (Figs.6.1B and D). In terms of disinfectant concentration, the extracellular protein and carbohydrate concentration in regrown biofilm were relatively higher when the isolated biofilm was conditioned at higher concentration of monochloramine (5 mg/L). In addition, the protein concentration exhibited similar trend with the carbohydrate in isolated biofilm, showing a decrease with increasing flow rate when regrow biofilm from flow cell fed with monochloramine of 5mg/L.

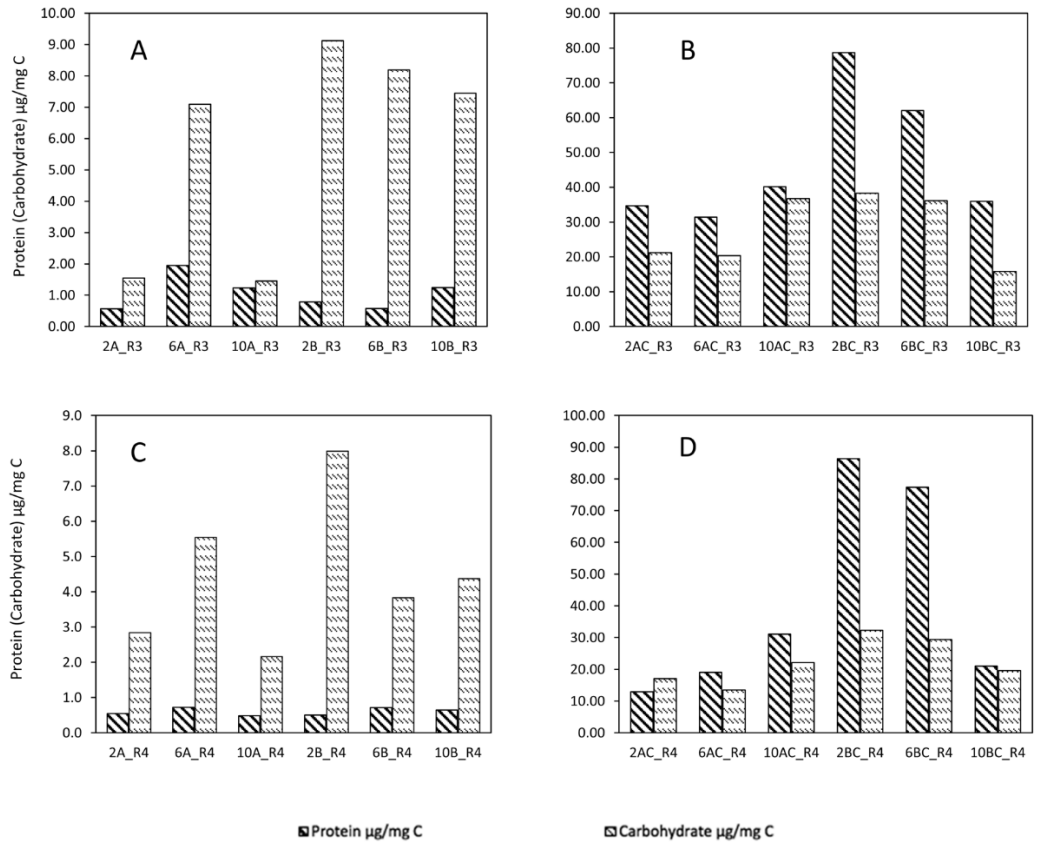

Figure 6.1 Total concentration of carbohydrate and protein within EPS of biofilms and regrown culture from different flow units. A. EPS extracted from isolated biofilm in test phases 3; B. EPS extracted from regrown culture in test phases 3; C. EPS extracted from isolated biofilm in test phases 4; D. EPS extracted from regrown culture in test phases 4.

Different from comparing EPS composition based on TOC, Table 6.1 and 6.2 shows the details of total extracellular protein and carbohydrate content produced by cell mass, and the ratio of total EPS mass (calculated by adding protein and carbohydrate together) and cell numbers. The ratio of carbohydrate and protein in isolated biofilm fluctuated more with operational conditions (from 2.73 to 16.07) when compared with that in regrown culture (range 0.37~1.32) (Table 6.1).

Table 6.1 Values of HPC cell numbers, protein, carbohydrate and concentration ratios (EPS) in isolated biofilm and regrown culture from different flow cell units and test phases.

Test code	Total cells		Protein (μg)		Carbohydrate (μg)		Carbohydrate:Protein	
	Biofilm (isolated)	Regrown culture	Biofilm (isolated)	Regrown culture	Biofilm (isolated)	Regrown culture	Biofilm (isolated)	Regrown culture
2A_R3	1.80E+07	5.70E+10	5.77	1030.60	15.74	630.92	2.73	0.61
6A_R3	4.86E+07	2.25E+11	18.05	1383.75	65.72	894.86	3.64	0.65
10A_R3	1.98E+08	6.15E+10	11.50	1726.66	13.50	1579.03	1.17	0.91
2B_R3	3.15E+07	1.50E+11	7.51	3412.81	87.06	1659.52	11.59	0.49
6B_R3	2.34E+07	8.00E+10	5.87	2568.32	82.94	1494.79	14.13	0.58
10B_R3	1.98E+07	1.75E+11	13.34	1317.21	79.76	579.44	5.98	0.44
2A_R4	5.40E+07	1.14E+11	5.36	559.73	27.91	740.43	5.21	1.32
6A_R4	2.91E+08	1.20E+11	7.30	892.41	55.99	630.92	7.66	0.71
10A_R4	6.30E+06	9.20E+10	4.85	1388.87	21.55	991.26	4.44	0.71
2B_R4	3.55E+08	1.62E+11	5.36	3719.90	86.13	1389.03	16.07	0.37
6B_R4	3.97E+08	8.00E+10	7.10	4359.67	38.02	1655.78	5.35	0.38
10B_R4	2.33E+08	3.60E+10	6.08	902.64	41.20	843.38	6.78	0.93

The EPS production ability of isolated biofilm and regrown culture was different as well (Table 6.2). There was a great decrease (around two order of magnitude) in the EPS-to-cell ratio when the biofilm regrown in culture media.

Table 6.2 Ratios of extracted EPS and cell mass for both isolated biofilm and regrown culture

	2A_R3	6A_R3	10A_R3	2B_R3	6B_R3	10B_R3	2A_R4	6A_R4	10A_R4	2B_R4	6B_R4	10B_R4
EPS/Cell μg/cell (isolated biofilm)	1.26E-07	1.72E-06	1.20E-06	4.70E-06	3.80E-06	3.00E-06	4.19E-06	2.18E-07	6.16E-07	2.03E-07	1.14E-07	2.58E-07
EPS/Cell μg/cell (regrown culture)	2.75E-08	4.39E-09	1.23E-08	3.81E-09	2.08E-08	1.26E-08	2.59E-08	1.27E-08	1.14E-08	4.85E-08	7.52E-08	3.15E-08

6.3.2 Chloramine Decay by Extracted EPS

Figs.6.2 and 6.3 illustrate the chloramine decay for series concentration of EPS from different test phases. The results indicate that there was no significant difference in chloramine decay between the varying amount of regrown biofilm EPS. As monochloramine was known as a slow-reacting disinfectant, the EPS reacted with it at slow rates and after the first 10 minutes of reaction, the residual remained relatively constant, although there was fluctuation in some cases. Compared with EPS extracted

from different samples, the fast decay rate (k_1) of chloramine was similar when reacted with the same concentration of NH_2Cl, while a higher rate was observed for reactions with chloramine concentration of 5mg/L.

For control, the diluted 2% EDTA solution was reacted with chloramine (Fig.6.4). Compared with EPS reactions, the difference in disinfectant residual between different TOC concentrations of EDTA solutions was rarer. However, in terms of the total decay rate, extracted EPS and EDTA reactions were similar.

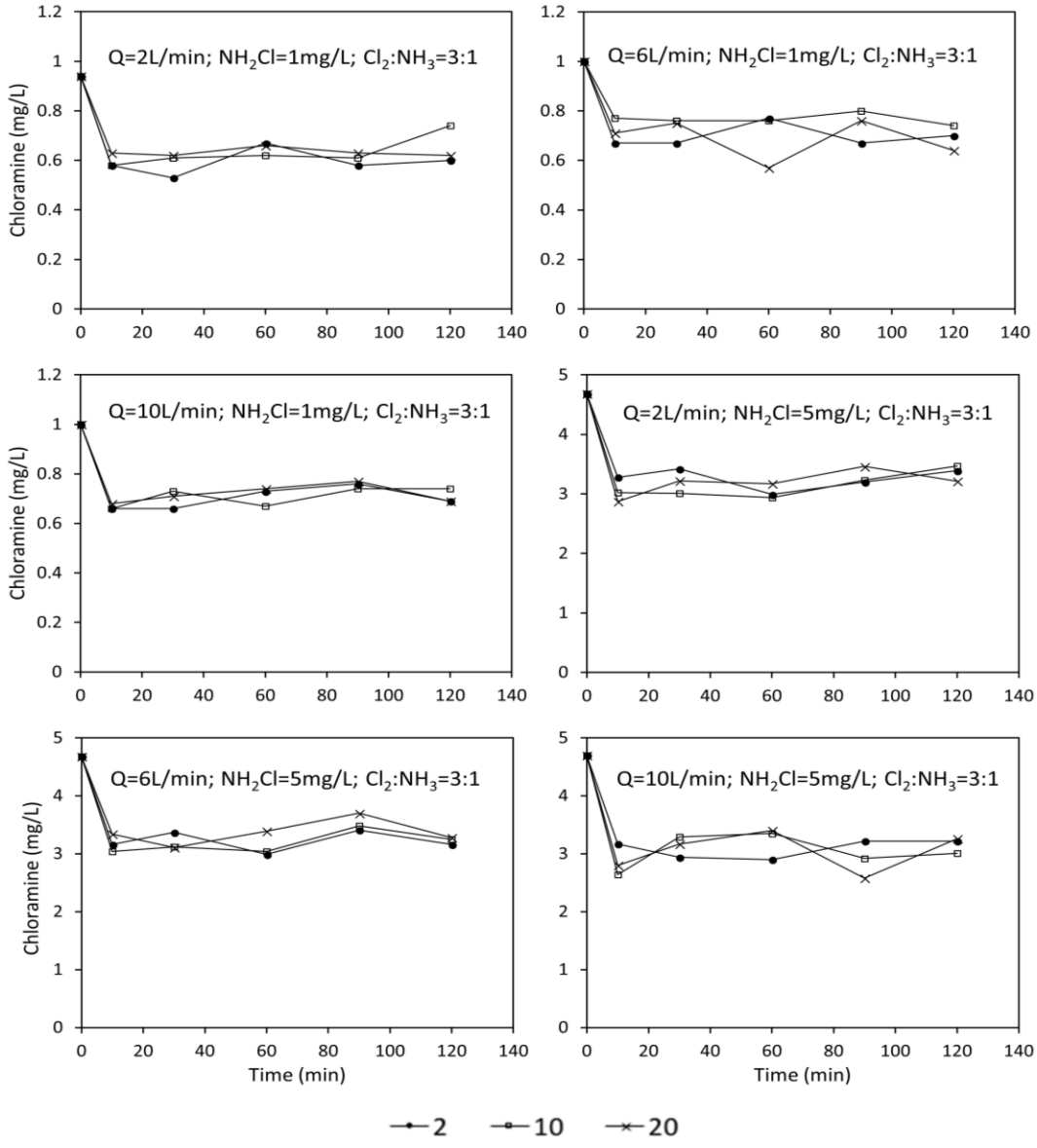

Figure 6.2 Monochloramine decay by extracted EPS of regrown culture based on different TOC concentration. The description in each figure corresponds to the original experimental conditions in test phase 3. Symbols: prepared EPS solution based on TOC concentration (2, 10 and 20 mg/L).

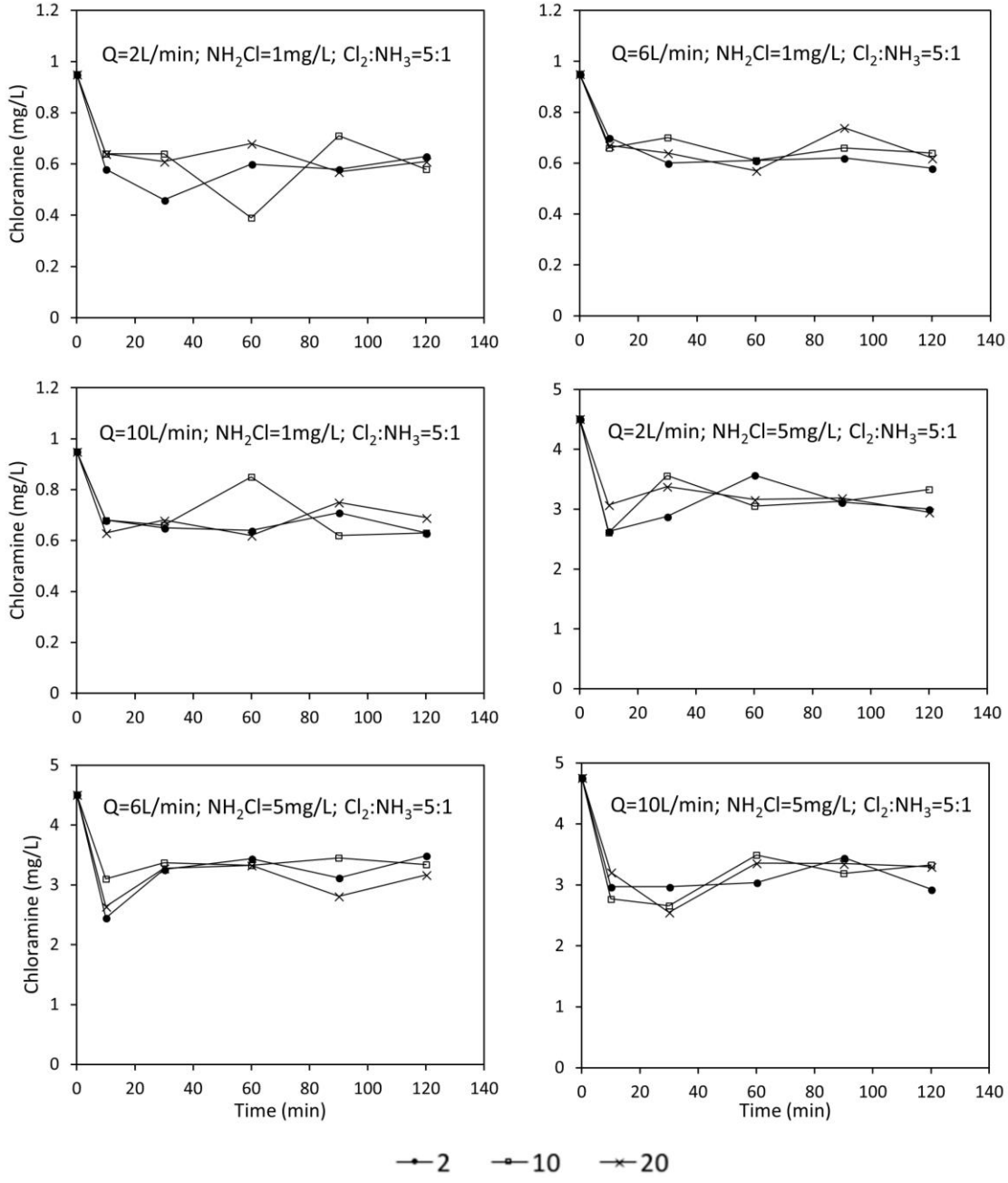

Figure 6.3 Monochloramine decay by extracted EPS of regrown culture based on different TOC concentration. The description in each figure corresponds to the original experimental conditions in test phase 4. Symbols: prepared EPS solution based on TOC concentration (2, 10 and 20 mg/L).

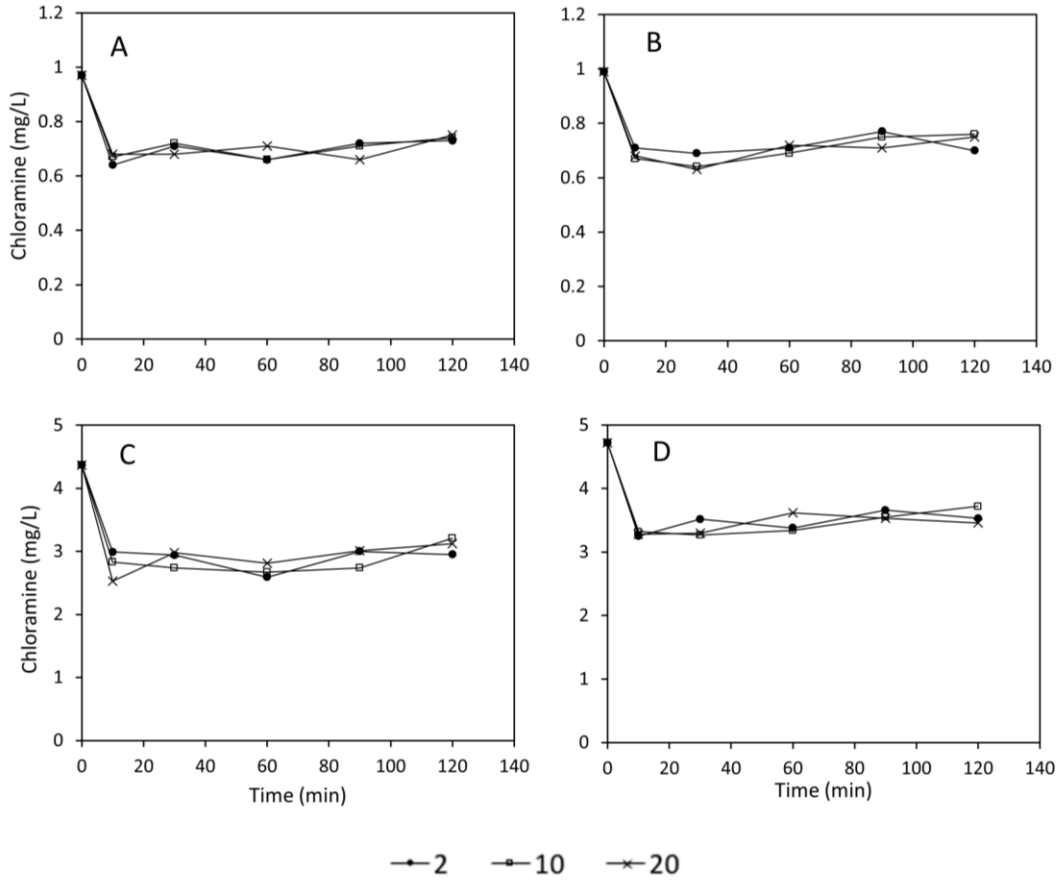

Figure 6.4 Chloramine decay by 2% EDTA solution based on different TOC concentration. A. NH_2Cl = 1mg/L and Cl_2/NH_3-N = 3:1; B. NH_2Cl = 1mg/L and Cl_2/NH_3-N = 5:1; C. NH_2Cl = 5mg/L and Cl_2/NH_3-N = 3:1; D. NH_2Cl = 5mg/L and Cl_2/NH_3-N = 5:1. Symbols: prepared EDTA solution based on TOC concentration (2, 10 and 20 mg/L)

6.3.3 Chlorine Decay by Extracted EPS

Compared with the reaction with chloramine, there was difference in chlorine residual between EPS amount (Fig.6.5 and 6.6). When a lower concentration of EPS (TOC=2 mg/L) is reacted with chlorine, a higher residual amount was observed for all the tests. For tests with EPS extracted from different samples, the fast decay rate (k_1) of chlorine varied in reaction when TOC in solution was 2 mg/L. However, when the concentration of TOC increased to 10 and 20 mg/L in all tests, the results indicated that no significant difference in the residual between the two reactions. These may be due to the high reactivity of chlorine, and a lack of tests for TOC in the range of 2~10 mg/L to verify TOC concentration effects on chlorine decay.

Fig.6.7 presents EDTA reactions with chlorine and the results indicate that chlorine decayed following similar trend with that in the EPS reactions, although difference in

k_1 occurred among tests.

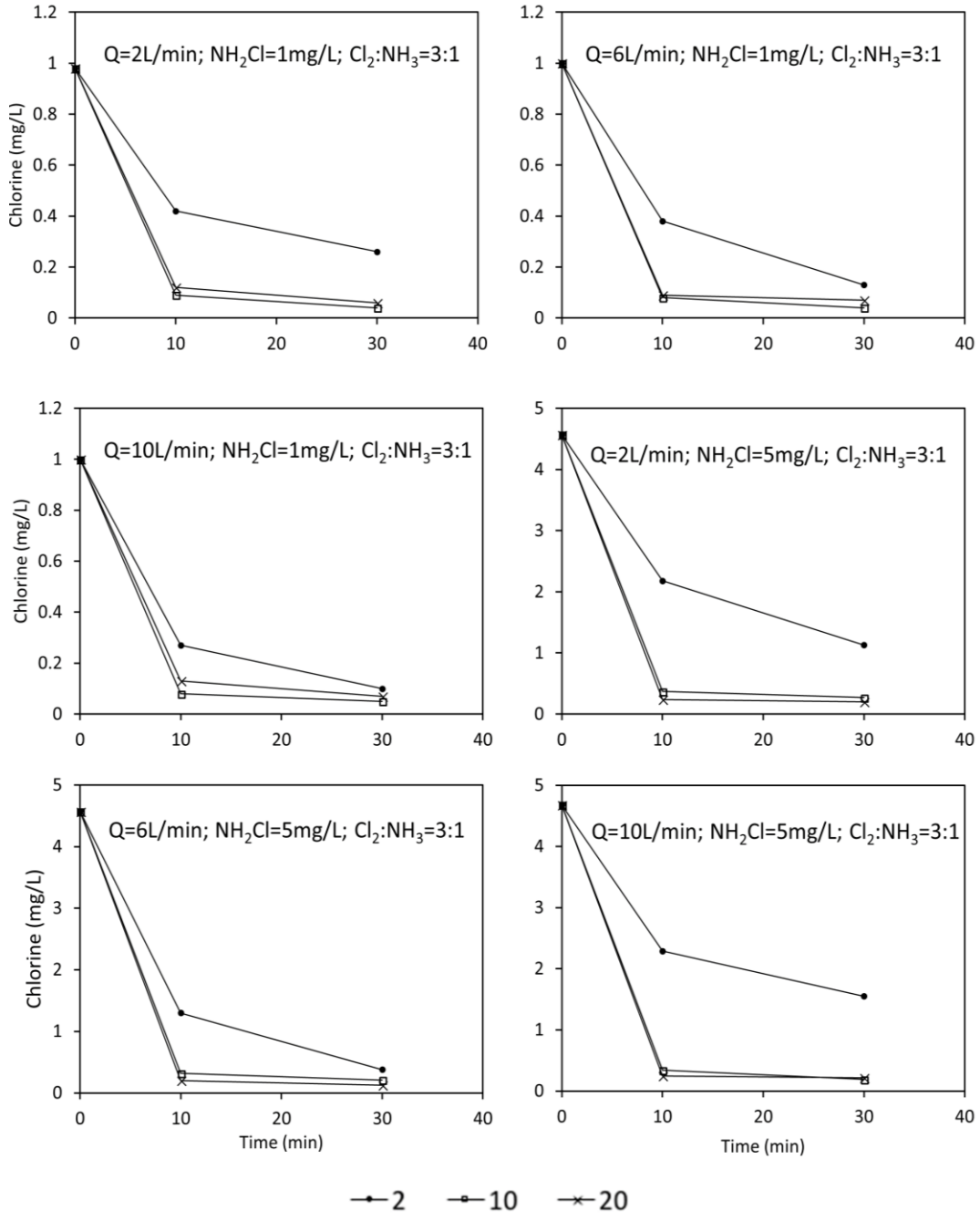

Figure 6.5 Chlorine decay by extracted EPS of regrown culture based on different TOC concentration. The description in each figure corresponds to the original experimental conditions in test phase 3. Symbols: prepared EPS solution based on TOC concentration (2, 10 and 20 mg/L).

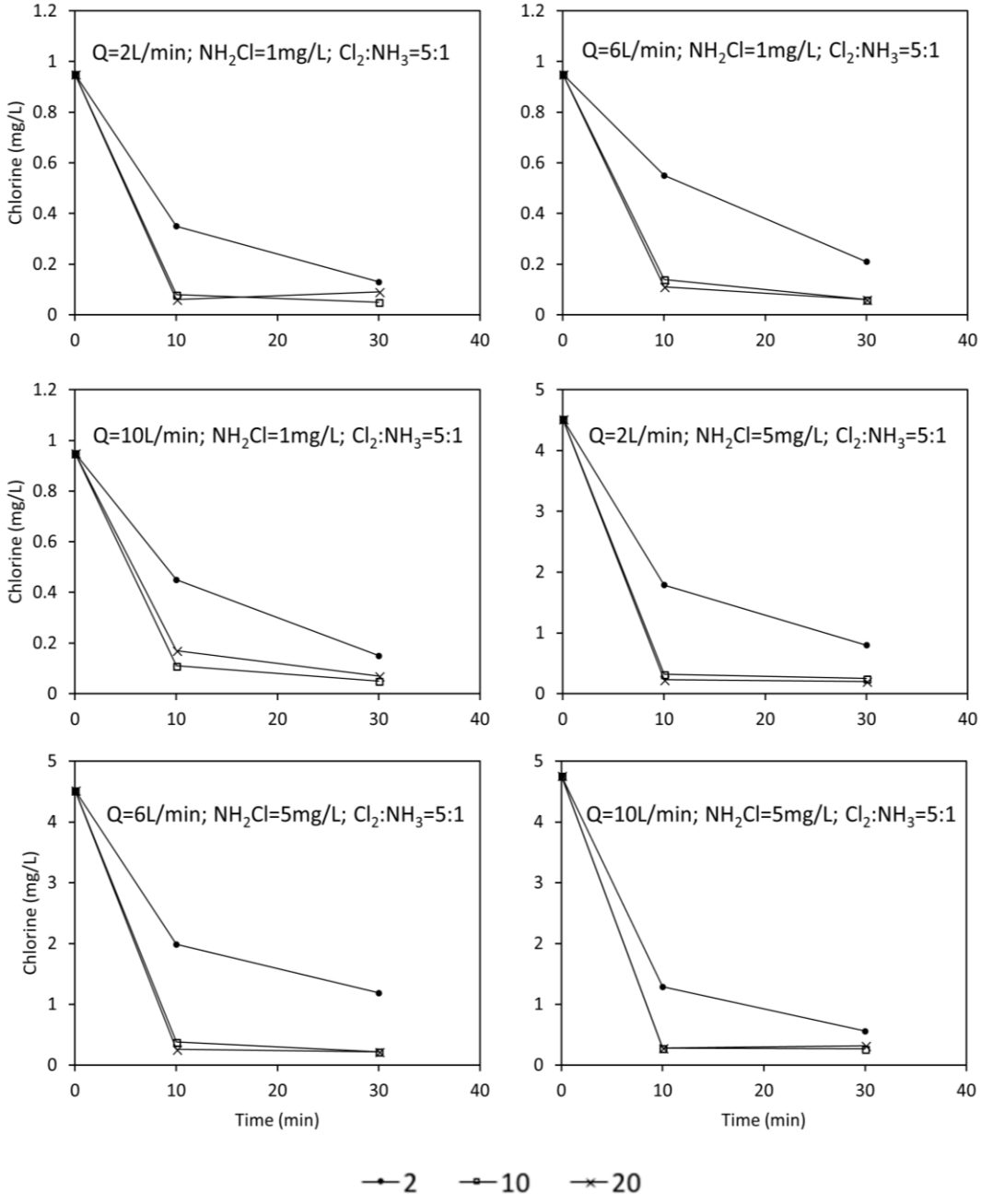

Figure 6.6 Chlorine decay by extracted EPS of regrown culture based on different TOC concentration. The description in each figure corresponds to the original experimental conditions in test phase 4. Symbols: prepared EPS solution based on TOC concentration (2, 10 and 20 mg/L).

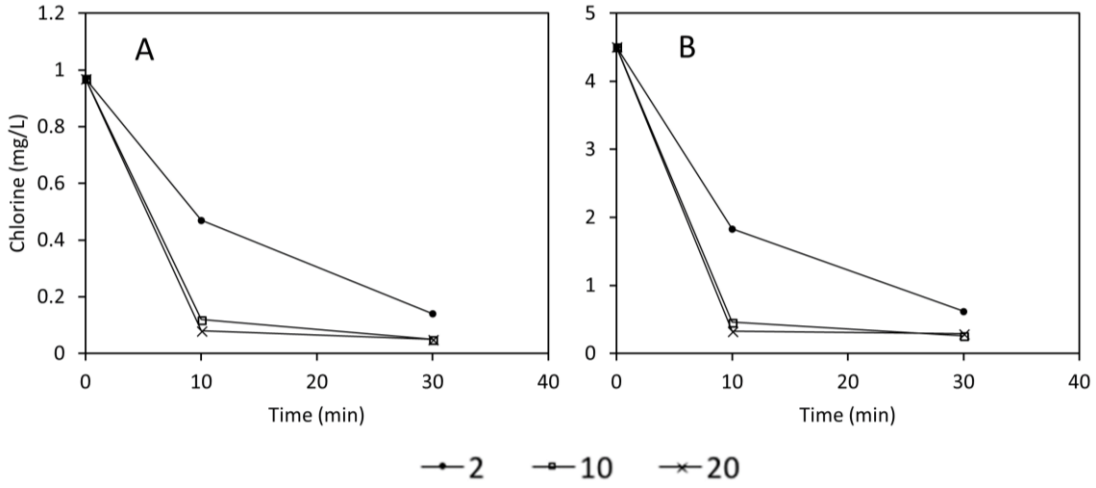

Figure 6.7 Chlorine decay by 2% EDTA solution based on different TOC concentration. A. Cl_2 = 1mg/L; B. Cl_2 = 5mg/L. Symbols: prepared EDTA solution based on TOC concentration (2, 10 and 20 mg/L).

6.4 Discussion

In this chapter, the EPS property from simulated chloraminated flow cell system and the interactions between operational condition and EPS structure were explored. In addition, previous studies have used only single bacteria strain to investigate the EPS composition and its impacts on water quality, such as disinfectant by products formation and disinfectant decay (Wang et al. 2012b; Xue et al. 2013a; Xue and Seo 2013b; Coburn et al. 2016), rather than using biofilm with mixed culture. In the current study, mixed culture biofilm from the experimental facility was regrown in $1/10^{th}$ LB broth and EPS was extracted from the enriched culture for investigating their impacts on disinfectant decay. The results of EPS characteristic analysis demonstrated a difference in EPS composition structure between isolated mixture biofilm and its regrown culture, highlighting the importance of using onsite biofilm if results are to have real world relevance.

It was suggested that biofilm EPS structure and composition were highly affected by the environment in which the biofilm is incubated, and the bacterial communities presented (Ahimou et al. 2007; Simões et al. 2007). Within the current study, carbohydrate was the dominant component of all biofilms from flow cell units (Table 6.1), as has been reported in other studies (Kilb et al. 2003). Fish et al. (2017) applied Confocal Laser Scanning Microscopy (CLSM) to evaluate EPS composition in a full-scale DWDS experimental facility and the results suggested carbohydrate was

dominant in EPS within all sample points. In contrast, biofilm's EPS composed with higher proportion of protein was observed by other researches (Jahn and Nielsen 1998; Ahimou et al. 2007; Celmer et al. 2008). Jahn et al. (1998) and Celmer et al. (2008) suggested a low carbohydrate to protein ratio (C/P) of between 0.25~0.6 and 0.1~0.8 for biofilm incubated in sewer and municipal wastewater, respectively. In the current study, although the C/P ratios of biofilm's EPS were all above 1, the value varied with different operational conditions. In most cases, without considering the disinfectant concentration and Cl_2/NH_3-N mass ratio, a higher proportion of carbohydrate was observed in biofilm incubated at flow rate of 6L/min, suggesting that carbohydrate synthesis was promoted (Table 6.1). These results were not expected as other studies reported a linear relationship between EPS composition and hydrodynamics (Simoes et al. 2005; Ahimou et al. 2007; Wagner et al. 2009) (i.e. more/less composition corresponding to high/low flow velocity/shear stress). For instance, carbohydrate concentration was reported to be positively correlated with the biofilm cohesive energy ($R^2 = 0.9$). This suggests a high potential of C/P ratio under high shear stress (Ahimou et al. 2007). This opinion was also supported by the filamentous nature and the ability of carbohydrate to form and fill spaces between cells (Ohashi et al. 1994; Wloka et al. 2004b; Flemming et al. 2010). On the contrary, Houghton et al. (1999) concluded that lower C/P ratio would induce a more stable and resilient biofilm, and hence to increase its resistance ability to high shear stress. However, since these studies used annual reactor with external nutrient or conducted in wastewater system, evidence for the interactions between hydraulic and EPS composition in DWDSs was not sufficient.

Hydraulic regime is a significant factor for biofilm development due to its effect on mass-transfer and material mobilization between biofilm and water (Beer et al. 1996; Stoodley et al. 2001; Beyenal et al. 2002). Previous studies suggested that lower flow rates or shear stress would result in thicker biofilm with more diverse bacterial community (Rickard et al. 2004b; Rochex et al. 2008; Wagner et al. 2009). In addition, Fish et al. (2017) observed greater volume of biomass in biofilm incubated at steady state hydraulic regimes, when compared with biofilm grown at varied flow condition. The author also demonstrated that since lower shear stress had less selection pressure on biofilm and therefore, less EPS-per-cell was produced from more diverse biofilm (Fish et al. 2017). If following the trends, biofilm incubated at flow rate of 2L/min

would have greater amount of biofilm but less EPS-per-cell than biofilm in flow cell running at 10L/min in the current study. However, this was not always the case (Table 6.2). In test phase 3, where the Cl_2/NH_3-N ratio was 3:1 and two concentrations of chloramine (1 and 5 mg/L) were tested, more biomass accumulated but less EPS-per-cell produced along with the increase of flow rate in biofilm conditioned by less chloramine (1 mg/L). On the other hand, when the disinfectant concentration changed to 5 mg/L, less biomass associated with less EPS production per cell were observed under higher flow rate. Moreover, there was no immediate relationship between hydrodynamic, biomass amount and the EPS-per-cell investigated in biofilm collected from test phase 4, although less biomass but more EPS production per cell was found regardless of hydraulic regime.

Results from the current study indicate that biomass accumulation and EPS amount within biofilm were not only influenced by the single operational condition, but is suggested to be affected by interactions between hydraulic regime and disinfectant strategy. In terms of hydraulic regimes, unlike the theory discussed above, a greater biomass might be the result of more turbulent flow, which would introduce greater mass-transfer of nutrient (including cells) to the attaching surface. This was observed by several studies, which found more materials were accumulated with increasing shear stress in biofilm incubated at industrial water-fed (Rochex et al. 2008) or nutrient rich (i.e. prepared culture media) reactors (Beyenal et al. 2002). At higher flow rate, although more bio-material might accumulate, less EPS-per-cell was expected due to old biofilm with more EPS being removed by high shear stress and consequently, more resources and energy remaining were converted to new biomass compared with EPS production. This was confirmed by Simoes et al. (2003, 2005) who observed less EPS (carbohydrate) formed per gram under higher velocity and also Kreft et al. (2001) who found a decrease of biofilm growth with the EPS production. Fish et al. (2017) also found limited biomass but more EPS per cell under low varied regimes, whereas high varied hydraulic regimes were associated with abundant biofilm but less EPS production per cell. These provided support to the explanation that under turbulent condition, EPS producers were removed by external shear stress and the remaining abundant were non-producers (Fish et al. 2017). Although the findings in current study cannot confirm the relationship between biofilm growth, EPS production and hydraulic

regimes, the theories above still explained part of the results on why less biomass is associated with more EPS-per-cell. The results also suggest hydraulic regimes and biofilm internal metabolism might work as combined effect on biofilm and EPS development and production process.

On the other hand, the disinfectant strategy might influence biofilm biomass and EPS per cell in terms of bacterial activity and EPS availability. A higher concentration of disinfectant was believed to have better disinfectant efficiency for controlling biomass within biofilm. However, from Table 6.1 and 6.2, in test phase 4, the biomass in biofilm conditioned by higher concentration of chloramine (5mg/L) was greater than that in biofilm from flow cells fed with lower disinfectant (1mg/L), while a reverse relationship was observed for EPS per cell. One of the functions of EPS is to protect biofilm against environmental stress (Weiner et al. 1995). Helbling and Vanbriesen (2007) observed a resistance mechanism adopted by many bacterial species, which would increase EPS production for defending against oxidative stress from disinfectants. Xue et al. (2013a) also suggested two mechanisms of EPS protection role on bacteria inactivity by both chlorine and chloramine. The author suggested EPS might work as either disinfectant consumer (for chlorine inactivation) or limiter that prevent the access of chloramine to the cell membrane (Xue et al. 2013a). In the current study, since nitrification was observed and this process would accelerate the decomposition of chloramine to free chlorine and ammonia (Oldenburg et al. 2002), hence the disinfectant affecting biofilm might be the combination of chloramine and chlorine. If the mechanisms described above were true, then the increased EPS produced would be consumed by chlorine and also work as protector to increase biofilm resistance ability to chloramine. Therefore, this opinion partly explains the less EPS per cell observed in biofilm conditioned by higher concentration of disinfectant in test phase 4. In addition, although the higher concentration of chloramine might remove more bacterial cluster from the biofilm, there still might be survivals and the redistributed cells would form more complex biofilm. This has been observed by Xue et al. (2013b), who used chlorine to detach cell clusters from single strain biofilm and then found that the redistributed biofilm had higher amount of biomass, greater thickness and more complex structure when compared with original biofilm. The findings in the current study lend support to this as more bio-material accumulated in

the system with higher concentration of disinfectant.

However, in test phase 3, disinfectant concentrations did not significantly affect the biomass and EPS-per-cell production in biofilms (Table 6.1 and 6.2). The different observations between the two test phases in the current study might be due to the difference in Cl_2/NH_3 mass ratios. The difference of the ratios reflects the amount of excessive free ammonia in the feed water. In systems undergoing nitrification, more free ammonia will be in favour of the process and the decay of chloramine will be accelerated by the produced nitrite. Consequently, the different mass ratio can further influence the proportion of the amount of chlorine/chloramine applied to the biofilm. In test phase 3, where the mass ratio was 3:1, free chlorine produced by the decay of chloramine was supposed to be the main biocide. LeChevallier et al. (1988) and Beer et al. (1994) suggested that compared with chloramine, chlorine dose not easily penetrate into biofilm. This property of chlorine might result in less inactivating pressure on microorganisms within biofilm and reduce the efficiency of higher concentration of disinfectant on controlling biofilm biomass.

As mentioned above, the structure of EPS composition was different between EPS from isolated biofilm and regrown culture, and the dominant composition changed from carbohydrate to protein (Fig.6.1). This was expected since not all the bacteria could be cultured due to the difference between culture media and the original biofilm incubation nutrient condition. Using the same regrowth culture media with current study, Wang et al. (2013) characterized the biomolecular composition of EPS for both mixed isolated and regrown biofilm. A more detailed difference of subunits of protein and carbohydrate was observed between these two kinds of EPS (Wang et al. 2013). Furthermore, there was no hydraulic effect on bacterial growth during regrowth in current experiments. The higher concentration of carbohydrate in isolated biofilm EPS further confirmed its role in maintaining biofilms mechanical stability and cohesion against additional shear stress (Korstgens et al. 2001; Ahimou et al. 2007). In addition, since the regrow culture was incubated with media without biocides, less EPS-per-cell was produced in the regrown biofilm (Table 6.2). The difference in EPS composition observed highlights the influence of environmental parameters on biofilm development and EPS properties.

Although the regrowth conditions were kept the same for all cultures, the EPS production per cell and structure were different between samples (Table 6.1 and 6.2). This was partly due to the difference in bacterial community within original biofilms, as EPS structure and composition were affected by microbial composition (Simões et al. 2007). Based on the results presented in Chapter 5, difference in microbial community between different operational conditions was observed in the same experimental facility, although the conditions were not the same as that within the current study. Combined with the findings from these two chapters, further research about the relationship between microbial community and EPS structure should be considered. In addition, some of the EPS producers from the corresponding biofilm might not be incubated or the incubation environment was not suitable for their EPS production. Consequently, the EPS amount and structure differed. As the EPS extracted from the regrown culture was further used for investigating their effects on disinfectant decay in the current study, the microbial composition difference mentioned above should be considered in the following discussion.

Based on TOC concentration, a series of regrown culture EPS solution were exposed to both chlorine and chloramine. The results showed a high reactivity with chlorine, while a relatively low reactivity with chloramine (Figs.6.2 to 6.7). According to the two-phase disinfectant decay model (Eq. 6.1), the rate constants of fast decay phase of chloramine-EPS (Figs.6.2 and 6.3) and chlorine-EPS (Figs.6.5 and 6.6) were 0.034~0.206 (min^{-1}) and 0.04~0.448 (min^{-1}), respectively. The difference of the disinfectant consumption rates between these two disinfectants indicate that there was a difference of reaction mechanism between chlorine and chloramine as disinfectant, and this has been raised by Neden et al. (1992) and Connell (1996). Chlorine will react with organics and inorganics without selection and hence the stability of this reactant is low when compared with chloramine. In contrast, chloramine is considered to be more stable and its mechanism of controlling bacterial growth is to penetrate to cell membrane to react with amino acids and disrupt bacterial metabolism (Connell 1996). Jacangelo et al. (1991) also raised the hypothesis that the protein-associated biological activity, such as respiration and bacterial transportation, would be inhibited in systems using chloramine for disinfection. This was further explored and confirmed by Coburn et al. (2016) who observed metabolic enzymes were affected by monochloramine.

In the chloramine decay test, no significant difference in disinfectant residual among different EPS amount was observed and the chloramine demand was low. This low disinfectant demand and slow reaction rates might help to inhibit the disinfection efficiency of chloramine for biofilm as the EPS would reduce the reaction sites on cell membrane (Kouame and Haas 1991; Coburn et al. 2016). As protein was the main EPS component in the current test, it was hypothesised that the protein-associated EPS would act as biofilm protector against disinfection. This opinion is supported by previous studies (Xue et al. 2013a; Coburn et al. 2016), which observed the functional group within protein to be consumed during disinfection through analysis of Fourier transform infrared spectroscopy (FTIR). To identify the effect of EPS component on disinfectant decay, Xue et al. (2013a) used both alginate-based EPS and alginate surrogate (bovine serum albumin - BSA) for comparison. The results showed that BSA was more reactive with chloramine than alginate EPS. Combined with inactivation test on bacterial strain, the author suggested rather than acting as disinfectant consumer, alginate EPS was a protector that limit or delay the reaction with chloramine (Xue et al. 2013a). However, this mechanism might not be sufficiently confirmed by the results of the current study since no significant difference in chloramine decay between EPS and EDTA (control) was observed. As the EPS extraction material, EDTA was considered as organics and took part in the disinfectant decay test. The similar trend of EPS and EDTA reactions might be due to the limited EPS contained within the solution (only 0.13~8.6 μg/ml, while 0~200 μg/ml in Xue et al. (2013a). When exposed to chloramine, the disinfectant was mostly interacted with EDTA and the combined chloroaromatic compounds would be detected as the total chlorine, and thereby the difference in chloramine residual between different concentrations of EPS solution was limited. As a result, there was no sufficient evidence from the current study for demonstrating whether EPS acts as simple organics to consume chloramine or limits the penetration of chloramine to cell membrane. Nevertheless, the rate constants of slow decay phase varied among samples from different original biofilms, although no statistical difference was found. This might be partially due to the difference in EPS component structure. To further investigate how EPS affects chloramine decay, the change of biomolecular compositions of EPS (i.e. amino acid and polysaccharide monomer) should be analysed and interference from other organics should be avoided

by adopting another EPS extraction method.

Unlike the chloramine test, chlorine performed as an oxidizer and its decay rates were observed to be rapid in all tests, and this has been reported by other researches (Gagnon et al. 2004). In addition, differences were found between EPS amount based on TOC concentration of 2 mg/L and 10 mg/L (Figs.6.5 and 6.6). The similar trend of 10 mg/L and 20 mg/L reactions within either single or different samples might be explained by the reason that the disinfectant demand for these two concentrations was too high for the chlorine present. All the disinfectant reacted with the materials exposed to it and therefore the chlorine residuals were similar. The high concentration of TOC also led to higher rate constants for fast decay phase than the 2 mg/L reactions. Compared with the decay trends with EDTA reaction (Fig.6.7), the limited difference observed suggests that EPS acted as an organic disinfectant consumer, which reacts with chlorine without selection and then decreases the available amount of chlorine for bacterial inactivation. However, EPS component and structure might still be an influencing factor due to the observation of differences of decay rate in 2 mg/L reactions between different samples. The biomolecular components of EPS might show different resistance ability to chlorine and this would further affect the chlorine decay rate. To verify the hypothesis, further researches need to focus on the role of more detailed EPS components on chlorine decay process.

6.5 Summary

This chapter presents the results of molecular characteristics of extracted EPS from chloraminated experimental flow cell facility running at different operational conditions, and also data about EPS effects on two different disinfectants. The main objective of this chapter was to investigate the effects of operational conditions on biofilm EPS characteristics, and also how EPS impacts on the decay of disinfectants. The following conclusions were derived from the study:

- The EPS composition and structure of isolated biofilm was investigated and the complex patterns observed suggest that there is no simple linear relationship between hydraulic regimes, EPS characteristics and disinfection strategy. Carbohydrate was the main components within biofilm's EPS, but the C/P ratio

varied with biofilm incubation conditions.

- Hydraulics did condition biomass availability and EPS production per cell, although no consistent effect was observed within current study.
- Chloramine concentration had effects on biofilm biomass and EPS-per-cell when the Cl_2/NH_3 mass ratio was 5:1. No obvious difference was observed between different disinfectant concentrations when the mass ratio was 3:1. The observations suggest that Cl_2/NH_3 mass ratio impacts on microbial inactivation and further influences biofilm and EPS properties in chloraminated water systems.
- The comparison between EPS composition of isolated biofilm and regrown culture confirmed nutrient incubation conditions would affect the EPS structure.
- The low ratio of carbohydrate and protein (C/P<1) of EPS from regrown culture suggests that the difference in structural function within biofilm between carbohydrate and protein. Less EPS production per cell in regrown biofilm suggests the protective role of EPS on withstanding detachment forces and disinfectants inactivation.
- The disinfectant decay tests suggest that the reaction mechanisms of chloramine and chlorine are different. Chlorine is a fast oxidizer and EPS potentially works as organic disinfectant consumer. EPS shows low reactivity with chloramine, but the reaction mechanism is not clear from this study.
- Although no statistical differences in disinfectant decay rate within different EPS samples were observed, the fluctuation of the rate might suggest possible effect of EPS composition and structure on disinfectant decay process.

In summary, how EPS property responds to different operational conditions, especially the hydraulic regime is investigated within this chapter. The understanding of the effects of EPS on disinfection was enhanced by the disinfectant decay tests. This study suggests that both hydraulics and disinfection strategies have impacts on biofilm EPS, and confirms that EPS can enhance biofilm resistance ability to disinfection.

Chapter 7 Conclusions and Future work

7.1 Main findings

Within the current study, an experimental flow cell facility was applied to investigate the effects of operational conditions, especially hydraulic conditions and disinfectant strategy on drinking water quality. Based on this facility and combined with engineering and microbiological techniques, the main findings of this study are as follows:

i. The current study has investigated how on-going nitrification responds to different hydraulic regimes and disinfection strategies within a flow cell experimental facility. This is the first work that provides insight into hydraulic regimes effects on microbial water quality problem in DWDS. It also evaluates the main nitrification indicators and suggests possible nitrification control strategies.
ii. The microbial community within biofilm and bulk water collected from flow cells under different operational conditions have been analysed by Illumina Miseq. The study investigates the difference in microbial community and structure between different hydraulic conditions and disinfection strategies.
iii. Biofilm EPS composition is characterized in this study and the effects of operational conditions, especially the hydraulic regimes, on EPS structure was analysed. The study also investigates the regrown biofilm EPS impacts on disinfection efficiency via disinfectant decay test. It is the first study that uses mix culture biofilm to identify EPS effects on disinfection, which can to some extent reveal real DWDS situation.

7.2 Conclusions

The main aim of this study is to investigate nitrification properties under different operational conditions, together with biofilm characteristics in chloraminated water distribution systems. In this thesis, the main aim together with individual research

objectives have been achieved. The main experimental findings and conclusions of current study are outlined herein.

1. Five hydraulic conditions were investigated within the flow cell units and to investigate their effects on nitrification process. Through evaluating various physic-chemical and biological parameters, nitrification process was suggested to be influenced by hydraulics. Although no direct linear relationship was observed between nitrification extent and hydraulic conditions, the activity of nitrifying bacteria was hypothesised to be favoured when the fluid flow is transforming from the laminar stage to the turbulent stage ($2300<Re<4000$).
2. Different disinfection strategies were operated within current facility to find whether nitrification could be effectively controlled by increasing total chlorine and ammonia nitrogen mass ratio. Compared the data from flow cell units fed with two chloramine concentrations (1 and 5 mg/L), increasing total chlorine concentration was found to inhibit nitrification for a short period in some cases. Combined with the less severe nitrification that was observed in the flow cells operated at higher flow rate (10L/min), a joint action is suggested to control nitrification by increasing both flow turbulence to a proper range and chloramine concentration within DWDSs.
3. To predict nitrification, statistical relationships between nitrite production and water parameters including pH, free chlorine residual, turbidity, TOC and HPC were analysed. In terms of evaluating nitrification extent in systems experiencing nitrification within the current study, it was feasible by taking into account nitrite, turbidity and TOC together.
4. After each test phase, biofilm and water samples were collected for further DNA extraction and sequencing. Through Miseq Illumina, the bacterial community composition and structure within each sample were detected. The results suggest a difference in microbial community between biofilm and bulk water. The Alpha diversity analysis shows that the species richness and diversity in biofilm tend to be higher at lower flow rates, while the diversity increases with the increase of shear stress when the flow rate is between 6 and 10 L/min. In addition, different hydraulic regimes affect the bacterial community composition and structure within bulk water, with a tendency of

higher richness and diversity detected at lower hydraulic regimes. This confirms the influence of hydraulic condition on biofilm mechanical structure and further material mobilization to water. Cl_2/NH_3-N mass ratio was found to have effect on microbial structure in biofilm and the results suggest that excessive ammonia would be a factor affecting chloramine penetration to biofilm and the microbial activity within biofilm.

5. After the tests the EPS composition and structure from collected biofilm were quantified and analysed to investigate whether there is relationship between EPS characteristics and operational conditions. The complex patterns observed suggest that there is no simple linear relationship between hydraulic regimes, EPS characteristics and disinfection strategy. In terms of EPS composition, carbohydrate was the main components, but the C/P ratio varied with biofilm incubation conditions. Hydraulics were also found can condition biomass availability and EPS production per cell, although no consistent effect was observed within current study.
6. The disinfectant decay tests were conducted to investigate how EPS affects the decay of chlorine/chloramine. The results suggest that the reaction mechanisms of chloramine and chlorine are different. Chlorine is a fast oxidizer and EPS potentially works as organic disinfectant consumer. EPS shows low reactivity with chloramine, but the reaction mechanism is not clear from this study.

Overall, current study provides new and unique data for water utilities about the impact of operational conditions on nitrification process and microbial community in biofilms and bulk water. These results could assist the operators to better evaluate and predict water quality in DWDS and to make further management strategy. Results from the disinfectant decay tests highlight the influence from biofilm EPS on water quality and encourage further research about their properties.

7.3 Future Work

Within the current study, experiments are conducted to evaluate water quality under different operational conditions. Although the experimental facility and procedures were designed to reveal real system as much as possible, there are still several factors that are not be fully represented. Based on the results obtained from the current study,

the following is a list of potential work that can be considered in the future:

- Due the limitation in laboratory, the current experimental facility is designed to recirculate feed water rather than having a continuous flow. Although a 'dump and fill' strategy has been applied to simulate the water flow in real system, the results from current facility could still be affected. In further research, a system which can have continuous in and out flow is suggested. In addition, the water age maintained within current study is three days, which is too long to secure water quality in real systems. Combined with the control strategies suggested in Chapter 4, shorter water age can be used in further research to verify the management approach. On the other hand, the experimental temperature controlled and kept constant in current study, and this may not reveal the real condition. Further research can introduce the temperature effect, together with different hydraulic regimes to identify whether on-going nitrification can still be affected by hydraulics.
- The sequencing technique used in current study cannot detect nitrifying bacteria, and this may be attributed to the low concentration of nitrifiers and the limited detection depth of this sequencing approach. In further research, a better understanding of the relationship between heterotrophs community and nitrifying bacteria can be achieved by using multiple molecular technique, such as q-PCR which can detect the community and abundance of target nitrifying groups. In addition, since biofilm and water samples for sequencing were collected at the end of each test phase without regular sampling during the experiment, results from the current study cannot reveal the change of microbial community to water quality. Further research can take advantage of the design of flow cell units and measure the change of microbial community with time. Such investigation can provide an understanding of the interactions of nitrification and microbial community.
- Although the EPS used for disinfection decay test in the current study was from mixed culture biofilm, the composition characterization results still suggest a difference in EPS structure between in-situ biofilm and culture regrown biofilm. This is due to the fact that most of the bacteria cannot be regrown properly by culture media, and biofilm properties are governed by various

environmental factors. Further research should focus on investigating the interactive effects between EPS composition and microbial community, and also operational conditions. The mechanism of EPS impacts on disinfectant decay is proven to be complex. It is encouraged that further research to investigate the process in combination with biofilm features, rather than isolating EPS composition.

References

Abe Y., Skali-Lami, S., Block, J. and Francius, G. (2012). Cohesiveness and hydrodynamic properties of young drinking water biofilms. Water research 46(4), pp. 1155-1166.

Agilent-Technologies. (2013). Agilent High Sensitivity D1000 ScreenTape System Quick Guide. Part Number: G2964-90131 Rev.B.

Ahimou F., Semmens, M.J., Haugstad, G. and Novak, P.J. (2007). Effect of protein, polysaccharide, and oxygen concentration profiles on biofilm cohesiveness. Appl Environ Microbiol 73(9), pp. 2905-2910.

Altman S.J., McGrath, L.K., Souza, C.A., Murton, J.K. and Camper, A.K. (2009). Integration and decontamination of Bacillus cereus in Pseudomonas fluorescens biofilms. J Appl Microbiol 107(1), pp. 287-299.

APHA. (1998). Standard Methods for the Examination of Water and Wastewater. 20th ed Am. Public Health Assoc, Washington, DC.

Araya R., Tani, K., Takagi, T., Yamaguchi, N. and Nasu, M. (2003). Bacterial activity and community composition in stream water and biofilm from an urban river determined by fluorescent in situ hybridization and DGGE analysis. FEMS Microbiology Ecology 43(1), pp. 111-119.

AWWA. (1992). Water industry database: Utility profiles. American Water Works Association: Denver, CO, USA.

AWWA. (2002). Effects of Water Age on Distribution System Water Quality. American Water Works Association: Denver, CO, USA, p. 19.

Beer D.D., Srinivasan, R. and Stewart, P.S. (1994). Direct measurement of chlorine penetration into biofilms during disinfection. Applied and Environmental Microbiology 60(12), pp. 4339-4344.

Beer D.D., Stoodley, P. and Lewandowski, Z. (1996). Liquid flow and mass transport in heterogeneous biofilms. Water Research 30(11), pp. 2761-2765.

Beumer A., King, D., Donohue, M., Mistry, J., Covert, T. and Pfaller, S. (2010). Detection of Mycobacterium avium subsp. paratuberculosis in drinking water and biofilms by quantitative PCR. Appl Environ Microbiol 76(21), pp. 7367-7370.

Beyenal H. and Lewandowski, Z. (2002). Internal and external mass transfer in biofilms grown at various flow velocities. Biotechnol Prog 18(1), pp. 55-61.

Blackburne R., Vadivelu, V.M., Yuan, Z. and Keller, J. (2007). Kinetic characterisation of an enriched Nitrospira culture with comparison to Nitrobacter. Water Research 41(14), pp. 3033-3042.

Boe-Hansen R., Albrechtsen, H., Arvin, E. and Jørgensen, C. (2002). Bulk water phase and biofilm growth in drinking water at low nutrient conditions. Water Research 36(18), pp. 4477-4486.

Böl M., Möhle, R.B., Haesner, M., Neu, T.R., Horn, H. and Krull, R. (2009). 3D finite element model of biofilm detachment using real biofilm structures from CLSM data. Biotechnology and Bioengineering 103(1), pp. 177-186.

Bollmann A., Bär-Gilissen, M. and Laanbroek, H.J. (2002a). Growth at low ammonium concentrations and starvation response as potential factors involved in niche differentiation among ammonia-oxidizing bacteria. Applied and Environmental Microbiology 68(10), pp. 4751-4757.

Bollmann A. and Laanbroek, H.J. (2002b). Influence of oxygen partial pressure and salinity on the community composition of ammonia-oxidizing bacteria in the Schelde estuary. Aquatic Microbial Ecology 28(3), pp. 239-247.

Boxall J.B. and Prince, R.A. (2006). Modelling discolouration in a Melbourne (Australia) potable water distribution system. Journal of Water Supply: Research and Technology - Aqua 55(3), p. 207.

Bridier A., Briandet, R., Thomas, V. and Dubois-Brissonnet, F. (2011). Resistance of bacterial biofilms to disinfectants: a review. Biofouling 27(9), pp. 1017-1032.

Brown M.J. and Lester, J.N. (1980). Comparison of bacterial extracellular polymer extraction methods. Appl Environ Microbiol 40(2), pp. 179-185.

Brunkard J.M., Ailes, E., Roberts, V.A., Hill, V., Hilborn, E.D., Craun, G.F., Rajasingham, A., Kahler, A., Garrison, L., Hicks, L., Carpenter, J., Wade, T.J., Beach, M.J. and Yoder Msw, J.S. (2011). Surveillance for waterborne disease outbreaks

associated with drinking water---United States, 2007--2008. MMWR Surveill Summ 60(12), pp. 38-68.

Burlingame G. and Brock, G. (1985). Water-quality deterioration in treated-water storage tanks. Journal American Water Works Association 77(4), pp. 60-60.

Butterfield P.W., Camper, A.K., Ellis, B.D. and Jones, W.L. (2002). Chlorination of model drinking water biofilm: implications for growth and organic carbon removal. Water Research 36(17), pp. 4391-4405.

Celmer D., Oleszkiewicz, J.A. and Cicek, N. (2008). Impact of shear force on the biofilm structure and performance of a membrane biofilm reactor for tertiary hydrogen-driven denitrification of municipal wastewater. Water Res 42(12), pp. 3057-3065.

Chandy J. and Angles, M. (2001). Determination of nutrients limiting biofilm formation and the subsequent impact on disinfectant decay. Water Research 35(11), pp. 2677-2682.

Chao A. (1984). Nonparametric estimation of the number of classes in a population. Scandinavian Journal of statistics, pp. 265-270.

Characklis W. and KC, M. (1990). Biofilms: A Basis for an Interdisciplinary Approach. New York: Wiley-Interscience.

Coburn K.M., Wang, Q., Rediske, D., Viola, R.E., Hanson, B.L., Xue, Z. and Seo, Y. (2016). Effects of Extracellular Polymeric Substance Composition on Bacteria Disinfection by Monochloramine: Application of MALDI-TOF/TOF-MS and Multivariate Analysis. Environ Sci Technol 50(17), pp. 9197-9205.

Connell G. (1996). The Chlorination/Chloramination Handbook. American Water Works Association, Denver.

Costerton J.W., Lewandowski, Z., Caldwell, D.E., Korber, D.R. and Lappin-Scott, H.M. (1995). Microbial biofilms. Annu Rev Microbiol 49, pp. 711-745.

Cowles M. (2015). Assessing the impact of biofouling on the hydraulic efficiency of pipelines. PhD thesis, Cardiff University.

Craun G.F., Brunkard, J.M., Yoder, J.S., Roberts, V.A., Carpenter, J., Wade, T., Calderon, R.L., Roberts, J.M., Beach, M.J. and Roy, S.L. (2010). Causes of outbreaks

associated with drinking water in the United States from 1971 to 2006. Clinical Microbiology Reviews 23(3), pp. 507-528.

Cunliffe D. (1991). Bacterial nitrification in chloraminated water supplies. Applied and environmental microbiology 57(11), pp. 3399-3402.

De Vet W., Dinkla, I., Muyzer, G., Rietveld, L. and Van Loosdrecht, M. (2009). Molecular characterization of microbial populations in groundwater sources and sand filters for drinking water production. Water Research 43(1), pp. 182-194.

Doederer K., Gernjak, W., Weinberg, H.S. and Farré, M.J. (2014). Factors affecting the formation of disinfection by-products during chlorination and chloramination of secondary effluent for the production of high quality recycled water. Water research 48, pp. 218-228.

Donlan R.M. (2002). Biofilms: Microbial Life on Surfaces. Emerging Infectious Diseases 8(9), pp. 881-890.

Donlan R.M. and Costerton, J.W. (2002). Biofilms: survival mechanisms of clinically relevant microorganisms. Clin Microbiol Rev 15(2), pp. 167-193.

Douterelo I., Sharpe, R.L. and Boxall, J.B. (2013). Influence of hydraulic regimes on bacterial community structure and composition in an experimental drinking water distribution system. Water Res 47(2), pp. 503-516.

Edgar R.C., Haas, B.J., Clemente, J.C., Quince, C. and Knight, R. (2011). UCHIME improves sensitivity and speed of chimera detection. Bioinformatics 27(16), pp. 2194-2200.

Edwards M., Marshall, B., Zhang, Y. and Lee, Y. (2005). Unintended consequences of chloramine hit home. proceedings of the Water Environment Federation 2005(1), pp. 240-256.

Eichler S., Christen, R., Höltje, C., Westphal, P., Bötel, J., Brettar, I., Mehling, A. and Höfle, M. (2006). Composition and dynamics of bacterial communities of a drinking water supply system as assessed by RNA-and DNA-based 16S rRNA gene fingerprinting. Applied and environmental microbiology 72(3), pp. 1858-1872.

Eisnor D. and Gagnon, G. (2003). A framework for the implementation and design of pilot-scale distribution systems.

Emtiazi F., Schwartz, T., Marten, S., Krolla-Sidenstein, P. and Obst, U. (2004). Investigation of natural biofilms formed during the production of drinking water from surface water embankment filtration. Water research 38(5), pp. 1197-1206.

Falkinham J.O., Norton, C. D. and LeChevallier, M.W. (2001). Factors influencing numbers of Mycobacterium avium, Mycobacterium intracellulare, and other Mycobacteria in drinking water distribution systems. Appl Environ Microbiol 67(3), pp. 1225-1231.

Feben D. (1935). Nitrifying bacteria in water supplies. Journal (American Water Works Association) 27(4), pp. 439-447.

Fish K., Osborn, A.M. and Boxall, J.B. (2017). Biofilm structures (EPS and bacterial communities) in drinking water distribution systems are conditioned by hydraulics and influence discolouration. Sci Total Environ 593-594, pp. 571-580.

Fleming K., Harrington, G. and Noguera, D. (2005). Nitrification potential curves: a new strategy for nitrification prevention. Journal (American Water Works Association) 97(8), pp. 90-99.

Fleming K., Harrington, G. and Noguera, D. (2008). Using nitrification potential curves to evaluate full-scale drinking water distribution systems. American Water Works Association. Journal 100(10), p. 92.

Flemming H.-C. (2002). Biofouling of Industrial Systems. Encyclopedia of environmental microbiology.

Flemming H.-C., Neu, T.R. and Wozniak, D.J. (2007). The EPS matrix: the "house of biofilm cells". Journal of bacteriology 189(22), pp. 7945-7947.

Flemming H.-C. and Wingender, J. (2010). The biofilm matrix. Nat Rev Micro 8(9), pp. 623-633.

Flemming H.-C., Wingender, J. and Griegbe, M.C. (2017). Physico-chemical properties of biofilms. pp. 19-34.

Furumai H. and Rittmann, B. (1992). Advanced modeling of mixed populations of heterotrophs and nitrifiers considering the formation and exchange of soluble microbial products. Water Science and Technology 26(3-4), pp. 493-502.

Furumai H. and Rittmann, B. (1994). Evaluation of multiple-species biofilm and floc processes using a simplified aggregate model. Water Science and Technology 29(10-11), pp. 439-446.

Gagnon G., C. O'Leary, K., J. Volk, C., Chauret, C., Stover, L. and Andrews, R. (2004). Comparative Analysis of Chlorine Dioxide, Free Chlorine and Chloramines on Bacterial Water Quality in Model Distribution Systems.

Gauthier V., Gérard, B., Portal, J.-M., Block, J.-C. and Gatel, D. (1999). Organic matter as loose deposits in a drinking water distribution system. Water Research 33(4), pp. 1014-1026.

Gjaltema A., Arts, P.A., van Loosdrecht, M.C., Kuenen, J.G. and Heijnen, J.J. (1994). Heterogeneity of biofilms in rotating annular reactors: Occurrence, structure, and consequences. Biotechnol Bioeng 44(2), pp. 194-204.

Gomez-Alvarez V., Revetta, R.P. and Santo Domingo, J.W. (2012). Metagenomic analyses of drinking water receiving different disinfection treatments. Appl Environ Microbiol 78(17), pp. 6095-6102.

Goodwin J. and Forster, C. (1985). A further examination into the composition of activated sludge surfaces in relation to their settlement characteristics. Water research 19(4), pp. 527-533.

Grady J., CP Leslie, Daigger, G.T., Love, N.G. and Filipe, C.D. (2011). Biological wastewater treatment. CRC press.

Groeneweg J., Sellner, B. and Tappe, W. (1994). Ammonia oxidation in Nitrosomonas at NH3 concentrations near Km: effects of pH and temperature. Water Research 28(12), pp. 2561-2566.

Hageskal G., Tryland, I., Liltved, H. and Skaar, I. (2012). No simple solution to waterborne fungi: various responses to water disinfection methods. Water Science and Technology: Water Supply 12(2), pp. 220-226.

Hallam N.B., West, J.R., Forster, C.F. and Simms, J. (2001). The potential for biofilm growth in water distribution systems. Water Res 35(17), pp. 4063-4071.

Hammes F., Berney, M., Wang, Y., Vital, M., Köster, O. and Egli, T. (2008). Flow-cytometric total bacterial cell counts as a descriptive microbiological parameter for drinking water treatment processes. Water Research 42(1), pp. 269-277.

Hardalo C. and Edberg, S.C. (1997). Pseudomonas aeruginosa: assessment of risk from drinking water. Critical reviews in microbiology 23(1), pp. 47-75.

Harms L.L. and Owen, C.A. (2004). Keys for controlling nitrification. In *AWWA WQTC*, November 2004, San Antonio, Texas.

Helbling D.E. and Vanbriesen, J.M. (2007). Free chlorine demand and cell survival of microbial suspensions. Water Res 41(19), pp. 4424-4434.

Henne K., Kahlisch, L., Brettar, I. and Höfle, M.G. (2012). Analysis of structure and composition of bacterial core communities in mature drinking water biofilms and bulk water of a citywide network in Germany. Applied and environmental microbiology 78(10), pp. 3530-3538.

Hoa P., Nair, L. and Visvanathan, C. (2003). The effect of nutrients on extracellular polymeric substance production and its influence on sludge properties. Water Sa 29(4), pp. 437-442.

Hockenbury M.R., Grady, C. and Daigger, G.T. (1977). Factors affecting nitrification. Journal of the Environmental Engineering Division 103(1), pp. 9-19.

Houghton J.I. and Quarmby, J. (1999). Biopolymers in wastewater treatment. Curr Opin Biotechnol 10(3), pp. 259-262.

Hua G., Reckhow, D.A. and Kim, J. (2006). Effect of bromide and iodide ions on the formation and speciation of disinfection byproducts during chlorination. Environmental Science & Technology 40(9), pp. 3050-3056.

Hulbert R. (1933). Ammonia-chlorine treatment yields nitrites in effluent.

Husband P.S., Boxall, J.B. and Saul, A.J. (2008). Laboratory studies investigating the processes leading to discolouration in water distribution networks. Water Res 42(16), pp. 4309-4318.

Husband S. and Boxall, J. (2010). Field Studies of Discoloration in Water Distribution Systems: Model Verification and Practical Implications.

Hwang C., Ling, F., Andersen, G.L., LeChevallier, M.W. and Liu, W.T. (2012). Microbial community dynamics of an urban drinking water distribution system subjected to phases of chloramination and chlorination treatments. Appl Environ Microbiol 78(22), pp. 7856-7865.

Jacangelo J., G, P. Olivieri, V. and Kawata, K. (1991). Investigating the Mechanism of Inactivation of Escherichia coli B by Monochloramine. pp. 80-87.

Jahn A., Griebe, T. and Nielsen, P.H. (1999). Composition of Pseudomonas putida biofilms: accumulation of protein in the biofilm matrix. Biofouling 14(1), pp. 49-57.

Jahn A. and Nielsen, P.H. (1998). Cell biomass and exopolymer composition in sewer biofilms. Water Science and Technology 37(1), pp. 17-24.

Jørgensen C., Boyd, H., Fawell, J. and Hydes, O. (2008). Establishment of a list of chemical parameters for the revision of the Drinking Water Directive. DHI.

Karanja D., Elliott, S.J. and Gabizon, S. (2011). Community level research on water health and global change: where have we been? Where are we going? Current opinion in environmental sustainability 3(6), pp. 467-470.

Katharine M., Hannah, R., Marissa, V., David, M., Virginia, A., Mia, M., Laura, A., Elizabeth, D., Timothy, J., Kathleen, E., Jonathan, S. and Vincent, R. (2017). Surveillance for Waterborne Disease Outbreaks Associated with Drinking Water — United States, 2013–2014. Morbidity and Mortality Weekly Report 66(44), pp. 1216-1221.

Kilb B., Lange, B., Schaule, G., Flemming, H.C. and Wingender, J. (2003). Contamination of drinking water by coliforms from biofilms grown on rubber-coated valves. Int J Hyg Environ Health 206(6), pp. 563-573.

Kirmeyer G.J. (2000). Guidance manual for maintaining distribution system water quality. American Water Works Association.

Kirmeyer G.J., Martel, K., Thompson, G., Radder, L., Klement, W., LeChevallier, M.W., Baribeau, H. and Flores, M. (2004). Optimizing chloramine treatment. American Water Works Association.

Kirmeyer G.J., Odell, L.H., Jacangelo, J., Wilczak, A. and Wolfe, R. (1995). Nitrification occurrence and control in chloraminated water systems. AWWA Res. Fdn., Denver.

Kjelleberg S. and Givskov, M. (2007). The biofilm mode of life: mechanisms and adaptations. Horizon Scientific Press.

Korstgens V., Flemming, H.C., Wingender, J. and Borchard, W. (2001). Uniaxial compression measurement device for investigation of the mechanical stability of biofilms. J Microbiol Methods 46(1), pp. 9-17.

Kouame Y. and Haas, C. (1991). Inactivation of E. coli by combined action of free chlorine and monochloramine. pp. 1027-1032.

Kozich J.J., Westcott, S.L., Baxter, N.T., Highlander, S.K. and Schloss, P.D. (2013). Development of a dual-index sequencing strategy and curation pipeline for analyzing amplicon sequence data on the MiSeq Illumina sequencing platform. Appl Environ Microbiol 79(17), pp. 5112-5120.

Kreft J.-U. and Wimpenny, J.W.T. (2001). Effect of EPS on biofilm structure and function as revealed by an individual-based model of biofilm growth. pp. 135-141.

Krishna K.C.B. and Sathasivan, A. (2010). Does an unknown mechanism accelerate chemical chloramine decay in nitrifying waters? pp. 82-90.

Krishna K.C.B., Sathasivan, A. and Chandra Sarker, D. (2012). Evidence of soluble microbial products accelerating chloramine decay in nitrifying bulk water samples. Water Res 46(13), pp. 3977-3988.

Krishna K.C.B., Sathasivan, A. and Ginige, M.P. (2013). Microbial community changes with decaying chloramine residuals in a lab-scale system. Water Res 47(13), pp. 4666-4679.

Kwon S., Moon, E., Kim, T.S., Hong, S. and Park, H.D. (2011). Pyrosequencing demonstrated complex microbial communities in a membrane filtration system for a drinking water treatment plant. Microbes Environ 26(2), pp. 149-155.

Larson T. (1939). Bacteria, corrosion and red water. Journal (American Water Works Association) 31(7), pp. 1186-1196.

Lawrence J.R., Swerhone, G.D.W. and Neu, T.R. (2000). A simple rotating annular reactor for replicated biofilm studies. Journal of Microbiological Methods 42(3), pp. 215-224.

LeChevallier M.W., Babcock, T.M. and Lee, R.G. (1987). Examination and characterization of distribution system biofilms. Appl Environ Microbiol 53(12), pp. 2714-2724.

LeChevallier M.W., Cawthon, C.D. and Lee, R.G. (1988). Inactivation of biofilm bacteria. Applied and environmental Microbiology 54(10), pp. 2492-2499.

LeChevallier M.W., Evans, T. and Seidler, R.J. (1981). Effect of turbidity on chlorination efficiency and bacterial persistence in drinking water. Applied and environmental microbiology 42(1), pp. 159-167.

LeChevallier M.W., Lowry, C.D. and Lee, R.G. (1990). Disinfecting biofilms in a model distribution system. Journal (American Water Works Association), pp. 87-99.

Lee W., Westerhoff, P. and Croué, J.-P. (2007). Dissolved organic nitrogen as a precursor for chloroform, dichloroacetonitrile, N-nitrosodimethylamine, and trichloronitromethane. Environmental science & technology 41(15), pp. 5485-5490.

Lee W.H., Wahman, D.G., Bishop, P.L. and Pressman, J.G. (2011). Free chlorine and monochloramine application to nitrifying biofilm: comparison of biofilm penetration, activity, and viability. Environ Sci Technol 45(4), pp. 1412-1419.

Lehtola M.J., Laxander, M., Miettinen, I.T., Hirvonen, A., Vartiainen, T. and Martikainen, P.J. (2006). The effects of changing water flow velocity on the formation of biofilms and water quality in pilot distribution system consisting of copper or polyethylene pipes. Water research 40(11), pp. 2151-2160.

Lehtola M.J., Miettinen, I.T., Keinänen, M.M., Kekki, T.K., Laine, O., Hirvonen, A., Vartiainen, T. and Martikainen, P.J. (2004). Microbiology, chemistry and biofilm development in a pilot drinking water distribution system with copper and plastic pipes. Water research 38(17), pp. 3769-3779.

Letterman R.D. and AWWA. (1999). Water quality and treatment - A handbook of community suppliers. McGraw-Hill.

Liang J.L., Dziuban, E.J., Craun, G.F., Hill, V., Moore, M.R., Gelting, R.J., Calderon, R.L., Beach, M.J. and Roy, S.L. (2006). Surveillance for waterborne disease and outbreaks associated with drinking water and water not intended for drinking—United States, 2003–2004. Morbidity and Mortality Weekly Report: Surveillance Summaries 55(12), pp. 31-65.

Lieu N.I., Wolfe, R.L. and Means, E.G. (1993). Optimizing chloramine disinfection for the control of nitrification. Journal of the American Water Works Association 85(2), pp. 84-90.

Life-Technologies. (2014). Quick Reference Qubit assays. Pub. no. MAN0010876, Rev. A.0.

Limpiyakorn T., Sonthiphand, P., Rongsayamanont, C. and Polprasert, C. (2011). Abundance of amoA genes of ammonia-oxidizing archaea and bacteria in activated sludge of full-scale wastewater treatment plants. Bioresource technology 102(4), pp. 3694-3701.

Lipponen M.T., Suutari, M.H. and Martikainen, P.J. (2002). Occurrence of nitrifying bacteria and nitrification in Finnish drinking water distribution systems. Water Research 36(17), pp. 4319-4329.

Liu R., Zhu, J., Yu, Z., Joshi, D., Zhang, H., Lin, W. and Yang, M. (2014). Molecular analysis of long-term biofilm formation on PVC and cast iron surfaces in drinking water distribution system. J Environ Sci (China) 26(4), pp. 865-874.

Liu S., Taylor, J.S., Randall, A. and Dietz, J.D. (2005). Nitrification modeling in chloraminated distribution systems. Journal (American Water Works Association) 97(10), pp. 98-108.

Liu Y. and Tay, J.H. (2001). Metabolic response of biofilm to shear stress in fixed-film culture. Journal of Applied Microbiology 90(3), pp. 337-342.

Love M.I., Anders, S. and Huber, W. (2017). Analyzing RNA-seq data with DESeq2. R package reference manual.

Lyon B.A., Dotson, A.D., Linden, K.G. and Weinberg, H.S. (2012). The effect of inorganic precursors on disinfection byproduct formation during UV-chlorine/chloramine drinking water treatment. Water research 46(15), pp. 4653-4664.

Lytle D.A., Sorg, T.J. and Frietch, C. (2004). Accumulation of arsenic in drinking water distribution systems. Environmental science & technology 38(20), pp. 5365-5372.

Machell J., Boxall, J., Saul, A. and Bramley, D. (2009). Improved representation of water age in distribution networks to inform water quality. Journal of Water Resources Planning and Management 135(5), pp. 382-391.

Mah T.-F.C. and O'Toole, G.A. (2001). Mechanisms of biofilm resistance to antimicrobial agents. Trends in microbiology 9(1), pp. 34-39.

Manuel C.M., Nunes, O.C. and Melo, L.F. (2007). Dynamics of drinking water biofilm in flow/non-flow conditions. Water Res 41(3), pp. 551-562.

Manz W., Szewzyk, U., Ericsson, P., Amann, R., Schleifer, K. and Stenström, T. (1993). In situ identification of bacteria in drinking water and adjoining biofilms by hybridization with 16S and 23S rRNA-directed fluorescent oligonucleotide probes. Applied and Environmental Microbiology 59(7), pp. 2293-2298.

Manz W., Wendt-Potthoff, K., Neu, T., Szewzyk, U. and Lawrence, J. (1999). Phylogenetic composition, spatial structure, and dynamics of lotic bacterial biofilms investigated by fluorescent in situ hybridization and confocal laser scanning microscopy. Microbial Ecology 37(4), pp. 225-237.

Martiny A.C., Albrechtsen, H.-J., Arvin, E. and Molin, S. (2005a). Identification of bacteria in biofilm and bulk water samples from a nonchlorinated model drinking water distribution system: detection of a large nitrite-oxidizing population associated with Nitrospira spp. Applied and environmental microbiology 71(12), pp. 8611-8617.

Martiny A.C., Albrechtsen, H.J., Arvin, E. and Molin, S. (2005b). Identification of bacteria in biofilm and bulk water samples from a nonchlorinated model drinking water distribution system: detection of a large nitrite-oxidizing population associated with Nitrospira spp. Appl Environ Microbiol 71(12), pp. 8611-8617.

Mathieu L., Bouteleux, C., Fass, S., Angel, E. and Block, J. (2009). Reversible shift in the α-, β-and γ-proteobacteria populations of drinking water biofilms during discontinuous chlorination. water research 43(14), pp. 3375-3386.

McCoy W.F. and Olson, B.H. (1986). Relationship among turbidity, particle counts and bacteriological quality within water distribution lines. Water Research 20(8), pp. 1023-1029.

Melo L. and Bott, T. (1997). Biofouling in water systems. Experimental thermal and fluid science 14(4), pp. 375-381.

Mi Z., Dai, Y., Xie, S., Chen, C. and Zhang, X. (2015). Impact of disinfection on drinking water biofilm bacterial community. pp. 200-205.

Moel P.J., Verberk, J.Q. and Van Dijk, J. (2007). Drinking water: principles and practices. World Scientific Publ.

Momba M.N. and Makala, N. (2004). Comparing the effect of various pipe materials on biofilm formation in chlorinated and combined chlorine-chloraminated water systems. Water SA 30(2), pp. 175-182.

Moradi S., Liu, S., Chow, C.W., van Leeuwen, J., Cook, D., Drikas, M. and Amal, R. (2017). Developing a chloramine decay index to understand nitrification: A case study of two chloraminated drinking water distribution systems. Journal of Environmental Sciences 57, pp. 170-179.

Muellner M.G., Wagner, E.D., McCalla, K., Richardson, S.D., Woo, Y.-T. and Plewa, M.J. (2007). Haloacetonitriles vs. regulated haloacetic acids: are nitrogen-containing DBPs more toxic? Environmental science & technology 41(2), pp. 645-651.

Neden D.G., Jones, R.J., Smith, J.R., Kirmeyer, G.J. and Foust, G.W. (1992). Comparing chlorination and chloramination for controlling bacterial regrowth. Journal (American Water Works Association), pp. 80-88.

Neu T.R. and Lawrence, J.R. 2009. Extracellular polymeric substances in microbial biofilms.Microbial Glycobiology. Elsevier, pp. 733-758.

Nielsen A.H., Vollertsen, J., Jensen, H.S., Wium-Andersen, T. and Hvitved-Jacobsen, T. (2008). Influence of pipe material and surfaces on sulfide related odor and corrosion in sewers. Water research 42(15), pp. 4206-4214.

Nielsen P.H. and Jahn, A. (1999). Extraction of EPS. pp. 49-72. Springer, Berlin, Germany.

Nieuwenhuijsen M.J., Grellier, J., Smith, R., Iszatt, N., Bennett, J., Best, N. and Toledano, M. (2009). The epidemiology and possible mechanisms of disinfection by-products in drinking water. Philosophical Transactions of the Royal Society of London A: Mathematical, Physical and Engineering Sciences 367(1904), pp. 4043-4076.

Niquette P., Servais, P. and Savoir, R. (2000). Impacts of pipe materials on densities of fixed bacterial biomass in a drinking water distribution system. Water research 34(6), pp. 1952-1956.

Noguera D., Goel, R., Harrington, G. and Yilmaz, L. (2009). Identification of Heterotrophic Bacteria that Colonize Chloraminated Crinking Water Distribution Systems. Water Environment Research Foundation.

Norton C.D. and LeChevallier, M.W. (1997). Chloramination: its effect on distribution system water quality. Journal-American Water Works Association 89(7), pp. 66-77.

Ochoa J.-C., Coufort, C., Escudié, R., Liné, A. and Paul, E. (2007). Influence of non-uniform distribution of shear stress on aerobic biofilms. Chemical engineering science 62(14), pp. 3672-3684.

Odell L.H., Kirmeyer, G.J., Wilczak, A. and Jacangelo, J.G. (1996). Controlling nitrification in chloraminated systems. American Water Works Association. Journal 88(7), p. 86.

Ohashi A. and Harada, H. (1994). Adhesion strength of biofilm developed in an attached-growth reactor. pp. 281-288.

Oldenburg P., S, Regan, J., W. Harrington, G. and Noguera, D. (2002). Kinetics of "Nitrosomonas europaea" inactivation by chloramine. pp. 100-110.

Organization W.H. (2009). World health statistics 2009. World Health Organization.

Pan P. and Umbreit, W. (1972). Growth of mixed cultures of autotrophic and heterotrophic organisms. Canadian journal of microbiology 18(2), pp. 153-156.

Paul E., Ochoa, J.C., Pechaud, Y., Liu, Y. and Line, A. (2012). Effect of shear stress and growth conditions on detachment and physical properties of biofilms. Water Res 46(17), pp. 5499-5508.

Percival S., Knapp, J., Wales, D. and Edyvean, R. (1999). The effect of turbulent flow and surface roughness on biofilm formation in drinking water. Journal of Industrial Microbiology and Biotechnology 22(3), pp. 152-159.

Pereira M., Vieira, M. and Melo, L. 2000. A simple flow cell for monitoring biofilm formation in laboratory and industrial conditions. In: *World congress of the international water association.* Paris.

Pereira M.O., Kuehn, M., Wuertz, S., Neu, T. and Melo, L.F. (2002). Effect of flow regime on the architecture of a Pseudomonas fluorescens biofilm. Biotechnol Bioeng 78(2), pp. 164-171.

Picioreanu C., Van Loosdrecht, M.C. and Heijnen, J.J. (2001). Two-dimensional model of biofilm detachment caused by internal stress from liquid flow. Biotechnology & Bioengineering 72(2), pp. 205-218.

Pintar K.D. and Slawson, R.M. (2003). Effect of temperature and disinfection strategies on ammonia-oxidizing bacteria in a bench-scale drinking water distribution system. Water Research 37(8), pp. 1805-1817.

Plewa M.J., Wagner, E.D., Muellner, M.G., Hsu, K.-M. and Richardson, S.D. 2008. Comparative mammalian cell toxicity of N-DBPs and C-DBPs. ACS Publications.

Potgieter S., Pinto, A., Sigudu, M., du Preez, H., Ncube, E. and Venter, S. (2018). Long-term spatial and temporal microbial community dynamics in a large-scale drinking water distribution system with multiple disinfectant regimes. Water research 139, p. 406.

Power K. and Nagy, L.A. (1989). Bacterial regrowth in water supplies. Urban Water Research Association of Australia.

Prakasam T. and Loehr, R. (1972). Microbial nitrification and denitrification in concentrated wastes. Water Research 6(7), pp. 859-869.

Price M.N., Dehal, P.S. and Arkin, A.P. (2009). FastTree: computing large minimum evolution trees with profiles instead of a distance matrix. Mol Biol Evol 26(7), pp. 1641-1650.

Purevdorj B., Costerton, J.W. and Stoodley, P. (2002). Influence of hydrodynamics and cell signaling on the structure and behavior of Pseudomonas aeruginosa biofilms. Applied and environmental microbiology 68(9), pp. 4457-4464.

Regan J.M., Harrington, G.W., Baribeau, H., De Leon, R. and Noguera, D.R. (2003). Diversity of nitrifying bacteria in full-scale chloraminated distribution systems. Water Research 37(1), pp. 197-205.

Regan J.M., Harrington, G.W. and Noguera, D.R. (2002). Ammonia- and nitrite-oxidizing bacterial communities in a pilot-scale chloraminated drinking water distribution system. Appl Environ Microbiol 68(1), pp. 73-81.

Revetta R.P., Gomez-Alvarez, V., Gerke, T.L., Curioso, C., Santo Domingo, J.W. and Ashbolt, N.J. (2013). Establishment and early succession of bacterial communities in monochloramine-treated drinking water biofilms. FEMS Microbiol Ecol 86(3), pp. 404-414.

Revetta R.P., Pemberton, A., Lamendella, R., Iker, B. and Santo Domingo, J.W. (2010). Identification of bacterial populations in drinking water using 16S rRNA-based sequence analyses. Water Res 44(5), pp. 1353-1360.

Richardson S.D., Plewa, M.J., Wagner, E.D., Schoeny, R. and DeMarini, D.M. (2007). Occurrence, genotoxicity, and carcinogenicity of regulated and emerging disinfection by-products in drinking water: a review and roadmap for research. Mutation Research/Reviews in Mutation Research 636(1), pp. 178-242.

Rickard A.H., Gilbert, P. and Handley, P.S. (2004a). Influence of growth environment on coaggregation between freshwater biofilm bacteria. J Appl Microbiol 96(6), pp. 1367-1373.

Rickard A.H., Gilbert, P., High, N.J., Kolenbrander, P.E. and Handley, P.S. (2003). Bacterial coaggregation: an integral process in the development of multi-species biofilms. Trends Microbiol 11(2), pp. 94-100.

Rickard A.H., McBain, A.J., Stead, A.T. and Gilbert, P. (2004b). Shear rate moderates community diversity in freshwater biofilms. Appl Environ Microbiol 70(12), pp. 7426-7435.

Rittmann B.E. and Manem, J.A. (1992). Development and experimental evaluation of a steady-state, multispecies biofilm model. Biotechnology and bioengineering 39(9), pp. 914-922.

Rittmann B.E., Regan, J.M. and Stahl, D.A. (1994). Nitrification as a source of soluble organic substrate in biological treatment. Water science and Technology 30(6), pp. 1-8.

Rochex A., Godon, J.J., Bernet, N. and Escudie, R. (2008). Role of shear stress on composition, diversity and dynamics of biofilm bacterial communities. Water Res 42(20), pp. 4915-4922.

Rossman L.A., Clark, R.M. and Grayman, W.M. (1994). Modeling chlorine residuals in drinking-water distribution systems. Journal of environmental engineering 120(4), pp. 803-820.

Rosswall T. 1982. Microbiological regulation of the biogeochemical nitrogen cycle.Nitrogen Cycling in Ecosystems of Latin America and the Caribbean. Springer, pp. 15-34.

Sathasivan A., Fisher, I. and Kastl, G. (2005). Simple method for quantifying microbiologically assisted chloramine decay in drinking water. Environ Sci Technol 39(14), pp. 5407-5413.

Sathasivan A., Fisher, I. and Tam, T. (2008). Onset of severe nitrification in mildly nitrifying chloraminated bulk waters and its relation to biostability. Water Res 42(14), pp. 3623-3632.

Sawade E., Monis, P., Cook, D. and Drikas, M. (2016). Is nitrification the only cause of microbiologically induced chloramine decay? Water research 88, pp. 904-911.

Schloss P.D. (2009). A High-Throughput DNA Sequence Aligner for Microbial Ecology Studies. PLOS ONE 4(12), p. e8230.

Schloss P.D. (2010). The Effects of Alignment Quality, Distance Calculation Method, Sequence Filtering, and Region on the Analysis of 16S rRNA Gene-Based Studies. PLOS Computational Biology 6(7), p. e1000844.

Schloss P.D. (2013). Secondary structure improves OTU assignments of 16S rRNA gene sequences. ISME J 7(3), pp. 457-460.

Schloss P.D., Gevers, D. and Westcott, S.L. (2011). Reducing the Effects of PCR Amplification and Sequencing Artifacts on 16S rRNA-Based Studies. PLOS ONE 6(12), p. e27310.

Schloss P.D., Westcott, S.L., Ryabin, T., Hall, J.R., Hartmann, M., Hollister, E.B., Lesniewski, R.A., Oakley, B.B., Parks, D.H., Robinson, C.J., Sahl, J.W., Stres, B., Thallinger, G.G., Van Horn, D.J. and Weber, C.F. (2009). Introducing mothur: Open-Source, Platform-Independent, Community-Supported Software for Describing and Comparing Microbial Communities. Applied and Environmental Microbiology 75(23), pp. 7537-7541.

Schmeisser C., Stöckigt, C., Raasch, C., Wingender, J., Timmis, K., Wenderoth, D., Flemming, H.-C., Liesegang, H., Schmitz, R. and Jaeger, K.-E. (2003). Metagenome survey of biofilms in drinking-water networks. Applied and environmental microbiology 69(12), pp. 7298-7309.

Schreiber I.M. and Mitch, W.A. (2007). Enhanced nitrogenous disinfection byproduct formation near the breakpoint: implications for nitrification control. Environmental science & technology 41(20), pp. 7039-7046.

Sedlak D.L. and von Gunten, U. (2011). The chlorine dilemma. Science 331(6013), pp. 42-43.

Seidel C.J., McGuire, M.J., Summers, R.S. and Via, S. (2005). Have utilities switched to chloramines? American Water Works Association 97(10), pp. 87-97.

Sekar R., Deines, P., Machell, J., Osborn, A.M., Biggs, C.A. and Boxall, J.B. (2012). Bacterial water quality and network hydraulic characteristics: a field study of a small, looped water distribution system using culture-independent molecular methods. J Appl Microbiol 112(6), pp. 1220-1234.

Shannon C.E. and Weave, W. (1949). The Mathematical Theory of Communication. University of Illionois Press, Urbana, IL.

Sharpe R.L., Smith, C.J., Boxall, J.B. and Biggs, C.A. (2010). Pilot Scale Laboratory Investigations into the Impact of Steady State Conditioning Flow on Potable Water Discolouration. . In: water Distribution System Analysis 2010 - WDSA2010, Tucson, AZ, USA, Sept., pp. 12-15.

Simoes L.C., Simoes, M. and Vieira, M.J. (2010). Adhesion and biofilm formation on polystyrene by drinking water-isolated bacteria. Antonie Van Leeuwenhoek 98(3), pp. 317-329.

Simões M., Pereira, M.O., Sillankorva, S., Azeredo, J. and Vieira, M.J. (2007). The effect of hydrodynamic conditions on the phenotype of Pseudomonas fluorescens biofilms. Biofouling 23(4), pp. 249-258.

Simoes M., Pereira, M.O. and Vieira, M.J. (2003). Monitoring the effects of biocide treatment of Pseudomonas fluorescens biofilms formed under different flow regimes. Water Sci Technol 47(5), pp. 217-223.

Simoes M., Pereira, M.O. and Vieira, M.J. (2005). Effect of mechanical stress on biofilms challenged by different chemicals. Water Res 39(20), pp. 5142-5152.

Skadsen J. (1993). Nitrification in a distribution system. American Water Works Association, pp. 95-103.

Skadsen J. (2002). Effectiveness of high pH in controlling nitrification. American Water Works Association 94(7), pp. 73-83.

Skadsen J. and Cohen, Y.K. (2006). Operational and treatment practices to prevent nitrification. Manual of water supply practices M 56.

Sommerfeld J. (1977). Unit operations of chemical engineering, 3rd edition, W. L. McCabe and J. C. Smith, McGraw-Hill, New York(1976). pp. 406-406.

Srinivasan R., Stewart, P.S., Griebe, T., Chen, C.I. and Xu, X. (1995). Biofilm parameters influencing biocide efficacy. Biotechnology and Bioengineering 46(6), pp. 553-560.

Staudt C., Horn, H., Hempel, D.C. and Neu, T.R. (2004). Volumetric measurements of bacterial cells and extracellular polymeric substance glycoconjugates in biofilms. Biotechnol Bioeng 88(5), pp. 585-592.

Stehr G., Böttcher, B., Dittberner, P., Rath, G. and Koops, H.-P. (1995). The ammonia-oxidizing nitrifying population of the River Elbe estuary. FEMS Microbiology Ecology 17(3), pp. 177-186.

Stein L.Y. and Arp, D.J. (1998). Ammonium limitation results in the loss of ammonia-oxidizing activity in Nitrosomonas europaea. Applied and environmental microbiology 64(4), pp. 1514-1521.

Stewart P.S. (2012). Mini-review: convection around biofilms. Biofouling 28(2), pp. 187-198.

Stoodley P., Dodds, I., Boyle, J. and Lappin - Scott, H. (1998). Influence of hydrodynamics and nutrients on biofilm structure. Journal of applied microbiology 85(S1).

Stoodley P., Hall-Stoodley, L. and Lappin-Scott, H.M. (2001). Detachment, surface migration, and other dynamic behavior in bacterial biofilms revealed by digital time-lapse imaging. Methods Enzymol 337, pp. 306-319.

Sun H., Shi, B., Bai, Y. and Wang, D. (2014). Bacterial community of biofilms developed under different water supply conditions in a distribution system. Science of the Total Environment 472, pp. 99-107.

Tarre S. and Green, M. (2004). High-rate nitrification at low pH in suspended-and attached-biomass reactors. Applied and environmental microbiology 70(11), pp. 6481-6487.

Teng F., Guan, Y. and Zhu, W. (2008). Effect of biofilm on cast iron pipe corrosion in drinking water distribution system: corrosion scales characterization and microbial community structure investigation. Corrosion science 50(10), pp. 2816-2823.

Teodosio J.S., Silva, F.C., Moreira, J.M., Simoes, M., Melo, L.F., Alves, M.A. and Mergulhao, F.J. (2013). Flow cells as quasi-ideal systems for biofouling simulation of industrial piping systems. Biofouling 29(8), pp. 953-966.

Teodosio J.S., Simoes, M., Melo, L.F. and Mergulhao, F.J. (2011). Flow cell hydrodynamics and their effects on E. coli biofilm formation under different nutrient conditions and turbulent flow. Biofouling 27(1), pp. 1-11.

Tinker S.C., Moe, C.L., Klein, M., Flanders, W.D., Uber, J., Amirtharajah, A., Singer, P. and Tolbert, P.E. (2009). Drinking water residence time in distribution networks and emergency department visits for gastrointestinal illness in Metro Atlanta, Georgia. Journal of water and health 7(2), pp. 332-343.

Tsvetanova Z. 2006. Study of biofilm formation on different pipe materials in a model of drinking water distribution system and its impact on microbiological water quality.Chemicals as intentional and accidental global environmental threats. Springer, pp. 463-468.

Tuomanen E., Cozens, R., Tosch, W., Zak, O. and Tomasz, A. (1986). The rate of killing of Escherichia coli byβ-lactam antibiotics is strictly proportional to the rate of bacterial growth. Microbiology 132(5), pp. 1297-1304.

Twort A.C., Ratnayaka, D.D. and Brandt, M.J. (2000). Water supply. Butterworth-Heinemann.

UKWIR. (2003). National Database of Mains Failures 2003.

Valentine R.L. (1998). Chloramine decomposition in distribution system and model waters. American Water Works Association.

Verhagen F.J. and Laanbroek, H.J. (1991). Competition for ammonium between nitrifying and heterotrophic bacteria in dual energy-limited chemostats. Applied and Environmental Microbiology 57(11), pp. 3255-3263.

Vieira M. and Melo, L. (1999). Intrinsic kinetics of biofilms formed under turbulent flow and low substrate concentrations. Bioprocess Engineering 20(4), pp. 369-375.

Vieira M., Oliveira, R., Melo, L., Pinheiro, M.M. and Martins, V. (1993). Effect of metallic ions on the adhesion of biofilms formed by Pseudomonas fluorescens. Colloids and Surfaces B: Biointerfaces 1(2), pp. 119-124.

Vigeant M.A.-S., Ford, R.M., Wagner, M. and Tamm, L.K. (2002). Reversible and irreversible adhesion of motile Escherichia coli cells analyzed by total internal reflection aqueous fluorescence microscopy. Applied and environmental microbiology 68(6), pp. 2794-2801.

Vikesland P.J., Ozekin, K. and Valentine, R.L. (2001). Monochloramine decay in model and distribution system waters. Water Research 35(7), pp. 1766-1776.

Villaverde S., Garcia-Encina, P. and Fdz-Polanco, F. (1997). Influence of pH over nitrifying biofilm activity in submerged biofilters. Water Research 31(5), pp. 1180-1186.

Vital M., Dignum, M., Magic-Knezev, A., Ross, P., Rietveld, L. and Hammes, F. (2012). Flow cytometry and adenosine tri-phosphate analysis: alternative possibilities to evaluate major bacteriological changes in drinking water treatment and distribution systems. Water research 46(15), pp. 4665-4676.

Volk C.J. and LeChevallier, M.W. (1999). Impacts of the reduction of nutrient levels on bacterial water quality in distribution systems. Applied and Environmental Microbiology 65(11), pp. 4957-4966.

Vreeburg I.J. and Boxall, J. (2007). Discolouration in potable water distribution systems: A review. Water research 41(3), pp. 519-529.

Vrouwenvelder J.S., Buiter, J., Riviere, M., van der Meer, W.G., van Loosdrecht, M.C. and Kruithof, J.C. (2010). Impact of flow regime on pressure drop increase and biomass accumulation and morphology in membrane systems. Water Res 44(3), pp. 689-702.

Wagner M., Ivleva, N.P., Haisch, C., Niessner, R. and Horn, H. (2009). Combined use of confocal laser scanning microscopy (CLSM) and Raman microscopy (RM): investigations on EPS-Matrix. Water Res 43(1), pp. 63-76.

Waines P.L., Moate, R., Moody, A.J., Allen, M. and Bradley, G. (2011). The effect of material choice on biofilm formation in a model warm water distribution system. Biofouling 27(10), pp. 1161-1174.

Wang H., Masters, S., Hong, Y., Stallings, J., Falkinham III, J.O., Edwards, M.A. and Pruden, A. (2012a). Effect of disinfectant, water age, and pipe material on occurrence and persistence of Legionella, mycobacteria, Pseudomonas aeruginosa, and two amoebas. Environmental science & technology 46(21), pp. 11566-11574.

Wang Z., Choi, O. and Seo, Y. (2013). Relative contribution of biomolecules in bacterial extracellular polymeric substances to disinfection byproduct formation. Environ Sci Technol 47(17), pp. 9764-9773.

Wang Z., Kim, J. and Seo, Y. (2012b). Influence of bacterial extracellular polymeric substances on the formation of carbonaceous and nitrogenous disinfection byproducts. Environmental science & technology 46(20), pp. 11361-11369.

Wäsche S., Horn, H. and Hempel, D.C. (2002). Influence of growth conditions on biofilm development and mass transfer at the bulk/biofilm interface. Water Research 36(19), pp. 4775-4784.

Watson S.W., Bock, E., Harms and H., K., H.P., and Hooper, A.B. . (1989). Nitrifying bacteria. Baltimore, Md.: Williams and Wilkins.

Weiner R., Langille, S. and Quintero, E. (1995). Structure, function and immunochemistry of bacterial exopolysaccharides. J Ind Microbiol 15(4), pp. 339-346.

Whittaker R.H. (1960). Vegetation of the Siskiyou Mountains, Oregon and California. Ecological Monographs 30(4), pp. 407-407.

Whittaker R.H. (1972). Evolution and Measurement of Species Diversity. pp. 213-251.

Wilczak A., Jacangelo, J.G., Marcinko, J.P., Odell, L.H., Kirmeyer, G.J. and Wolfe, R.L. (1996). Occurrence of nitrification in chloraminated distribution systems. Journal-American Water Works Association 88(7), pp. 74-85.

Williams M.M. and Braun-Howland, E.B. (2003). Growth of Escherichia coli in model distribution system biofilms exposed to hypochlorous acid or monochloramine. Applied and Environmental Microbiology 69(9), pp. 5463-5471.

Williams M.M., Domingo, J.W., Meckes, M.C., Kelty, C.A. and Rochon, H.S. (2004). Phylogenetic diversity of drinking water bacteria in a distribution system simulator. J Appl Microbiol 96(5), pp. 954-964.

Williams M.M., Santo Domingo, J.W. and Meckes, M.C. (2005). Population diversity in model potable water biofilms receiving chlorine or chloramine residual. Biofouling 21(5-6), pp. 279-288.

Wloka M., Rehage, H., Flemming, H.-C. and Wingender, J. (2004a). Rheological properties of viscoelastic biofilm extracellular polymeric substances and comparison to the behavior of calcium alginate gels. pp. 1067-1076.

Wloka M., Rehage, H., Flemming, H.C. and Wingender, J. (2004b). Rheological properties of viscoelastic biofilm extracellular polymeric substances and comparison to the behavior of calcium alginate gels. Colloid and Polymer Science 282(10), pp. 1067-1076.

Wolfe R.L. and Lieu, N.I. (2001). Nitrifying bacteria in drinking water. Encyclopedia of Environmental Microbiology.

Wolfe R.L., Lieu, N.I., Izaguirre, G. and Means, E.G. (1990). Ammonia-oxidizing bacteria in a chloraminated distribution system: seasonal occurrence, distribution and disinfection resistance. Applied and environmental microbiology 56(2), pp. 451-462.

Wolfe R.L., Means III, E.G., Davis, M.K. and Barrett, S.E. (1988). Biological nitrification in covered reservoirs containing chloraminated water. Journal-American Water Works Association 80(9), pp. 109-114.

Wu C., Wu, Y., Gao, J. and Zhao, Z. (2005). Research on water detention times in water supply network. J. Harbin Inst. Technol 12(1), pp. 188-193.

Wu H., Zhang, J., Mi, Z., Xie, S., Chen, C. and Zhang, X. (2015). Biofilm bacterial communities in urban drinking water distribution systems transporting waters with different purification strategies. Applied microbiology and biotechnology 99(4), pp. 1947-1955.

Xue Z., Hessler, C.M., Panmanee, W., Hassett, D.J. and Seo, Y. (2013a). Pseudomonas aeruginosa inactivation mechanism is affected by capsular extracellular polymeric substances reactivity with chlorine and monochloramine. FEMS Microbiol Ecol 83(1), pp. 101-111.

Xue Z., Lee, W.H., Coburn, K.M. and Seo, Y. (2014). Selective reactivity of monochloramine with extracellular matrix components affects the disinfection of biofilm and detached clusters. Environmental science & technology 48(7), pp. 3832-3839.

Xue Z. and Seo, Y. (2013b). Impact of chlorine disinfection on redistribution of cell clusters from biofilms. Environ Sci Technol 47(3), pp. 1365-1372.

Yang J., Harrington, G.W. and Noguera, D.R. (2008). Nitrification modeling in pilot-scale chloraminated drinking water distribution systems. Journal of Environmental Engineering 134(9), pp. 731-742.

Yang J., Harrington, G.W., Noguera, D.R. and Fleming, K.K. (2007). Risk analysis of nitrification occurrence in pilot-scale chloraminated distribution systems. Journal of Water Supply: Research and Technology-Aqua 56(5), pp. 293-311.

Yilmaz L.S., Goel, R., Harrington, G.W. and Noguera, D. (2008). Identification of heterotrophic bacteria that colonize pilot- and full-scale chloraminated distribution systems. American Water Works Association Reasearh Foundation, pp. 2577-2596.

Yu J., Kim, D. and Lee, T. (2010). Microbial diversity in biofilms on water distribution pipes of different materials. Water Science and Technology 61(1), pp. 163-171.

Zacheus O.M., Lehtola, M.J., Korhonen, L.K. and Martikainen, P.J. (2001). Soft deposits, the key site for microbial growth in drinking water distribution networks. Water Research 35(7), pp. 1757-1765.

Zhang Y. and Edwards, M. (2009a). Accelerated Chloramine Decay and Microbial Growth by Nitrification in Premise Plumbing (PDF). Journal-American Water Works Association 101(11), pp. 51-62.

Zhang Y., Griffin, A. and Edwards, M. (2008). Nitrification in premise plumbing: role of phosphate, pH and pipe corrosion. Environmental science & technology 42(12), pp. 4280-4284.

Zhang Y., Griffin, A., Rahman, M., Camper, A., Baribeau, H. and Edwards, M. (2009b). Lead contamination of potable water due to nitrification. Environmental science & technology 43(6), pp. 1890-1895.

Zhang Y., Love, N. and Edwards, M. (2009c). Nitrification in drinking water systems. Critical Reviews in Environmental Science and Technology 39(3), pp. 153-208.

Zhang Y., Zhou, L., Zeng, G., Deng, H. and Li, G. (2010). Impact of total organic carbon and chlorine to ammonia ratio on nitrification in a bench-scale drinking water distribution system. Frontiers of Environmental Science & Engineering in China 4(4), pp. 430-437.

Zhou J., Bruns, M.A. and Tiedje, J.M. (1996). DNA recovery from soils of diverse composition. Appl Environ Microbiol 62(2), pp. 316-322.

Zhou L., Zhang, Y. and Li, G. (2009). Effect of pipe material and low level disinfectants on biofilm development in a simulated drinking water distribution system. Journal of Zhejiang University SCIENCE A 10(5), pp. 725-731.

Appendices

A. Supporting data for Chapter 3

A.1 TOC and TN analyser calibration data

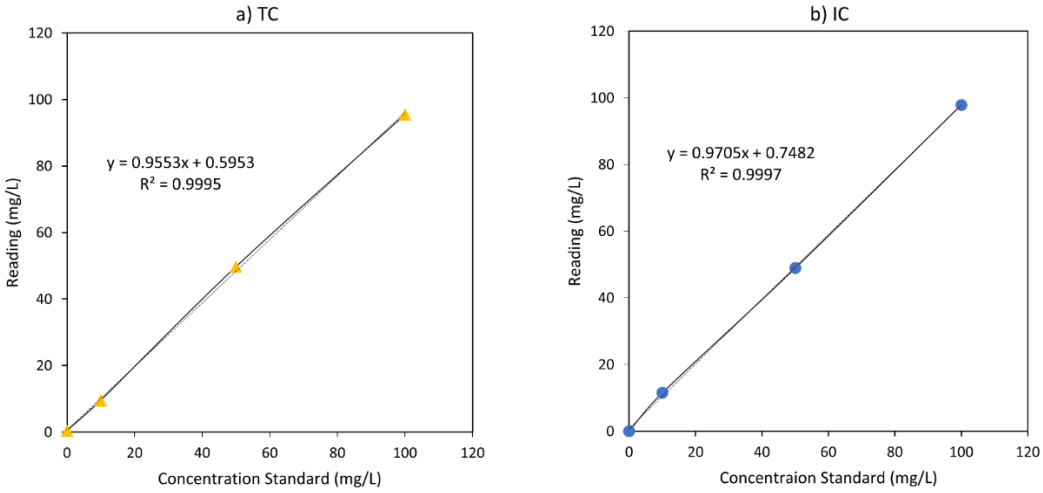

Figure A-1 Typical calibration curves for a) TC and b) IC using the TOC and TN analyser (Shimadzu TOC-V_{CPH})

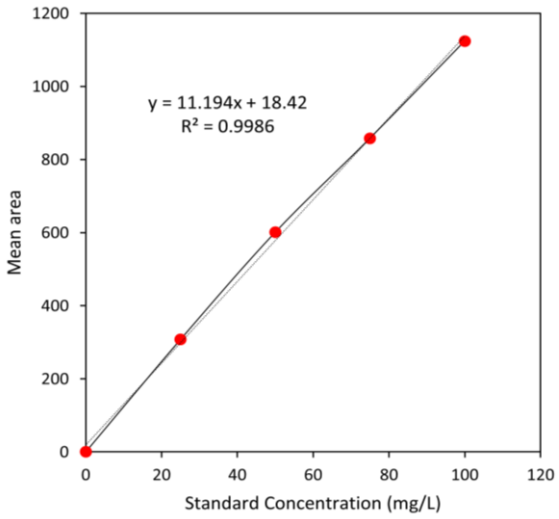

Figure A-2 Typical calibration curve for TN

A.2 EPS calibration data

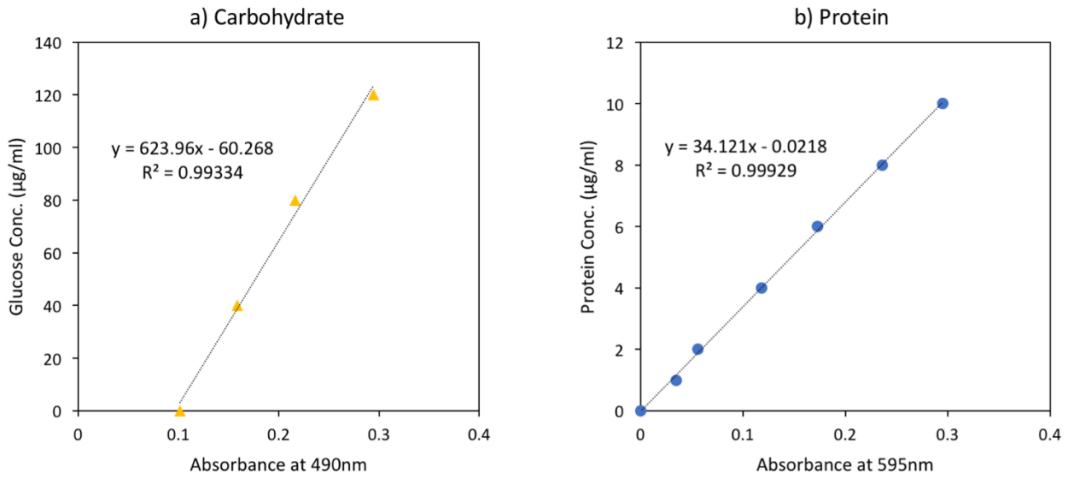

Figure A-3 Typical a) Carbohydrate and b) protein standard curve for EPS quantification

A.3 Images of coupon before and after incubation

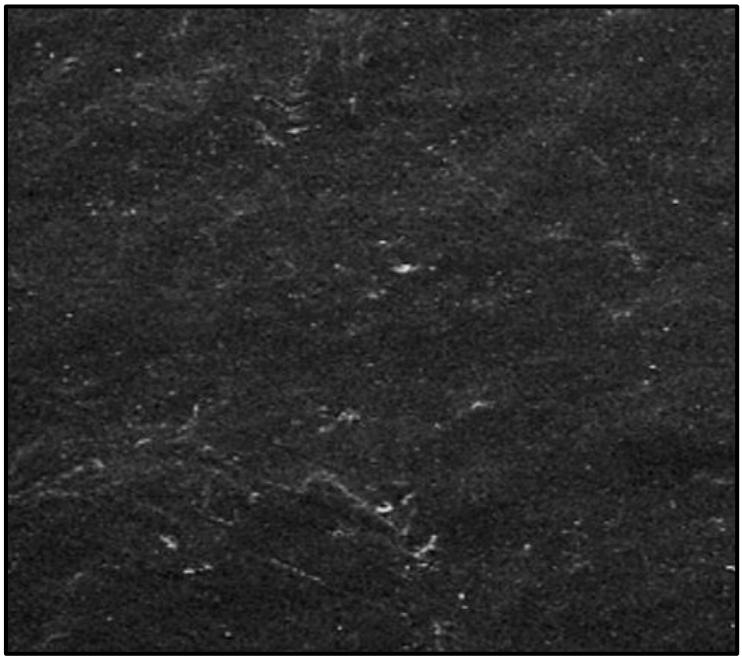

Figure A-4 Photomicrographs captured by polarizing microscopy (Nikon ECLIPSE LV100) of coupons before incubation

a) 2A-R3 at × 10 mag

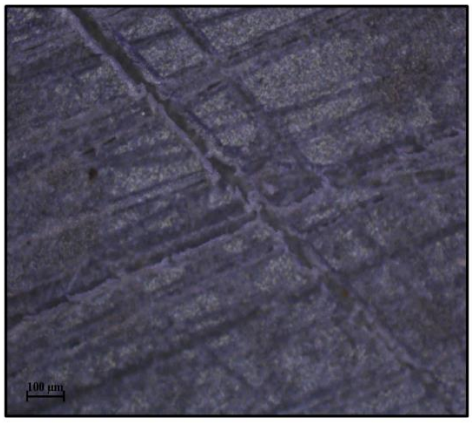

b) 2A-R3 at × 100 mag

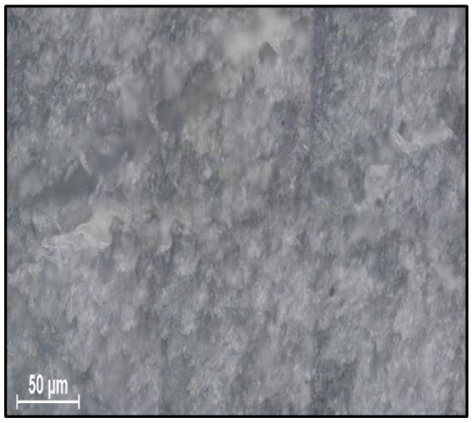

c) 6A-R3 at × 10 mag

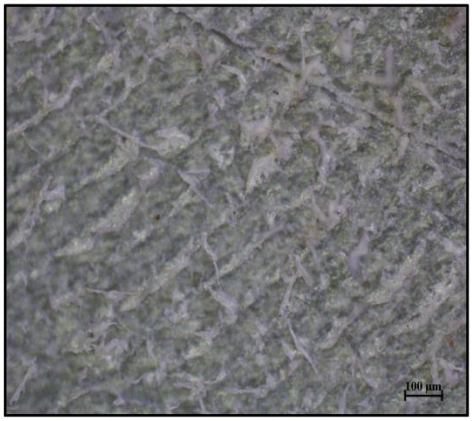

d) 6A-R3 at × 100 mag

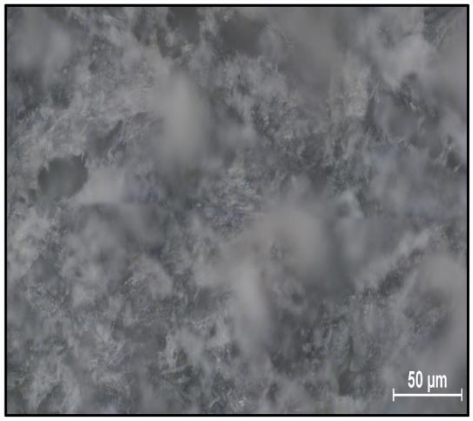

e) 10A-R3 at × 10 mag

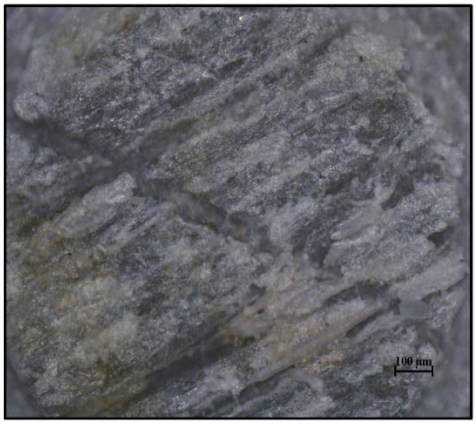

f) 10A-R3 at × 100 mag

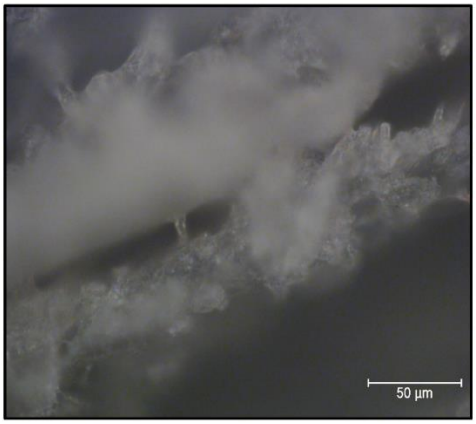

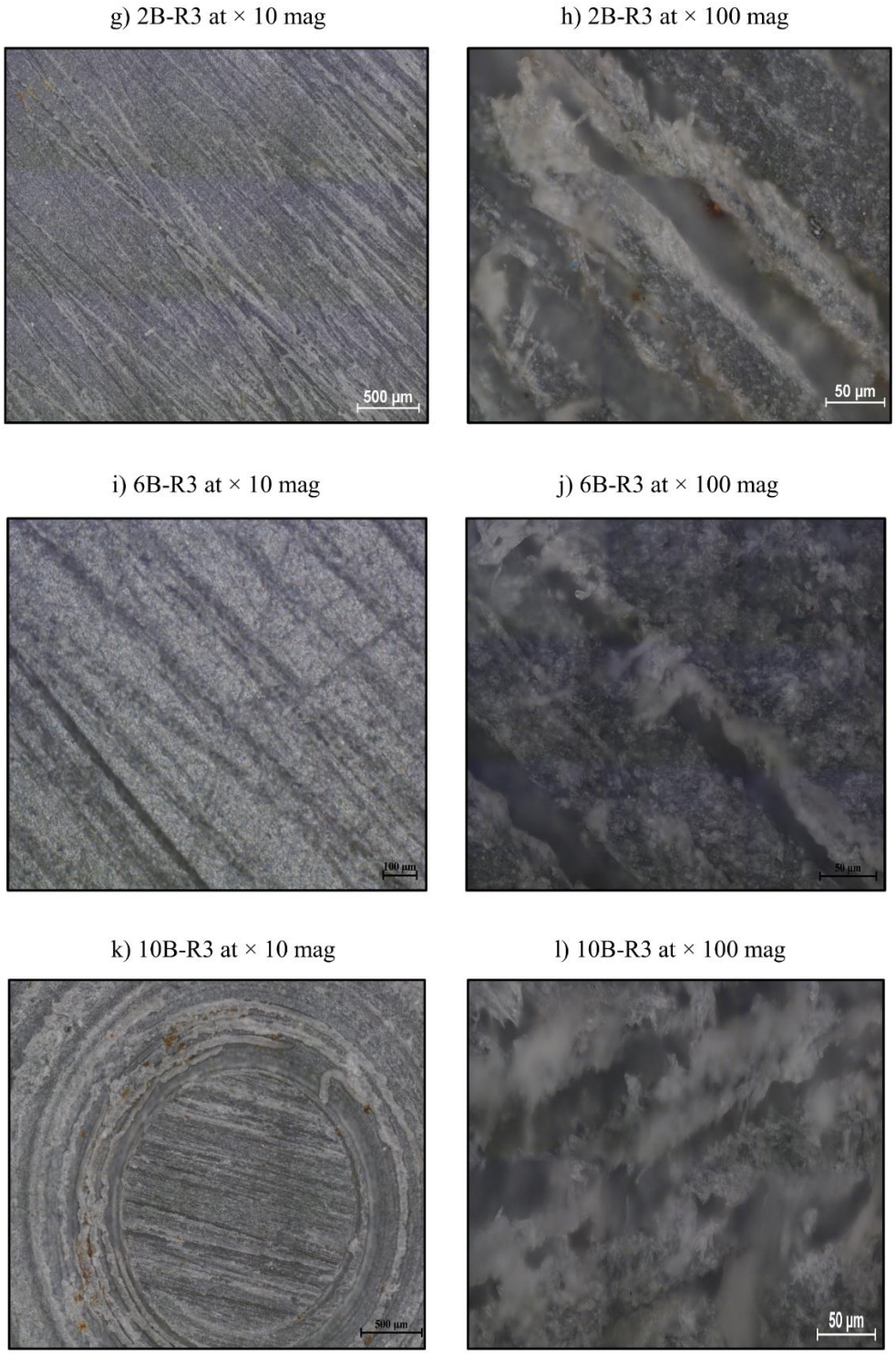

Figure A-5 Photomicrographs captured by polarizing microscopy (Nikon ECLIPSE LV100) of coupons post incubation, including the a) 2A_R3 × 10 mag; b) 2A_R3 × 100 mag; c) 6A_R3 × 10 mag; d) 6A_R3 × 100 mag; e) 10A_R3 × 10 mag; f) 10A_R3 × 100 mag; g) 2B_R3 × 10 mag; h) 2B_R3 × 100 mag; i) 6B_R3 × 10 mag; j) 6B_R3 × 100 mag; k) 10B_R3 × 10 mag; l) 10B_R3 × 100 mag.

a) 2A-R4 at × 10 mag

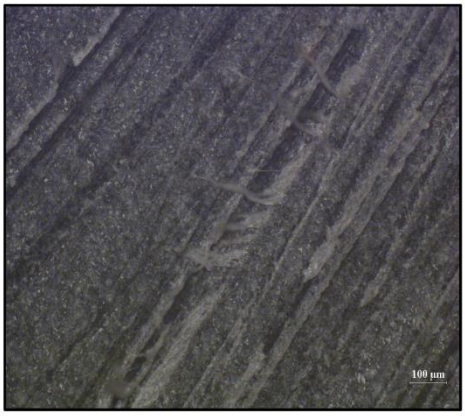

b) 2A-R4 at × 100 mag

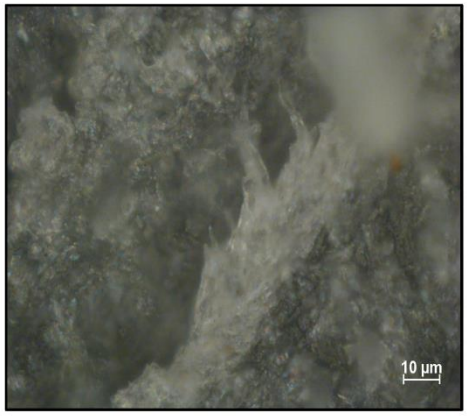

c) 6A-R4 at × 10 mag

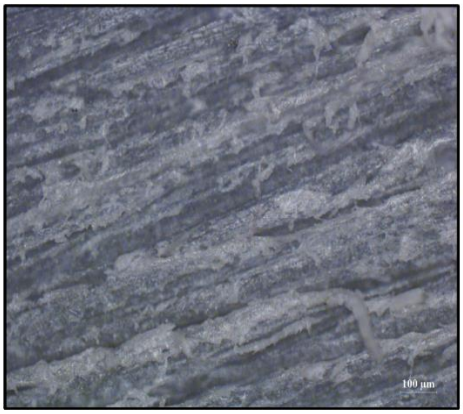

d) 6A-R4 at × 100 mag

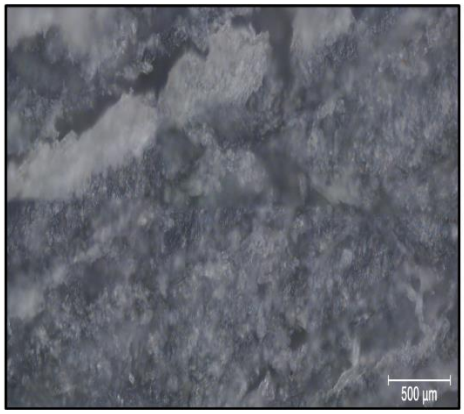

e) 10A-R4 at × 10 mag

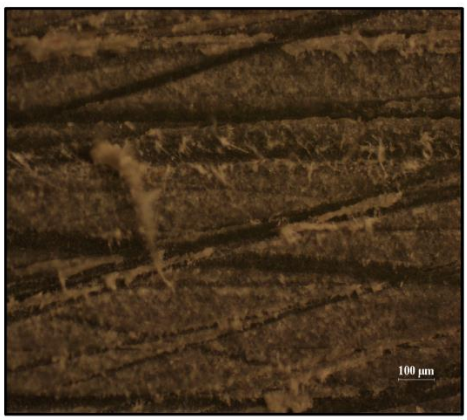

f) 10A-R4 at × 100 mag

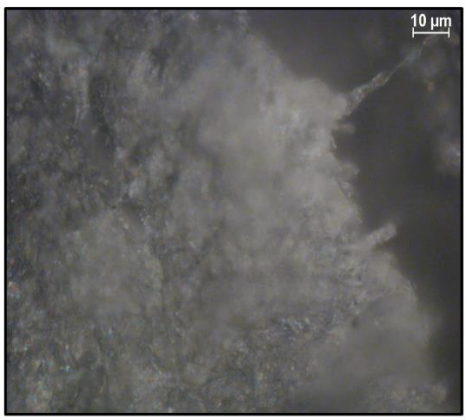

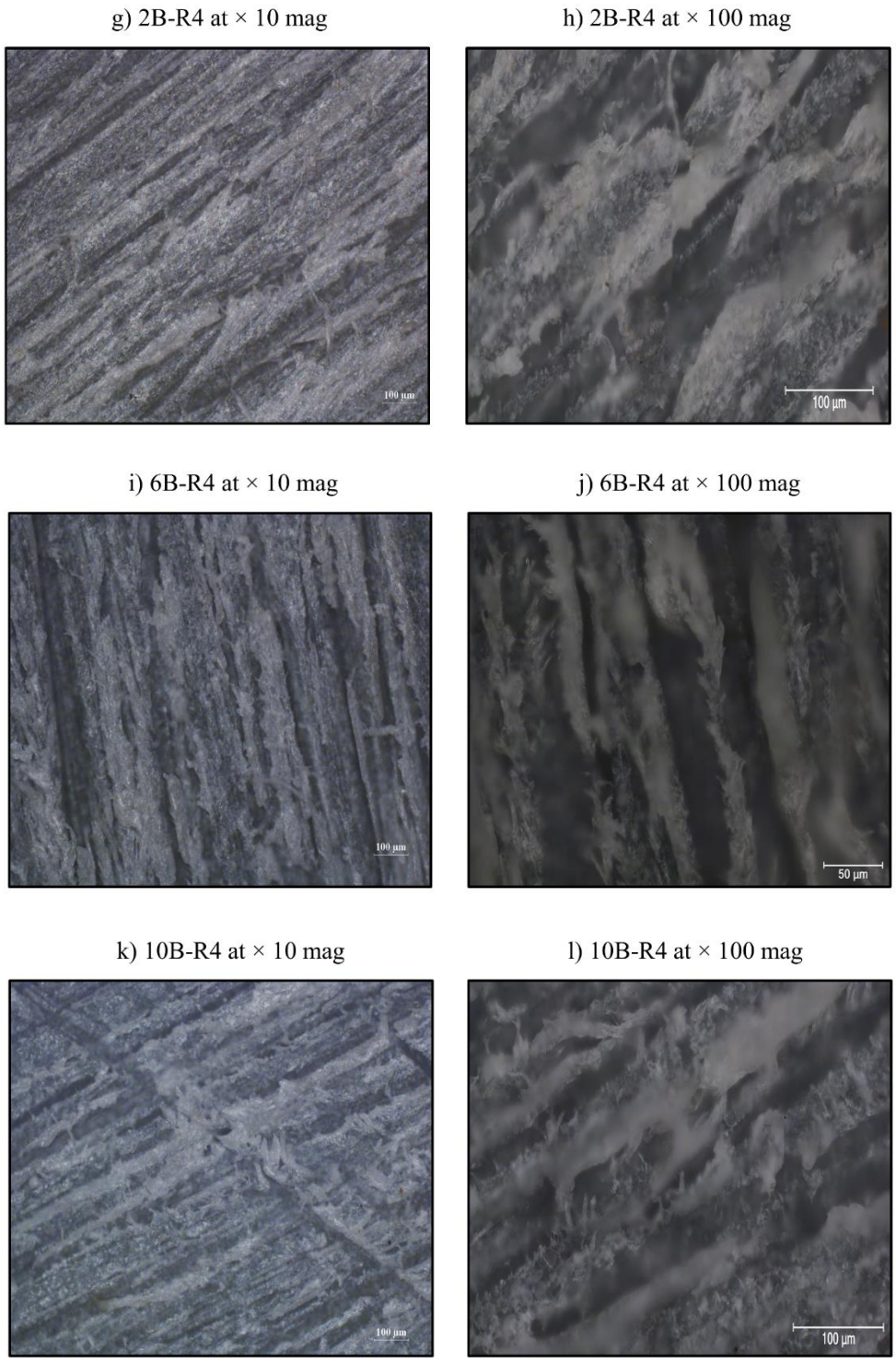

Figure A-6 Photomicrographs captured by polarizing microscopy (Nikon ECLIPSE LV100) of coupons post incubation, including the a) 2A_R4 × 10 mag; b) 2A_R4 × 100 mag; c) 6A_R4 × 10 mag; d) 6A_R4 × 100 mag; e) 10A_R4 × 10 mag; f) 10A_R4 × 100 mag; g) 2B_R4 × 10 mag; h) 2B_R4 × 100 mag; i) 6B_R4 × 10 mag; j) 6B_R4 × 100 mag; k) 10B_R4 × 10 mag; l) 10B_R4 × 100 mag.

A.4 Raw data of Qubit DNA concentration and DNA quality

Table A-1 Data of Qubit DNA concentration and DNA quality

Sample name	Qubit concentration ng/µl	DIN
2A biofilm	59.8	6.3
2A bulk water	238	6.9
4A biofilm	17.5	6.6
4A bulk water	480	1
6A biofilm	42.8	6.4
6A bulk water	1000	1
8A biofilm	5.63	6.4
8A bulk water	593	6.4
10A biofilm	5.99	6.2
10A bulk water	567	4.1
2B biofilm	228	4.4
2B bulk water	161	7.4
4B biofilm	102	1
4B bulk water	340	6.3
6B biofilm	236	1
6B bulk water	585	
8B biofilm	39.9	4.1
8B bulk water	367.5	1
10B biofilm	70.4	6
10B bulk water	1000	6.3

B. Supporting data for Chapter 4

B.1 TOC and TN in feed water

Table B-1 TOC and TN concentration in feed water

Test phase 2			Test phase 3					Test phase 4				
Time (day)	TOC (mg/L)	TN (mg/L)	Time (day)	TOC (mg/L)		TN (mg/L)		Time (day)	TOC (mg/L)		TN (mg/L)	
				Cl_2=1 mg/L	Cl_2=5 mg/L	Cl_2=1 mg/L	Cl_2=5 mg/L		Cl_2=1 mg/L	Cl_2=5 mg/L	Cl_2=1 mg/L	Cl_2=5 mg/L
1	1.64	1.689										
2	0.96	1.704	1	1.31	2.962	-0.4	5.292	1	1.12	0.62	2.61	3.819
3	2.28	1.653	2					2			2.823	4.104
4	1.88	1.667	3	1.35	3.091			3	1.6		2.602	3.801
5	1.91	1.576	4	1.37	3.153	1.68	5.372	4	-1.1	1.24	2.525	3.812
6	1.56	1.549	5	-0.44	3.147			5	1.38		2.596	3.72
7	1.49	1.487	6	1.59	2.96	1.69	5.105	6	2.27	1.55	2.615	3.903
8	1.5	1.504	7	1.6	2.76	1.48	4.993	7	0.4	0.05	2.448	3.78
9	1.35	1.5	8	1.36	2.657	1.46	4.927	8	0.54	0.24	2.618	3.802
10	1.61	1.339	9	0.12	2.5	0.25	4.739	9	0.84	0.29	2.519	3.874
11	1.87	1.673	10	1.57	2.389	1.76	4.561	10	0.5	0.42	2.439	3.662
12	1.56	1.688	11	1.47	2.518	1.59	4.645	11	0.44	-0.26	2.486	3.674
13	1.79	1.758	12	0.41	2.447	0.99	4.493	12	1.67	1.45	2.476	3.714
14	2.29	1.822	13	0.3	2.456	-0.05	4.484	13	0.43	0.41	2.422	3.61
15	1.57	1.749	14	1.3	2.381	1.43	4.53	14	0.07	-0.01	2.357	3.545
16	1.54	1.677	15	1.68	2.519	1.63	4.528	15	0.61	0.32	2.229	3.534
17	1.83	1.69	16	1.98	2.48	0.31	4.704	16	6.76	0.43	2.271	3.463
18	1.74	1.668	17	0.79	2.374	0.86	4.505	17	0.02	0	2.103	3.415
19	1.72	1.677	18	0.46	2.296	0.5	4.417	18	0.21	-0.12	2.09	3.322
20	1.51	1.663	19	0.82	2.335	-0.45	4.417	19	1.83	1.02	2.082	3.322
21	1.62	1.765	20	-0.31	3.498	0.13	4.429	20	0.81	0.98	2.072	3.13
22	1.58	1.622	21	0.19	2.403	0.08	4.47	21	0.5	0.9	2.006	2.994
23	1.46	1.603	22	0.06	2.536	-0.2	4.529	22	0.02	0.25	1.712	3.078
24	1.69	1.676	23	0.26	2.553	-0.12	4.669	23	0.81	0.21	1.872	2.995
25	1.88	1.474	24	-1.06	2.755	-0.48	4.917	24	1.06	0.23	1.776	3.018
26	2.83	1.417	25	0.18	2.757	-0.37	4.944	25	2.17	1.73	1.827	1.816
27	2.91	1.458	26	-0.57	2.822	-0.69	4.929	26	0.41	-0.64	1.769	3.002
28	2.67	1.454	27	0.63	2.806	1.58	5.48	27	0.76	0.87	1.79	2.818
29	1.66	1.394	28	0.44	3.387	0.85	5.176	28	1.37	1.5	1.752	2.781
30	2.17	1.337	29	0.07	2.895	0.48	4.993	29	1.97	2.27	1.63	2.679
			30	1.54	2.924	0.91	5.052	30	1.66	1.62	1.626	2.567
			31	2.04	2.645	2.19	4.918	31	0.98	1.67	1.499	2.482
			32	0.44	2.541	0.61	4.682	32	0.84	-0.05	1.477	2.477
								33	1.1	2	1.567	2.42

Table B-2 DO concentration (mg/L) in flow cell units during test phase 3 and 4

Test phase 3							Test phase 4						
	1 mg/L			5 mg/L				1 mg/L			5 mg/L		
Time (day)	10L/min	6L/min	2L/min	10L/min	6L/min	2L/min	Time (day)	10L/min	6L/min	2L/min	10L/min	6L/min	2L/min
0	8.45	9.44	9.59	9.1	9.18	9.92	0	8.59	8.84	8.74	8.62	8.63	8.56
1	10.15	10.08	10.39	9.9	9.56	10.83	3	8.64	8.29	7.97	8.49	8	8.42
3	10.35	9.66	9.49	9.97	9.32	10.34	6	8.65	8.56	8.58	8.89	8.68	9.07
6	10.62	9.83	10.48	11.77	9.91	11.06	9	9.6	8	9.09	8.48	8.74	8.77
9	10.02	9.87	10.37	9.29	10.31	9.15	10	9.38	8.69	8.77	7.86	8.83	9.09
10	8.92	10.51	9.46	8.85	8.79	9.22	11	9.62	8.92	9.14	8.79	9.07	9.55
11	10.39	11.92	9.71	10.45	9.84	11.63	12	9.56	8.87	8.64	8.97	9.35	9.09
12	10.98	10.82	10.79	11.66	10.69	9.8	13	10.71	9.14	9.16	9.65	10.06	9.61
13	10.24	8.89	9.78	9.09	9.04	9.64	14	9.98	9.27	9.11	8.78	9.63	9.09
14	9.16	9.12	8.85	9.3	9.23	9.03	15	9.52	8.76	8.56	8.39	8.8	8.69
15	8.98	8.68	8.97	8.46	8.48	8.23	16	8.49	8.31	8.8	8.91	7.63	7.97
16	8.21	8.46	8.6	9.23	8.98	8.85	18	10.5	8.86	9.87	10.02	8.97	9.44
18	9.77	9.05	8.2	9.23	9.27	9.01	21	10.16	9.83	9.41	9.58	8.87	8.86
21	10.42	9.09	9.27	8.68	9.34	8.6	24	9.51	11.32	9.79	9.62	8.56	8.92
24	10.7	9.82	9.28	9.5	9.23	9.98	27	11.89	8.93	10.39	9.62	9.61	9.37
27	9.87	10.54	10.58	9.44	10.21	10.48	30	10.75	9.2	10.42	9.57	9.79	8.85
30	9.78	8.72	9.66	10.25	9.7	9.61	33	10.84	8.93	8.94	7.94	9.32	8.85
33	9.43	8.65	8.7	8.76	8.54	8.47	39	8.86	7.6	7.12	7.72	8.14	7.35

Table B-3 Nitrate concentration (mg/L) in feed water

Test phase 3			Test phase 4		
Time (day)	1 mg/L	5 mg/L	Time (day)	1 mg/L	5 mg/L
0	1.3	2.9	0	1.4	2.8
1	1.2	2.8	3	1.2	2.7
3	1.4	2.7	6	1.4	2.9
6	1.3	2.8	9	1.3	2.8
9	1.2	2.9	10	1.3	2.7
10	1.4	2.8	11	1.2	2.8
11	1.3	2.7	12	1.4	2.7
12	1.3	2.7	13	1.3	2.9
13	1.4	2.9	14	1.3	2.7
14	1.2	2.8	15	1.4	2.8
15	1.5	2.9	16	1.3	2.8
16	1.4	2.7	18	1.4	2.7
18	1.2	2.8	21	1.2	2.9
21	1.4	2.8	24	1.3	2.8
24	1.3	2.7	27	1.3	2.9
27	1.3	2.9	30	1.4	2.7
30	1.2	2.8	33	1.4	2.8
33	1.4	2.8	36	1.2	2.9

B.2 Results of Mann-Whitney U test

Table B-4 Results of Mann-Whitney U test for test phase 1

pH						**Cl_2**					
		2A	4A	6A	8A			2A	4A	6A	8A
4A	Wilcoxon	305				4A	Wilcoxon	301			
	p value	0.004**					p value	0.001**			
6A	Wilcoxon	364.5	294			6A	Wilcoxon	353	320		
	p value	0.218	0.002**				p value	0.097	0.008**		
8A	Wilcoxon	230	220	249.5		8A	Wilcoxon	383.5	285.5	316.5	
	p value	0.000**	0.000**	0.000**			p value	0.429	0.000**	0.006**	
10A	Wilcoxon	328	273	377	310	10A	Wilcoxon	387	277	308	396
	p value	0.026**	0.000**	0.372	0.007**		p value	0.491	0.000**	0.003**	0.670
TOC						**Turbidity**					
		2A	4A	6A	8A			2A	4A	6A	8A
4A	Wilcoxon	383.5				4A	Wilcoxon	336			
	p value	0.430					p value	0.023**			
6A	Wilcoxon	397.000	356			6A	Wilcoxon	340	396.5		
	p value	0.672	0.112				p value	0.037**	0.682		
8A	Wilcoxon	323	288	327.5		8A	Wilcoxon	401	332	342	
	p value	0.014**	0.000**	0.023**			p value	0.681	0.022**	0.05**	
10A	Wilcoxon	259.5	247	261	328	10A	Wilcoxon	389	388.5	392.5	384
	p value	0.000**	0.000**	0.000**	0.013**		p value	0.548	0.474	0.609	0.548
Nitrite						**Nitrate**					
		2A	4A	6A	8A			2A	4A	6A	8A
4A	Wilcoxon	340				4A	Wilcoxon	355			
	p value	0.372					p value	0.647			
6A	Wilcoxon	220.5	252			6A	Wilcoxon	353.5	342.5		
	p value	0.000**	0.001**				p value	0.611	0.410		
8A	Wilcoxon	356.5	333.5	220.5		8A	Wilcoxon	332.5	363	319.5	
	p value	0.681	0.279	0.000**			p value	0.258	0.825	0.130	
10A	Wilcoxon	370	348.5	254	367	10A	Wilcoxon	356	351	367.5	331.5
	p value	0.998	0.520	0.001**	0.919		p value	0.667	0.567	0.929	0.249
Ammonia						**TN**					
		2A	4A	6A	8A			2A	4A	6A	8A
4A	Wilcoxon	272				4A	Wilcoxon	363			
	p value	0.004**					p value	0.827			
6A	Wilcoxon	276.5	318			6A	Wilcoxon	313	334.5		
	p value	0.006**	0.124				p value	0.093	0.293		
8A	Wilcoxon	364.5	250.5	256		8A	Wilcoxon	274	289	254	
	p value	0.861	0.000**	0.130			p value	0.005**	0.019**	0.001**	
10A	Wilcoxon	330.5	296	315	341.5	10A	Wilcoxon	351	342	327	341
	p value	0.242	0.029**	0.104	0.396		p value	0.569	0.405	0.204	0.543
HPC						**Fm**					
		2A	4A	6A	8A			2A	4A	6A	8A
4A	Wilcoxon	24				4A	Wilcoxon	18			
	p value	0.465					p value	0.047**			
6A	Wilcoxon	19	23			6A	Wilcoxon	18	26		
	p value	0.076	0.347				p value	0.047**	0.754		
8A	Wilcoxon	21	24	27		8A	Wilcoxon	24	18	18	
	p value	0.175	0.465	0.917			p value	0.459	0.047**	0.047**	
10A	Wilcoxon	22.5	20	16	17	10A	Wilcoxon	21.5	15.5	17	27
	p value	0.295	0.117	0.016**	0.028**		p value	0.207	0.012**	0.028**	0.917

n=20 for pH, Cl_2, TOC, Turbidity, Nitrite, Nitrate, Ammonia and TN; n=5 for HPC and Fm; ** indicates significant difference between datasets.

Table B-5 Results of Mann-Whitney U test for test phase 2

pH						**Cl_2**					
		2A	4A	6A	8A			2A	4A	6A	8A
4A	Wilcoxon	259				4A	Wilcoxon	229.5			
	p value	0.850					p value	0.901			
6A	Wilcoxon	226	218.5			6A	Wilcoxon	216.5	219.5		
	p value	0.151	0.085				p value	0.506	0.085		
8A	Wilcoxon	262.5	263.5	231.5		8A	Wilcoxon	189.5	177.5	176.5	
	p value	0.955	0.985	0.219			p value	0.074	0.985	0.219	
10A	Wilcoxon	142	141	139	145	10A	Wilcoxon	162.5	148.5	148.5	206.5
	p value	0.000**	0.000**	0.000**	0.000**		p value	0.004**	0.000**	0.000**	0.000**
TOC						**Turbidity**					
		2A	4A	6A	8A			2A	4A	6A	8A
4A	Wilcoxon	213.5				4A	Wilcoxon	196			
	p value	0.431					p value	0.129			
6A	Wilcoxon	222.000	231			6A	Wilcoxon	206	231		
	p value	0.663	0.950				p value	0.270	0.950		
8A	Wilcoxon	177	167	170.5		8A	Wilcoxon	194.5	158	173.5	
	p value	0.021**	0.007**	0.010**			p value	0.113	0.002**	0.014**	
10A	Wilcoxon	140.5	136	146	207.5	10A	Wilcoxon	165	141	155	218.5
	p value	0.000**	0.000**	0.000**	0.3		p value	0.005**	0.000**	0.001**	0.560
Nitrite						**Nitrate**					
		2A	4A	6A	8A			2A	4A	6A	8A
4A	Wilcoxon	230				4A	Wilcoxon	179			
	p value	0.917					p value	0.024**			
6A	Wilcoxon	199.5	195			6A	Wilcoxon	213	202.5		
	p value	0.171	0.119				p value	0.414	0.204		
8A	Wilcoxon	184	183	166.5		8A	Wilcoxon	158	186.500	168.5	
	p value	0.044**	0.040**	0.006**			p value	0.002**	0.051	0.007**	
10A	Wilcoxon	143.5	149.5	146	203	10A	Wilcoxon	200.5	126	176.5	124
	p value	0.000**	0.001**	0.000**	0.220		p value	0.174	0.000**	0.018**	0.000**
Ammonia						**TN**					
		2A	4A	6A	8A			2A	4A	6A	8A
4A	Wilcoxon	199.5				4A	Wilcoxon	216			
	p value	0.170					p value	0.494			
6A	Wilcoxon	210.5	228.5			6A	Wilcoxon	209	221		
	p value	0.361	0.868				p value	0.330	0.633		
8A	Wilcoxon	165.5	148	156.5		8A	Wilcoxon	182.000	170	167	
	p value	0.005**	0.000**	0.002**			p value	0.036**	0.010**	0.007**	
10A	Wilcoxon	188.5	158.5	184	193	10A	Wilcoxon	158	148	185	121
	p value	0.067	0.002**	0.044**	0.100		p value	0.002**	0.000**	0.049**	0.000**
HPC						**Fm**					
		2A	4A	6A	8A			2A	4A	6A	8A
4A	Wilcoxon	23				4A	Wilcoxon	38			
	p value	0.347					p value	0.064			
6A	Wilcoxon	22	26			6A	Wilcoxon	34	39		
	p value	0.251	0.754				p value	0.018**	0.085		
8A	Wilcoxon	26	24	25		8A	Wilcoxon	50.5	40.5	33	
	p value	0.754	0.465	0.602			p value	0.798	0.125	0.013**	
10A	Wilcoxon	27	24	24	25	10A	Wilcoxon	46	44.5	39	49.5
	p value	0.917	0.465	0.465	0.602		p value	0.406	0.306	0.085	0.701

n=16 for pH, Cl2, TOC, Turbidity, Nitrite, Nitrate, Ammonia and TN; n=5 for HPC and Fm; n=5 and n=7 for HPC and Fm respectively. ** indiates significant difference between datasets

Table B-6 Results of Mann-Whitney U test for test phase 3

pH							**Cl_2**						
		2A_R3	6A_R3	10A_R3	2B_R3	6B_R3			2A_R3	6A_R3	10A_R3	2B_R3	6B_R3
6A_R3	Wilcoxon	317.5					6A_R3	Wilcoxon	290				
	p value	0.623						p value	0.795				
10A_R3	Wilcoxon	330.5	330				10A_R3	Wilcoxon	283	273			
	p value	0.937	0.924					p value	0.616	0.396			
2B_R3	Wilcoxon	260					2B_R3	Wilcoxon	265.5				
	p value	0.021**						p value	0.021**				
6B_R3	Wilcoxon		190.5		306.5		6B_R3	Wilcoxon		273		296.5	
	p value		0.000**		0.401			p value		0.397		0.972	
10B_R3	Wilcoxon			322	269.5	212.5	10B_R3	Wilcoxon			290.5	284	285.5
	p value			0.727	0.044**	0.000**		p value			0.808	0.641	0.678
TOC							**Turbidity**						
		2A_R3	6A_R3	10A_R3	2B_R3	6B_R3			2A_R3	6A_R3	10A_R3	2B_R3	6B_R3
6A_R3	Wilcoxon	287					6A_R3	Wilcoxon	261.5				
	p value	0.718						p value	0.213				
10A_R3	Wilcoxon	295	295				10A_R3	Wilcoxon	250.5	236.5			
	p value	0.931	0.959					p value	0.104	0.035**			
2B_R3	Wilcoxon	220.5					2B_R3	Wilcoxon	282				
	p value	0.008**						p value	0.592				
6B_R3	Wilcoxon		248.5		263.5		6B_R3	Wilcoxon		286.5		287.5	
	p value		0.091		0.242			p value		0.704		0.730	
10B_R3	Wilcoxon			274.5	224	249	10B_R3	Wilcoxon			271	296.5	274.5
	p value			0.428	0.011**	0.095		p value			0.360	0.972	0.428
Nitrite							**Nitrate**						
		2A_R3	6A_R3	10A_R3	2B_R3	6B_R3			2A_R3	6A_R3	10A_R3	2B_R3	6B_R3
6A_R3	Wilcoxon	216					6A_R3	Wilcoxon	265				
	p value	0.005**						p value	0.253				
10A_R3	Wilcoxon	291	255				10A_R3	Wilcoxon	297	280.5			
	p value	0.822	0.143					p value	0.986	0.555			
2B_R3	Wilcoxon	281					2B_R3	Wilcoxon	287				
	p value	0.569						p value	0.715				
6B_R3	Wilcoxon		167		216		6B_R3	Wilcoxon		230		258.5	
	p value		0.000**		0.025**			p value		0.018**		0.177	
10B_R3	Wilcoxon			292	286	225	10B_R3	Wilcoxon			234.5	254.5	297
	p value			0.850	0.692	0.049**		p value			0.029**	0.135	0.986
Ammonia							**TN**						
		2A_R3	6A_R3	10A_R3	2B_R3	6B_R3			2A_R3	6A_R3	10A_R3	2B_R3	6B_R3
6A_R3	Wilcoxon	229.5					6A_R3	Wilcoxon	254				
	p value	0.019**						p value	0.134				
10A_R3	Wilcoxon	266.5	285				10A_R3	Wilcoxon	278	293			
	p value	0.285	0.666					p value	0.502	0.877			
2B_R3	Wilcoxon	158					2B_R3	Wilcoxon	169				
	p value	0.000**						p value	0.000**				
6B_R3	Wilcoxon		170		278.5		6B_R3	Wilcoxon		164		278	
	p value		0.000**		0.513			p value		0.000**		0.502	
10B_R3	Wilcoxon			229.5	254	272	10B_R3	Wilcoxon			206	254	256
	p value			0.019**	0.134	0.380		p value			0.002**	0.134	0.153
HPC							**Fm**						
		2A_R3	6A_R3	10A_R3	2B_R3	6B_R3			2A_R3	6A_R3	10A_R3	2B_R3	6B_R3
6A_R3	Wilcoxon	42					6A_R3	Wilcoxon	52				
	p value	0.180						p value	0.949				
10A_R3	Wilcoxon	46	52				10A_R3	Wilcoxon	42.5	45.5			
	p value	0.406	0.949					p value	0.200	0.370			
2B_R3	Wilcoxon	63.5					2B_R3	Wilcoxon	48				
	p value	0.954						p value	0.565				
6B_R3	Wilcoxon		43.5		52		6B_R3	Wilcoxon		44		47.5	
	p value		0.148		0.093			p value		0.277		0.522	
10B_R3	Wilcoxon			59.5	59	50	10B_R3	Wilcoxon			44	51.5	50
	p value			0.602	0.345	0.059		p value			0.277	0.898	0.749

n=18 for pH, Cl2, TOC, Turbidity, Nitrite, Nitrate, Ammonia and TN; n=7 for HPC and Fm; ** indicates significant difference between datasets

Table B-7 Results of Mann-Whitney U test for test phase 4

pH						
		2A_R3	6A_R3	10A_R3	2B_R3	6B_R3
6A_R3	Wilcoxon	449				
	p value	0.279				
10A_R3	Wilcoxon	334	347			
	p value	0.000**	0.001**			
2B_R3	Wilcoxon	476.5				
	p value	0.664				
6B_R3	Wilcoxon		304.5		339.5	
	p value		0.000**		0.000**	
10B_R3	Wilcoxon			460	367.5	283.5
	p value			0.411	0.003**	0.000**

Cl_2						
		2A_R3	6A_R3	10A_R3	2B_R3	6B_R3
6A_R3	Wilcoxon	405.5				
	p value	0.234				
10A_R3	Wilcoxon	385	428.5			
	p value	0.085	0.552			
2B_R3	Wilcoxon	412.5				
	p value	0.321				
6B_R3	Wilcoxon		441		375.5	
	p value		0.787		0.053	
10B_R3	Wilcoxon			334.5	423.5	330.5
	p value			0.003**	0.480	0.002**

TOC						
		2A_R3	6A_R3	10A_R3	2B_R3	6B_R3
6A_R3	Wilcoxon	279				
	p value	0.000**				
10A_R3	Wilcoxon	248.5	430			
	p value	0.000**	0.589			
2B_R3	Wilcoxon	359.5				
	p value	0.021**				
6B_R3	Wilcoxon		338.5		246	
	p value		0.004**		0.000**	
10B_R3	Wilcoxon			410	366	315
	p value			0.296	0.031**	0.001**

Turbidity						
		2A_R3	6A_R3	10A_R3	2B_R3	6B_R3
6A_R3	Wilcoxon	271.5				
	p value	0.000**				
10A_R3	Wilcoxon	448.5	260			
	p value	0.939	0.000**			
2B_R3	Wilcoxon	436				
	p value	0.695				
6B_R3	Wilcoxon		416.5		291.5	
	p value		0.378		0.000**	
10B_R3	Wilcoxon			419	433.5	323
	p value			0.411	0.649	0.001**

Nitrite						
		2A_R3	6A_R3	10A_R3	2B_R3	6B_R3
6A_R3	Wilcoxon	288.5				
	p value	0.000**				
10A_R3	Wilcoxon	374	288.5			
	p value	0.050**	0.002**			
2B_R3	Wilcoxon	401.5				
	p value	0.208				
6B_R3	Wilcoxon		333.5		261	
	p value		0.003**		0.000**	
10B_R3	Wilcoxon			336.5	437.5	340
	p value			0.004**	0.724	0.005**

Nitrate						
		2A_R3	6A_R3	10A_R3	2B_R3	6B_R3
6A_R3	Wilcoxon	438.5				
	p value	0.735				
10A_R3	Wilcoxon	302.5	262.5			
	p value	0.000**	0.000**			
2B_R3	Wilcoxon	365.5				
	p value	0.028**				
6B_R3	Wilcoxon		303.5		281.5	
	p value		0.000**		0.000**	
10B_R3	Wilcoxon			434.5	438.5	304.5
	p value			0.667	0.742	0.000**

Ammonia						
		2A_R3	6A_R3	10A_R3	2B_R3	6B_R3
6A_R3	Wilcoxon	382.5				
	p value	0.081				
10A_R3	Wilcoxon	361.5	412			
	p value	0.023**	0.318			
2B_R3	Wilcoxon	275.5				
	p value	0.000**				
6B_R3	Wilcoxon		314		360.5	
	p value		0.001**		0.022**	
10B_R3	Wilcoxon			288	419.5	313
	p value			0.000**	0.421	0.000**

TN						
		2A_R3	6A_R3	10A_R3	2B_R3	6B_R3
6A_R3	Wilcoxon	388				
	p value	0.110				
10A_R3	Wilcoxon	300	322.5			
	p value	0.000**	0.001**			
2B_R3	Wilcoxon					
	p value	0.000**				
6B_R3	Wilcoxon				388	
	p value		0.012**		0.110	
10B_R3	Wilcoxon				422	345
	p value			0.003**	0.458	0.007**

HPC						
		2A_R3	6A_R3	10A_R3	2B_R3	6B_R3
6A_R3	Wilcoxon	52				
	p value	0.093				
10A_R3	Wilcoxon	59	50			
	p value	0.345	0.059			
2B_R3	Wilcoxon	57				
	p value	0.248				
6B_R3	Wilcoxon		59		50	
	p value		0.345		0.059	
10B_R3	Wilcoxon			44	50	44
	p value			0.165	0.487	0.165

Fm						
		2A_R3	6A_R3	10A_R3	2B_R3	6B_R3
6A_R3	Wilcoxon	22				
	p value	0.006**				
10A_R3	Wilcoxon	37	23			
	p value	0.748	0.010**			
2B_R3	Wilcoxon	32.5				
	p value	0.297				
6B_R3	Wilcoxon		26		39	
	p value		0.037**		1.000	
10B_R3	Wilcoxon			39	29.5	32
	p value			1.000	0.127	0.261

n=22 for pH, Cl2, TOC, Turbidity, Nitrite, Nitrate, Ammonia and TN; n=8 and n=6 for HPC and Fm respectively; ** indicates significant difference between datasets

B.3 Results of Kruskal-Wallis test

Table B-8 Results of Kruskal-Wallis test for test phase 1

	pH	Cl_2	TOC	Turbidity	Nitrite	Nitrate	Ammonia	TN	HPC	Fm
X^2	45.356	22.363	32.746	6.679	25.932	2.593	20.249	11.167	8.889	12.004
df	4	4	4	4	4	4	4	4	4	4
p value	0.000**	0.000**	0.000**	0.094	0.000**	0.628	0.000**	0.025**	0.064	0.017**

Table B-9 Results of Kruskal-Wallis test for test phase 2

	pH	Cl_2	TOC	Turbidity	Nitrite	Nitrate	Ammonia	TN	HPC	Fm
X^2	36.83	19.732	26.247	22.092	24.011	30.392	20.872	27.006	1.839	10.330
df	4	4	4	4	4	4	4	4	4	4
p value	0.000**	0.001**	0.000**	0.000**	0.000**	0.000**	0.000**	0.000**	0.765	0.035

Table B-10 Results of Kruskal-Wallis test for test phase 3

Total Cl_2=1 mg/L										
	pH	Cl_2	TOC	Turbidity	Nitrite	Nitrate	Ammonia	TN	HPC	Fm
X^2	0.073	0.687	0.084	5.666	6.256	1.031	4.447	1.730	1.655	1.619
df	2	2	2	2	2	2	2	2	2	2
p value	0.964	0.706	0.959	0.059	0.044**	0.597	0.108	0.421	0.437	0.445
Total Cl_2=5 mg/L										
	pH	Cl_2	TOC	Turbidity	Nitrite	Nitrate	Ammonia	TN	HPC	Fm
X^2	11.422	0.264	7.094	0.466	9.637	2.738	2.319	3.108	0.831	0.351
df	2	2	2	2	2	2	2	2	2	2
p value	0.003**	0.876	0.029**	0.792	0.008**	0.254	0.314	0.211	0.660	0.839

Table B-11 Results of Kruskal-Wallis test for test phase 4

Total Cl_2=1 mg/L										
	pH	Cl_2	TOC	Turbidity	Nitrite	Nitrate	Ammonia	TN	HPC	Fm
X^2	18.387	3.174	29.988	29.539	18.314	25.599	6.141	18.310	4.835	9.589
df	2	2	2	2	2	2	2	2	2	2
p value	0.000**	0.205	0.000**	0.000**	0.000**	0.000**	0.046**	0.000**	0.089	0.008**
Total Cl_2=5 mg/L										
	pH	Cl_2	TOC	Turbidity	Nitrite	Nitrate	Ammonia	TN	HPC	Fm
X^2	30.918	9.085	28.950	18.094	20.242	21.917	12.090	6.881	3.843	2.411
df	2	2	2	2	2	2	2	2	2	2
p value	0.000**	0.011**	0.000**	0.000**	0.000**	0.000**	0.002**	0.032**	0.146	0.299